Photoelectrochemistry

PRINCIPLES AND PRACTICES

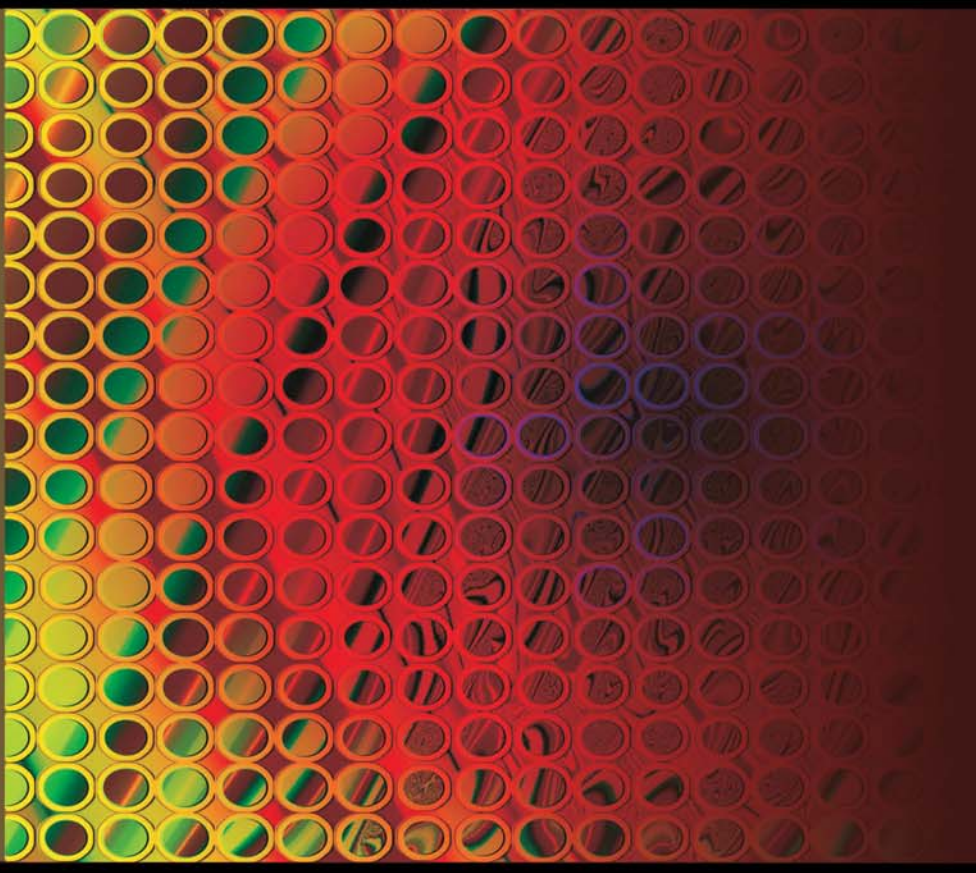

B. Viswanathan
M. Aulice Scibioh

Alpha Science

Photoelectrochemistry

Principles and Practices

Photoelectrochemistry

Principles and Practices

B. Viswanathan
M. Aulice Scibioh

Alpha Science International Ltd.
Oxford, U.K.

Photoelectrochemistry
Principles and Practices
198 pgs. | 26 figs. | 56 tbls.

B. Viswanathan
M. Aulice Scibioh
National Centre for Catalysis Research
Indian Institute of Technology Madras
Chennai

ALPHA SCIENCE INTERNATIONAL LTD.
7200 The Quorum, Oxford Business Park North
Garsington Road, Oxford OX4 2JZ, U.K.

www.alphasci.com

ISBN 978-1-84265-712-6

E-ISBN 978-1-78332-078-3

Printed in India

Preface

Over the last four or five decades, the subject of photo-electro-chemistry and photo-catalysis has been receiving considerable attention both academically and also for scientific research and practice. Research in this area is exploding in terms of number of publications. This subject has also been realized as essential for development of effective energy conversion devices and sustainability of life on earth. The authors have been considering formulating a monograph on this subject for a number of years since young researchers who are initiating research in this field find it hard to assimilate all the available knowledge and information in a short period. It has also been reflected and realized during the various special courses that the National Centre for Catalysis Research (NCCR) at Indian Institute of Technology, Madras has conducted on this topic. However, the hesitation to bring out a monograph lingered on due to the fact that every week, the literature in this field is expanding. Hence there was a fear that the coverage may look outdated when the monograph appears in print. This fear being fully present even now, the authors took the bold step of providing a level of knowledge with the fear that the coverage can not be comprehensive nor will be most upto date.

Having felt the need from various points of view, the authors considered the contents of the monograph and decided to restrict to some specific aspects on this branch of science for obvious reasons like affordability, available time for assimilating the knowledge and other related issues. Hence it should not be considered that this is a comprehensive monograph on this subject but has the bias of the authors and also other considerations mentioned above. It is also gratifying to note that many authoritative reviews are appearing on various aspects of this subject from time to time on regular basis and there are other authoritative sources of information on this subject and the readers should peruse these reviews for their knowledge assimilation. At most this monograph can be an introduction to this wealth of knowledge made available on this subject from time to time.

The authors felt that research in this field will have far reaching consequences for life sustainability on earth and hence introduction of these

subjects in the educational curriculum may become possible only when a suitable and appropriately tailored document is available as a reading source material. NCCR has introduced one such course in their Master's curriculum and attempted to experiment with the contents of this proposed monograph as a viable text. It is hoped that this compilation will also serve the purpose of an available text book and the educational curricula of the various institutions may introduce this subject at appropriate levels. It is fully realized that this compilation does not cover all aspects of this branch of science and it is hoped that it will kindle interest in the minds of the readers to dwell deep in this subject and experience the thrill of being in frontier in Science.

In a subject like this, there can be many gaps and limitations and the authors will be grateful if these aspects are brought to their attention so that these left out aspects can be included in subsequent attempts if there were to be some.

The authors wish to thank their learned colleagues and research scholars who have consistently contributed to the formulation and production this monograph. The inquisitive academic atmosphere provided by them especially the colleagues at NCCR has been one of the motivating factors and it is our duty to thank them for the same. We do hope that these colleagues will experiment introducing this course. One of the authors experimented this material in a course on Photo-catalysis for M Tech students in Indian Institute of Technology, Madras. They also wish to thank the *Department of Science and Technology*, Government of India for not only supporting the National Centre for Catalysis Research but also encouraged conducting these short term courses at NCCR.

Finally, the authors will be grateful for pointing out any shortcomings in this compilation.

B. Viswanathan
M. Aulice Scibioh

Contents

1 History of Photocatalysis

1.1 INTRODUCTION

There is generally a conception that Photo-catalysis originated with the discovery of Photo-electrochemical decomposition of water by Fujishima and Honda [1] in the 70s. Photo-catalysis which is a phenomenon where in an acceleration of a chemical reaction in the presence of photons and catalyst has been reported in the literature in 50s (possibly even earlier to this) by Markham and Laidler [2]. Rev. Sister Markham followed this with a publication in chemical education [3] wherein she reported the photo-catalytic properties of oxides. In fact, Sister Markham had a number of subsequent publications on the photo-catalytic transformations on irradiated zinc oxide [4]. Photo-catalysis deals with the absorption of photons by the solid which generate electron hole pair which are utilized in the generation free radicals (hydroxyl radicals (.OH). The chemical consequence of this process today goes with the name of advanced oxidation process (AOP; which may or may not involve TiO_2 and Photons). Langford has written a concise article on photo-catalysis as introduction to a special issue of catalysts dealing with this hybrid area of catalysis [5].

Photo-chemistry has been an integral part of life on earth. One often associates photo-catalysis with photosynthesis. However the term photo-catalysis found mention in an earlier work by Plotnikov in the 1930's in his book entitled Allaemeine photochemie. The next major systematic development as stated in the previous paragraph was in the 1950's when Markham and Laidler performed a kinetic study of photo oxidation on the surface of zinc oxide in an aqueous suspension. By the 1970's researchers started to perform surface studies on photo-catalysts like Zinc Oxide and Titanium dioxide. The most commonly employed photo-catalyst is Titanium dioxide. TiO_2 exists mainly in three crystallographic forms, namely Brookite, Anatase and Rutile. There have been a number of studies on the three modifications of titania. The energetics of the titania polymorphs were studied by high temperature oxide melt drop solution calorimetry. It has been shown

that relative to bulk rutile, bulk brrokite is 0.71 ± 0.38 kJ/mol and bulk anatase is 2.61 ± 0.41 kJ/mol higher in enthalpy [6]. The effect of particle size on phase stability and phase transformation during growth of nanocrystalline aggregates and the mixed phases transform to brookite and/or rutile before brookite transforms to rutile have been reported by Zhang and Banfield [7]. Among these three forms, the most often used photo-catalyst is the anatase phase either in pure form or in combination with rutile form. There are various reasons for this preference of TiO_2 as photo-catalyst. These reasons include that it was the first system studied by Fujishima and Honda and TiO_2 exhibits possibly maximum photon absorption cross section (i.e., it absorbs maximum number of photons of correct wavelength). This preference over TiO_2 is seen from the data given in Table 1.1.

Table 1.1 ***Statistical distribution of scientific publications dealing with nano-materials for PEC/Photo-catalysis hydrogen production [8].***

Materials	*Percentage of Study*
TiO_2	36.2
Non-TiO_2 Oxides	10.9
Oxy-sulphides	18.8
Oxy-nitrides	5.1
Other semiconductors	5.8
Composites and Mixtures	17.4
Non Semiconductors	5.8
Total	**100**

Degussa P25 Titanium dioxide generally employed as catalyst in many of the studies reported in literature and hence, considered as standard for photo-catalytic activity comparison, contains both anatase (about 80 per cent) and rutile (about 20 per cent).

It is in general impossible to completely trace the history of Photo-catalysis. Even Fujishima and his coworkers [9] have expressed concern on completely outlining the history of photo-catalysis. The main difficulty appears to be that photo-catalysis unlike other chemical reactions involves simultaneously both oxidation and reduction reactions on a surface possibly assisted by photons of appropriate wavelength corresponding to the band gap of the semiconductor employed as catalyst. In 1921 Renz reported that titania was partially reduced when it was illuminated with sunlight in the presence of organic substrates like glycerol [10]. In 1924, Baur and Perret [11] probably were the first to report the photo-decomposition of silver salt on ZnO to produce metallic silver. Probably Baur and Neuweiler [12] were the first to recognize that both oxidation and reduction are taking place simultaneously on the production of hydrogen peroxide on ZnO. This was followed by the work of Renz in

1932 [13] who reported the photo-catalytic reduction of silver nitrate and gold chloride on TiO_2. Goodeve and Kitchener [14] studied the photo-catalytic decomposition of dye on titania surfaces and even reported the quantum yields. In 1953, it has been recognized that the organic substrate was oxidized and oxygen was reduced. Unfortunately, these studies have been carried out on ZnO surfaces and hence could have been hampered because of the inevitable problem of photo corrosion of ZnO [2]. There were few attempts in between for the production of hydrogen peroxide and decomposition of dyes on illuminated semiconductor surfaces. There were attempts to study the photo-catalytic oxidation of organic substrates on a variety of oxide surfaces from other parts of the world in and around this period. In the 1960s photo-electrochemical studies on ZnO with various redox couples were started. All these studies culminated in the photo-electrochemical decomposition of water by Fujishima and Honda which opened up means for solar energy conversion and also for the generation of fuel hydrogen. Subsequently Kraeutler and Bard have demonstrated that illuminated TiO_2 could be used for the decontamination of water by photo-catalytic decomposition. This has led to new photo-catalytic routes for environmental clean-up and also for organic synthesis. These aspects will be dealt with in separate chapters in this monograph. Fujishima et al.,[9] have provided a more detailed and authentic write-up on the history of photo-catalysis.

1.2 BASIC PRINCIPLE OF PHOTO-CATALYSIS

According to the glossary of terms used in photo-chemistry [IUPAC 2006 page 384] photo-catalysis is defined "as the change in the rate of a chemical reaction or its initiation under the action of ultraviolet, visible or infra red radiation in the presence of a substance the photo-catalyst that absorbs light and is involved in the chemical transformation of the reaction partners." When a semiconductor (or an insulator) is irradiated with light of suitable wavelength corresponding to the energy of the band gap, electrons occupying the usually or mostly filled energy levels in the valence band will be transferred to an allowed energy state in the normally empty conduction band thus creating a hole in the valence band. This electron-hole pair is known as exciton. These photo-generated electron-hole pairs promote the so called redox reaction through the adsorbed species on the semiconductor or insulator surface. However, the band gap of the insulators will be usually high and as such generating of such high energy photons will not be comparatively easy and hence insulators are not considered as possible candidates for Photo-catalysis. Generally, metals cannot be employed as photo-catalysts since their occupied and unoccupied energy states are overlapping with respect to energy and hence the recombination of

electron-hole pair will be the most preferred process and hence the conversion of photon energy to chemical energy using metals will not be advantageous.

It is generally considered that the energy position of the top of the valence band of a semiconductor is a measure of its oxidizing power and the bottom of the conduction band is a measure if its reducing capacity. It is therefore necessary one has to know with certainty the energy positions of the top of the valence band and bottom of the conduction band so that the reactions that these excitons can promote can be understood. One such compilation is given in Table 1.2.

Photo-catalytic destruction of organic pollutants in water is based on photo-chemical process involving semiconductors. When a semiconductor is irradiated with UV (usually but it can be any other radiation as well) light of wavelength appropriate for excitation from valence band to the conduction

Table 1.2 ***Electro-negativity, [χ], Band gap,(E_g) energy levels of the conduction band bottom (E_{CB}) and energy position of the top of valence band (E_{VB}) [data extracted from Y. Xu and M.A.A. Schoonen, American Mineralogist, 85, 543-556 (2000)].***

Substance Oxide	*Electro-negativity* (χ)	*Band Gap* (E_g)	*Conduction Band,* E_{CB}	*Valence Band,* E_{VB}
$BaTiO_3$	5.12	3.30	-4.58	-7.88
Bi_2O_3	6.23	2.80	-4.83	-7.63
$CoTiO_3$	5.76	2.25	-4.64	-6.89
CuO	5.81	1.70	-4.96	-6.66
Fe_2O_3	5.88	2.20	-4.78	-6.98
Ga_2O_3	5.35	4.80	-2.95	-7.75
$KNbO_3$	5.29	3.30	-3.64	-6.94
$KTaO_3$	5.32	3.50	-3.57	-7.07
$MnTiO_3$	5.59	3.10	-4.04	7.14
Nb_2O_3	6.29	3.40	-4.59	-7.99
NiO	5.75	3.50	-4.00	-7.50
$NiTiO_3$	5.79	2.18	-4.70	-6.88
PbO	5.42	2.80	-4.02	6.82
SnO_2	6.25	3.50	-4.50	-8.00
$SrTiO_3$	4.94	3.40	-3.24	-6.64
TiO_2	5.81	3.20	-4.21	-7.41
V_2O_5	6.10	2.80	-4.70	-7.50
WO_3	6.59	2.70	-5.24	-7.94
ZnO	5.79	3.20	-4.19	-7.39
ZrO_2	5.91	5.00	-3.41	-8.41

Table 1.3 ***Oxidizing power of the common oxidizing agents.***

Oxidant	*Oxidation Potential(V)*
Hydroxy radical	2.80
Ozone	2.07
Hydrogen Peroxide	1.77
ClO_2	1.49
Chlorine (Cl_2)	1.35

band of the chosen semiconductor an exciton is created. The photo-chemical oxidation of the organic substrate normally proceeds by the adsorption of the substrate on the surface of the semiconductor with transfer of electrons with the hole generated. However other possible oxidation processes can also take place with radicals generated (OH radical if the solvent is water) at the surface of the semiconductor surface. Thus a variety of surface reactions will take place on the photo-excited semiconductor surface, the preferred reaction depends on the nature of the substrate under consideration and its nature of adsorption and activation on the semiconductor surface. In Fig. 1.1, a simple representation of these possible processes are shown by considering simple general reactions water giving hydroxyl radicals and organic substrate being oxidized all the way to carbon dioxide and water in order to get an idea of what can takes place on the surface of semiconductor as a result of photo-excitation and catalysis.

Since it is possible that the organic substrate can be completely degraded to carbon dioxide and water, this process has been considered to be a viable method for the decontamination of water. In addition, it should be kept in mind that hydroxyl radical is a powerful oxidizing agent as compared to other common oxidizing agents as can be seen from the data given in Table 1.3. It is clear from the data given in Table 1.3 that the aqueous phase reactions will still be preferred in Photo-catalysis.

1.3 LIMITATIONS OF PHOTO-CATALYSIS

Though Photo-catalytic technology has been emerging as a viable technology for the remediation of pollutants from water, it can be applied to a variety of compounds. One of the factors to be considered is the possibility of mass transfer limitations due to the characteristics imposed in the reaction chamber by the existence of the catalyst in various forms in dispersed state. In fact the construction of a appropriate photo-chemical reactor itself has been a major issue and various designs have been proposed in literature. A simple reactor design conventionally employed is shown in Fig. 1.2.

Sclafani et al., [16] postulated external mass transfer limitations to interpret their results in a packed bed reactor filled with spheres of semiconductor

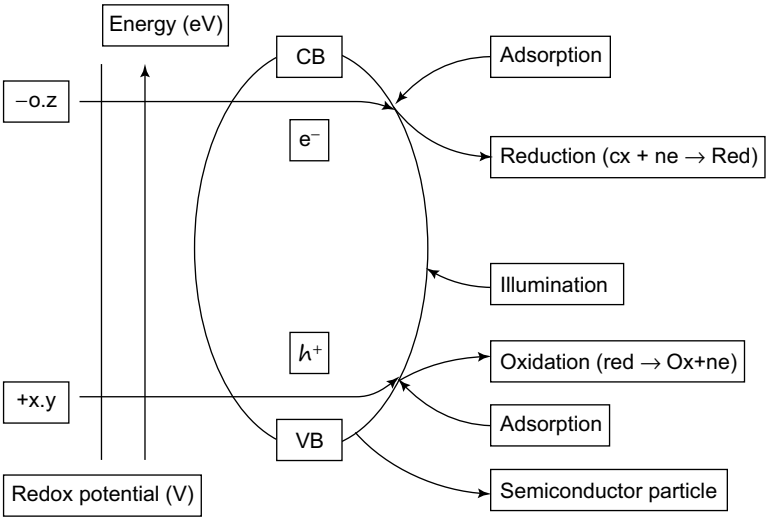

Figure 1.1 ***Schematic representation of the principle of photocatalysis showing the energy band gap of a semiconductor particle. Typical reactions considered are: water → hydroxyl radical; organic substrate + hydroxy radical → carbon dioxide + water + mineral acid.***

catalyst (in this case pure titanium dioxide (ca. 0.12 cm in diameter)). Chen and Ray [17] studied internal and external mass transfer limitations in catalytic particles of photo-catalytic reactors and concluded only mild mass transfer restrictions since the effectiveness factor observed was near 0.9 and hence rotating disc photo reactor when the spherical particles of the semiconductor fixed on a solid support mass transfer limitations are negligible. The specific role of mass transfer was analyzed in terms of one of the dimensionless Damkhler numbers. In other reactor configurations, particularly films and membrane reactors other quantitative observations of internal mass transfer limitations have been published [18,19]. and many others (see for example one of the reviews on this topic in Legrini et al., [20]. Unfortunately, these limitations have not been examined with other type of reactors like slurry reactors. In addition, since photons are coupling with a heterogenous system, this can result in gradients in concentration or the coupling of the photon field with the scattering particles.

The points that emerge from the data presented in Table 1.2 are that the top of the valence band is nearly the same for the oxide semiconductors and the bottom of the conduction band depends on the cation involved and hence the oxide semiconductors will be more or less behaving in a similar manner.

The other chemical limitations involved in the photo-catalytic degradation of pollutants from water are: The adsorption of the pollutant species on

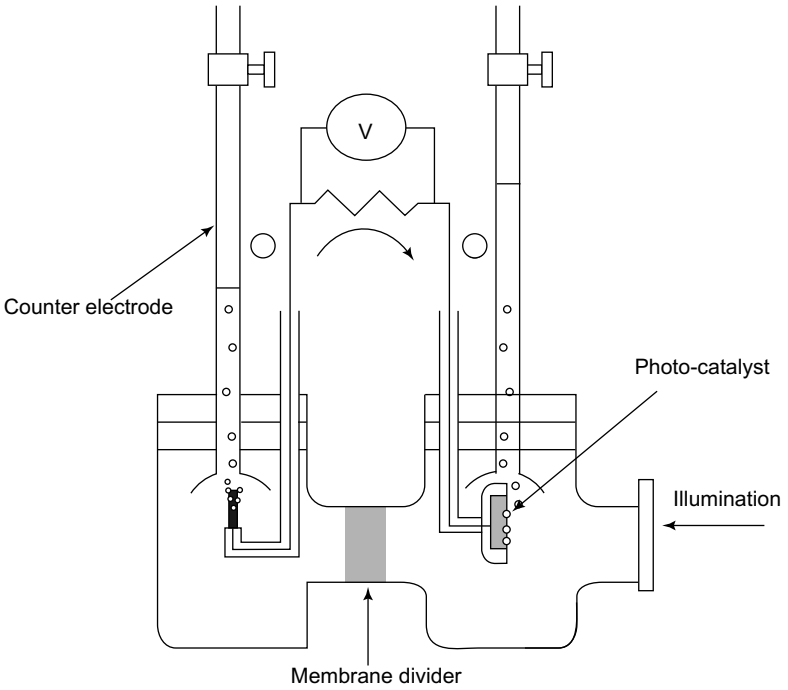

Figure 1.2 ***Typical reactor design conventionally employed for the photo-splitting of water.***

the surface of the semiconductor. This fact has been recognized in the literature but still not many quantitative relationships have emerged indicating the importance of this step in the photo-degradation processes. However, the importance of this step is apparent since the charge transfer from the semiconductor to the substrate and hence cause their degradation is possible only in the adsorbed state of the substrate since charge transfer has restrictions with respect to distances involved. In addition the adsorption is directly related to the surface area of the photo-catalyst and hence it is conventional to optimize the surface area of the photo-catalyst.

The pH may also have an effect on the photo-degradation of organic pollutants since the nature of the species involved can change with respect to pH. In addition in aqueous medium the potential changes by 59 milli-volts per pH unit and this also can affect the process of degradation.

In solution phase, the presence of both type of counter ions namely, anions and cations can affect the photo-degradation process due to reasons like photon absorption by the ions and also the type of species that will be generated as a result of photon absorption. When the composite solar radiation is employed for photo-degradation process, the temperature of the system can affect all

the reactions (normally increase is noticed) except for the electron hole creation step. However, the solubility of oxygen will decrease with increase in temperature and this can also affect the rate of photo-degradation reaction.

In a separate chapter, the studies reported on the application of photo-catalysis for the decontamination of water will be considered. This field seems to assume importance in these days due to various reasons. However, the studies reported in this area have to be considered with care since the products of oxidation and their effects have not yet been established though it is mostly assumed to be carbon dioxide.

As seen earlier that one of the areas in which photo-catalysis has been extensively employed is the decontamination of water. Water covers over tow thirds of earth's surface and less than a third is the land area. Oceans, rivers and other inland waters are continuously polluted by human activities leading to a gradual decrease in the quality of water. There are specified limits of concentration beyond which the presence of some substances is considered as polluting water. In Table 1.5, the recommended tolerance limits of pollutants are given.

Table 1.4 ***Band positions of semiconductor photo-catalysts in aqueous solution at pH = 1 and Positions are given in volts versus NHE.***

Semiconductor Material	*Valence Band (V vs NHE)*	*Conduction Band (V vs NHE)*	*Band Gap (eV)*	*Band Gap (Wavelength)*
TiO_2	+3.1	-0.1	3.2	387
SnO_2	+4.1	+0.3	3.9	318
ZnO	+3.0	-0.2	3.2	387
ZnS	+1.4	-.2.3	3.7	337
WO_3	+3.0	+0.2	2.8	443
CdS	+2.1	-0.4	2.5	496
CdSe	+1.6	-0.1	1.7	729

The common pollutants in water are classified as inorganic contaminants and organic pollutants. The main inorganic contaminants are the metal ions, nitrates, nitrites, nitrogen dioxide, ozone, ammonia, azide and halide ions. There are various studies reported in literature that deal with the photo-catalytic decomposition or transformation of these inorganic contaminants. This will be dealt with in a separate chapter.

Photocatalytic decomposition (mostly oxidation) of organic pollutants has been of great interest. In these studies, the reaction is carried out in presence of molecular oxygen or air for complete oxidation to carbon dioxide and water and possibly inorganic mineral acids as the final products. It has been shown

Table 1.5 ***Recommended tolerance limits of pollutants in water [Data collected from K.C. Agarwal, Industrial power engineering and Applications, Butterworth-Heinemann, pp. 565 (2001)].***

S.No	*Parameter*	*Recommended Tolerance Level*
1	Biological Oxygen Demand (BOD)	30 mg/l
2	Chemical Oxygen Demand (COD)	250 mg/l
3	Alkali traces	Maximum upto pH 9
4	Acid	Note less than pH 5.5
5	Total suspended solitds	100 mg/l
6	Oil and grease	10 mg/l
7	Dissolved phosphates as P	5 mg/l
8	Chlorides as (Cl)	600 mg/l
9	Sulphates (as SO_4)	1000 mg/l
10	Cyanides as (CN)	0.2 mg/l
11	Total chromium	2 mg/l
12	Hexavalent chromium	0.1 mg/l
13	Zinc as Zn	0.25 mg/l
14	Iron	3 mg/l
15	Total heavy metals	7 mg/l
16	Total phenoloic compounds	1 mg/l
17	Lead (Pb)	0.1 mg/l
18	Copper as Cu	2.0 mg/l
19	Nickel as Ni	2.0 mg/l
20	Bioassay test	90% survival after 96 hours

that many of the organic-chlorides, pesticides, herbicides and surfactants are completely oxidized to carbon dioxide, water and hydrochloric acid.

It may be worthwhile to realize the effect of some of the pollutants on human health. The data collected from literature are given in Table 1.6. It is to be remarked the effects of pollutants generally affect the human health in a variety of ways basically affecting the nervous system.

In addition there are some Persistent Organic Pollutants (POP) like aldrin, chlordane DDT, hexachlorbenzene, furans, polychlorinated biphenyls, Polycycic aromatic hydrocarbons (PAHs) and so on. These substances some of which are called the dirty dozen cause many disorders including cancer breast cancer, damage to reproductive system, neuro-behavioural disorders and health related concerns.

Table 1.6 ***Possible pollutants in water and their effect on human health.***

Pollutant	*Adverse Effect on Human Health*
Atrazine	Cancer, damage to nervous system
Benzene	Cancer and anemia
Pentachlorophenol	Liver and kidney damage and cancer
Trichloroethylene	Cancer
Trichlorethane	Damage to Kidney, liver and nervous system
Bromoform	Damage to nervous system and muscle
Carbofuran	Damage to nervous system, kidney, reproductive system and liver
Carbon tetrachloride	Cancer
Chlorobenzene	Damage to nervous system, kidney and liver
Dibromochloroethane	Damage to nervous system and muscle and cancer
Endrin	Damage to nervous system, kidney, liver, anemia and cancer
Ethylbenzene	Damage to nervous sytem, liver and kidney
Heptachlor	Cancer
Hetachlor epoxide	Cancer
Hexachlorocycopentadiene	Damage to kidney and stomach
Lindane	Damage to nervous system, liver and kidney
Simazine	Damage to nervous system, cancer
Styrene	Damage to nervous system, kidney and liver
Tetrochloroethylene	Damage to nervous system, cancer
Toluene	Damage to nervous system, liver and kidney
1,2,4-trichlorobenzene	Damage to liver and kidney
Xylene pesticides	Damage to nervous system, liver, kidney lungs and membranes

1.4 ADVANCED OXIDATION PROCESSES (AOP)

Irrespective of the method of generation of hydroxyl radicals, the methods which utilize hydroxyl radicals for carrying out the oxidation of the pollutants are grouped as Advanced Oxidation Processes.

Hydroxyl radicals are extraordinarily reactive species and have one of the highest oxidation potential (2.8 V). The values of rate constants in reactions with organic substrates are in the range of $10^6 - 10^9$ $M^{-1}s^{-1}$ [21-23] (Table 1.7). In addition hydroxyl radicals do not show any selectivity with respect to the position of attack on the organic substrates which is useful aspect for the treatment of water. The fact that the production of hydroxyl radicals can be

Table 1.7 ***Values of second order rate constants for the oxidation by ozone and hydroxyl radical for a variety of compounds [data a- from Hoigne and Bader, 1983; b- from Farhataziz and Ross, 1977].***

Organic compound	*Value of Rate Constant* $M^{-1}s^{-1}$	
	Ozone[a]	OH* radical[b]
Benzene	2	7.8×10^9
n-butanol	0.6	4.6×10^9
t-butanol	0.03	0.4×10^9
Chlorobenzene	0.75	4×10^9
Tetrachloroethylene	<0.1	1.7×10^9
Toluene	14	7.8×10^9
Trichloroethylene	17	4.0×10^9

a- from Hoigne and Bader, 1983; b- from Farhataziz and Ross, 1977.

made by a variety of methods adds to the versatility of Advanced Oxidation Processes thus allowing a better compliance with the specific treatment requirements. An important consideration to be made in the application of AOP to waste water treatments is the requirement of expensive reactants like hydrogen peroxide and/or ozone. Hence, AOP cannot replace the application of more economical treatment methods such as biological degradation whenever possible. A list of the different possibilities offered by AOP are briefly given in Table 1.8.

Table 1.8 ***Sources involved in the various Advanced Oxidation Processes.***

Source of Oxidants	*Name of the Processes*
H_2O_2/Fe^{2+}	Fenton
H_2O_2/Fe^{3+}	Fenton like
H_2O_2/Fe^{2+}, Fe^{3+}/UV	Photoassisted fenton
TiO_2, $h\nu/O_2$	Photocatalysis
O_3 or H_2O_2/UV	photoassisted oxidation

1.5 HETEROGENEOUS PHOTO-CATALYSIS

Among the AOPs mentioned, photo-catalysis is the promising method. This is attributed to its potential to utilize energy from the sun without the addition of others forms of energy or reagents. The reactions carried out by the photo-catalysts are classified into two categories namely homogeneous or Heterogeneous photo-catalysis.

Heterogeneous photo-catalysis is based on the semiconductors which are employed for carrying out various desired reactions in both liquid and vapour phases. Photo-catalysis involves the formation of highly reactive electrons and holes in the conduction and valence bands respectively. The electrons are capable of carrying out reduction reactions and holes can carry out oxidation reactions. There are also other processes that take place in the semiconductor. The electron and hole can react with acceptor or donor molecules respectively or recombine at surface trapping sites. They can also be trapped at bulk trapping sites and recombine with the release of heat. The electron hole can be exploited in a number of ways:

(i) For producing electricity(solar cells)-Photo-voltaics.
(ii) For decomposing or removing pollutants-Photo-oxidation.
(iii) For the synthesis and production of useful chemicals-Photo-catalysis.
(iv) For the photo-electrolysis of water-(photo-electro-chemistry).

As the recombination of the photogenerated electron and hole occurs on a pico second time scale, electron transfer at the interface can kinetically compete with recombination only when the donor or acceptor is adsorbed on the surface of the semiconductor before irradiation. Hence adsorption of the substrate prior to irradiation is important for efficiency of the heterogeneous photocatalyic process [24]. Hydroxyl groups or water molecules adsorbed on the surface can serve as traps for the photogenerated hole, leading to the formation of hydroxyl radicals in the case of metal oxide suspensions. Strong adsorption of acetone and 2-propanol on ZnO has been observed during temperature programmed desorption [25]. Metal oxide surfaces have a surface density of about 4-5 hydroxy groups/nm^2 as has been shown by the continuous distribution of adsorption energies in the Freundlich isotherm. Many organic substrates were found to play the role of adsorbed traps for the photo-generated holes. For example, in a colloidal suspension of TiO_2 in acetonitrile, radical ions are detected directly during flash excitation [25].

Apart from materials derived from TiO_2 by modifications like doping, coupling with an additional phase or morphological changes different compounds with distinct composition and structure have also been examined. Various tantalates, [26-27], niobates [28], Oxides of bismuth like $Bi_2W_2O_9$, Bi_2MoO_6, $Bi_2Mo_3O_{12}$ and oxides of Indium as In_2O_3, $Ba_2In_2O_5$, MIn_2O_4 (M = Ca,Sr) were found to be capable of photo-splitting water. Tantalum nitride and tantalum oxynitriede were aslo found to be effective catalysts for water splitting.

References

1. Akira Fujishima and Kenichi Honda, Electrochemical photolysis of water at a semiconductor electrode, Nature, 238: 37-38 (1972).

2. M. C. Markham and K. J. Laidler, A kinetic study of photo-oxidations on the surface of zinc oxide in aqueous suspensions, J. Phys. Chem., 57: 363-369 (1953).
3. M. C. Markham, Photocatalytic properties of oxides, J. Chem. Edu, 540-543 (1955).
4. J. C. Kuriacose and M. C. Markham, J. Catalysis, 1: 498-507 (1962).
5. Cooper H. Langford, Photocatalysis, A special issue on a unique hybrid area of Photocatalysis, catalysts, 2: 327-329(2012).
6. M. R. Ranade, A. Navrotsky, H. Z. Zhang, J. F. Banfield, S. H. Elder, A. Zeban, P. H. Borse, S. K. Kulkarni, G. S. Doran and H. J. Whitefield, Energetics of Nanocrystalline TiO_2, PNAS, 99: 6476-6481 (2002).
7. H. Zhang and J. F. Banfield, Understanding polymorphic phase transformation behaviour during growth nanocrystalline aggregates: Insights from TiO_2, J. Phys. Chem., B, 104: 3481-3487 (2000).
8. J. Zhu and M. Zach, Nano-structured materials for photo-catalytic hydrogen production, Current opinion in Colloid and Interface Science, 14: 260-269 (2009).
9. A. Fujishima, X. Zhang, and D. A. Tyrk, TiO_2 Photo-catalysis and related surface phenomena, Surface Science Reports, 63: 515-582 (2008).
10. C. Renz, Helv. Chim. Acta, 4: 961-968 (1921).
11. E. Baur and A. Perret, Helv. Chim. Acta, 7: 910-915 (1924).
12. E. Baur and C. Neuweiler, Helv. Chim. Acta, 10: 901-907 (1927).
13. C. Renz, Helv. Chim. Acta, 1077-1084 (1932).
14. C. F. Goodeve and J. A. Kichener, Trans. Faraday Soc., 34: 570-579, 902-908 (1938).
15. B. Kraeutler and A. J. Bard, J. Am. Chem. Soc., 100: 4317-4318 (1978).
16. A. Sclafani, L. Palmisano and E. Devi, Photo-catalytic degradation of Phenol in aqueous titanium dioxide dispersion: The influence of Iron (3+) and Iron (2+) and silver (1+) on the reaction rate, J. Photochem. Photobiol A: Chemistry, 56: 113 (1991).
17. D. Chen and A. K. Ray, Photodegradation kinetics of 4-nitrophenol in TiO_2 suspension, Water. Res., 32: 3223 (1998).
18. M. F. J. Dijkstra, H. Buwalda, A. W. F. de Jong, A. Michorius, J. G. M. Winkelman and A. A. C. M. Beenackers, Experimental comparison of three reactor designs for photocatalytic water purification, Chem. Eng. Sci., 56: 547 (2001).
19. J. Chen, D. F. Ollis, W. H. Rulkens and H. Bruning, Kinetic process of photocatalytic mineralization of alcohols on metallized titanium dioxide, Water. Res., 33: 1173 (1999).

20. O. Legrini, E. Oloveros and A. M. Braun, Photochemical process for water treatment, Chem. Revs., 93: 671-698 (1993).
21. J. Hoigne and H. Bdar, Rate constants of reaction of ozone with organic and inorgnaic compounds in water, Part II dissociating organic compounds, Water Resour., 17: 185-194 (1983).
22. R. Andreozzi, V. Capiro, A. Insola and R. Marotta, Advanced Oxidation Processes (AOP) for water purification and recovery, Catal. Today, 53: 51-59 (1999).
23. A. Farhataziz and B. Ross, Selective specific rates of reactions of transients in water and aqueous solution Part III Hydroxyl radical and perhydroxyl radical and their radical ions, Natational Standard Reference Data Series USA (NBS) 59: 22-67 (1977).
24. M. A. Fox and M. T. Dulay, Heterogeneous photocatalysis, Chem. Rev., 93: 341-37 (1993).
25. M. A. Fox, C. C. Chen, and R. A. Lindig, Transients generated upon photolysis of colloidal titanium dioxide in acetonitrile containing organic redox couples, J. Am. Chem. Soc., 104: 5828-5829(1982).
26. F. E. Osterloh, H_2 and O_2 over lanthanum doped $NaTiO_3$ photocatalysts with high crystallinity and surface nanostructure, J. Am. Chem. Soc., 125: 3082-3089 (2003).
27. F. E. Osterloh, Inroganic materials as catalysts for photochemical splitting of water, Chem. Mater., 20: 35-54 (2008).
28. Y. Ebina, N. Sakai and T. Sasaki, Photocatalyst of lamellar aggregates of RuO_2 loaded perovskite nanosheets for overall water splitting, J. Phy. Chem., B 109: 17212-17216 (2005).

2 Developments for Photoelectrochemistry (PEC)

2.1 WORLD ENERGY OUTLOOK

It is interesting to watch the growing debate over the future of energy in global platforms. Ever soaring oil prices and increasing energy demands accelerated environmental, ecological and global climate changing problems. The challenges in energy security, environmental security, national security, and economic security can be met by addressing the energy demands in a sustainable fashion, not only through increased energy efficiency, and by introducing new methods of using the existing carbon-based fuel sources, but by haunting for new carbon-neutral energy. We are now witnessing the beginning of a global paradigm shift toward clean energy. The search for alternative energy is set. The finding of secure, clean, sustainable energy is an inevitable issue faced by the scientific, technological and policy making communities.

Alternative energy can generally be classified into two categories. The first one is to looking for substitutes to the excising petroleum - liquids such as ethanol, biodiesel, biobutanol, dimethyl ether, coal-to-liquids, tar sands, oil shale - from biomass and/or fossil feed stock. The second one is to look for alternatives to the generation of electric power and power-storage technologies - wind, solar, photovoltaics, solar thermal, tidal, biomass, fuel cells, batteries. In the decades ahead, the world will need to expand energy supplies in safe, secure, affordable and environmentally responsible ways.

What can we foresee for the next 25-30 years? The answer to this question may vary by region, based on diverse economic and demographic trends, evolution of technologies and energy policies set by governments. The growth in primary energy demand is shown in Fig. 2.1. It can be seen that the global energy demand increases by one-third from 2010 to 2035, with India and China accounting for 50% of the growth. In the countries belonging to the Organization for Economic Cooperation and Development (OECD), including North America and Europe, we see that the energy usage appears to remain flat, even as these countries achieve economic growth and higher living standards. In contrast, Non-OECD energy demand will surge by close to 50%. China's

demand for energy will extend over the next two decades and then gradually flatten as its economy and population mature.

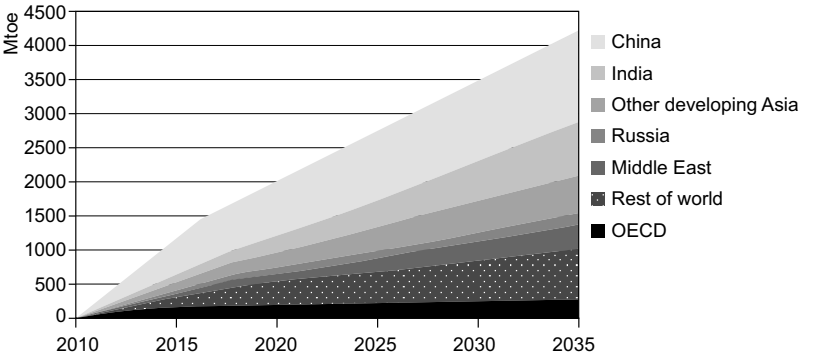

Figure 2.1 ***Growth in primary energy demand [Source: World Energy Outlook 2012, by International Energy Agency].***

In order to shift concerns about oil security, changing scenario in oil net imports are set, as shown in Fig. 2.2. The United States oil imports drop due to rising domestic output and improving transport efficiency; the European Union oil imports overtake those of the US around 2015; China becomes the largest importer around 2020. As new technologies and sources emerge, we witness that the energy has been used more efficiently with diverse energy supplies.

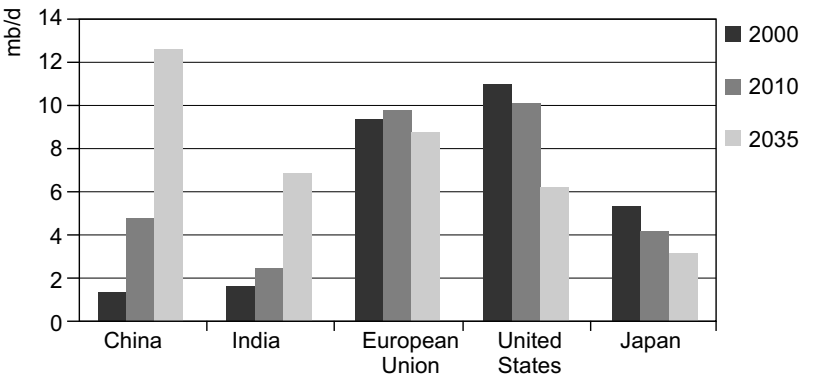

Figure 2.2 ***Net imports of oil [Source: World Energy Outlook 2012, by International Energy Agency].***

Population and income growth (gross domestic product, GDP) are the two most powerful driving forces besetting energy demands. It can be evidenced from the following data (Fig. 2.3). Since 1900, world population has more than quadrupled, real income has grown by a factor of 25, and primary energy consumption by a factor of 22.5. The next two decades are likely to see continued global integration, and rapid growth of low and medium income

economies. Population growth appears to trending down, but income growth is treading up. In the past two decades, the world population has increased by 1.6 billion, and it is projected to increase by 1.4 billion in the coming 20 years. At the outset, in the global level, the fundamental relationship in energy economics remains robust, as more people with more income means that the production and consumption of energy will hike.

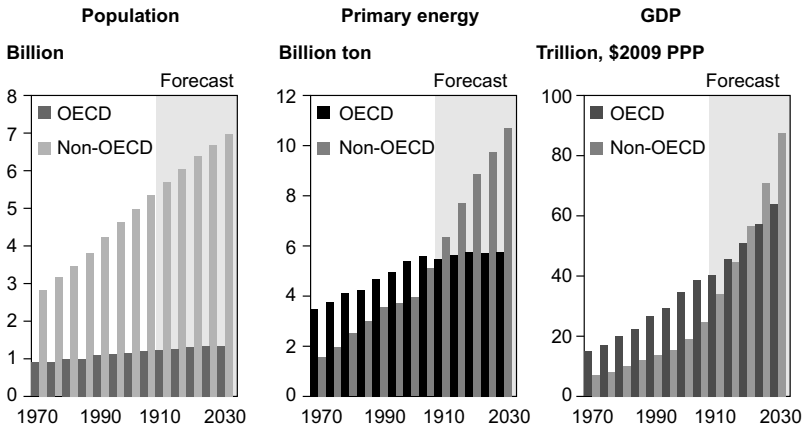

Figure 2.3 ***Population, income growth and primary energy usage [Source: BP Statistical Review of World Energy, London, UK, 2011].***

The energy consumption and the fuel mix are shown in Fig. 2.4. The first wave of industrialization was based almost entirely on a truly disruptive technology, the steam engine and on coal. Coal remained as a dominant fuel until after World War II. The next major transition came with electricity and the internal combustion engine, which enabled diversification away from coal. Oil replaced coal usage, in transport. While coal remains as the principal fuel in power generation, it is gradually being replaced first by natural gas and now by renewable.

Figure 2.4. (a) World commercial energy use (b) Contribution to total energy growth [Source: BP Statistical Review of World Energy, London, UK, 2011] The global energy consumption is projected to increase, in spite of substantial declines in energy intensity, at least two-fold by midcentury relative to the present, because of population and economic growth. Several sources indicate that there are ample fossil energy reserves, in some form or other, to supply this energy at tolerable cost. The World Energy Assessment Report estimates of the total reserves, and of global resource base including both conventional and non-conventional sources, based on 1998 consumption rates. We deliberately provide the decade old data, so as to provide a chance for us to examine with the present day trends with the projected data, and we find that the historical energy data is compatible with the projected data. Accordingly, 40-80 years

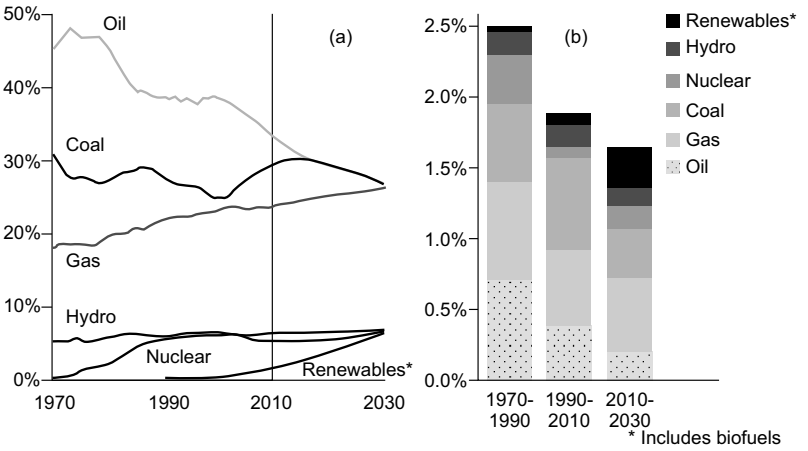

Figure 2.4 ***(a) World commercial energy use (b) Contribution to total energy growth [Source: BP Statistical Review of World Energy, London, UK, 2011].***

of proven conventional and unconventional oil reserves exist globally in our planet, and 50-150 years of oil are available if the estimated resource base is included. 60-160 years of reserves of natural gas are present, and between 207-590 years of gas resources, excluding the natural gas potentially available in the form of methane clathrates at the continental shelves, which are in the estimated resource base. A 1000-2000 years supply of coal, shales, and tar sands are in the estimated resource base. Therefore, the estimated fossil energy resources could support a 25-30 TW energy consumption rate globally for at least several centuries [1]. However, consumption of fossil energy at that rate will result in catastrophic global issues. Historical trend reveals that the mean carbon intensity i.e., the kg of C emitted to the atmosphere as CO_2 per year per W of power produced from the fuel, in the global energy mix is declining. This is because, in the past two centuries, the energy mix has shifted from being dominated by wood to coal to oil and now more to natural gas. Such a shift has produce a decrease in the average carbon intensity of the energy mix, since oil and gas have higher H/C ratios, and hence upon combustion yield more water and less CO_2 per unit of heat released than the coal. Figure 2.5, indicate that gas and renewable win in the fuel share coverage, and the energy supply mix diversifies.

It can be seen that oil continues to suffer a long run decline, while gas steadily gains in the market share. Coal's recent gains in market share due to rapid industrialization in China and India are reserved by 2030. The diversifying fuel mix can be seen most clearly in terms of contributions to growth. Over the period 1990-2010, fossil fuels contributed 83% percent of

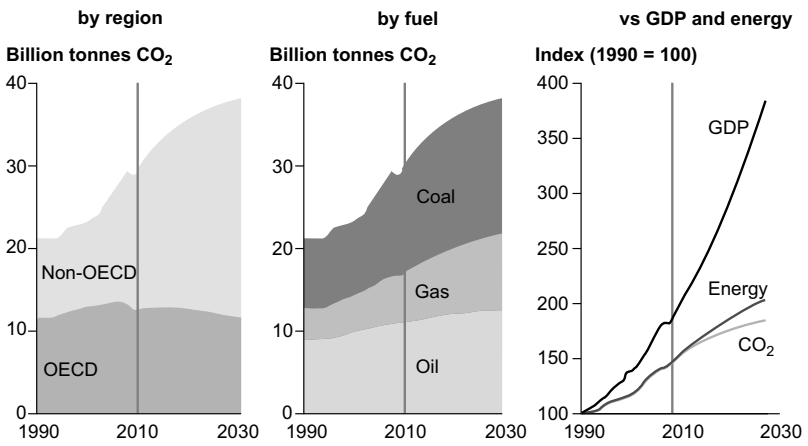

Figure 2.5 ***Shares of world primary energy and energy sources contribution to growth [Source: BP Statistical Review of World Energy, London, UK, 2011].***

the growth in energy; over the coming 20 years, fossil fuels contribute 64% of the growth. Piecing together, the contribution of all non-fossil fuels to growth the next 20 years (36%) is, for the first time, larger than that of any single fossil fuel. Renewables including biofuels account for 18% of the growth in energy to 2030. The rate at which renewables penetrate the global energy market is similar to the emergence of nuclear power in the 1970s and 1980s. For many centuries, CO_2 emissions are building up in the atmosphere. The CO_2 equilibrates on an approximately 10 to 30 years timescale between the atmosphere and the near surface layer of the ocean [2], which accounts for the reason why only 50% of the anthropogenic CO_2 emissions remain in the atmosphere, and the remainder partitioning into the biosphere and the oceans. Since there are no destruction mechanisms of CO_2 in the atmosphere, the long-term removal of CO_2 must occur by convection. The time required for the relevant mixing between the near surface ocean layer and the deep ocean is between 400 to several thousand years [2, 3]. Therefore, in the absence of geoengineering or active intervention, whatever environmental effects might be caused by the atmospheric CO_2 accumulation over the next five decades will persist globally for the next 500 to 2000 years or more. Though the precise future effects of such anthropogenic CO_2 emission are uncertain, the emission levels are viewed with caution in historical prospective. The data from Vostok ice core indicate that the atmospheric CO_2 concentration has been between 210 and 300 ppm for the 420, 000 years [4], and a later study of Dome Concordia ice cores have extended this time line to 650,000 years [5]. The CO_2 concentrations in the past five decades have been rising due to anthropogenic CO_2 emissions from fossil fuel consumption, and now they are exceeding

380 ppm. Figure 2.5 can also be considered to depict the global CO_2 emission from energy use.

Strong growth in non-OECD energy consumption, particularly of coal translates into continued growth of global CO_2 emissions. The growth of global CO_2 emissions from energy averages 1.2% per annum over the next two decades, compared to 1.9% per annum, in the years 1900-2010, leaving the emissions in 2030, 27% higher than in the present days. Even with the implementation of carbon abatement policies in the OECD, the levels of CO_2 can only be reduced to an extent of 10% in 2030. Non-OECD emissions may grow by 2.2% per annum on average, up 53% by 2030. The energy policies in non-OECD countries focus on reducing the carbon intensity of economic growth. Carbon per unit of GDP falls by 42% in 2030, and the rate of fall accelerates steadily. By 2020-30, non-OECD emissions are growing by 1.3% per annum, compared to 5.2% per annum growth over 2000-2010. Cumulatively, this trend implies some progress towards climate change goals, but enough to put the planet on a path to stabilization at 450 ppm. The only way by which we can reduce the mean carbon intensity is by adapting to carbon-free power. Three general options are available to produce such daunting amount of carbon-neutral power. Nuclear fission is one method, but it would require widespread implementation of breeder reactors. The estimated terrestrial uranium sources are sufficient to produce nearly 100 TW-per year electricity using conventional once-through uranium reactor technology. Hence, if 10 TW of power were obtained from conventional nuclear fission, the terrestrial uranium resource would be exhausted in less than a decade. Moreover, the construction of nuclear power plant would need to proceed at a very rapid rate by historical standards—1 gigawatt electric power plant every 1.6 days for the next 45 years. The international thermonuclear experimental reactor (ITER)—magnetic confinement fusion experiment is scheduled to demonstrate an energy breakdown point in 35 years, for a few minutes of operational time. Though the fusion might possibly provide a credible option to the amount of carbon-neutral energy production, the ITER time line is too far in the future to meet any reasonable atmospheric CO_2 concentration target in the next 5 decades. The second approach comprises the carbon capture and storage. In this approach, the CO_2 is dissolved in underground aquifers. To make this technology viable, the CO_2 must not leak at a globally averaged rate of 1% in a time scale for centuries. If not, the emitted flux will be greater than that intended to be mitigated initially. Realizable experiments at scale are needed, along with extensive modeling, monitoring, and validation, to ascertain $>99\%$ confidence that the leak rate will be low for 500-1000 years. Caution must be exercised to the fact that each reservoir is geologically different and hence the proof that one sequestration works technically at one may not be considered as

a general proof to the process at a global level. The global reservoir capacity has been estimated to be equivalent to 100-150 years of carbon emissions. Therefore, sequestration could buy time, if it works technically well and is so validated within the next 2-3 decades. An additional requirement is that the energy distribution and end-use chain must be transformed to handle massive quantities of carbon-free fuels such as hydrogen or electricity on the required time-scale to mitigate carbon emissions. The third approach is to employ renewable energy. Among various renewable energy sources, the largest resource is provided by the sun. If solar energy is to become a practical alternative to fossil fuels, we must have ways to convert photons into electricity, fuel and heat.

2.2 RADIATION AS A RENEWABLE SOURCE

Naturally, the sun has always held the attention of humanity and been the subject of worship by many cultures over the millennia, such as Egyptians, Incans, Greeks, Indians, and Mayans among many others. The sun provides enormous amount of energy to our planet earth, sufficient to power the great oceanic and atmospheric currents, the cycle of evaporation and condensation that brings fresh water inland and drives rivers flow, and typhoons, tornadoes and hurricanes that so easily destroy the natural and men-made landscape. Solar energy is energy force that sustains life on earth for all plants, animals and people. It offers a compelling solution to all societies to meet their needs for clean, abundant sources of energy in the future. The source of solar energy is the nuclear interactions at the core of the sun, from in where the energy originates by the conversion of hydrogen into helium. The amount of energy from sunlight strikes the earth in one hour is 4.3×10^{20} J, which is greater than all of the energy currently consumed on the planet in one year (4.1×10^{20} J). Earth's ultimate recoverable resource of oil, estimated at 3 trillion barrels, contains 1.7×10^{22} J of energy, which the sun supplies to earth in 1.5 days. The staggering power that the sun continuously delivers to earth, 1.2×10^{5} terawatts, dwarfs every other energy source, renewable or non-renewable. Sunlight is readily available, secure from geopolitical tensions, and poses no threat to our environment and our global climate systems from pollutants emissions. Although the solar energy source is inexhaustible and free, it is not the most convenient energy source because it is not constant during the day and not readily dispatched. However, there are ways to overcome these shortfalls. The vast supply of solar energy is complemented by its versatility, as depicted in Fig. 2.6. Sunlight can be converted into electricity by exciting electrons in a solar cell. It can yield chemical fuel via natural photosynthesis in green plants or artificial photosynthesis in human-engineered systems. Either concentrated or unconcentrated sunlight can produce heat for direct use or

further conversion to electricity. In general, solar energy utilization requires (a) solar energy capture and conversion and (b) storage.

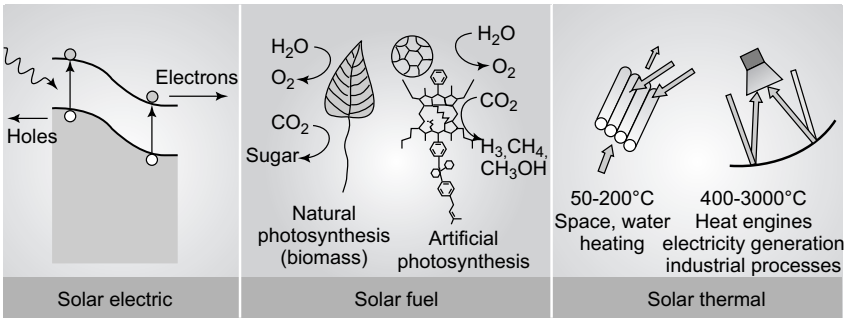

Figure 2.6 ***Solar photons convert naturally into three forms of energy electricity, chemical fuel, and heat [6].***

Solar energy capture and conversion can be accomplished by photovoltaics (PV). The challenge here is to dramatically lowering the cost per W of delivered solar electricity. Solar cells capture photons by exciting electrons across the bandgap of a semiconductor, which creates electron-hole pair that are then charge separated, by typical p-n junctions introduced by doping. The space charge at the p-n junction interface drives electrons in one direction and holes in the other, which results in a potential difference equal to the band at the external electrodes gap as shown in the first picture in Fig. 2.6. The principle and device are similar to a semiconductor diode, except that electrons and holes are introduced into the junction by photon excitation and are removed at the electrodes. Compared to fossil sources, solar energy is diffuse, and therefore material cost must be inexpensive to realize a solar-based power source. In the absence of cost-effective storage, solar electricity can never be a primary energy source, because of diurnal variation in local insolation. In principle, storage in a battery is possible, but at present no battery is inexpensive enough, when amortized over the 30 year lifetime of a solar device, to satisfy the needed cost per W targets for the whole system. A second option is to store the electrical energy mechanically. For example, electricity could be used to drive turbines to pump water uphill. This method is relatively cheaper for storing large quantity of energy at modest charge and discharge rates, but is not well suited to being charged and discharged every 24 hours to compensate for the diurnal cycle. For instance, buffering a day/night cycle in the US energy demand by this route would require a pumping capacity equivalent to >5, 000 Hover dams, filling and emptying reservoirs every 24 hours. Presently, the cheapest method of solar energy capture, conversion and storage is solar thermal technology, which costs about \$0.10–0.15 per kW-hr for electricity production. Advancement in this important technology will require new

materials for the harvesting, as well as advancements in thermochemical cycles for solar energy. A third approach for storage is to mimic the design of nature, in which chemical bonds are cleaved and formed to produce solar fuels in an artificial photosynthesis process. Natural photosynthesis itself is inefficient, when scaled on a yearly average basis per unit area of insolation. For instance, one of the fastest growing crops, switch-grass yields energy stored in a biomass at a yearly averaged rate of $1\ Wm^{-2}$ [1]. Whereas the biofuels derived from existing plants could provide a notable contribution to liquid fuels for transportation. One viable proposition is to develop artificial photosynthetic process with an average efficiency significantly higher than plants or algae. The primary steps in photosynthesis involve the conversion of sunlight into a wireless current. In all cases, to form a useful fuel, O_2 must evolve and it can be released into our oxygen-rich atmosphere, and used elsewhere as an oxidizing agent for fuel consumption. The reduced fuel could either be hydrogen from water reduction, or it could be an organic species, such as methane or methanol, which is derived from the fixation of atmospheric CO_2. Recombination of the reduced fuel with the released O_2 would then regenerate the original species, completing the cycle in a carbon-neutral fashion. In natural photosynthesis, the anodic charge of the wireless current is used at the oxygen-evolving complex to oxidize water to oxygen with the concomitant release of four protons. The cathodic charge of the wireless current is captured by photosystem to reduce the protons to hydrogen, with the reduced hydrogen equivalents stored through the conversion of NADP to NADPH. Thereby, the overall primary events of photosynthesis store sunlight through the rearrangement of the chemical bonds of water, to form oxygen and nature's form of hydrogen. In essence, the sun has a unique role in sustainable energy production, as it is an undisputed champion of energy. From the materials points of view, chemistry will assume a prime role for solar energy capture, conversion and storage, because new catalysts are required for the desired chemical bond conversions.

2.3 SCOPE OF PHOTOELECTROCHEMITRY (PEC)

A number of authors have provided definitions for photoelectrochemistry (PEC). Kuwana [7] defined it as follows:

(a) Introduction of photo-excitation into the electrochemical system.
(b) Creation of the excited state through the electrochemical process.

Kenichi Honda [8] defined as: (a) Reaction at the electrode in excited state: (i) Excitation of the electrode (metal or semiconductor); (ii) Excitation of substances (adsorbed molecules, etc.,) at the interface between the electrode and solution; (iii) Excitation of reactive species in a solution. (b) Generation of electronically excited state by electrode reaction: (c) Combination

of photochemical and electrode reactions; (d) Alternate generation of photochemical and electrode reaction: In this section, we set to discuss on introduction of photo-excitation into the electrochemical system' as described above. We classify our discussion based on the following three perspectives according to the region at which the electronically excited state is formed during the photo-irradiation in the electrochemical system. The light irradiation mode can be: (1) electrode (e.g., photocatalysis, water decomposition); (2) interfacial layer (e.g., dye sensitization); (3) bulk solution (e.g., photogalvanic cell). Figure 2.7, is a schematic sketch of these three modes.

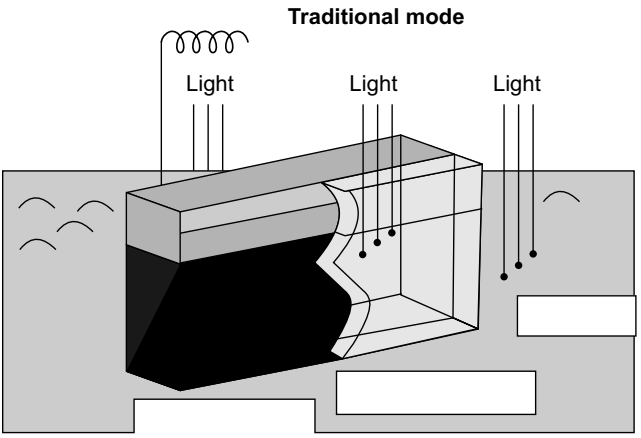

Figure 2.7 *Irradiation mode of the electrochemical system [9].*

2.3.1 Historical Sketch

Becquerl Effect The French scientist Edmond Becquerel immersed two different metal electrodes such as platinum, gold, silver, brass and silver coated with silver halogenide on the surface into the acidic, neutral and alkaline electrolyte solutions. By exposing one of the electrodes to sunlight, he found that electric current flows through the external circuit between two electrodes. The current was very small, as the pointer in the galvanometr moved only to several degrees. At the age of 18, Becquerel reported this effect at Academy in Paris in 1839 [10]. His study was considered as the first paper in photoelectrochemistry, and this phenomenon is named as Becquerel effect. Figure 2.8, illustrates Becquerel experiment. This invention, opened up a new branch namely photoelectrochemistry in the field of electrochemistry. The era of 1950s, witnessed a tremendous escalation in the research activities of semiconductor materials, in both electrochemistry and photoelectochemistry fields in the aspects of fundamental and applied research.

Although photoelectrochemistry continued to draw attention in 1950s through 1960s, no attempts were to reexamine Becquerel's research in

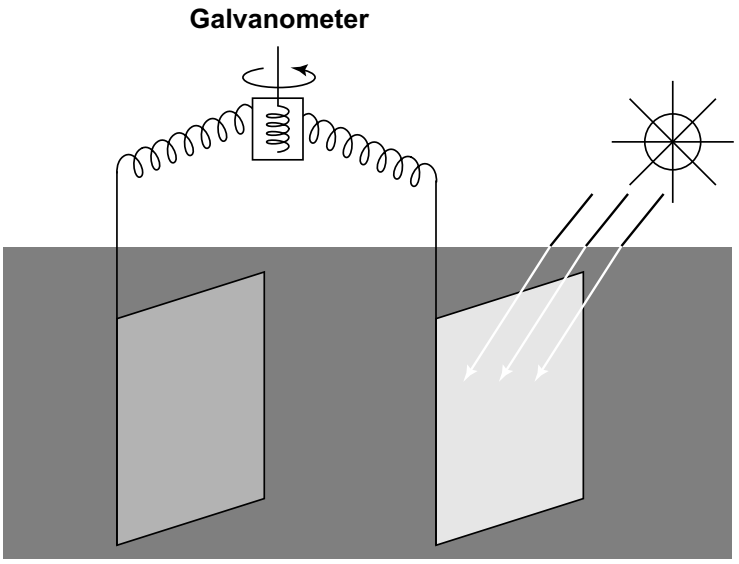

Figure 2.8 *Diagrammatic representation of Becquerel's experiment (1839) [9].*

quantitative perspective. In 1966, Honda carried out research by immersing two smooth platinum sheet electrodes in sulfuric acid solution, irradiating one of the electrodes with high pressure mercury lamp, and measured the photovoltaic effect, as shown in Fig. 2.9 [11]. Simply by tuning the light on and off, the photovoltaic changes of several 10 mV were found.

Excitation of the Solution The dawn of the twentieth century witnessed a spurt of research activities on photoelectrochemical and electrochemical studies, by irradiating the electrolyte solution as depicted in Fig. 2.7, and such phenomenon is named as Swensson-Becquerel effect. This is an example of photogalvanic system, involving photochemistry and electrochemistry in subsequent steps as follows.

Photochemistry: $A^* + D \rightarrow (h\nu)\ A + D +$ First cell
Electrochemistry: $A \rightarrow A + e$
Ground state electrochemistry: $D^+ + e \rightarrow D$ Second cell

In these systems, the products of the photochemical reaction in the first cell return to their initial states via the conventional reverse electrochemical reactions in the first and the second cells, generating current. This system stands for the conversion of light energy to electrical energy. The study of

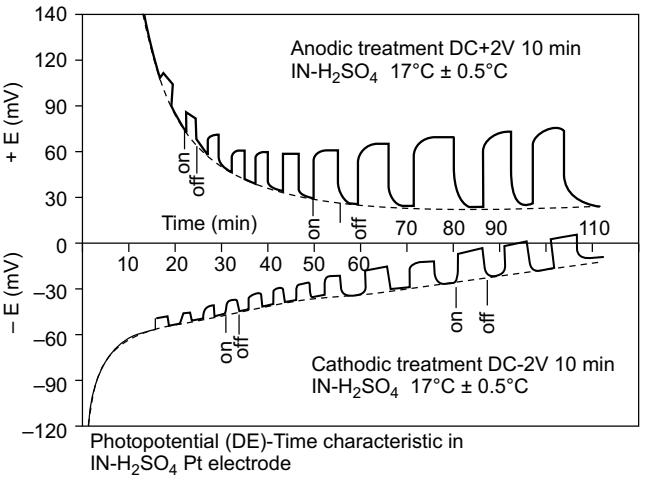

Figure 2.9 ***Effect of light irradiation at platinum electrode [11].***

Rabinowitch using thionine and Fe^{2+} is well known [12]. In order to realize a practical application, the reactants are to be completely recycled for harvesting light energy. Examples of this kind include the studies of Goldmann [13], Baur [14], Iimori [15], Rabinowitch [16] and Eisenberg and Silvermann [17].

Excitation of Electrode Both metal and semiconductor electrodes are generally employed, and the following diagram (Fig. 2.10) depicts the photo-process in these two types of electrodes.

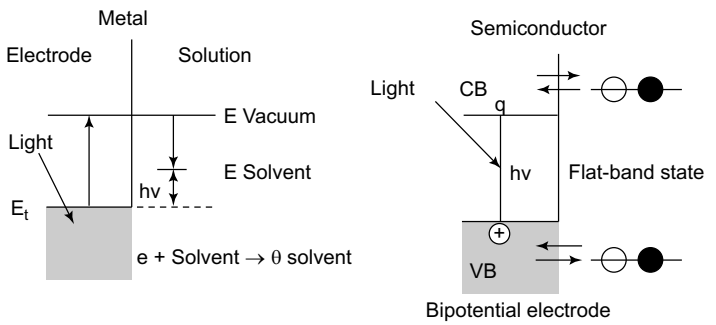

Figure 2.10 ***Excitation of electrode [9].***

The discharge of photoelectrons from metal is a known physical phenomenon. In 1960s, especially in the field of polarography with droping mercury electrodes, generation of photocurrent through light irradiation on electrodes in immersed in electrolyte solution started to appear. Though several theories on the mechanism are proposed, it is understood through experiments

in the present days that the difference between the work function E_f of the metal electrode and the salvation energy of the electrode E_{sol} corresponds to the photoenergy required to generate photocurrent. Examples of this kind, where metal electrodes are employed, include the studies of Berg et al., [18], Heyrovsky [19], and Brodsky and Pleskov [20] in the years 1967, 1963 and 1972 respectively.

With the advancement of knowledge of semiconductor properties, semiconductors are widely employed as electrodes in electrochemistry. Photoconduction is a notable property of semiconductors. Brattain and Garrett [21], the Nobel Prize winner of the year 1955, reported the photoreaction properties of germanium electrode, and their work is considered to be a milestone on semiconductor photoelectrochemistry and for the dawn of progress in this field. Figure 2.11 shows the photo-response characteristics with typical current-potential trace of n-Ge in their report.

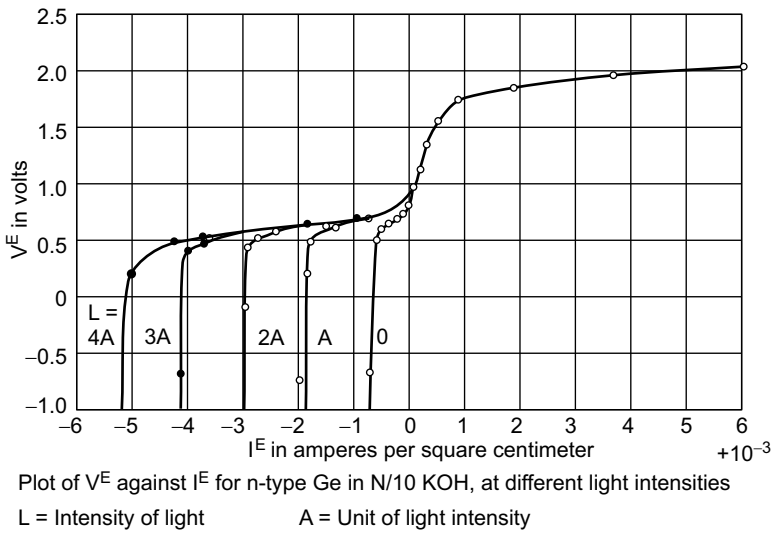

Figure 2.11 ***Current (I) vs Potential (V) curve of n-Ge as a function of Intensity of Light [21].***

During negative polarization, typical rectification can be found in the dark, though the current is increasing in proportion to irradiated light intensity, L. As shown in Fig. 2.10 for the semiconductor electrodes, electrons in the conduction band and holes in the valence band generated by light absorption cause charge transfer through the interface of the chemical species in the solution at different potential levels corresponding to the band width. Research activities on the theories and dynamics of semiconductor photoelectrode reactions are continue to emerge till date and numerous reports are available.

Emergence of TiO_2 After the prominent research by Brattain et al., [21], the focus of monocyrstalline semiconductor research in 1960s has been shifted to single crystals in the field of photoelectrochemistry, as single crystals are indispensible from scientific standpoint. Here we list such semiconductor materials in a chronological order in terms of their period of study.

Semiconductor Material	*Year of Study*
N-Ge	1955
n-Si	1958
n-CdS	1960
N-, p-GaAs	1965
n-ZnO	1966
p-NiO	1966
n-Znse	1967
n-,p-GaP	1968
n-Sno_2	1968
n-$KTaO_3$	1968

Semiconductor materials other than Ge and Si include oxide semiconductors, chalcogenide semiconductors, III-V group semiconductor among others. Mostly they are of n-type, while few of them belong to p-type. As indicated in his article [9], Honda employed single crystals of Ge, Si, CdS, ZnO etc., for his research. In spite of their importance, single crystals are often expensive and difficult to obtain. For an n-type semiconductor, as shown in Fig. 2.11, the anode photocurrent is proportional to the intensity of the light. For oxide semiconductors ($M^{2+}O^{2-}$), such a reaction can be represented as follows.

$$MO + 2h \rightarrow MO + 2e^- + 2p^+ \text{ (Step 1)}$$
$$MO + 2p^+ \rightarrow M^{2+} + 1/2\ O_2$$
$$\text{Or} \quad MO + 2p^+ + Red \rightarrow M^{2+} + 1/2\ O_2 + Oxi \text{ (Step 2)}$$

Step 1, indicates the dissolution reaction (etching) of the semiconductor itself. Step 2 indicates the oxidation reaction of the reductant, Red, in the electrolytic solution to Oxi induced by photo-generated holes in the electrode. This reaction represents the evolution of oxygen when water molecules become the donor. The reactions are competitive when both steps occur simultaneously. In this case, the etching of the electrode is inevitable. In the year 1969, at University of Tokyo, in the lab next to Honda's coincidently, the experiments on electrophotography using TiO_2 as the photoreceptor has been carried out. Fujishima, a co-researcher of Honda, obtained TiO_2 by following the suggestion of Prof. Iida, and used it as a photoelectrode and found that only oxidation reaction of the chemical species takes place in the solution without

any etching of the electrode [22]. Then using platinum as the counter electrode, in 1972, Fujishima and Honda [23] constructed a cell as shown in Fig. 2.12, irradiated the light from a high pressure mercury lamp on the TiO_2, and found that oxygen is generated on TiO_2 by the decomposition of water due to anode reaction, and hydrogen is generated by cathode reaction of the Pt electrode. At the same time, electrons flow in the arrow direction through the external circuit, achieving electrochemical photolysis of water.

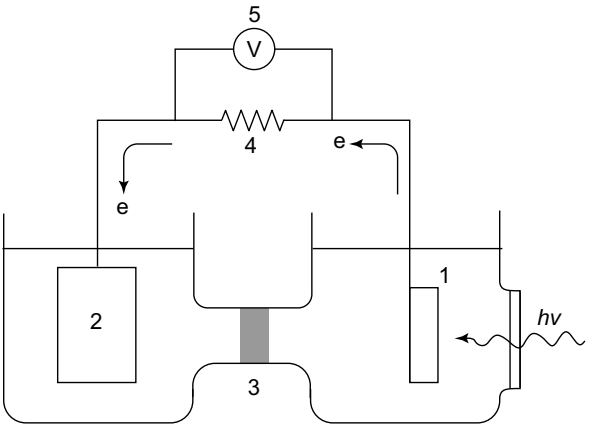

Electrochemical cell in which the TiO_2 electrode is connected with a platinum electrode. The surface area of the platinum black electrode used was approximately 30 cm^2

Figure 2.12 ***Cell for the decomposition of water with TiO2 Photoanode [23] A similar figure is also given in chapter 1.***

Though this study was carried out from a purely academic perspective of photoelectrochemistry, as it was a coincident with the Oil Shock in 1973, it drew prominent attention of the world and considered as a doorway to the use of solar energy. It was also greatly anticipated as a means of producing hydrogen fuel. As the cost of the single crystal of TiO_2 used in this research was expensive than diamond, for practical application inexpensive materials are indispensable. In an attempt to reduce the cost, Honda et al., [24] tried to form TiO_2, as oxide film on the surface by heating titanium metal available in the market using a heating burner. Water decomposition experiments by sunlight outdoors were made using this as a large photoanode for the first time. The results indicated that hydrogen can be generated by natural light without supplying any external energy. The view of TiO_2 photoanode formed by Ti plate and used at that time is shown in Fig. 2.13.

In this fashion, the outstanding characteristic of TiO_2 as a photoelectrode has been attributed to its strong oxidizing power. For comparison, in Fig. 2.14, we show a graphical representation of the positions of conduction band (CB)

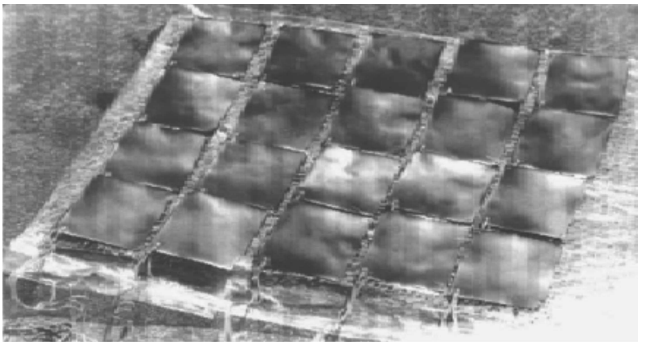

Figure 2.13 *View of TiO2 photoanode formed by heating Ti plate [9].*

and valence band (VB) of the generally used n-type semiconductors. Lower portion of the valence band is equivalent in representing to greater oxidation ability. It shows that TiO_2 exhibits the lowest point among others. Since the report on TiO_2, several reports emerge using new semiconductor materials, hybrid semiconductors, doped systems etc., and for details one can refer to the respective literature.

Dye Sensitization of Photoelectrochemical Process Always, photoelectrochemical process takes place after semiconductor electrodes absorb light with the wavelength of the intrinsic absorption band. Most semiconductors absorb a part of sunlight spectrum. For effective utilization of sunlight, the working wavelength band of the photoelectrode reaction has to be expanded. By 1873, Vogel [25] already discovered dye sensitization employing silver halide photosensitive material. Since then, voluminous

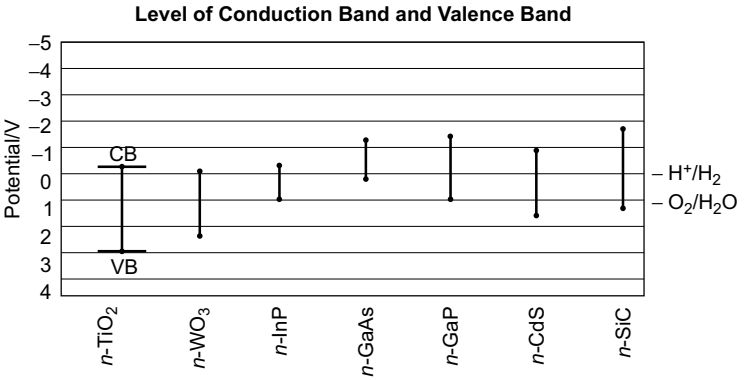

Figure 2.14 *Levels of conduction band (CB) and valence band (VB) of n-type semiconductor electrodes [9].*

knowledge on dye sensitization has been evolved. Becquerel was truly captivated by this study, and carried out immense research in photographitic and photoelectrochemistry fields, and reported his notable research on photosensitization by chlorophyll [26]. Studies on dye sensitization in the arena of photoelectrochemistry dated back to the end of 19th century for metal electrodes. Since 1960, the year in which semiconductor electrodes made their emergence systematic studies were carried out in this direction. As a historical sketch, Fig. 2.15 shows the sensitization curve by methyl violet and malachite green of copper oxide electrode [27], from the studies of Audubert in 1931. The extent of sensitization is represented by the photopotential. Realization of sensitization in longer wavelength can be seen. Remarkably, Audubert predicted in his article [27], that electrochemical photolysis of water would be realized in the future. Major studies on dye sensitization carried out using semiconductors between 1960s and 1970s are listed in chronological order as follows: ZnO [28, 29], GaP, GaAs, Cu_2O [30], p-GaP [31], TiO_2 [32], and CdS [33, 34], in the years 1968, 1969, 1971, and 1974, 1975 respectively. The dyes employed for the dye sensitizations are of general category such as xanthane. It has been indicated that most of the dyes used in these earlier studies were not satisfactory in terms of sensitization efficiency and durability. In 1991, Gratzel and his team [35] reported that the ruthenium bipyridyl complex exhibited high sensitization efficiency and durability. Subsequently, research solar cells using dye as a sensitizer has been ever expanding. In an exclusive chapter on dye sensitization in this book, we set to discuss the later advancements in detail.

2.3.2 Configurations of Photoelectrochemical Cells (PEC)

Photoelectrochemical cells convert light energy into a useful product via photo-induced chemical reactions. The product is usually electrical energy, but can also be useful chemicals such as hydrogen and oxygen, or even the degradation of hazardous wastes into harmless chemicals. A photoelectrochemical cell is defined as a cell in which the irradiation of an electrode in contact with an appropriate electrolyte produces a change in the electrode potential with respect to a reference electrode (under open circuit conditions) or produces a change in the current flowing in the galvanic cell containing the electrode (under closed-circuit conditions).

Wet photovoltaic (WPV) cells (liquid junction solar cells) These cells are composed of a semiconductor photoelectrode, either n-or p-type, a solution of a redox couple appropriate to the photoelectrode, and a counter electrode, usually kept in dark, which is reversible to the same redox couple. The cell generates electric power when the semiconductor photoelectrode is illuminated and there is ideally no net chemical change since the same reaction occurs in

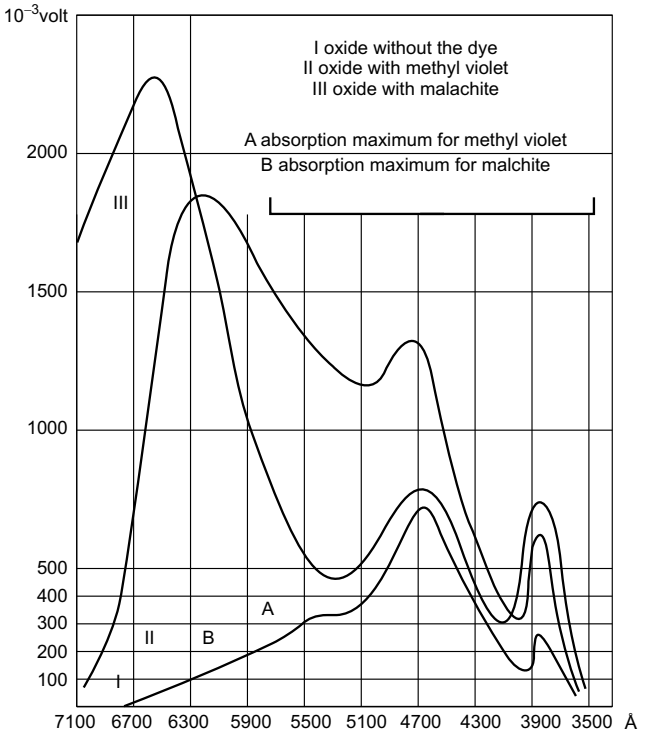

Figure 2.15 ***Review of the photoelectrochemical dye sensitization work by Audubert[27].***

opposite directions at the two electrodes. The principles of this type of cell are depicted in Fig. 2.16.

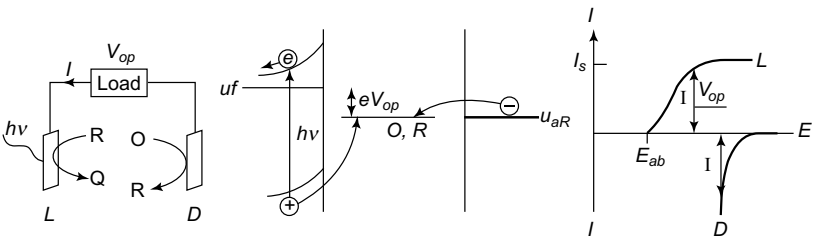

Figure 2.16 ***Basis for function of a WPV cell depicting electrode reactions, band diagram and I/E curves, for n- type photocathode (L), redox couple (O, R), reversible dark electrode (D) and output voltage (V_{op})[36].***

The open circuit voltage (V_{op}) of these cells depends on the energy difference between the Fermi level in the solution and the flat-band potential, and for the efficiency should exceed 0.5 V. The current I_s is generated from the electron-hole pairs photogenerated in the seminconductor reduced by

recombination, concentration polarization at the dark electrode and other loss mechanisms. If the WPV cell is to operate in sunlight, the semiconductor has to be an efficient absorber of sunlight, with a band gap around 1.5 eV. Table 2.1 summarizes the major results obtained in 1980s for WPV cells. The power conversion efficiency of some cells, were up to 15% in full sunlight, which is equivalent to that of commercially available silicon PV cells, but around half the best efficiency was realized in the laboratory for advanced solid state devices the same area in that era. Large area photoanodes of polycrystalline cadmium chalcogenides, prepared by using vacuum evaporation, electrodeposition or screen printing showed good results with power conversion efficiencies of about half to two-thirds of the efficiency exhibited by single crystal device.

Table 2.1 ***Major developments in WPV cells in 1980s.***

Photoanode/Redox Couple	*Efficiency%*	*Reference*
n-CdSe/Se|$Fe(CN)_6{}^{3-}$/$Fe(CN)_6{}^{4-}$	12-14	37, 38
n-$CdSe_{0.65}Te_{0.35}$|Sn^{2-}/S^{2-}	12.7	39
n-WSe_2|$I_3{}^-$/I^-	10-13	40
	13.3	41
n-$CuInSe_2$|$I_3{}^-$/I^-	12	42
n-$CuInSe_2$| $I_3{}^-$ /I^- (Cu^+ , HI)	12.2	43
p-InP| V^{3+} / V^{2+}	12	44
n-GaAs| $Se_2{}^{2-}$ / $Se_2{}^{2-}$	13	45
n-GaAs (Os^{3+})| $Se_2{}^{2-}$/$Se_2{}^{2-}$	15	46
n-$GaAs_{0.6}P_{0.4}$ — $Te_2{}^{2-}$ / $Te_2{}^{2-}$	18 (458 nm)	47
n-Si / Ti_2O_3 — Fe $(CN)_6{}^{3-}$ / Fe $(CN)_6{}^{4-}$	14	48
n-Si / Li-MgO / Pt — Br_2 / Br^-	13	49
n-Si / MgO / Pt — Br_2 / Br^-	11	49
n-$GaAs_{0.72}P_{0.28}$ | Fe^+ /Fe in CH_3CN (Fe = Ferrocene)	13	45

Fuel Producing Cells Fuel producing cells are the most common category of photoelectrochemical cells using semiconductor electrodes. They covert the cheap, readily available material such as water into useful high energy fuel such as hydrogen. This class of cell can be classified into three basic types.

Photoelectrolysis Cells (PE Cells) This type of cell is operated in a short circuit mode under light irradiation to produce maximum flux of fuel but no electric power. Both electrodes are immersed in the same electrolytic solution at constant pH. The principle of this type of cell is shown in Fig. 2.17, for the water-splitting n-$SrTiO_3$/ 1M NaOH/Pt cell.

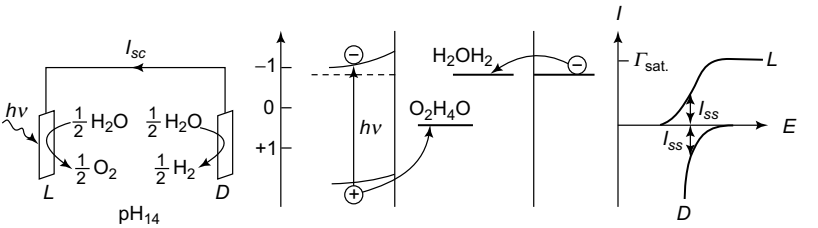

Figure 2.17 ***Basis for operation at the short-circuit current I_{sc} of an unbiased PE Cell for water splitting showing electrode reactions, band diagram and I/E curves [36].***

Photo-assisted Electrolysis Cells (PAE Cells) The cells operate under irradiation plus an assisting bias, which serves either to drive electrolytic reactions for which the photon energy is insufficient or to increase the rate of fuel production by reducing the recombination rate of electrons and holes in the bulk semiconductor through the reduced band-bending. **(a) Chemically biased PAE Cells:** Chemical bias is obtained by using different electrolytes in two half cells, with the electrolytes being chosen to reduce the voltage required to cause the chemical splitting. For example, the use of 1 M NaOH and 0.5 M H_2SO_4 as electrolytes in the half cells of Fujishima and Honda [23] yields a pH difference of 14 and reduces the minimum photovoltage required for decomposition of water from 1.23 V to about 0.4 V. Production of hydrogen, of course, draws work from both the incident radiation and the electrolytes causing the acidic and alkaline pH values to converge. The operational principles of such cells are shown in Fig. 2.18.

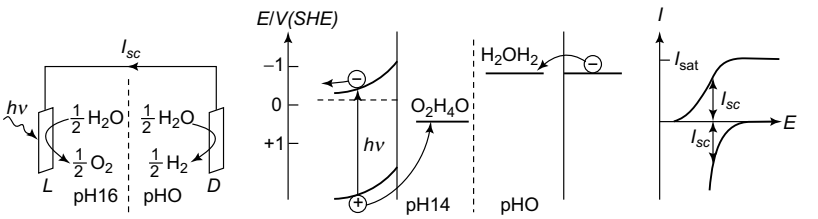

Figure 2.18 ***Basis for operation of pH-based PAE cell for water splitting showing electrode reactions, band diagram and I/E curves [36].***

(b) Electrically biased PAE Cells: The electrical energy input required for a given fuel output is reduced by the contribution of the incident radiation. If the cell is to have the capability of storing solar radiation in the form of the fuel produced, then the operating voltage under irradiation must be smaller than that in dark. An example of the principles of this type of cell is shown in Fig. 2.19.

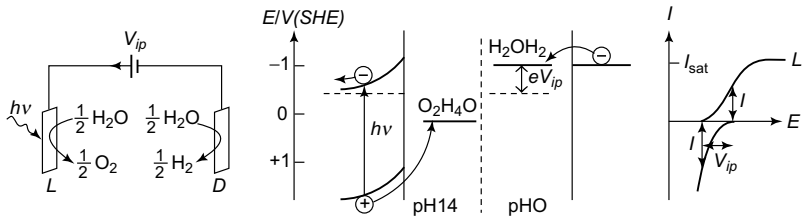

Figure 2.19 ***Electrically-biased PAE cell for water splitting showing electrode reactions, band diagram, I/E curves for assisting input voltage V_{ip} [36].***

Photovoltaic electrolysis cells (PVE Cells) These devices produce both fuel and electrical power via a low energy electrolytic reaction, as shown in Fig. 2.20 for splitting of hydrogen iodide. The definition of the efficiency of the fuel producing cells, which have multiple input powers of different kinds, requires careful consideration.

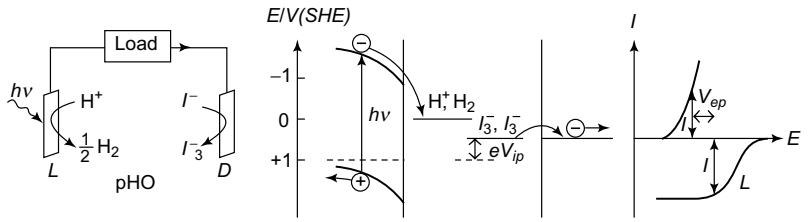

Figure 2.20 ***Basis for a operation of a PVE cell for water splitting showing electrode reactions, band diagram, I/E curves for assisting output voltage V_{op} [36].***

A detailed discussion is offered by Archer and Bolton [36], and their definitions are shown here. They showed that the Gibbs energy storage efficiency is the most appropriate figure-of-merit for all three types of fuel producing cell, where η_g = [E_{cell} - V']I / E_0 where, V' = 0 for PE Cells, V_{ip} for electrically biased cells, and V_{op} for PVE cells; I = photocurrent density; E_0 = irradiance; E_{cell} = e m f of cell reaction. Some of the major achievements in improving the efficiencies of fuel producing cells in 1980 s are given in Table 2.2.

Photoelectrochemical storage cells (PES Cells) PES cells can be viewed as secondary batteries which are recharged by the light absorption. The absorption of light energy in one part of the PES cell produces photoreaction products which are stored and/or reacted in a different part of the cell, in the dark, to produce electricity, and regenerate the original state. PES cells may have just the photoelectrode and the storage electrode, but then both must operate in reverse during the discharge cycle. The cell efficiency can be improved by the addition of one or more auxiliary electrodes. In a three-electrode cell,

Table 2.2 ***Major advances in fuel-producing cells during 1980s.***

Cell Structure	*Efficiency (%)*	*Ref.*
Splitting of water PE Cells		
n, p-GaAs(RuO_2) | 5M H_2SO_4 | (Pt) n, p-GaAs	7.8	50
Pt | 0.5 M H_2SO_4 | p-BP	8	51
PAE Cells		
n-$BaTiO_3$ | 1M NaOH | Pt	3	52
Splitting of hydrogen halides PE Cells		
n-$MoSe_2$ | HBr, $NaClO_4$ | (Pt) p-InP	8 (633 nm)	53
n-Si / p-Si (Ir)| HBr, HBr | (Pt) n-Si /p-Si	8	54
n-Si / p-Si (Pt)| HI, HBr | Pt	8	55
N, p-GaAs (Ti / RuO_2)| HCl, NaCl | (Pt) n, p-GaAs	8	50
PAE Cells		
Pt (RuO_2)| HCl, KCl | (Ru) p-InP	12	56
n-$MoSe_2$ | HBr, $NaClO_4$ |(Pt) p-InP	11	53
PAE Cells		
p-InP (Ru) | HI, $NaClO_4$ | n-$MoSe_2$	7 (514 nm)	53

the auxiliary is chosen to be efficient to the reverse of the photoreaction. In a four-electrode cell, the reverse of the photoreaction occurs through the auxiliary electrodes and these may be placed in a separate cell. An example of a three-electrode device is shown in Fig. 2.21. This PES cell, devised by Licht et al., [57], was the most efficient PES of 1980s, and generated constant current to the load by careful choice of electrode areas. Two half-cells of a PES cells are normally separated by a semi-permeable membrane, as shown by dotted lines in Fig. 2.21. The storage and auxiliary electrodes should be non-polarizing, but otherwise, their form and material is not critical. The notable works on PES cells in 1980s are listed in Table 2.3. More than 10% photo efficiencies were realizable, as compared to the overall efficiencies of crystalline silicon PV molecules of 14% feeding secondary batteries of 70% power efficiency. One of the most exciting developments in PES technology in the late 1970s was the Texas Instruments device. This was a closed loop system in which microspheres of semiconductor silicon solar cells were embedded in a glass matrix that were used to electrolyze aqueous solutions of hydrogen bromide. The reaction products, hydrogen and tribromide in a fuel cell produced electricity and regenerated the hydrogen bromide solution. Both charge and discharge cycles operated near the reversible potential and the operational efficiency for splitting of hydrogen bromide was 8.6%. Though this was technically successful, the long-term reliability and cost-effectiveness

of this system is unable to match with those of conventional PV modules plus storage battery, and the development was discontinued in 1983.

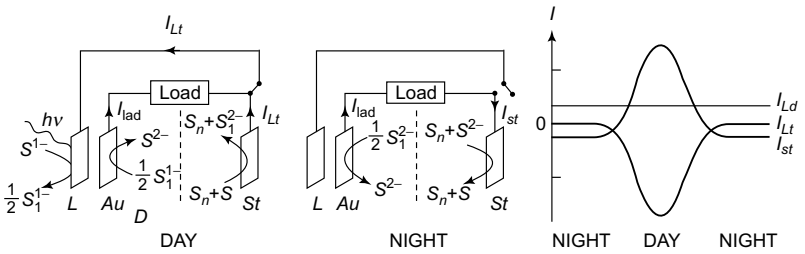

Figure 2.21 ***Basis for operation of a PES cell, as designed by Licht et al [57]. The constant load current is ensured by choice of electrode areas. Electrode reaction and positive current directions are shown for day- and night-time operation. L = 0.08 cm^2 , n-CdSe$_{0.65}$Te$_{0.35}$; Au = 3 cm^2; CoS, St = 3 cm^2 Sn, SnS [36].***

Table 2.3 ***Major developments in PES devices during 1980s.***

Materials	*Efficiency (%)*	*Ref.*
Single crystal photoelectrodes		
n-$CdSe_{0.65}Te_{0.35}$ | Cs_2S_4, CsSH, CsOH		
CsHS, CsOH | SnS, Sn CoS | *	11.3	57
p-WSe_2 | AQ, AQH_2, H_2SO_4 I_2,		
KI, Na_2SO_4, H_2SO_4 | Pt AQ = anthraquinone	10 (633 nm)	58
n-WSe_2 or n-MoS | KI, Na_2S_4O , H_2SO_4		
AQ, H_2SO_4 | C	10 (633 nm)	58
n-GaP | $K_3Fe(CN)_6$, K_4 Fe $(CN)_6$		
$NiSO_4$ | Ni	1.9	59
Polycrystalline photoelectrodes		
n-CdSe | S, Na_2S, NaOH Na_2		
Zn $(OH)_4$, NaOH | Zn Ni |*	3	60
n-CdSe, Se | $CdSO_4$ | p-CdTe, Cd	10^{-7}	61

*The discharge electrode is shown on the left, under the charge electrode, with the auxiliary electrode on the right. The line represents semi permeable membrane that separates two half cells.

In summary, photoelectrochemical reactions between the electrode materials and the electrolyte are rarely completely reversible and side reactions can occur with dissolution of the electrodes. PE cells are thus liable to degrade over periods of time, ranging from minutes to years, depending on the materials of choice, their form and the energy densities involved.

2.4 A COMPARISON: PHOTOSYNTHESIS, PHOTOVOLTAICS, PHOTOELECTROCHEMISTRY

There are at present, three known methods of converting light into energy sources. Among these three the first one is the remarkable nature's path namely Photosynthesis. Probably this may be the most preferred pathway by which nature provides energy sources for living beings on earth. The total solar energy reaching the earth surface per year is approximately $3850{,}000 \times 10^{18}$ joules. Possibly the energy utilized in photosynthesis can account for about 3000×10^{18} joules. Thus, it can be seen that only a tiny fraction of the total solar energy is harnessed by the plants, but still this level of energy storage is sufficient to support living systems on earth. It is clear that energy conversion by photosynthesis appears to be a possible means of providing the energy requirements of earth. There are two alternate methods of energy conversion that have been proposed and are being developed for increasing the efficiency of the processes. One of them is termed as Photovoltaics in the last 3-4 decades. A photovoltaic cell consists of two different types of solids connected at an abrupt but defined junction. This type of cell promotes the current flow in only one direction in the external circuit and thus produces electrical power. Unlike the photosynthesis, wherein solar energy is utilized to produce fuel, photovoltaics produce electricity directly. This brings us to the concept of electron versus fuel for energy conversion. There are some distinct advantages of Photovoltaics, like the device can be compact in nature and net efficiencies achievable even today is nearly the Carnot efficiency and are durable and can last nearly 20 or more years. The third possibility is the Photo-electrochemical cells. The main component of the phtoto-electrochemical cells is the photoactive electrode which is usually a semiconductor. Metals are not very effective in this operation since the energy levels are continuous (between occupied and unoccupied states) and hence excitation in these systems will lead to fast recombination and hence the net free energy change cannot be harnessed. For conventional redox reactions, one is interested in either reduction or oxidation of a substrate. For example consider that one were interested in the oxidation of Fe^{2+} ions to Fe^{3+} ions then the oxidizing agent that can carry out this oxidation is chosen from the relative potentials of the oxidizing agent with respect to the redox potential of Fe^{2+}/Fe^{3+} redox couple. The oxidizing agent chosen should have more positive potential with respect to Fe^{2+}/Fe^{3+} couple so as to affect the oxidation, while the oxidizing agent undergoes reduction spontaneously. This situation throws open a number of possible oxidizing agents from which one of them can be easily chosen. However, in the case of water splitting one has to carry out both the redox reactions simultaneously namely, the reduction of hydrogen ions ($2H^+ + 2e^- \rightarrow H_2$) as well as ($2OH^- + 2H^+$

$\rightarrow H_2O + 1/2O_2$) oxygen evolution from the hydroxyl ions. The system that can promote both these reactions simultaneously is essential. Since in the case of metals the top of the valence band (measure of the oxidizing power) and bottom of the conduction band (measure of the reducing power) are almost identical they cannot be expected to promote a pair redox reactions separated by a potential of nearly 1.23 V. Another aspect is that metals liberate hydrogen preferentially and if these semiconductors can be designed to have enhanced metallic/reducing properties it may be advantageous. But this aspect is not considered in this presentation. Therefore one has to resort to systems where the top of the valence band and bottom of the conduction band are separated at least by 1.23 V in addition to the condition that the potential corresponding to the bottom of the conduction band has to be more negative with respect to $2H^+ + 2e^- \rightarrow H_2$ while the potential of the top of the valence band has to be more positive to the oxidation potential of the reaction $2OH^- + 2H^+ \rightarrow H_2O + 1/2\ O_2$. This situation is obtainable with semiconductors as well as in insulators. However insulators are not appropriate due to the high value of the band gap which demands high energy photons to create the appropriate excitons for promoting both the reactions. The available photon sources for this energy gap are expensive and again require energy intensive methods. Hence insulators cannot be employed for the purpose of water splitting reaction. Therefore, it is clear that semiconductors are alone suitable materials for the promotion of water splitting reaction. In the operation mode, the semiconductor electrode-electrolyte interface is the key factor and a complete understanding of this interface alone can lead to a successful development of highly efficient photo-electrochemical cells. In some sense, photo-electrochemical cells can be considered as a notional hybrid of photo-synthesis and photo-voltaics since these cells can generate either or both electricity and fuel. However, the development of Photo-electrochemical cells with the desired efficiency appears to be one of the major issues calling the attention of the developers. It is better to comment further between the similarities and also differences between PEC and Photosynthesis and Photovoltaics. Photosynthesis appears to provide remarkable efficiencies due to various factors. The essential points of relevance are (i) The absorption of the photon takes place in the chlorophyll dimmer or the special pair' facilitated by the antenna and chlorophyll pigment. (ii) The excited electron- electron vacancy (hole) pair could normally undergo de-excitation thus releasing the optical energy as heat without producing fuel or electricity. However, in the photo-synthetic reaction centre the separation of the excited electron from its vacancy is achieved by the presence of a series of electron acceptors that are not only strategically located in the protein but could also adjust their redox potentials like in an escalator thus positioning the acceptor states

suitable for harnessing the energy. (iii) In addition, the presence of a series of electron acceptors make the electron to move from one species to another thus spatially separating the electron hole farther away thus restricting the thermodynamically feasible recombination of the excited electron and hole thus bringing in a kinetic control. This alone facilitates the use of the excited electron to perform the chemical reactions in photosynthesis and is responsible for fuel production. In the case of Photovoltaics, the free energy gradient caused by the potential energy gradient present at the junction of the two solids is the cause for the flow of electrons or electricity. In the case of photoelectrochemical cells also the driving force is the electrical field gradient that is available at the semiconductor/electrolyte interface and also the interaction of the photon field in the semiconductor adds cumulatively for this field gradient which is responsible for the vectorial transfer of electrons and also for driving the chemical reaction in the electrolyte. Hence, PEC can thus produce electricity, chemical reaction or both. However, PEC can be operated exclusively in the current mode if the reaction that takes place at the counter electrode to the semiconductor electrode (usually a metallic electrode) is simply the reverse of the anodic reaction that takes place at the semiconductor. In this mode of operation (for example the oxygen evolution and oxygen reduction were to occur at the two electrodes) then the PEC is presumed to operate similar to Photovoltaic cell as an energy conversion device. However, if the energetics of the electrons is suitable it is possible to reduce water to hydrogen at the counter electrode instead of the reduction of oxide ions and this process may be considered as fuel production produced by the use of photon energy and also the electrical field gradient. Depending on the net energetics, it is possible to produce both fuels and also electricity. In this sense the PEC appears to be unique if one were to understand and implement both the process in the same cell. It is also possible that other concurrent reactions can also take place in the PEC like corrosion and passivation processes of the semiconductor electrode can compete with the desired energy conversion process. These dissolution or degradation processes can restrict the life time of the electrodes. Secondly some trap states can be present in the materials which will lead to loss processes for the effective conversion of excited states into energy and thus contribute to the lowering of the conversion efficiency. Third parameter is the Electrode electrolyte interface which may not give rise to a large free energy gradient so that effective charge separation is achieved at the interface. This is an important component of PEC and deserves careful attention.

2.5 CONCLUDING REMARKS

A number of promising devices have emerged for the conversion of solar energy to chemical energy or electricity, based on the R&D efforts at a

number of laboratories. Stable and efficient systems have been demonstrated, but economically useful and practical systems have yet to be realized. Developments in such systems will require new materials and configurations, improvements in efficiencies with polycrystalline and amorphous materials, and fundamentally a better understanding of semiconductor materials and the nature of semiconductor/electrolyte interface.

References

1. Nathan S. Lewis and Daniel G. Nocera, Proceedings of National Academy of Sciences, 103 (43): 2006, 15729-15735.
2. T. M. I. Wigley, R. Richels and J. A. Edmonds, World Energy Assessment Report: Energy and the Challenge of Sustainability (United Nations, New York).
3. E. Maier-Reimer and K. Hasselmann, Climate Dyn., 2: 1987, 63-90.
4. J. R. Petit, J. Jouzel, D. Raynaud, N.I. Barkov, J-M. Barnola, I. Basile, M. Bender, J. Chappellaz, M. Davis, G. Delaygue, et al., Nature, 399: 1999, 429-436.
5. U. Asiegenthaler, T.F. Stocker, E. Monnin, D. Lathi, J. Schwander, B. Stauffer, D. Raynaud, J-M. Barnola, H. Fischer, V. Masson-Delmotte, et al., Science, 310: 2005, 1313-1317.
6. G. W. Crabtree and N. S. Lewis, Physics Today, 60: 2007, 37-42.
7. T. Kuwana, Electroanalytical Chemistry, Vol. 1, Marcel Dekker Inc., New York, 1966, p. 197.
8. K. Honda, J. Chem. Soc. Jpn. Ind. Chem. Sec., 72: 1969, 63.
9. K. Honda, J. Photo Chem. Photo Biol., A, 166: 2004, 63-68.
10. E. Becquerel, Compt. Rend., 9: 1839, 58.
11. S. Kikuchi, T. Yura, K. Honda, Seisankenkyu, 18: 1966, 165.
12. E. Rabinowitch, J. Chem. Phys., 8: 1940, 551.
13. A. Golgmann, Ann. Physik 27: 1908, 449.
14. E. Baur, Z. Physik Chem., 63: 1908, 683.
15. S. Iimori, J. Tokyo Chem. Soc., 38: 1917, 507.
16. E. Rabinowitch, J. Chem. Phys., 8: 1940, 551.
17. M. Eisenberg, H.P. Silverman, Electrochim. Acta, 5: 1961, 1.
18. H. Berg, H. Schweiss, E. Stutter, K. Weller, J. Electroanal. Chem. 15: 1967, 415.
19. M. Heyrovsky, R. G. W. Norrish, Nature, 200: (1963) 880.
20. A. M. Brodsky, Y. V. Pleskov, Progress in Surface Science, Vol. 2, part 1, Pergamon Press, 1972.

21. W. H. Brattain, C. G. B. Garrett, Bell System Tech. J., 34: 1955, 129.
22. A. Fujishima, S. Kikuchi, K. Honda, J. Chem. Soc. Jpn. Ind. Chem. Sec., 72: 1969, 108.
23. A. Fujishima, K. Honda, Nature, 238: 1972, 37-38.
24. A. Fujishima, K. Kohayakawa, K. Honda, J. Electrochem. Soc., 122: 1975, 1487.
25. H. Vogel, Ber. Bunsen. Phys. Chem., 6: 1873, 1302.
26. E. Becquerel, Compt. Rend., 79: 1874, 185.
27. R. Audubert, Les piles sensibles l'action de la lumire, Hermann et Cie, Paris, 1931, p. 16.
28. K. Hauffe, J. Range, Z. Naturforsch. 23B: 1968, 736.
29. H. Gerischer, H. Tributsch, Ber. Bunsen. Phys. Chem., 72: 1968, 437.
30. H. Tributsch, H. Gerischer, Ber. Bunsen. Phys. Chem., 73: 1969, 850.
31. R. Memming, H. Tributsch, J. Phys. Chem., 75: 1971, 562.
32. A. Fujishima, E. Hayashidani, K. Honda, Seisankenkyu, 23: 1971, 363.
33. H. Gerischer, Faraday Disc. Chem. Soc., 58: 1974, 219.
34. A. Fujishima, T. Iwase, T. Watanabe, K. Honda, J. Am. Chem., Soc. 97: 1975, 4134.
35. B. O'Regan, M. Grtzel, Nature, 353: 1991, 737.
36. M. D. Archer and J. R, Bolton, Photoconversion of Solar Energy, Wiley Interscience, New York, 1991.
37. K. W. Frese, Appl. Phys. Lett., 40: 1982, 275-277.
38. J. Reichman and M. A. Russak, J. Electrochem. Sot., 131: 1984, 796-798
39. S. Licht, R. Tenne, G. Dagan, G. Hodes, J. Manassen, D. Cahen, R. Triboulet, J. Rioux and C. Levy-Clement, Appl. Phys. Lett., 46: 1985, 608 - 610.
40. G. Kline, K. Kam, D. Canfield and B. A. Parkinson, Sol. Energy Mater., 4: 1981, 301-308.
41. R. Tenne and A. Weld, Appl. Phys. Lett., 59: 1985, 2249-2251.
42. D. Cahen, Y. W. Chen, R. Noufi, R. Ahrenkiel, R. Matson, M. Tomkiewicz and W. M. Shen, Sol. Cells, 16: 1986, 529-548.
43. S. Menezes, H. J. Lewerenz and K. J. Bachmann, Nature (London), 305: 1983, 615-616.
44. A. Heller, J. Vat. Sci. Technol., 21: 1982, 559-561.
45. C. M. Gronet and N. S. Lewis, J. Phys. Chem., 88: 1984, 1310-1317.
46. B. J. Tufts, I. L. Abrahams, P. G. Santangelo, G. N. Ryba, L. S. Casagrande and N. S. Lewis, Nature (London), 326: 1986, 861-863.
47. W. S. Hobson and A. B. Ellis, Appl. Phys. Lett., 41: 1982, 891-893.

48. J. A. Switzer, J. Electrochem. Sot., 133: 1986, 722-728.
49. A. T. Howe and T. H. Fleisch, J. Electrochem. Sot., 134: 1987, 72-76.
50. J. Murphy and J. O. M. Bockris, Znt. J. Hydrogen Energy, 9: 1984, 557-561.
51. J. Lee, A. Fujishima, K. Honda and Y. Kumashiro, Bull. Chem. Sot. Jpn., 58: 1985, 2634-2637.
52. J. F. Juliao, An. Simp. Bras. Electroquim. Electroanal. 3rd, 1: 1982, 341-347.
53. C. Levy-Clement, A. Heller, W. A. Bonner and B. A. Parkinson, J. Electroanal. Chem., 129: 1982, 4116-4120.
54. E. L. Johnson, Recent Progress in Photovoltaic/Electrochemical Energy System Application, in U. Landau, E. Yeager and D. Korton (eds.), Electrochemistry in Industry, Plenum, New York, 1982, p. 299-306.
55. Y. Nakato, M. Yoshimura, M. Hiramoto, A. Tsumura, T. Murahashi and H. Tsubomura, Bull. Chem. Sot. Jpn., 57: 1984, 355-360.
56. A. Heller and R. G. Vadimsky, Phys. Rev, Lett., 46: 1981, 1153-1156.
57. S. Licht, G. Hodes, R. Tenne and J. Manassen, Nature (London), 326: 1987, 863-864.
58. B. Keita and L. Nadjo, J. Electroanal Chem., 163: 1984, 171-188.
59. H. Yonezawa, M. Okai, M. Ishino and H. Hada, Bull. Chem. Soc. Jpn., 56: 1983, 2873-2876.
60. P. Bratin and M. Tomkiewicz, J. Electrochem. Soc., 129: 1982, 2469-2473.
61. H. J. Gerritson, W. Ruppel and P. Wuerfel, J. Electrochem. Soc., 131: 1984, 2037-2041.

3 Principles of Photo-electrochemistry (PEC)

3.1 INTRODUCTION

Photo-electrochemistry has gained importance in the last four decades after the announcement by Fujishima and Honda that water can be decomposed using TiO_2 and solar radiation. The electrolysis of water is a well known phenomenon but not widely used industrially for the production of hydrogen since considerable over-voltages are required to decompose water over the conventional thermodynamic reversible decomposition potential of water that is 1.229 V. The observation that water decomposition involves over-voltage means that the efficiency of the process will be considerably less than one. However if one wants pure hydrogen without the impurity of carbon oxides which are invariably present if hydrogen was obtained from steam reforming of naphtha, then direct electrolysis may be resorted to. Though photo-electrochemistry assumed importance from the point of view of water decomposition or generation of hydrogen from renewable source, water, it has assumed considerable importance today in many areas including the reduction of carbon dioxide as well as synthesis of ammonia from nitrogen which are most challenging propositions.

3.2 BASIC ELECTROCHEMISTRY AND SOLID STATE SCIENCE

The study of photo-electrochemistry needs some fundamental knowledge of Electrochemistry and Solid State Physics. However since this monograph basically deals with only photo-electrochemistry and its manifestations, it is not our intention to outline the basis of electrochemistry or solid state physics in any manner. However, since it is necessary that one comprehends the various values of redox potentials and their significance in a concise manner, even with the fear of repetition, the values of standard redox potentials of many of the commonly employed redox couples are given in Table 3.1 and the same is schematically represented in Fig. 3.1.

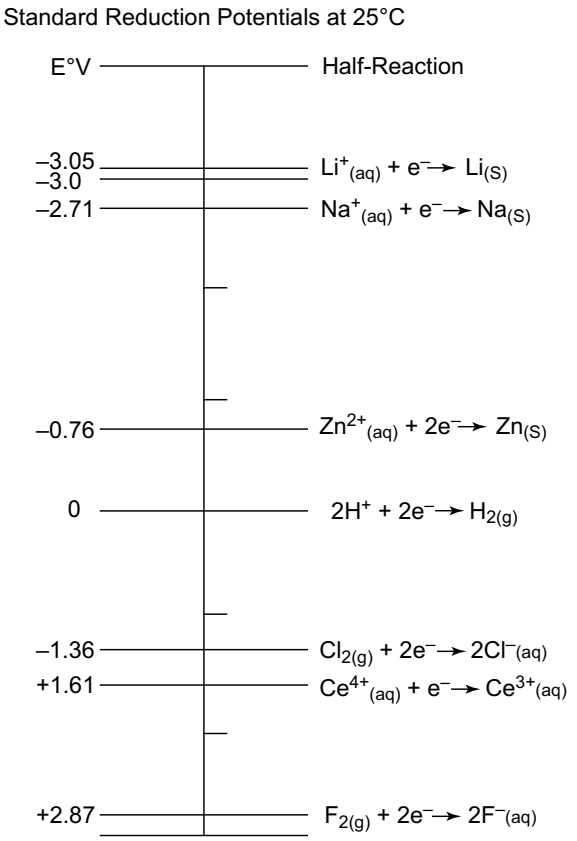

Figure 3.1 ***Standard reduction potential at 298 K.***

Table 3.1 ***Standard Reduction Potentials at 273 K for various Redox Reactions.***

Half Reaction	*Standard Reduction Potential in Volts*
$Li^+(aq) + e \rightarrow Li(s)$	−3.05
$K^+(aq) + e \rightarrow K(s)$	−2.93
$Ba^{2+}(aq) + 2e \rightarrow Ba(s)$	−2.90
$Sr^{2+}(aq) + 2e \rightarrow Sr(s)$	−2.89
$Ca^{2+}(aq) + 2e \rightarrow Ca(s)$	2.87
$Na^+(aq) + e \rightarrow Na(s)$	−2.71
$Mg^{2+}(aq) + 2e \rightarrow Mg(s)$	−2.37
$Be^{2+}(aq) + 2e \rightarrow Be(s)$	−1.85

Table 3.1 ***(Continued)***

Half Reaction	*Standard reduction Potential in Volts*
$Al^{3+}(aq) + 3e \rightarrow Al(s)$	−1.66
$Mn^{2+}(aq) + 2e \rightarrow Mn(s)$	−1.66
$2H_2O + 2e \rightarrow H_2\ (g) + 2OH^-(aq)$	−0.83
$Zn^{2+}(aq) + 2e \rightarrow Zn(s)$	−0.76
$Cr^{3+}(aq) + 3e \rightarrow Cr(s)$	−0.74
$Fe^{2+}(aq) + 2e \rightarrow Fe(s)$	-0.44
$Cd^{2+}(aq) + 2e \rightarrow Cd(s)$	-0.40
$PbSO_4(s) + 2e \rightarrow Pb(s) + SO_4^{2-}\ (aq)$	-0.31
$Co^{2+}\ (aq) + 2e \rightarrow Co(s)$	-0.28
$Ni^{2+}(aq) + 2e \rightarrow Ni(s)$	-0.25
$Sn^{2+}(aq) + 2e \rightarrow Sn(s)$	-0.14
$Pb^{2+}(aq) + 2e \rightarrow Pb(s)$	-0.13
$2H^+\ (aq) + 2e \rightarrow H_2(g)$	0.00
$Sn^{4+}(aq) + 2e \rightarrow Sn^{2+}(aq)$	+0.13
$Cu^{2+}(aq) + e \rightarrow Cu^+(aq)$	+0.15
$AgCl(s) + e \rightarrow Ag(s)\ Cl^-(aq)$	+0.22
$Cu^{2+}(aq) + 2e \rightarrow Cu(s)$	+0.34
$O_2(g) + 2H{-}2O + 4e \rightarrow 4OH^-(aq)$	+0.40
$I_2(s) + 2e{\rightarrow}\ 2I^-(aq)$	+0.53
$MnO_4{}^-(aq) + 2H_2O + 3e \rightarrow MnO_2\ (s) + 4OH^-$	+ 0.59
$O_2(g) + 2H^+(aq) + 2e \rightarrow H_2O_2(aq)$	+0.68
$Fe^{3+}(aq) + e \rightarrow Fe^{2+}(aq)$	+0.77
$Ag^+(aq) + e \rightarrow Ag(s)$	+0.80
$Hg_2{}^{2+}(aq) + 2e \rightarrow 2Hg(l)$	+0.85
$2Hg^{2+}(aq) + 2e \rightarrow Hg_2{}^{2+}(aq)$	+0.92
$Br_2(l) + 2e \rightarrow 2Br^-(aq)$	+1.07
$O_2(g) + 4H^+(aq) + 4e \rightarrow 2H{-}2O$	+1.23
$MnO_2(s) + 4H^+(aq) + 2e \rightarrow Mn^{2+}(aq) + 2H_2O$	+1.23
$Cr_2O_7{}^{2-}(aq) + 14H^+(aq) + 6e \rightarrow 2Cr^{3+}(aq) + H_2O$	+1.33
$Cl_2(g) + 2e \rightarrow 2Cl^-(aq)$	+1.36
$Au^{3+}(aq) + 3e \rightarrow Au(s)$	+1.50
$Ce^{4+}(aq) + e \rightarrow Ce^{3+}$	+1.61
$PbO_2(s) + 4H^+(aq) + SO_4{}^{2-}(aq) + 2e \rightarrow PbSO_4(s) + 2H_2O$	+ 1.70
$H_2O_2(aq) + 2H^+(aq) + 2e \rightarrow 2H_2O$	+ 1.77
$Co^{3+}(aq) + e \rightarrow Co^{2+}(aq)$	+1.82
$O_3(g) + 2H^+(aq) + 2e \rightarrow O_2(g) + H_2O(l)$	+2.07
$F_2(g) = 2e \rightarrow 2F^-(aq)$	+2.87

Figure 3.1 has some messages for understanding the redox processes from the point of electrochemistry. For any electrochemical processes to be feasible, the net free energy change (standard free energy change) has to be negative which means that the net potential has to be positive since $\Delta F^0 = -nFE^0$ where n is the number of electrons transferred in the redox process and F is the Faraday constant which is the product of charge on the electron $\times$ Avogadro number = $1.6022 \times 10^{-19} \times 6.0221 \times 10^{23}$ = 96485 Coulombs/mole (= F Faraday constant). The feasible half cell reactions should have positive values of potential while the reverse of the reactions are feasible for the processes with negative values of potential. Secondly the two ends of the electochemical potential scale are represented by the flourine reduction and lithium ion reduction. This denotes the magnitude of potentials that can be realized using these redox species.

3.3 ELECTRODE-ELECTROLYTE INTERFACE

Photo-electrochemical cells are the simplest devices consisting of a semiconductor and metallic electrodes immersed into an electrolyte and the semiconductor electrode is preferentially exposed to sun light or light irradiation. The semiconductor electrode absorbs the light and creates energetically separated electrons and holes which drive the chemical reaction to evolve chemicals (it will be hydrogen if the electrolyte contains water) or fuels. These simple devices if they can be efficient at least greater than 15% (or capable of over coming the conventional Carnot limitation) can become a source of fuel conversion device. There are at present, three known methods of converting light into usable energy sources. Among these three, the first one is the remarkable nature's path namely Photosynthesis. Probably this may be the most preferred pathway by which nature provides energy sources for all the living beings on earth. The total solar energy reaching the earth surface per year is approximately $3850{,}000 \times 10^{18}$ joules/yr or 120,000 TW. Out of this estimated resource only less than 0.02% will be sufficient to replace the energy requirement now met by fossil fuels and nuclear energy. The total solar energy received by earth is given by 1366 watts per square meter ($\pm$6.9%) $\times$ 127,4000,000 km^2 = 174 $\pm$ 3.5 % peta watts from which at least half (89 PW) reaches the earth surface. The total solar energy reaching the earth in a year is more than twice of all the energy stored in various forms like coal, oil and all other conceivable forms of energy. Possibly the energy utilized in photosynthesis can account for about 3000×10^{18} joules. Thus, it can be seen that only a tiny fraction of the total solar energy is harnessed by the plants, but still this level of energy storage is sufficient to support living systems on earth. It is clear that energy conversion by photosynthesis appears to be a possible means of providing the energy requirements of earth. There are two

alternate methods of energy conversion that have been proposed and are being developed for increasing the efficiency of the processes. One of them is termed as Photovoltaics. A photovoltaic cell consists of two different types of solids connected at an abrupt but defined junction. This type of cell promotes the current flow in only one direction in the external circuit and thus produces electrical power. Unlike the photosynthesis, wherein solar energy is utilized to produce fuel, photovoltaics produce electricity directly. This brings us to the concept of electron versus fuel for energy conversion. Which route is better and why can be another debate. There are some distinct advantages of Photovoltaics, like the device can be compact in nature and net efficiency achievable even today is nearly the Carnot efficiency or more and are durable and can last nearly 20 or more years. The positive features mentioned are only indicative figures and in practice they can be different.

3.4 PHOTO-ELECTROCHEMICAL CELLS

The third possibility is the Photo-electrochemical cells. The main component of the phtoto-electrochemical cells is the photo-active electrode which is usually a semiconductor. Metals are not so much effective in this operation (see the chapter on plasmonic photocatalysis where metal particles in the nano state can be active) since the energy levels are continuous (between occupied and unoccupied states) and hence excitation in these systems will lead to fast recombination and hence the net free energy change can not be harnessed. For conventional redox reactions, one is interested in either reduction or oxidation of a substrate. For example consider that one were interested in the oxidation of Fe^{2+} ions to Fe^{3+} ions then the oxidizing agent that can carry out this oxidation is chosen from the relative potentials of the oxidizing agent with respect to the redox potential of Fe^{2+}/Fe^{3+} redox couple. The oxidizing agent chosen should have more positive potential with respect to Fe^{3+}/Fe^{2+} couple so as to affect the oxidation, while the oxidizing agent undergoes reduction spontaneously. This situation throws open a number of possible oxidizing agents from which one of them can be easily chosen. However, in the case of water splitting one has to carry out both the redox reactions simultaneously namely, the reduction of hydrogen ions ($2H^+ + 2e^- \rightarrow H_2$) as well as ($2OH^- + 2H^+ \rightarrow H_2O + 1/2O_2$) oxygen evolution from the hydroxyl ions. The system that can promote both these reactions simultaneously is essential. Since in the case of metals the top of the valence band (measure of the oxidizing power) and bottom of the conduction band (measure of the reducing power) are almost identical they cannot be expected to promote a pair redox reactions separated by a potential of nearly 1.23 V. Another aspect is that metals liberate hydrogen preferentially and if these semiconductors can be designed to have enhanced metallic/reducing properties

it may be advantageous. But this aspect is not considered in this presentation. Therefore one has to resort to systems where the top of the valence band and bottom of the conduction band are separated at least by 1.23 V in addition to the condition that the potential corresponding to the bottom of the conduction band has to be more negative with respect to $2H^+ + 2e^- \rightarrow H_2$ while the potential of the top of the valence band has to be more positive to the oxidation potential of the reaction $2OH^- \rightarrow H_2O + O_2$. This situation is obtainable with semiconductors as well as in insulators. However insulators are not appropriate due to the high value of the band gap which demands high energy photons to create the appropriate excitons for promoting both the reactions. The available photon sources for this energy gap are expensive and again require energy intensive methods. Hence insulators may not be employed for the purpose of water splitting reaction. Therefore, it is clear that semiconductors are alone suitable materials for the promotion of water splitting reaction. In the operation mode, the semiconductor electrode-electrolyte interface is the key factor and a complete understanding of this interface alone can lead to a successful development of highly efficient photo-electrochemical cells. In some sense, photo-electrochemical cells can be considered as a notional hybrid of photo-synthesis and photo-voltaics since these cells can generate either or both electricity and fuel. However, the development of Photo-electrochemical cells with the desired efficiency appears to be one of the major issues calling the attention of the developers. It is better to comment further between the similarities and also differences between PEC and Photosynthesis and Photovoltaics. Photosynthesis appears to provide remarkable efficiency due to various factors. The essential points of relevance are (i) The absorption of the photon takes place in the chlorophyll dimer or the special pair' facilitated by the antenna and chlorophyll pigment. (ii) The excited electron-electron vacancy (hole) pair could normally undergo de-excitation thus releasing the optical energy as heat without producing fuel or electricity. However, in the photo-synthetic reaction centre the separation of the excited electron from its vacancy is achieved by the presence of a series of electron acceptors that are not only strategically located in the protein but could also adjust their redox potentials like in an escalator steps thus positioning the acceptor states suitable for harnessing the energy. (iii) In addition, the presence of a series of electron acceptors makes the electron to move from one species to another thus spatially separating the electron hole farther away thus restricting the thermodynamically feasible recombination of the excited electron and hole thus bringing in a kinetic control. This alone facilitates the use of the excited electron to perform the chemical reactions in photosynthesis and is responsible for fuel production. In the case of Photovoltaics, the free energy gradient caused by the potential energy gradient present at the junction of

the two solids is the cause for the flow of electrons or electricity. In the case of photoelectrochemical cells also the driving force is the electrical field gradient that is available at the semiconductor/electrolyte interface and also the interaction of the photon field in the semiconductor adds cumulatively for this field gradient which is responsible for the vectorial transfer of electrons and also for driving the chemical reaction in the electrolyte. Hence, PEC can thus produce electricity, chemical reaction or both. However, PEC can be operated exclusively in the current mode if the reaction that takes place at the counter electrode to the semiconductor electrode (usually a metallic electrode) is simply the reverse of the anodic reaction that takes place at the semiconductor. In this mode of operation (for example the oxygen evolution and oxygen reduction were to occur at the two electrodes) then the PEC is presumed to operate similar to Photovoltaic cell as an energy conversion device. However, if the energetics of the electrons is suitable it is possible to reduce water to hydrogen at the counter electrode instead of the reduction of oxide ions and this process may be considered as fuel production caused by the use of photon energy and also the electrical field gradient. Depending on the net energetics, it is possible to produce both fuels and also electricity. In this sense the PEC appears to be unique if one were to understand and implement both the process in the same cell. It is necessary therefore to define some specific parameters for the operation of PEC. The term short circuit current (I_{SC}) refers to the current that will flow in low resistance ammeter when the two electrodes of PEC are in direct short circuit. The term open circuit voltage (V_{OC}) is the maximum Gibbs free energy that can be obtained from the cell and usually measured with a high resistance voltmeter. The term fill factor refers to the maximum power that can be produced by a photo-electrochemical cell. It will be clear that all these three parameters have to be optimized. See for example Fig. 3.2.

It is also possible that other concurrent reactions can take place in the PEC, like corrosion and passivation processes of the semiconductor electrode can compete with the desired energy conversion process. These dissolution or degradation processes can restrict the life time of the electrodes. Secondly some trap states can be present in the materials which will lead to loss processes for the effective conversion of excited states into energy and thus contribute to the lowering of the conversion efficiency. Third parameter is the electrode-electrolyte interface which may not give rise to a large free energy gradient so that effective charge separation is not achieved at the interface. This is an important component of PEC and deserves careful attention. Even though the focus of this presentation will be on the conversion of solar energy into useful forms of energy like electricity or fuels or both,it is possible to make use of the concept of PEC for the treatment of waste water and for other

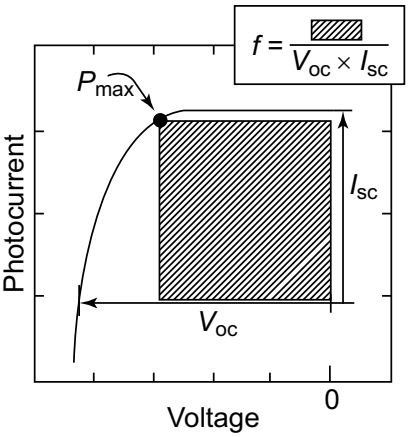

Figure 3.2 ***i-V curve to explain the parameters like V_{OC} , I_{SC} and fill factor.***

organic synthetic oxidation reactions. These two aspects will be dealt with in separate chapters.

3.5 SELECTION CRITERIA FOR ELECTRODES

It has been stated earlier, that semiconductor materials are commonly employed as electrodes in PECs. It is therefore necessary that one outlines some governing principles of electron transfer in semiconducting materials before one considers the semiconductor-electrolyte interface. Unlike in simple molecular systems, wherein the energy levels take discrete and specified energy values, the energy levels in semiconductors are close together instead of the discrete energy levels and hence give rise to energy bands of allowed energy levels. Normally one mole of any substance will contain Avogadro number of species and hence the frontier orbitals of these systems should consist of multiples of Avogadro number of eigen states, each with double occupancy with paired spins. If the occupied density of states (DOS) overlaps with density of states of unoccupied states, then the material can be considered to possess metallic conduction, which is normally identified by the decrease in conductance value with increase in temperature. However in the case of other materials, the occupied valence band is separated from the usually unoccupied conduction band and depending on the band gap values the materials can be either semiconductors or insulators. This situation is usually depicted in terms of a box type diagram shown in Fig. 3.3, though this is not the real picture arising from three dimensional solids. In the case of semiconductors, the band gap is usually or the order of 0 to 4 eV. A compilation of band gap values of the some of the known semiconductors is given in Table 3.2. The value of the band gap (E_g) has important implications in the application as

electrodes in PEC. One is normally interested in the electrochemical potential of the electrons for the redox reactions of interest, the position of the highest occupied state or more precisely the Fermi level (it should be Fermi surface for three dimensional systems) of the solid system on hand. Essentially, one is tempted to denote the Fermi level in the conceived two dimensional box type diagram in between the top of the valence band and the bottom of the conduction band, more precisely considering the energy position where the probability of finding the electron is 0.5. However, the more precise definition should be based on the electrochemical potential of the electrons but since it is a conceived concept, one takes the route of a visual and manageable parameter of probability function. The distribution of electrons in the frontier bands in the solids has to be rationalized in terms of well defined distribution functions containing at least two distinct constants related to energy of the electrons and also to the total number of electrons in the system considered.

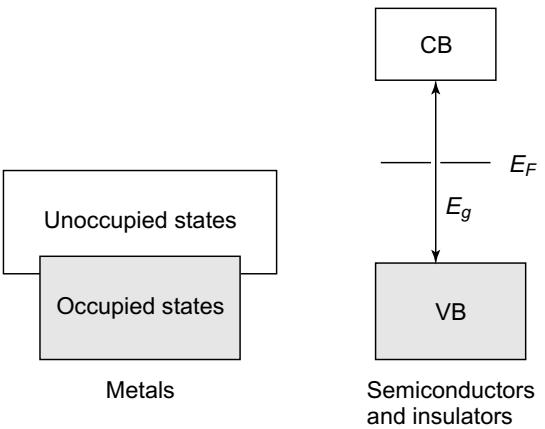

Figure 3.3 ***The energy band positions in metals, semiconductors and insulators (E_g = band gap and E_F Fermi level.***

There are various ways the energy states of the frontier wave functions (namely the energy states of the valence and conduction bands) can be altered by appropriate substitutions in the solid matrix or even the solid matrix can sustain small amounts of alter valent ions and thus can give rise to extra allowed wave functions in the so called forbidden gap which is termed as band gap (E_g). Depending on the eigen-value of these allowed wave functions in the forbidden gap, they can be either acceptor states near the top of valence band (mainly contributing to conduction by positive holes and hence called p-type semiconductor). If on the other hand, the added species were to generate allowed energy states very near to the bottom of the conduction band, then these states are denoted as donor states, since these states are usually occupied

and hence called n-type semiconductors. The electrical behavior that arises out of the incorporation of the foreign species in a given semiconductor lattice and hence termed as extrinsic semiconductors. However, the energy states namely acceptor and donor states can also be intrinsically generated in a given semiconductor without the addition of foreign altervalent species and these are termed as intrinsic semiconductors. The statements that have been made so far refer to the single crystals of semiconductors. In the case of amorphous and poly crystalline semiconductors, the additional energy levels can be generated from the inherent defects in them like grain boundaries, trap states and defects. The presentation given is one of the simplest and for more rigorous treatments, it would be good the reader refers to some text book on solid state physics to understand the electronic structure of semiconductor materials. There are various ways the energy states of the frontier wave functions (namely the energy states of the valence and conduction bands) can be altered by appropriate substitutions in the solid matrix or even the solid matrix can sustain small amounts of alter valent ions and thus can give rise to extra allowed wave functions in the so called forbidden gap which is termed as band gap ($\mathrm{E_g}$). Depending on the eigen-value of these allowed wave functions in the forbidden gap, they can be either acceptor states near the top of valence band (mainly contributing to conduction by positive holes and hence called p-type semiconductor). If on the other hand, the added species were to generate allowed energy states very near to the bottom of the conduction band, then these states are denoted as donor states, since these states are usually occupied and hence called n-type semiconductors. The electrical behavior that arises out of the incorporation of the foreign species in a given semiconductor lattice and hence termed as extrinsic semiconductors. However, the energy states namely acceptor and donor states can also be intrinsically generated in a given semiconductor without the addition of foreign altervalent species and these are termed as intrinsic semiconductors. The statements that have been made so far refer to the single crystals of semiconductors. In the case of amorphous and poly crystalline semiconductors, the additional energy levels can be generated from the inherent defects in them like grain boundaries, trap states and defects. The presentation given is one of the simplest and for more rigorous treatments, it would be good the reader refers to some text book on solid state physics to understand the electronic structure of semiconductor materials.

3.6 STRUCTURE AND DYNAMICS OF ELECTRODE/ELECTROLYTE INTERFACE

The primary purpose of this presentation is to examine the structure and dynamics of the electrode-electrolyte interface. When a metal electrode is

immersed in an electrolyte, and since these two systems are in electrical contact, there will be equalization of the Fermi levels in both systems which will result in the transfer of charge. Under these equilibrium conditions, the electrochemical potential of the electrons is conventionally given by the Nernst Equation

$$E_{redox} = E^0{}_{redox} + (RT/nF) \ln (a_{ox}/a_{red})$$

Where a_{ox} and a_{red} stand for the activities of the oxidized and reduced species in the redox couple and E^0_{redox} can be identified with the Fermi level in the electrolyte. At this point, one must realize that one is dealing with two scales for energy. The electrochemical scale of energy which is of relevance for PEC assumes that the potential of the standard hydrogen electrode (SHE) as reference value and assigns the value of zero. However, the solid state community has adopted the more reasonable reference value for the energy scale and assigned the zero value for the free electron in vacuum. It is therefore possible now to connect both the electrochemical scale and that of the energy scale with reference to free electron in vacuum as zero by the relationship that the zero of the electrochemical scale (namely the potential of SHE) is at $\sim$ 4.5 eV with respect to the energy of the free electron in vacuum. Now if a semiconductor is immersed in a redox electrolyte, the electrochemical potential (for this discussion it is the Fermi level of the two phases) are different at the interface. A second point to be noted is that the field gradient is varying in some form from the interface to the solution side as well as inside the semiconductor. However in the case metal-electrolyte interface the field gradient is prominent only in the solution side and not very deep within the metallic electrode. In the case of semiconductor-electrolyte interface, equilibration of the interface Fermi levels thus necessitates the flow of charge from one phase to another and hence the eigen values of the allowed energy levels also vary with respect to distance from the interface inside the semiconductor. This variation of the values of allowed energy levels within the semiconductor is usually visualized as band bending. In reality it only shows how the allowed energy levels get altered due to the free charge flow across the semiconductor, this alteration can also be due to the accumulation or adsorption of charged species from the electrolyte on the semiconductor electrode. This redistribution of allowed energy levels in the semiconductor gives rise to build of voltage V_{SC} (SC = space charge) within the semiconductor.

The charge injection as a result of Fermi level equilibration can lead to alteration of the Fermi level in either of the directions (namely it can be more stabilized or can also be more destabilized, though it is conventionally denoted as moving “down” or “up”). Essentially this alteration of the Fermi level can take place till the Fermi level equilibration takes place. The concepts that have

been described so far namely band bending or Fermi level equilibration are not unique to the semiconductor/electrolyte interface and any interface can give rise to readjustment of electronic energy levels if electron transfer is feasible at the interface. However it must re-emphasized that the potential drop or the charge accumulation (may be appropriately charge density change) is mainly concentrated at the surface or at the most few nanometers from the surface (skin depth), which could be due to high electronic conductivity of the metals which cannot support a net electric field within the bulk metal. This is the reason why electrochemists have been successful in explaining the electrochemical electron transfer process at the metal/electrolyte interface in terms of Helmholtz region. In the case of semiconductors the field penetrates inside the semiconductor as in the electrolyte region and this is called **Garrett-Brattain space charge region**. The point of relevance is that the behavior of metal/electrolyte interface is different from that of semiconductor/electrolyte interface. The differences have been examined in terms some kind visualizable equivalent circuits, but it is not yet clear if this description is quite sufficient and adequate. It is realized now that there is a definite region in the semiconductor where the charge distribution is altered because of equilibration. Beyond this region, may be the electro-neutrality condition is holding good. One is concerned with the space charge region or the layers where the charge density alteration exists. The potential distribution in this interface region can be expressed under certain conditions by the equation

$$V(x) = -(e_0 N_D/2\varepsilon_s)x^2 \quad \text{where } x\ (0 \leq\ x \leq\ w)$$

In this equation,ε s is the static dielectric constant of the semiconductor and e_0 is the electronic charge. The quantitative equation for the value of V_{SC} is therefore given by

$$\mathrm{V}_{SC} = -(\mathrm{e}_0 \mathrm{N}_D/2\varepsilon_s)w^2$$

where w stands for the field penetration depth and in the case of charge depletion it is depletion layer width. It is therefore clear that the value of N_D can be considered to be equal to doping level or impurity level. It may be necessary one understands the difference between the concept of doping or dissolution or solid solution formation. The doped species (in the ionic state) must be accommodated in the crystalline lattice positions while in solid solution this condition need not be satisfied. This implies that only certain species which satisfy conditions like ionic size and extent (read percentage) of doping will have restrictions which can be in the order of 10^{16} to 10^{18} cm^{-3} for the situation of light or heavy doping respectively decides the field penetration depth and this is of the order of 10 to 1000 nm for most of the semiconductors as compared to the typical Helmholtz layer width of 0.4 to 0.6 nm. It is therefore clear that if one were to extend the

science of metal/electrolyte interface to semiconductor/electrolyte interface, the layer width has to be considerably reduced. The potential difference across a semiconductor electrolyte can be mathematically written by simple extrapolation of the metal/solution interface as

$$V_t = V_{SC} + V_H + V_G$$

where V_t denotes the total potential difference between the semiconductor electrode and the counter metallic electrode. It is generally realized that V_{SC} depends on the nature of the semiconductor and also that of the electrolyte and its magnitude is sometimes difficult to estimate so also that of V_H and V_G. Another contributing factor for the uncertainty in the determination of these values is the specific adsorption of the electrolyte on the surface of the electrode. In the case of metallic electrodes this is simpler since there are only one type of surface sites that are available and also the field effects are posssibly known while in the case of semiconductor these factors are not yet fully certain and one has to make some striking approximations which may not be representing the true situation existing at the interface. It is necessary that one estimates the extent of so called band bending (though in reality this is band alteration) which can be assessed by a parameter called the flat band potential V_{fb}, that is the potential that need to be applied to make the band to be flat. The value of this parameter can be determined from the Mott-Schottky relation which is given by the expression for a n-type semiconductor

$$1/C^2_{SC} = 2/N_D e_{os} [(V - V_{fb}) \ kt/e_o]$$

Where C_{SC} is the semiconductor depletion layer capacitance and this relation itself is derived invoking the Poisson distribution.. It must be noted that V_{fb} itself depends on many parameters like the specific adsorption of the electrolyte and also the trap states in the semiconductor. When the value of the flat band potential V_{fb} is known then the Fermi level of the semiconductor is defined. This provides a means to delineate the position of the top of the valence band and also the bottom of the conduction band which essentially correspond to the oxidation and reduction potential of the semiconductor and this also provides a means of estimating the band gap which facilitates the choice of the wavelength of the radiation necessary to make an exciton in a semiconductor. Having identified that the oxidation and reduction capabilities of the semiconductor are associated with the energy positions of the top of the valence band and bottom of the conduction band of the semiconductor, it is seen that the so called band bending associated with the semiconductor/electrolyte interface positions or alters the Fermi level of the semiconductor in the direction for favourable redox reaction. In other words the band bending probably is capable of tracking the redox

potential changes that occur in the system. So far we have considered an ideal semiconductor/electrolyte interface. However in reality semiconductors necessarily have abrupt termination of the lattice and this situation can give rise to co-ordinatively unsaturated positions which are different from that of the species in the bulk of the lattice. The presence of such species in the surface can result in some kind of surface reconstruction of the surface or the unsaturation has to be satisfied by extraneous species. In both these cases, the electronic energy states take discrete values in the forbidden band gap region rather than forming one of the energy levels in the continuously varying with respect to energy valence or conduction bands. Depending on the occupancy of these states, it is possible that these energy levels can exchange charge either with the valence or conduction bands or with the redox electrolyte. If the value of V_{SC} (that is the band bending in the semiconductor) is not altered with change in the value of the redox potential of the solution redox couple, then the Fermi level is said to be pinned. This extent of Fermi level pinning is reflected from the plot of variation of V_{SC} (any other parameter equivalent to it) versus E_{redox}. If the slope of this plot were to be zero then the Fermi level is completely pinned and any other variation with a slope value up to 1 denotes the possible variation in V_{SC}. It should be noted that the argument given is applicable only for under non-irradiated condition. Under irradiation of the semiconductor, there can be changes in the values of V_H and also that of V_{SC} which can complicate and alter the situation. Depending on the magnitude of the values of N_D and ε_s, it is possible that the values of V_H can become sizable fraction of the potential drop exceeding the value of V_{SC}. The Fermi level pinning can also be associated with the extent of defect states in the crystalline lattice. The charge transfer process of semiconductor/electrolyte interface in the dark follows simple electrochemical principles. Let us consider the electrode/electrolyte under equilibrium conditions. Under these conditions the forward current and the reverse currents exactly balance each other and there is no net current across the interface. If the system sustains a bias voltage, then the net current will flow in either of the directions depending on the number of majority carriers that are generated in the space charge region in the semiconductor. This argument is based on the assumption that the voltage drop essentially takes place in the space charge region and hence one is modulating the population of majority charge carriers only in the surface layers. This situation gives rise to exponential dependence of the current on the applied potential when $V < 0$ cathodic bias and when $V > 0$ (anodic bias) the current is independent of the applied potential.

Under these conditions one has to consider the value of i_0 which is conventionally termed as the exchange current density, that is the current that flows at equilibrium when the cathodic and anodic currents exactly

balances each other. The value of i_0 should therefore naturally depend on the concentration of the redox species in solution and also on the extent of band bending, which is dependent on the extent of doping or other alterations that cause a change in the Fermi level in the semiconductor. The magnitude of i_0 is therefore a measure of the rectification that can be realized in the system. In the dark under no illumination condition, there can be hole injection in the VB of the semiconductor. These holes can recombine with electrons either through the surface states or by the occupied states in the space charge region.

Now if the semiconductor is exposed to the radiation of energy equal to or greater than the band gap (E_g) then these radiations can give rise to excitation of an electron from the occupied valence band to an unoccupied state in the conduction band. If all these electrons thus excited could be harnessed in the external circuit, then the process can be said to have high quantum efficiency. However there are other concomitant processes that are possible. Essentially they arise due to scattering and also absorption of radiation by the electrolyte and other components of the assembly and these radiations have to be quantitatively assessed for calculating the net quantum efficiency. As stated earlier the number of carriers that are collected in the external circuit versus those that are generated by optical absorption is conventionally termed as quantum yield, it is clear even though one can estimate the conversion efficiency, there are uncertainties in the estimation of the absorption of the photons by the semiconductor alone. Secondly, it is assumed that the photon field and electric field are acting on the semiconductor independent of each other. The validity of this assumption has not been explicitly addressed even though there are indications that there can be photon enhanced field emission. Irradiation of semiconductor results in some kind of charge redistribution in the density of states of valence and conduction bands. The superimposing electric field can give rise to distortion of the energy states. Similarly if the charge distribution in the valence and conduction bands are perturbed by the electric field, then the application of the photon field can give rise to altered redistribution and hence the net effect can not be considered to be an algebraic sum of the individual field effects though that is how it is considered mostly so far. It is possible that the extent of band bending and also the extent of effective space charge region might get altered and hence the kinetics of charge transfer process can be generally altered either way.

3.7 PERSPECTIVE AND CONCLUDING REMARKS

Having outlined the physics of semiconductor/electrolyte interface necessary for energy conversion processes, it is now possible to briefly comment on the strategies for the choice of semiconductors for PEC applications. What one hopes at this stage is to delineate the semiconductor system that will provide

efficient fuel production from decomposition of water. Unfortunately, in spite of intense research efforts for more than four decades this projection appears to be a distant future due to many obstacles. The competing components are the large band gap or small band gap materials. Large band gap materials show low efficiency and low band gap materials are susceptible for photo-corrosion and other related process like passivation which restrict the life time of the system. The presentation given has shown that the kinetic stability limitation has to be overcome than any apprehension over thermodynamic limitation. The prime factor that is responsible for this situation is the anxiety to utilize maximum extent of solar radiation instead of searching for kinetically compatible reagents to prevent photocorrosion or photopassivation processes. It may be possible or desirable to use non-aqueous electrolytes instead of solvents that promote photocorrosion. Another approach can be to modify the surface of semiconductors with surface enriching co-catalysts instead of substitution or doping. These possibilities have been explored but yet success appears to be far off.

Another approach that has been attempted is to alter the position of the top of the valence band by substitution at anionic positions of the semiconductors with species like nitrogen, phosphorus, sulphur and carbon, or alter the position of the bottom of the conduction band by doping in the cationic positions. These attempts also have provided a marginal success only. Coupling of the semiconductors is also possibly aimed in this direction only. The focus has been only to show hydrogen evolution in the decomposition of water but it should have been on the realization of storichiometric evolution of oxygen and hydrogen. Secondly, the search could have been on the surface of the semiconductors which can effectively activate the molecule employed for decomposition. Use of scavenging agents to restrict the photocorrosion has also not yielded the desired level of activity for fuel production. These studies show that the limitation for not achieving desired level of activity does not lie either in thermodynamic parameter barrier or kinetic rate limitation alone but above these two conventionally blamed parameters there is need for some intrinsic evaluation of the required parameters. It has been tempting to identify this parameter with the usual choice of parameters like 'd' electron configuration (d^0 or d^{10}, band gap value) (this is proved to be not true from the studies on band gap engineering studies) or intrinsic bond character, but the truth appears to lie above all these known variables that are amenable for study. It is hoped that the search will continue in the years to come and possibly, the solution is possibly blurred with our polarized vision.

References

Only typical references alone are given, they are not the selected ones. There are many earlier references

1. Ming X. Tan, Paul E. Laibinis, Sonbinh T. Nguyen, Janet M. Kesselman, Colby E. Stanton and Nathan S. Lewis, Principles and applications of semiconductor photoelectrochemistry, Progress in Inorganic chemistry, Vol. 41, 21-144 (1994).and references cited therein.
2. A. Fujishima and K. Honda, Electrochemical photolysis of water at a semiconductor electrode, Nature, 238, 37-38 (1972).
3. Frank E. Osterloh, Inorganic nanostructures for photo-electrochemical and photo-catalytic water splitting, Chem. Soc. Rev., 2013, 42, 2294 and the references cited therein.
4. Prashant V. Kamat and Juan Bisquert, (eds.) Solar Fuels. Photocatalytic Hydrogen Generation The Physical Chemistry C., Virtual Issue all the 27 articles in this issue. DOI: 10.1021/jp406523w
5. Xiaobo Chen, Shaohya Shen, Liejin Guo and Samuel S. Mao, Semiconductor-based photocatalytic hydrogen generation, Chem. Rev., 110, 6503-6570 (2010).
6. Michael G. Walter, Emily L. Warren, James R. Mckone, Shannon W. Boettcher, Qixi Mi, Elizabeth A. Santori and Nathan S. Lewis, Solar water splitting cells, Chem. Rev., 110, 6446-6473 (2010).
7. Krishnan Rajeshwar, Fundamentals of semiconductor electro-chemistry and photo-electrochemistry, Encyclopedia of Electrochemistry, Wiley, DOI:10.1002/97835227610426.bard060100.
8. Jeanne L. Mchale, Hierarchal light harvesting aggregates and their potential for solar energy applications, The Journal of Physical Chemistry letters, 3, 587-597 (2012).
9. Yabi Wu, Predrag Lazic, Geoffroy Hautier, Kristin Persoon and Gerbrand Ceder, First principles high throughput screening of oxynitrides for water-splitting photo-catalysts, Energy and Environmental Science, DOI. 10.1039/c2ee23482c (2012).
10. Prashant V. Kamat, Manipulation of charge transfer across semiconductor interface A Criterion that cannot be ignored in photocatalyst design, The Journal of Physical Chemistry Letters, 3, 663-672 (2012).
11. Zhen Zhang and John T. Yates, Band Bending in semiconductors: Chemical and Physical consequences at surfaces and interfaces, Chem. Revs., DOI.org/10.1021/cr3000626 (2012).

12. Halming Zhu and Tlanquan Lian, Wavefunction engineering in quantum confined semiconductor nanoheterostructures for efficient separation and solar energy conversion, Energy Environment Science, 5, 9406 (2012)
13. Aulice M. Scibioh and B. Viswanathan, Hydrogen Future: Facts and Fallacies, Bulletin of the Catalysis Society of India, 3, 72-81 (2004).
14. B. Viswanathan, Photo-catalytic processes - Selection Criteria for the Choice of Materials, Bulletin of the Catalysis Society of India, 2, 71-74 (2002).

4 Dye Sensitized Solar Cells (DSSC)

4.1 INTRODUCTION

The phenomenon of sensitization is well known to mankind. The semiconducting materials are often functioning by the sensitization of their charge carriers namely the electrons and holes. In the case of wide band gap semiconductors, the separation of the charge carriers requires considerable expansion of energy. The life on earth has always been sustained by solar power either directly or indirectly. It appears that mankind has resorted to the direct use of solar power for their energy needs and hence a variety of options are being examined including direct conversion of photons into electricity which is termed as photo-voltaics. Since the photons are used for the separation of electron hole pair, one has to resort to materials where the occupying state of the electron (valence band) should be different from the state (conduction band) from which the electron is displaced in terms of energy and symmetry. Since the energy levels of both occupied and unoccupied states are continuous in conductors, the excited state of the electron will tend to recombine easily with the hole generated. Hence it is necessary that the states from which electrons are removed must be energetically different from the states at which the electrons are placed on excitation. This situation is obtainable in semiconductors or insulators where valence band (the state from which electron is excited) and conduction band (the state to which the electron is excited) are separated both in terms of energy and the symmetry of the wave functions is also mostly different. However, the anxiety to utilize solar energy for excitation places a restriction on the use of semiconductors and that too only small band gap semiconductors since most of the radiation (in terms of energy) from the solar spectrum can be harnessed. However, not all small band semiconductors are stable under strong illumination conditions or amenable to be used as photo-anodes in the photo-voltaic devices. Among the available and exploited semiconductors (nearly 400 in number [1]), only a handful of them appear to be promising. For application in Dye Sensitized Solar Cells (DSSC) the most studied systems are TiO_2, ZnO and tin oxide [2].

Unfortunately all these three systems are wide band gap semiconductors and absorb only UV radiation which is only about 5-8% of the total solar radiation. Secondly the conversion efficiency, (photon to electricity) is also governed by the process of recombination which is the predominant mode of decay when excitation is carried out in the semiconductor itself. It appears therefore, necessary that some kind of charge injection is resorted to. This may be possible if the excitation by photon is carried out in another system and the excited electron takes occupancy in the conduction band states of the wide band gap semiconductor so that the electron can be moved in the external circuit. The auxiliary system where photo-excitation is taking place is termed as the sensitizer. It is therefore clear that the sensitizer has to fulfill some specifications. The important ones are:

(i) The system chosen should be capable of absorbing light in visible and infra red region of the solar spectrum.

(ii) The energy state of the electron on excitation in the sensitizer should be on par or suitable with that of the conduction band of the semiconductor so that charge injection can be feasible.

(iii) The sensitizer employed should be capable of being dispersed on the semiconductor so that the photon absorption can be maximized.

(iv) The sensitizer should be stable under strong illumination conditions since electron excitation may ultimately after electron transfer lead to an oxidized form of the sensitizer and it should be capable of easily reduced by the shuttled electron from the counter electrode.

(v) The sensitizer should be stable on the semiconductor surface (good adhesion). It is therefore appropriate to note that the sensitizers may be any substance that can absorb low energy photons (visible and IR region) and also is capable of providing the electrons in the external circuit to draw the power.

There are various motivations for including this chapter in this monograph. We list them as follows:

(i) This technology is threatening to be a viable for the conversion of solar energy into electricity for nearly 20 years now.

(ii) Efficiency of this type of solar cell has been consistently improving over the years either from the point of utilizing major portion of the solar radiation by appropriate choice of the dyes (the HOMO and LUMO levels of the dye could be altered to suit the available solar radiation) and/or their suitability with the semiconductor which is being sensitized.

(iii) Various structural modifications of the dye are feasible and also tried.

(iv) The cost of these solar cells has been considerably reduced with respect to time.

(v) As of now, these devices appear to be environmentally acceptable and the available infrastructure may be able to sustain this technology.

(vi) These devices may be universally accepted, and

(vii) Above all, market penetration is possible.

In view of these reasons, in recent years there have been a number of perspective articles and reviews on this topic [only selected ones in 3-7]. It is a fact that vast literature is already available on this topic, as this topic is very contemporary and hence it is necessary to assess the scientific and technological developments at periodical intervals so that one does not miss out the important advances that are taking place in such an application area. The contents of this chapter therefore will be focusing on the various possible sensitizers that have been already examined for DSSC applications as well as other relevant aspects of this emerging technology. It may be appropriate at this stage to draw the comparison with the natural photosynthesis. Both DSSC and photo synthesis make use of photon absorption by a molecular dye (it is chlorophyll a and b in the case of photosynthesis). The excited electron is transferred effectively in the case of photosynthesis since it is an escalator type redox species and hence most of the excited electrons are effectively transferred and utilized in the reduction reaction. In photo synthesis the excited electron gets transferred to a variety of species so that effective and efficient electron transfer can take place to the species undergoing reduction. In essence, in photosynthesis after initial photo-excitation the electron takes appropriate energetic position in terms of reduction potential so as to be suitable for the species undergoing reduction. Such a situation is not realizable in the case of laboratory driven reduction processes since one has only fixed value redox couples and hence effective transfer of electron and thus efficient reduction of carbon dioxide could not realized in the laboratory. However, in the case of DSSC, the excited electron has to be transported via the conduction band of the semiconductor and hence it is necessary to match the LUMO level of the molecular dye employed for sensitization and that of the bottom edge of the conduction band of the semiconductor. In addition, the electron mobility in the semiconductor has to be high enough so that fast electron transfer takes place without the concurrent recombination process. This similarity makes the DSSC to be considered as a form of bio-mimicry. However it should be emphasized that the efficiency of DSSC cannot reach the levels of efficiency of photosynthesis. The basic principles of photosynthesis will be outlined in a separate chapter.

4.2 CONFIGURATION OF A DYE SENSITIZED SOLAR CELL

There are various forms of Photo-electrochemical cells (PEC). Some of these forms are considered in this book. Among them, Dye Sensitized Solar Cells

(various abbreviations are employed in the literature the important ones are DSSC, DSC or DYSC) are the prominent ones. These cells are simpler in construction compared to solid state solar cells. The first cell was constructed by Michael Gratzel and Brain O'Regan in 1991 [8]. Dye sensitized solar cells (DSSC) have been claimed to be promising for energy conversion to electricity with the possibility of low fabrication cost, easy manufacturing feasibility and fairly high efficiency. In general, the conversion efficiency is less than that of the best thin film cells, but this could be compensated in terms of price/performance ratio which could be as much favourable as that of fossil fuel to electricity generation and hence these types of cells can be expected to be possible mode of energy converters in the near future. If one were to combine an electron rich semiconductor (n-type) with an electron deficient semiconductor (p-type) then one can visualize the transfer of electrons from n to p due to the difference in the electrochemical potential of the electrons in the two semiconductors. This shuttling of the electron (partly formed by photo-excitation in n-type semiconductor) in the external circuit is made use of to derive energy so that the electron returns back to the n-semiconductor in the valence band as it was in the original state before photo-excitation. Therefore, the harnessing of energy is related to the extent to which one can make use of the photons for increasing the electrochemical potential of the electrons. This manifests itself in the extent of the available number of appropriate energy photons and also the absorption capacity of the semiconductor employed. The origin of the dye sensitized solar cells is in this direction meant to increase the extent of photon absorption (as dyes are good photon absorbers) and possibly also favours smooth transport of the electrons through the conventional semiconductor namely TiO_2 in the external circuit. Configurationally, dye sensitized solar cells consist of conventional semiconductor (usually TiO_2 which is the work horse semiconductor for photo-electrolysis) and a counter metallic (Pt) electrode usually in supported mode to reduce the extent of requirement of the noble metal. However, the oxide semiconductor has a surface coating of the dye (mostly mimicking chlorophyll in the leaves). This coating can be achieved in a variety of ways like dipping the semiconductor in a solution of the dye whereby the dye molecules are adsorbed on the semiconductor by probably covalent bonding. However other variations of the loading of the dye on the semiconductor can also be pursued. These include loading the dye with appropriate binder, preparing the electrode (in this case it functions as anode) materials from semiconductor oxide and the dye from a slurry. Improvements in the stability of DSSC have also been achieved in alternate use of the plasticized polymer electrolyte instead of the conventional I_3^-/I^- system. For an elementary description of the dye sensitized solar cells, readers are referred to the site http://www.science20.com/mei/blog/dye_sensitized_solar_cell-75581.

4.3 SENSITIZERS

It may be appropriate if one makes some comments on the sensitizers (not necessarily dyes alone) normally employed in DSSC since this is the central part of these cells. In a sense, they are the real converters of photon energy into electrons which are injected into the semiconductor to be passed on to the counter electrode for the reduction reaction. A variety of substances have been employed probably taking the clues from the natural photosynthesis process. The type of molecules that have been tried include a variety of ruthenium based complexes like cis $Ru(L)_2(NCS)_2$ where L is bipyrine carboxylic acid, or RuL'$(NCS)_3$ where L' is a tripyridine carboxylic acid or RuL_3, [9] or the corresponding analogs of Os [10] (These species give rise to intense (in the visible region) metal-to-ligand charge transfer (MLCT) bands with a favourable energetics for possible activation-less charge injection into the semiconductor. In essence, several organic [11] and inorganic compounds have been investigated for the sensitization of the semiconductor which include chlorophyll derivatives [12], porphyrins [13], phtalocyanines [14, 15], platinum complexes [16, 17], fluorescent dyes [18], carboxylated derivatives of anthracene [19], polymeric films [20], and coupled semiconductors [21, 22] with lower-energy band-gaps, natural dyes like anthocyanin [23] from black rice, carotenoid [24] from erythinka and chlorophyll from variegata, rose bengal, porphyrin complexes especially that of zinc [25], inorganic species like copper diselenium, [26], and iodide (doped in ZnO)[27], and organic dyes without the metal ions. A complete listing of 86 sensitizers that have been tried and their characteristics are given in a recent book [28]. In recent years a number of other possibilities are being examined. The relevant data on these systems are briefly given in Table in the appendix to this chapter. Based on cost considerations, attempts have been made to use metal free dyes for DSSC applications., However, these systems exhibit lower efficiencies as compared to the metal containing dyes [3, 4, 29-31].

It may be useful to place some general remarks on the dyes or essentially on the types of sensitizers conventionally employed in DSSC in terms of materials selection and logistics for consideration.

(i) The sensitizers conventionally provide the excited electrons to the semiconductor and hence they should be stable enough in the oxidized state such that it will return to the original state by electron injection from the cathode. This means that the dyes chosen should be capable of providing electrons of suitable energy so that the electrons can be injected into the conduction band of the semiconductor employed. This brings a condition that the energy of the excited electron in the dye must match at least with bottom of the conduction band of the semiconductor.

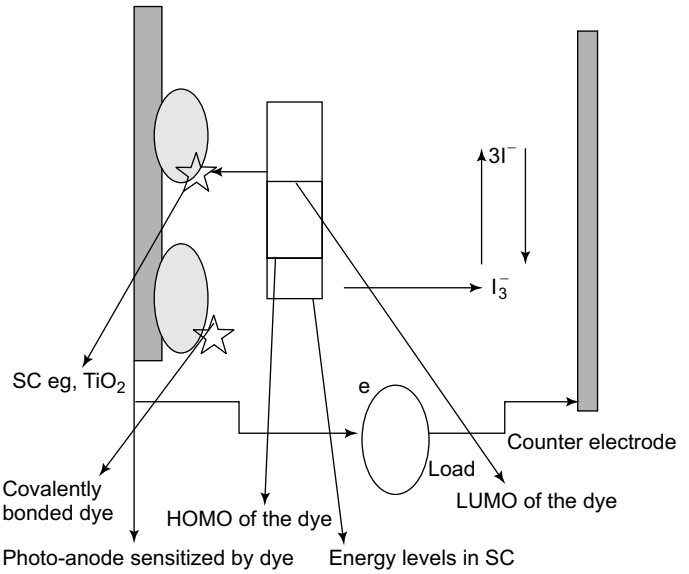

Figure 4.1 ***Schematic diagram of a dye sensitized solar cell. The photo-anode consists of semiconductor usually TiO_2 and occasionally, ZnO or other semiconductors to which the dye is covalently attached and the photon absorption by the dye gives rise to electron injection into the semiconductor conduction band from where it is transported in the external circuit through the load to the cathode which is conventionally carbon supported metal system which injects the electrons to carry out the reduction reaction in the tri-iodide/iodide couple I_3^- / I^-. Other couples or electron shuttles can be employed to facilitate the electron reinjection into the dye. A variety of electrolytes have been employed.***

(ii) Since the electrons are directly injected into the conduction band of the semiconductor from the excited state of the sensitizers, the hole-electron recombination within the semiconductor does not take place or at least less likely.

(iii) The choice of the semiconductors are based on the spectral region where the absorption of photons can take place and it is usually preferred to extend the absorption region as low energy as possible namely to visible and IR region. Hence the molecular structures of the sensitizers are chosen such that they will have absorption in the spectral region of the choice.

(iv) Since sensitizers (for this presentation it can be read as dyes) and the semiconductor are in electrical contact, there can be alterations of the electronic energy levels at the interface and it is preferable that the electron energy state in the sensitizers must be on par with that of the energy of the bottom of the conduction band of the semiconductor. This

means that the energy band positions must be suitably altered at the semiconductor/sensitizer interface. This brings us to a limitation that the sensitizers chosen should be such that their energy levels of the excited electrons should be capable of stabilizing the bottom of the conduction band edge. This is usually termed as moving the bottom of the conduction band edge downwards or negative conduction band shift due to favourbale dipolar field exerted by the sensitizer to the semiconductor. This may be at variance to conventional metal ion containing sensitizers like heteroleptic Ru(II)-dyes for which an opposite dipole effect has been reported thus increasing the value of the open circuit voltage, V_{OC} [32].

(v) In a recent publication, [33] there has been an attempt to use an inverse sensitized photo-cathode in combination with the conventional sensitized photo-anodes (where electron injection was conceived to take place) so as to increase photon to electron yield several times as compared to the conventional n-DSCs. This type of tandem pn-DSCs may be one of the possible alternatives however, it should be remarked that the available dyes for p-DSC are till now poor performers and hence there is a need to develop new systems which can function in this mode. These authors claim that the donor-acceptor dyes, studied as photo-cathodic sensitizers, comprise a variable-length oligothiophene bridge, which provides control over the spatial separation of the photo-generated charge carriers.

(vi) It is appropriate that some comments are also available in the nature and structure of the sensitizers that have been tried for DSSC. The logic for

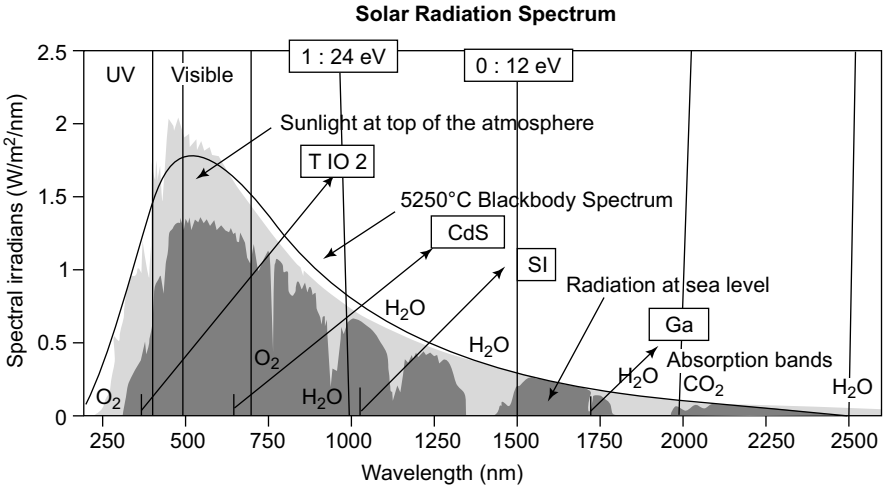

Figure 4.2 ***The typical solar spectrum with relevant details marked in terms of energy and some typical semiconductor absorption maximum***

the selection of sensitizers must be (i) the required excitation energy must fall in the IR or visible region so that most part of the solar spectrum can be used. It means one has to have a fair idea of the available solar spectrum which is shown in Fig. 4.2. (ii) The chosen sensitizer should be capable of covalently bonded to the semiconductor employed.

(i) As mentioned elsewhere, there must be appropriate energetic position of the conduction band of the semiconductor which must be overlapping with the excited state energy of the electron in the sensitizer.

(ii) The hole electron recombination within the sensitizer should be minimum, this can be achieved to an extent from smaller size (length in case of polyene dyes) of sensitizers or in other words the electron path in the dye system should be as short as possible so that the electron is injected into the semiconductor before recombination takes place.

(iii) The sensitizers in the excited state should not prefer the de-excitation route through intermolecular interaction with the acceptor species in the electrolyte.

(iv) The dyes in general used in DSSCs tend to degrade over time, thus leading to decreased efficiency and also the life time of the dyes are also limited and hence needs replacement of costly dyes. Attempts are being made to enhance the life time of the dyes in DSSCs in a variety of ways [34, 35] and it is hoped that the stability problems may eventually be overcome in the near future.

(v) Even though it is generally claimed that the DSSCs are affordable in terms of cost, it is to remarked that most of the contemporary DSSCs use complexes of the relatively rare metals like ruthenium or osmium and other noble metals as sensitizing species which may not be amenable for large scale applications. Research efforts are made for designing alternate dyes including metal-free organic and natural dyes [36-38]. However, it should be remembered that metal free and natural dyes are generally show lower efficiencies as compared to the metal containing dyes [6, 38, 39-42].

(vi) The reported efficiencies of dyes sensitized solar cells are in the range of 5-11%. This is lower than most other solar cells like solid state photo-voltaics. DSSCs with metal free sensitizers show lower efficiencies in the range of 5%. The reason for this may be that metal free dyes may show high molar extinction coefficients (50,000-20,000 $M^{-1}cm^{-1}$) but narrow range of absorption ($\Delta\lambda \approx 250$ nm) while metal containing dyes may show low molar absorption coefficient (5000-20,000 $M^{-1}cm^{-1}$) but fairly broad absorption spectra ($\Delta\lambda \approx 350$ nm)[43]. The overall conversion efficiency of the dye sensitized cell is

normally estimated form the measured values of photocurrent measured at short circuit current, I_{SC}, the open circuit photo-voltage, V_{oc}, the fill factor of the cell (ff) and the intensity of the incident light (I_S) and is given as =[I_{Ph}.V_{oc}. (ff)]/I_S. The search for the type of dyes employed for sensitization has centred around the following points: The dyes normally employed in DSSCs have good capacity to convert a photon into an electron almost around 80% efficiency. This limitation can indicate that the DSSC based arrays may have to be sufficiently larger than solid state photovoltaic arrays to produce the same amount of power. However this disadvantage is offset by the lower cost and greater construction flexibility of DSSCs. Any improvement in efficiency will make DSSCs to be competitive to other types of energy conversion devices. Since DSSCs employ a liquid electrolyte, its operation at lower temperatures will be of still lower efficiency and also will lead to other problems due to freezing of the electrolyte [44] Even though alternatives that would prevent the freezing problem are being considered, it is unlikely that DSSCs will probably be suitable for cold climates in the near future. The net conversion efficiency of the DSSC depends on the dynamics of the various processes that take place in the cell. Unfortunately all the possible processes in a DSSC are not of the same time scale and hence some processes proceed faster than others and hence the net conversion efficiency does not reach high and desirable levels. Secondly the electron has to be transported from the excited state of the dye to the conduction band of the semiconductor and there-from it is transported in the external (load) circuit to the cathode where it reduces the charge carriers which regenerate the dye from its oxidized state. Generally the diffusion length of the electron controls this process and the diffusion length is given by the equation, $L_n = (D_n \times \tau_n)^{1/2}$ where D_n is the diffusion coefficient of the electron, τ_n is the life time of the electron. It is therefore necessary that we know the time scales of the various processes that take place in a DSSC. Some estimates of these times are given in terms of the values of rate constants in Table 4.1.

The second important parameter of concern is the life time of the dye and various governing criteria have been evolved either in terms of number of cycles (a figure 50 million cycles is claimed) or in terms of time of continuous exposure (this is of the order of 1000s hours) before the dye degradation sets in. (iii) There is always a concern on the nature of the dye with respect to the electrolyte medium employed. If the electrolyte medium is aqueous then the dyes chosen should have hydrophobic character so that they will be fairly well anchored on the semiconductor electrode. (iv) For improving the

Table 4.1 ***Values (in ranges) of the rate constants (in*** $sec^{-}1$***) for the various electron transfer process in a dye sensitized solar cell.***

Specific Electron Transfer Process in DSSC	*Values(ranges) of Rate Constant in* sec^{-1}
Electron excitation in the dye	10^8 - 10^{10}
Electron transfer from excited state of the dye to the semiconductor (electron injection)	10^10 - 10^12
Back electron transfer from semiconductor to the dye	10^6 - 10^7
Electron transfer from semiconductor to external circuit	10^0-10^2
Oxidized state to the reduced state in the electrolyte at the cathode	10^8 - 10^9
Direct electron transfer in the electrolyte at the anode	10^8 - 10^1

stability of the DSSC (either with respect to temperature or chemicals) solid state gel or polymer gel electrolyte or melt of multiple salts have been employed. These studies showed some improvements in terms of efficiency, however, improving the efficiency alone cannot be considered as a sole criterion for designing DSSCs. (v) Designing of appropriate dyes for DSSCs (either with or without metal linkages) has been made by a variety of ways. The main factors considered in these studies include the HOMO-LUMO energy gap in the dye (usually estimated through semi-empirical quantum mechanical calculations like DFT or variations thereon [45]), the estimation of the life time or properties (dipole moment) of the excited states of the dye and other relevant spectroscopic properties. (vi) In order to increase the light harvesting in DSSCs electron relay dyes have been employed where in the excitation takes place in energy relay dye from which the transfer takes place by Foster energy transfer process to the sensitizing dye. This architecture permits broader spectral absorption, increase in the amount of the dye loading and gives rise to flexible design features for the DSSCs. An increase of nearly 25% in power conversion efficiency has already been achieved [43]. (vii) The degradation of the dye and the long term durability of the DSSCs are other factors of concern and it has been briefly mentioned above. Conventional photon induced de-carboxylation or decomposition

may take place and it is possible that one can device methods to restrict this kind of degradation. However, it should be remembered that the dye molecules are in the presence of relay species which can be I^-/I^{3-} (alternatively Br^-/Br^{3-}) or other amine in the electrolyte and these can also induce (or at least promote) the degradation of the dye. Since the DSSCs cannot be operated without these kinds of electrolyte media, more attention is needed on the dye degradation process [46].

4.4 THE SEMICONDUCTOR ELECTRODE

The commonly used anode material is based on TiO_2 (ZnO is also employed and a variety of other materials are also employed [47-58]) for the following reasons. (i) The energetics of the conduction band of TiO_2 is well established and hence the appropriate dye could be employed so that the electron transfer from the excited state of the dye can be facilitated. This transfer probably restricts the recombination of the electron with the hole generated. (ii) Since this transfer has to take place between the dye and the semiconductor, the dye should be capable being adsorbed on the semiconductor and also the coverage (θ) by the dye on the semiconductor should be almost near to 1, since otherwise, the photon will be absorbed or scattered (loss) by the semiconductor. (iii) The semiconductor employed must be amenable for surface modification so that the dye molecule can be easily anchored on the surface and also the excitation energy (the difference between HOMO and LUMO levels of the dye) can be suitably modulated so that the absorption range can be extended to visible and even to IR region of the solar spectrum [59].

4.5 ELECTROLYTE

The electrolyte and the medium to be used in DSSC generally control the potential of the positive electrode. In any form of electrochemical cells, the electrolyte has a significant role in the electron transfer since the medium permits the diffusion of the redox species forth and back to the counter electrode. Generally, high conversion efficiencies are reported in DSSCs in which electrolyte is an acetonitrile solution of iodine ions (I^-/I_3^-). The physical properties of the organic medium in this case acetonitrile (like melting/boiling point and the decomposition potential) control the concentration (due to evaporation at higher temperatures or decomposition due to potential) and hence causes drop of conversion efficiency at higher temperatures or with long-term use. Alternate methodologies have also been tried like sealing the electrolyte (that controls the evaporation loss) solidification of the electrolyte or employing solid electrolytes like CuI or CuSCN, Conductive polymers like polypyrrole, low molecular weight materials like triphenyldiamine or amorphous organic compounds. At this moment, the selection of electrolyte

does not seem to attract much attention though there are sporadic reports on the use of alternate electrolyte medium.

4.6 COUNTER ELECTRODE

The counter electrode acts as the conduit for the return of the electron to the dye. Since the electrolyte can be corrosive, it is essential that the material of the counter electrode is fairly corrosion resistant, and is also capable of reducing tri-iodide to iodide ion. The appropriate material can be conductive glass electrode having a dispersion of Pt. However carbon electrodes and conductive polymers can also be the alternate choices. However, these materials cannot come up to Pt in terms of the reduction rate.

4.7 PACKAGING OF THE DSSCs

It is known that this technology is threatening to be commercially viable for a number of years in recent times. This means a neat packaging of this technology must be in place if this technology were to be adopted for energy conversion process. Since packaging may lead to efficiency loss, it is necessary to encapsulate DSSC appropriately like in optical nanofibers [60, 61]. Various single cell configurations for long term stability and also for grid connection possibilities are being examined with plastic substrate [62, 63].

4.8 POSSIBLE ROUTES FOR ELECTRON TRANSFER IN DSSC

The values of rate constants of for electron transport in DSSC have already been considered in an earlier section. It is essential that one considers the dynamics of this transport both from the points of view of electron transport feasibility and also the flexibility. This section addresses these aspects in some detail. A pictorial representation of the various possible processes for the electron excitation, de-excitation, electron injection, transport, recombination, and utilization in regeneration is given in Fig. 4.3. The photon is absorbed by the dye and the electron is excited from the HOMO level of the dye to the LUMO level of the dye. The excited electron from the LUMO level of the dye is injected into the conduction band of the semiconductor. This injection rate constant is assumed to be of the order of $5 \times 10^{13}\mathrm{s}^{-1}$ for perylene derivatives [64] and it is of the order of $4 \times 10^{14}\mathrm{s}^{-1}$ for Ru complexes. It is also assumed that the injection rate of the electrons from the sensitizer to the semiconductor is of the same order of magnitude in both electrolyte and solid state solar cells. However it should be remarked that the transfer rate may depend on the density of states in the conduction band of the semiconductor and also the symmetry of the wave functions that constitute the electronic states in the

conduction band of the semiconductor. The excitation in the dye takes place in femto-second time scale while the charge injection from the excited state dye D^* to the conduction band of the semiconductor (typically in TiO_2 (CB) takes place in sub-pico second time scale. This statement of the time scales is based on the assumption that the excited state dye does not undergo intra-molecular relaxation which not only can alter the time scale of electron injection but also may complicate the injection process itself.

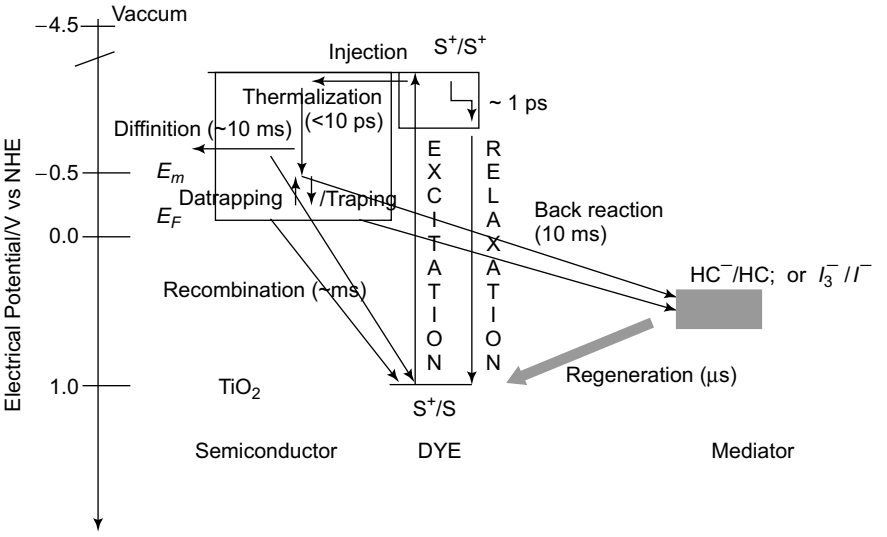

Figure 4.3 ***Schematic representation of the various possible processes for the generation, transfer, recombination of the electron that is electron transfer processes occur in parallel and in competition in DSSC [adopted from ref. 64]***

The electrons in the semiconductor can be thermalized by lattice collisions and phonon emissions in the time scale of femto-seconds. If the relaxation of the excited state dye takes place in the time scale of nanoseconds, then the efficiency of electron injection process in the semiconductor can become nearly unity. In this case the excited state dye has to be regenerated by the iodide ions from the mediator. This process will be in the domain of microsecond. This regeneration may prevent the recombination of the electron from conduction band of the semiconductor with the HOMO level of the dye which could be in the range of mill-second time scale. This favourable time scales facilitate the electron percolation and the capture of the electron by the oxidized relay namely I_3^- which takes place in millisecond or higher time scales. The processes that take place in a DSSC are given in the form of equations below:

$$D/TiO_2 + h\nu \rightarrow D^*/TiO_2(\text{Excitation of the Dye}) \qquad (4.1)$$

$$D^*/TiO_2 \rightarrow D^+/TiO_2 + e(CB\ TiO_2)\ \text{(Charge injection into SC)} \quad (4.2)$$

$$D^*/TiO_2 \rightarrow D/TiO_2 + h\nu + \Delta\ \text{(Relaxation)} \quad (4.3)$$

$$D^+/TiO_2 + 2I^- \rightarrow D/TiO_2 + I_2\ \text{(Regeneration of the dye)} \quad (4.4)$$

$$D^+/TiO_2 + \frac{3}{2}I^- \rightarrow D/TiO_2 + \frac{1}{2}I_3^- \quad (4.5)$$

$$D^+/TiO_2 + e(CB) \rightarrow D/TiO_2\ \text{(Recombination)} \quad (4.6)$$

$$\frac{1}{2}I_3^- + e^- \rightarrow \frac{3}{2}I^-; I_3^- + 2e \rightarrow 3I^-\ \text{Cathode reactions} \quad (4.7)$$

It may be appropriate if some general remarks are made on the statements made in this section

(i) The electron transfer routes outlined in equation (4.6) are only indicative of the various possibilities. It should not be considered exhaustive since the possibilities like the trapping of the electrons in defect or surface states of the semiconductor, and other possible electron transfers with impurities and other species present in the system are not considered and they can also contribute for the loss of efficiency.

(ii) The life times that are given are indicative and they may not be exact. In addition the life times given are for pure species namely the time indicated for the excitation in the dye is when the dye is in the isolated state while in the experiments the dye will be in the adsorbed state on the semiconductor and hence the time required for excitation can be different. This could be due to the fact that in the adsorbed state, the molecular structure of the dye molecule might have changed depending on how and with what functionalities the dye molecule is adsorbed on the semiconductor. Similar arguments may hold good for the mediator species as well.

(iii) Even though the reactions are shown in a sequence, the process can take place in a competitive and also concurrent manner thus accounting for the loss in efficiency.

(iv) The other parameters on which the rate of electron injection depends include the length of the spacer between the electron donor and acceptor, the density of acceptor states in the semiconductor, the interaction between the dye and the semiconductor (already mentioned). The total electron transfer rate is related to the density of states (DOS) at the appropriate energy relative to the bottom of the conduction band edge of the semiconductor, the reorganization energy and the temperature T. The electron injection in the semiconductor depends on the magnitude of DOS in the semiconductor in the conduction band. When the dye is adsorbed on the semiconductor (most probably through functional

groups (like carboxyl groups in the dye) the electron transfer essentially takes place between the π^* orbital of the sensitizer dye and the conduction band energy levels (which is essentially the unoccupied d states of the transition metal in the semiconductor for example Ti d states). Since the number of states in the conduction band of the semiconductor can be large (of the order of Avogadro number) the electron injection into the semiconductor takes place at a higher rate compared to the relaxation from the excited state to the ground state (that is relaxation through emission). It may be realized that this electron injection is the key for the higher efficiency and hence the choice of the semiconductor and the dye should be such that the energetic positions of the conduction band of the semiconductor and the energy of the excited state are appropriately matched.

(v) The injected electron is transported through the semiconductor to the back contact and this could be slower in the nano-crystalline semiconductor as compared to single crystal dye sensitized semiconductor.

(vi) The recombination of the electron with the excited state of the dye can occur over a time period of picoseconds to millisecond. This wide time scale arises due to the charge trapping possibilities by the localized surface states in the semiconductor. In addition the photon field may alter the energy states of the semiconductor (thus altering the position of the quasi Fermi level) and thus may favour the occupancy of the trap states.

(vii) The electron transport can also be controlled by the composition of the electrolyte employed and also the applied potential.

(viii) The recombination is also dependent on the nature and structure of the dye employed.

In the operation of DSSC, the regeneration of the dye is an important step. The life time of the cationic form of the dye can be of the order of milliseconds in the presence of pure solvents and can be altered by the nature of the electrolyte. The most widely employed redox system is I^-/I_3^-. The regeneration of the dye depends on the concentration of iodide ions. The relative energetic positions of the mediator and dye decide the open circuit potential achievable. Till now I^-/I_3^- redox system is the best electrolyte for DSSC. Efficiency of more than 11% with acetonitrile based electrolyte and 8% and long term stability with other low volatile electrolytes have been reported [65-68]. Other ionic liquids with fairly high ionic conductivity have also been examined like pure imidazolium I^-/I_3^- [69 -73]. Quasi solid electrolytes by gelation with aliphatic gels, polymer and even nano particles have also been examined for DSSC application [74-78]. Other redox couple that has also been

tried is Br^-/Br_3^- [79]. In addition hole conductors like CuSCN, CuI, organic hole conductors like triarylamines, polymer hole conductors like poly (3-alkyl thiophene, polyaniline) have also been tried in DSSC [80-88].

4.9 CURRENT VOLTAGE CHARACTERISTICS OF DSSC

The standard illumination on a DSSC is usually referred as AM 1.5 with an intensity of $1000 W/m^2$ also referred to as 1 sun. This spectrum corresponds to sunlight that passes through the atmosphere 1.5 times longer than when the sun is directly overhead. The current voltage characteristics of DSSCs are monitored under standard illumination conditions by varying the external load from zero value (short circuit condition) to infinite load (open circuit condition). A parameter called fill factor is defined as follows:

$$FF = J_{powermax} \times V_{powermax} / J_{sc} \times V_{oc} \tag{4.8}$$

The solar cell efficiency is given by the ratio of the power generated and power of the incident light

$$\eta = P_{out}/P_{in} = (J_{sc} \times V_{oc} \times (FF)/P_{in} \tag{4.9}$$

Another parameter of relevance is the Incident Photon to Current Conversion Efficiency (IPCE) which denotes how efficiently the light of a particular wavelength is converted into current and is given by the expression

$$\begin{aligned} IPCE &= h \times c/\lambda \times J_{sc}(\mathrm{mA/cm^2/q})/P_{in}(\mathrm{mW/cm^2}) \\ &= 1240\, J_{sc}(\mathrm{mA/cm^2})/\lambda nm.P_{in}(\mathrm{mW/cm^2}) \end{aligned} \tag{4.10}$$

The parameter Absorbed Photon to current conversion efficiency (APCE) denotes how efficiently the absorbed photons are converted into current, the IPCE and APCE are related to each other through light harvesting efficiency (LHE), Transmittance (T) and Absorbance (A) according to the following equation

$$APCE(\%) = [IPCE(\%)/LHE(\%)] \times 100\, LHE = 1 - T\ \&\ T = 1 - 10^{-A} \tag{4.11}$$

IPCE itself can be expressed as

$$IPCE(\%) = LHE \times \Phi_{inj} \times \eta_{reg} \times \eta_{cc} \tag{4.12}$$

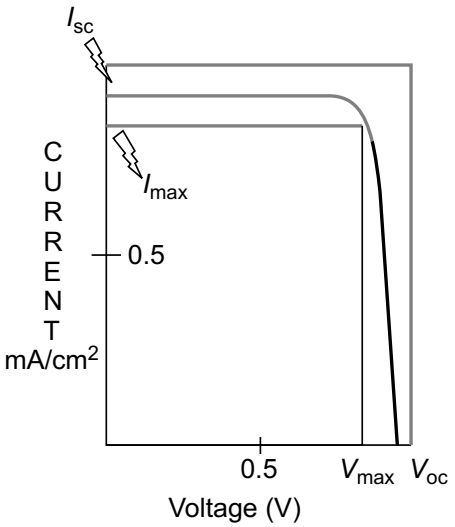

Figure 4.4 ***Typical representation of current Voltage characteristics of a DSSC denoting the short circuit current (J_{sc}), open circuit voltage V_{oc} Current at maximum power point (J_{max}) and voltage at maximum power point (V_{max}).***

Where $(\Phi_{inj}), (\eta_{reg})$, and (η_{cc}) denote the quantum yield of charge injection, dye regeneration and charge collection efficiency respectively. The efficiency of a DSSC can also be examined from another point of view. Essentially the efficiency of DSSC depends on how many photons are converted and collected in the external circuit in the form of electrical power. This conversion efficiency (IPCE)(λ)(incident photon to current efficiency) depends on three factors namely, the light harvesting efficiency (LHE) which denotes the number of photons absorbed by the dye, the electron injection efficiency (Φ_{inj}) which is a measure of how many absorbed photons result in injection of electrons into the semiconductor, (this probably accounts for the return of the excited of the dye to the ground state) and charge collection efficiency $\eta(c)$ (probably accounts for the loss in the semiconductor itself without transfer to the external circuit).

$$IPCE(\lambda) = LHE(\lambda) \times \Phi_{inj} \times \eta c \tag{4.13}$$

All of three processes in the DSSC are kinetic in nature and hence their efficiency is determined by how fast they occur relative to competing processes like de-excitation of the dye, electron loss in the semiconductor and processes internal to the system. One has to therefore consider the essential characteristics of the dye since the photon to electron conversion critically depends how best the dye absorbs the photon.

4.10 DYE CHARACTERISTICS

In this section, the important characteristics of the dye will be considered in addition to what has already been discussed in the section on sensitizers (subsection 3) The light harvesting dye is clearly the crucial and central component of the DSSC design. These dyes need to fulfill several functions: adsorption onto metal or semiconductor surface, its absorption spectrum must overlap effectively with the solar spectrum, the dyes should be capable of injecting electrons efficiently into metal oxide and must be stable for many cycles. These aspects have been already outlined. Adsorption of the dye onto the metal oxide surface is normally facilitated by inclusion of a functional substituents that will adsorb readily. In the case of metal complexes like ruthenium species, ligands which have capacity to bind to the metal ions, are preferred, the well studied ligands are those containing carboxyl-substituted ligands. The possibility of adsorbing the ruthenium complex on TiO_2 surface is shown pictorially in Fig. 4.5. It is given as an example for the process of adsorption and one can visualize alternate modes of adsorption of the dye on the semiconductor surface.

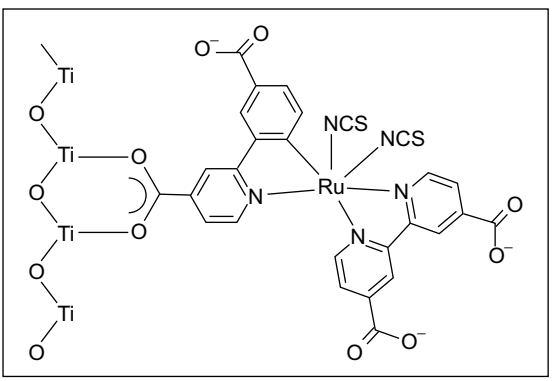

Figure 4.5 ***Typical and possible bonding scheme of the ruthenium based dye with the TiO_2 surface.***

In the table given in the appendix to this chapter the typical listing of the sensitizing species so far employed and their structures are given. It may be conceived that these species will be adsorbed on the semiconductor surface (TiO_2, or ZnO or any other semiconductors) through the functional groups contained in them. The spectral absorption of the dye or adsorbed sensitizer should be such that it overlaps with the solar spectrum so that as much of the sun's energy as possible is utilized in exciting the sensitizer. Most of the dyes or sensitizers normally employed in DSSCs absorb in the visible and near infrared region (in the region 400 to 700 nm), capturing about half the available power and a third of the available photons from the

solar radiation. The ruthenium complexes which are currently employed as sensitizers have a limitation in that their extinction coefficients (approxmately 2×10^4 $M^{-1}cm^{-1}$) are comparatively low. This means that one must have sufficient number of sensitizers adsorbed on the semiconductor surface thus necessitating the metal oxide semiconductors have to be prepared with very high surface areas. It is expected that normally efficiencies of greater than 15% is preferable, the designed DSSCs will have to absorb about 80% of light between 350 to 900 nm. In order to extend the spectral region, complexes of osmium has been examined in place of ruthenium, which extended the absorption further into the low energy red region and enhanced the response of the cell to light relative to the ruthenium analogues. The charge transfer transitions in osmium are more intense than in ruthenium complexes. Organic dyes have also been used successfully as seen from the data given in the table in the appendix. For facile electron transfer from the excited state of the dye to the semiconductor, it is necessary that the energy of the excited state of the dye is suitable with respect to the bottom of the conduction band of the semiconductor so that energetically the electron transfer process will be a downhill process in addition the electron injection process into the semiconductor must be faster than the relaxation process in the excited state of the dye by luminescence or non-radiative decay. It has been pointed out elsewhere in this presentation the relative time scale of each of these processes. In the case of ruthenium species, the injection takes place in the time scale of femto second while the decay process is taking place leisurely in the sub-picosecond time scale. However as pointed out earlier, it is necessary to assess if these time scales determined in the molecular scale will be applicable to the adsorbed state [89]. Nevertheless, the very fact that fairly efficient DSSCs are available supports these contentions, it is necessary that caution is required in ensuring that efficiency of the DSSCs is not reduced by other design factors of the cell. One way of ensuring that the dye or sensitizer absorbs sufficiently in the red region, one has to lower the LUMO level of the dye or sensitizer, but this option has to be carefully considered since this lowering cannot be done in such way that the LUMO is lower than the conduction band of the semiconductor and also the position of LUMO level should be such that facile electron injection will take place without considerable activation barrier. In a recent publication, the group from Stanford has coupled luminescent choromophores which absorb high energy photons and pass their energy to the sensitizing dyes. These options possibly can show some improvement in the net efficiency [43].

4.11 SEMICONDUCTOR MATERIAL

After the successful injection of the electron into the semiconductor, the electron should be transported in the external circuit through the load to

the working electrode. Semiconductors like TiO_2 or ZnO are the common material employed in DSSCs. The normal criterion for the choice of the type of semiconducting material is that they must be relatively inert, cheap, and must be amenable for flexible and scalable synthesis with high surface area. The factors that contribute to the choice of anatase form of TiO_2 as the choice of the semiconductor are: (i) Anatase has a higher band gap (3.2 eV) as compare to rutile (3.0 eV). Hence the anatase phase absorbs limited range of the solar spectrum and the remaining region is available for absorption by the sensitizer. (ii) The recombination of the electron with the hole in the valence band is slower than it has been observed with Rutile form. It must be remarked that the multilayer semiconductors with varying nm sized particles have been advocated as best materials from the point of view of increasing the exposed surface area which could sustain considerable layers of the sensitizer molecules so that improved Photon absorption conditions could be ensured. The time taken for the electron to percolate through the external circuit to the transparent conducing electrode is of the order of 100s of microseconds. Even though this time scale is longer, it is lower than the conduction band dye recombination or other conduction band decay process within the semi conductor. In order to effectively transfer the electron in the external circuit it will be advantageous to employ one dimensional nano tubes or nano rods rather than bulk materials. These configurations can be expected to facilitate vectorial transfer of charge [90]. This aspect may be addressed in the future [90].

4.12 ELECTROLYTE AND REGENERATION

The electrolyte contains the redox couple, which regenerates the oxidized dye D^+ which was formed by the injection of electron from the dye to the semiconductor layer. The redox couple should be efficient enough at reducing the dye cation (D^+) back to the original state for another cycle, but should not intercept or capture the electrons being injected. The most commonly employed redox couple for this electron transfer is tri-iodide/iodide (I_3^-/I^-) system for the transfer of electron from the conduction band of the semiconductor to the oxidized form of the dye or sensitizer. Even though the time scales of this electron transfer process in the tri-iodide/iodide couple may be favourable for the DSSC application, the redox chemistry of tri-iodide/iodide couple is not very well understood even now. This places some restrictions in the selection of appropriate dyes as sensitizers. One of the alternate possibilities may be to use solid state redox couples. This may allow the use of higher concentrations of the redox couple and possibly can extend the applicability of the device.

4.13 SUMMARY

Dye-sensitized solar cells is receiving considerable attention in recent times and threatening to be one of the possibilities for alternative renewable energy converter. The principle of operation is to harvest light efficiently by a sensitizer and pass on the energy to a semiconductor surface, which connects to an external circuit generating current. The light harvesting dye is regenerated by means of a suitable redox couple. It appears that each of the process steps in DSSC like the electron excitation, electron injection into the semiconductor, electron transport in the external circuit, the redox species that facilitates the back transfer of the electron to the sensitizer, and the times scales for each of these processes can offer a wide variety of options and examining them and making an appropriate combination appears to be the job on hand in this exciting area.

References

1. Frank E. Osterloh, Chem. Mater., 2008, 20 (1), 35-54; Chnm. Soc. Rev., 2013, 42, 2294.
2. http://en.wikipedia.org/wiki/Dye-sensitized_solar_cell
3. Michael Grtzel, "Photoelectrochemical Cells", Nature, Vol. 414, 15 November 2001.
4. Michael Grtzel, "Solar Energy Conversion By Dye-Sensitized Photovoltaic Cells", Inorganic Chemistry, 2005, Vol. 44, issue 20 6841-6851.
5. Jiu Kawakita, Trends of research and development of Dye-sensitized solar cells, Science and technology Trends, original Japanese version was published in 2009 see also http://www.nistep.go.jp/achiev/ftx/eng/stfc/stt035e/qr35pdf/STTqr3505.pdf
6. N. Sekar and Visal Y. Gehlot, Metqal complex dyes for dye sensitized solar cells: Recent Developments, Resonance, 819-831 (2010).
7. Gratzel, M. (2003). "Dye-sensitized solar cells", Journal of Photochemistry and Photobiology C: Photochemistry Reviews 4: 145. doi:10.1016/S1389-5567(03)00026-1. http://photochemistry.epfl.ch /EDEY/DSC_review.pdf.
8. Brian O'Regan, Michael Grtzel (24 October 1991). "A low-cost, high-efficiency solar cell based on dye-sensitized colloidal TiO_2 films". Nature 353 (6346): 737-740. doi:10.1038/353737a0
9. M. K. Nazeeruddin, A. Kay, I. Rodicio, et al., Conversion of light to electricity by cis-Xbis(2,2-bipyridyl-4,4-dicarboxylate)ruthenium(II)

charge-transfer sensitizers (X=Cl, Br, I, CN, and SCN) on nanocrystalline TiO_2 electrodes, Journal of the American Chemical Society, Vol. 115, No. 14, pp. 6382-6390, 1993.

10. G. Sauv, M. E. Cass, G. Coia, et al., Dye sensitization of nanocrystalline titanium dioxide with osmium and ruthenium polypyridyl complexes, Journal of Physical Chemistry B, vol. 104, no. 29, pp. 6821-6836, 2000.
11. Tamotsu Horiuchi, Hidetoshi Miura and Satoshi Uchida, Highly efficient metal-free organic dyes for dye-sensitized solar cells, Journal of Photochemistry and Photobiology A: Chemistry, 164, 29, (2004).
12. A. Kay and M. Graetzel, Artificial photosynthesis. 1. Photosensitization of TiO_2 solar cells with chlorophyll derivatives and related natural porphyrins, The Journal of Physical Chemistry, Vol. 97, No. 23, pp. 6272-6277, 1993.
13. F. Odobel, E. Blart, M. Lagre, et al., Porphyrin dyes for TiO_2 sensitization, Journal of Materials Chemistry, Vol. 13, No. 3, pp. 502-510, 2003.
14. M. K. Nazeeruddin, R. Humphry-Baker, M. Grtzel, et al., Efficient near-IR sensitization of nanocrystalline TiO_2 films by zinc and aluminum phthalocyanines, Journal of Porphyrins and Phthalocyanines, Vol. 3, No. 3, pp. 230-237, 1999.
15. J. He, A. Hagfeldt, S. E. Lindquist, et al., Phthalocyanine-sensitized nanostructured TiO_2 electrodes prepared by a novel anchoring method, Langmuir, vol. 17, no. 9, pp. 2743-2747, 2001.
16. W. Paw, S. D. Cummings, M. A. Mansour, W. B. Connick, D. K. Geiger, and R. Eisenberg, Luminescent platinum complexes: tuning and using the excited state, Coordination Chemistry Reviews, Vol. 171, No. 1, pp. 125-150, 1998.
17. A. Islam, H. Sugihara, K. Hara, et al., Dye sensitization of nanocrystalline titanium dioxide with square planar platinum(II) diimine dithiolate complexes, Inorganic Chemistry, Vol. 40, No. 21, pp. 5371-5380, 2001.
18. J. M. Rehm, G. L. McLendon, Y. Nagasawa, K. Yoshihara, J. Moser, and M. Grtzel, Femtosecond electron-transfer dynamics at a sensitizing dye-semiconductor (TiO_2) interface, Journal of Physical Chemistry, Vol. 100, No. 23, pp. 9577-9578, 1996.
19. P. V. Kamat and W. E. Ford, Photochemistry on surfaces: triplet-triplet energy transfer on colloidal TiO_2 particles, Chemical Physics Letters, Vol. 135, No. 4-5, pp. 421-426, 1987.
20. S. Das, C. S. Rajesh, C. H. Suresh, et al., Photo- physical and photoelectrochemical behavior of poly[styrene-co-3-

(acrylamido)-6-aminoacridine], Macromolecules, Vol. 28, No. 12, pp. 4249-4254, 1995.

21. D. Liu and P. V. Kamat, Photo-electrochemical behavior of thin CdSe and coupled TiO_2/CdSe semiconductor films, Journal of Physical Chemistry, Vol. 97, No. 41, pp. 10769-10773, 1993.
22. K.T. Ranjit and B.Viswanathan, Photocatalysis, Principles and some selected results,in Selected Studies in Heterogeneous Catalysis, Editor: B. Viswanathan, Department of Chemistry, Indian Institute of Technology, Madras (Chennai), India, pp. 150-178, May, 1996.
23. Cherepy, Nerine J.; Smestad, Greg P.; Grtzel, Michael; Zhang, Jin Z. (1997). "Ultrafast Electron Injection: Implications for a Photoelectrochemical Cell Utilizing an Anthocyanin Dye-Sensitized TiO_2 Nanocrystalline Electrode". The Journal of Physical Chemistry B 101 (45): 9342-51. doi:10.1021/jp972197w. http://solideas.com/papers/JPhysChemB.pdf.
24. Sancun Hao, Jihuai Wu, Yunfang Huang and Jianming Lin, Natural dyes as photosensitizers for dye-sensitized solar cell, Solar energy, 80, 209, (2006); M. S. Roy, P. Balraju, Manish Kumar and G. D. Sharma, Dye-sensitized solar cell based on Rose Bengal dye and nanocrystalline TiO_2, Solar Energy Materials and Solar Cells 92, 909 (2008)
25. Porphyrin-based photosensitizer dyes for dye-sensitized solar cells, United States Patent Application 20100125136
26. http://en.wikipedia.org/wiki/Dye-sensitized_solar_cell
27. Y-Z Zheng, X. Tao, Q. Hou, D. T. Wang, W. L. Zhou and J. F. Chen, Iodine doped Zno nanocrystalline aggregates for improved dye-sensitized solar cells, Chem. Mater., 23, 3 (2011)
29. Tamotsu HoriuchiJun-ichi FujisawaSatoshi UchidaMichael Gratzel, Data book on Dye-sensitized Solar Cells, CMC Publishing CO.,LTD (2008).
30. Patrocnio, A., Mizoguchi, S., Paterno, L., Garcia, C., and Iha, N. (2009). Efficient and low cost devices for solar energy conversion: Efficiency and stability of some natural-dye-sensitized solar cells. Synthetic Metals, 159(21/22), 2342-2344. doi:10.1016/j.synthmet.2009.08.027
31. http://www.elp.uji.es/juan_home/research/solar_cells.htm
32. Horiuchi T., Miura H.,and Uchida S. (2004). Highly efficient metal-free organic dyes for dye-sensitized solar cells. Journal of Photochemistry and Photobiology A: Chemistry, 164 (1-3), 29-32.
33. Chen P., Yum J. H., De Angelis F., Mosconi E., Fantacci S., Moon S. J., Baker R. H., Ko J., Nazeeruddin M., Grtzel M., Nano let., 2009 Jun; 9(6): 2487-92.

34. A. Nattestad, A. J. Mozer, M. K. R. Fischer, Y.-B. Cheng, A. Mishra, P. Buerle and U. Bach, Nature Materials, 9: 31 (2010)
35. Sommeling, P., Spth, M., Smit, H., Bakker, N., and Kroon, J. (2004). Long-term stability testing of dye-sensitized solar cells. Journal of Photochemistry and Photobiology A: Chemistry, 164 (1-3), 137-144. doi:10.1016/j.jphotochem. 2003.12.017
36. Nogueira, V., Longo, C., Nogueira, A., Soto-Oviedo, M. and Paoli, M. (2006). Solid-state dye-sensitized solar cell: Improved performance and stability using a plasticized polymer electrolyte. Journal of Photochemistry and Photobiology A: Chemistry, 181(2/3), 226-232. doi:10.1016/j.jphotochem.2005.11.028
37. T. Horiuchi, H. Miura, and S. Uchida, Highly efficient metal free organic dyes for dye-sensitized solar cells, Journal of photochemistry and photobiology, A Chemistry, 164, (2004) 29-32.
38. T. Horiuchi, H. Miura, K. Sumioka and S. Uchida, High eficency of dye sensitized solar cells on metal-free indoline dyes J.Am.Chem.Soc., 126 (2004) 12218.
39. C. Teng, X. Yang, C. Yuan, C. Li, R. Chen, H. Tian, S. Li, A. Hagfeldt and L. Sun, Two novel carbazole dyes for dye-sensitized solar cells with open circuit voltagtes upto to 1 V based on Br^{-}/Br^{3-} electrolytes, Organic Letters, 11 (2009),5542.
40. F. O. Lenzmann and J.M. Kroon, Recent advances in Dye sensitized solar cells, Advances in optoelectronics, (2007) Article ID 65073 DOI:1155/2007/76507.
41. Tannia Marinado, Ph.D. Thesis, Photoelectrochemical studies of dye-sensitized solar cells using organic dyes, School of chemical Science and Engineering, Kungliga Tekniska Hogskolar, Stockholm, (2009)
42. M. Sokolsky and J. Cirak, Dye-Sensitized solar cells: Materials and processes, Acta Electrochimca et informatica 10, (2010)78.
43. K. Hara, T. Sato, R. Katoh, A. Furube, T. Yoshihara, M. Murai, M. Kurashige, S. Ito, A. Shinpo, S. Suga and H. Arakawa, Novel conjugated organic dyes for efficient Dye-sensitized solar cells, Advanced functional Materials,15 (2005) 246 and references cited therein.
44. B. E. Hardin, E. T. Hoke, P. B. Armstrong, J-Hyum, P. Comte, T. Torres, J.M.J. Frechet, M.K. Nazeeruddin, M. Gratzel and M D McGehee, Increased light harvesting in dye-sensitized solar cells with energy relay dyes, Nature Photoniccs 3, (2009)406.
45. Nogueira, V., Longo, C., Nogueira, A., Soto-Oviedo, M., and Paoli, M. (2006). Solid-state dye-sensitized solar cell: Improved performance

and stability using a plasticized polymer electrolyte. Journal of Photochemistry and Photobiology A: Chemistry, 181(2/3), 226-232. doi: 10.1016/j.jphotochem.2005.11.028

46. B. N. Wong and J. G. Cordaro, Coumarin dyes for Dye-sensitized solar cells; A long range corrected density functional study.
47. H. Tananka et al., Solar energy Materials and Solar cells, 93, 1143 (2009)
48. He, J. J., Lindstrom, H., Hagfeldt, A. and Lindquist, S. E. Dye-sensitized nano-structured p-type nickel oxide film as a photocathode for a solar cell. J. Phys. Chem. B 103, 8940-8943 (1999).
49. Borgstrom, M. et al. Sensitized hole injection of phosphorus porphyrin into NiO: Toward new photovoltaic devices. J. Phys. Chem. B 109, 22928-22934 (2005).
50. He, J. J., Lindstrom, H., Hagfeldt, A. and Lindquist, S. E. Dye-sensitized nanostructured tandem cell-first demonstrated cell with a dye-sensitized photocathode. Sol. Energy Mater. Sol. Cells 62, 265-273 (2000).
51. Mizoguchi, Y.and Fujihara, S. Fabrication and dye-sensitized solar cell performance of nanostructured NiO/Coumarin 343 photocathodes. Electrochem. Solid State Lett. 11, K78-K80 (2008).
52. Morandeira, A., Boschloo, G., Hagfeldt, A. and Hammarstrom, L. Photoinduced ultrafast dynamics of coumarin 343 sensitized p-type-nanostructured NiO films. J. Phys. Chem. B 109, 19403-19410 (2005).
53. Morandeira, A. et al. Improved photon-to-current conversion efficiency with a nanoporous p-type NiO electrode by the use of a sensitizer-acceptor dyad. J. Phys. Chem. C 112, 1721-1728 (2008).
54. Mori, S. et al. Charge-transfer processes in dye-sensitized NiO solar cells. J. Phys. Chem. C 112, 16134-16139 (2008).
55. Qin, P. et al. Design of an organic chromophore for p-type dye-sensitized solar cells. J. Am. Chem. Soc. 130, 8570-8572 (2008).
56. Vera, F. et al. Preparation and characterization of Eosin B- and Erythrosin J-sensitized nanostructured NiO thin film photocathodes. Thin Solid Films 490, 182-188 (2005).
57. Zhu, H., Hagfeldt, A. and Boschloo, G. Photoelectrochemistry of mesoporous NiO electrodes in iodide/triiodide electrolytes. J. Phys. Chem. C 111, 17455-17458 (2007).
58. Nattestad, A., Ferguson, M., Kerr, R., Cheng, Y.-B. and Bach, U. Dye-sensitized nickel(II) oxide photocathodes for tandem solar cell applications. Nanotechnology 19, 295304-295313 (2008).

59. Nakasa, A. et al. A high voltage dye-sensitized solar cell using a nanoporous NiO photocathode. Chem. Lett. 34, 500-501 (2005).
60. H. Burcksummer et al, Organic letters, 12, 3666(2010)
61. Bourzac, Katherine (2009-10-30). "Wrapping Solar Cells around an Optical Fiber". Technology Review. http://www.technologyreview.com/energy/23829/. Retrieved 2009-10-31.
62. Benjamin Weintraub, Yaguang Wei, Zhong Lin Wang (2009-10-22). "Optical Fiber/Nanowire Hybrid Structures for Efficient Three-Dimensional Dye-Sensitized Solar Cells". Angewandte Chemie International Edition 48 (47): NA. doi:10.1002/anie.200904492. PMID 19852015
63. http://innovation.nikkeibp.co.jp/etb/20080228-00.html; and also large scale module for direct outdoor se[http://www.fujikura.co.jp/rd/field/mt.html.
64. Chrubin, Noumissing Sao, Dye-sensitized solar cells based on perylene derivatives, Dissertation, for the Degree Doctor of Natural Sciences, Universitt Kassel (2009).
65. P. Wang, C. Klein, R. Humphry-Baker, S. M. Zakeeruddin, M. Grtzel, J. Am. Chem. Soc. 2005, 127, 808
66. M. Grtzel, J. Photochem. Photobiol. A 2004, 164, 3.
67. P. Wang, C. Klein, R. Humphry-Baker, S. M. Zakeeruddin, M. Grtzel, Appl. Phys. Letts. 2005, 86, 123508
68. D. Kuang, C. Klein, S. Ito, J. E. Moser, R. Humphry-Baker, S. M. Zakeeruddin, M. Grtzel, Adv. Func. Mater. 2007, 17, 154.
69. P. Wasserscheid, T. Welton, Ionic Liquids in Synthesis; Wiley: Weinheim, Germany, 2002.
70. R. D. Dogers, K. R. Seddon, Science 2003, 302, 792.
71. J. Dupont, R. F. de Souza, P. A. Z. Suarez, Chem. Rev. 2002, 102, 3667.
72. W. Xu, C. A. Angell, Science 2003, 302, 422.
73. D. B. Kuang, P. Wang, S. Ito, S. M. Zakeeruddin, M. Grtzel, J. Am. Chem. Soc. 2006, 128, 7732.
74. W. Kubo, K. Murakoshi, T. Kitamura, Y. Wada, K. Hanabusa, H. Shirai, S. Yanagida, Chem. Lett. 1998, 27, 1241.
75. W. Kubo, S. Kambe, S. Nakade, Kitamura, T. K. Hanabusa, Y. Wada, S. Yanagida J.Phys. Chem. B 2003, 107, 4374.
76. P. Wang, S. M. Zakeeruddin, I. Exnar, M. Grtzel, Chem. Commun. 2002, 2972.

77. F. Cao, G. Oskam, P. C. Searson, J. Phys. Chem. 1995, 99, 17071.
78. P. Wang, S. M. Zakeeruddin, P. Comte, I. Exnar, M. Grtzel, J. Am. Chem. Soc. 2003, 125, 1166.
79. J. Desilvestro, M. Grtzel, L. Kaven, J. Moser, J. Am. Chem. Soc. 1985, 107, 2988.
80. B. O'Regan, F. Lenzmann, J. Phys. Phys. Chem. B 2004, 108, 4342.
81. B. O'Regan, F. Lenzmann, R. Muis, J. Wienke, Chem. Mater. 2002, 14, 5023.
82. B. O'Regan, D. T. Schwartz, S. M. Zakeeruddin, M. Grtzel, Adv. Mater. 2000, 12, 1263.
83. T. Taguchi, X. T. Zhang, I. Sutanto, K. Tokuhiro, T. N. Rao, H. Watanabe, T. Nakamori, M. Uragami, A. Fujishima, Chem. Comm. 2003, 2480.
84. A. Konno, T. Kitagawa, H. Kida, G. R. A. Kumara, K. Tennakone, Cuur. Appl. Phys. 2005, 5, 149.
85. G.R.A. Kumara, A. Konno, K. Shiratsuchi, J. Tsukahara, K. Tennakone, Chem. Mater. 2002, 14, 954.
86. H. Snaith, S. M. Zakeeruddin, Q. Wang, P. Pechy, M. Grtzel, Nano Lett. 2006, 6, 2000.
87. D. Gebeyehu, C.J. Brabec, N.S. Sariciftci, Thin Solid Film 2002, 403-404, 271.
88. S. Tan, J. Zhai, M. Wan, Q. Meng, Y. Li, L. Jiang, D. Zhu, J. Phys. Chem. B 2004, 14. 108, 18693.
89. ChunHung Law, Shehan C. Pathirana, Xaioe Li, Assaf Y. Anderson, Piers R. F. Barnes, Andrea Listorti, Tarek H. Ghaddar, Brian C. ORegan, Water-Based Electrolytes for Dye-Sensitized Solar Cells, Advanced Materials, 22, (2010), pages 4505-4509; Koops SE, O'Regan BC, Barnes PR, Durrant JR., Parameters influencing the efficiency of electron injection in dye-sensitized solar cells., J. Am. Chem. Soc., 2009, 131, 4808).
90. Pagliaro, http://photochemistry.wordpress.com/2009/08/17/dye-sensitised-solar-cells-dssc/ ; Nanochemistry aspects of titania in dye-sensitized solar cells, Pagliaro, M., Palmisano, G., Ciriminna, R. and Loddo, V., Energy Environ. Sci., 2009, 2, 838-844.
Advancing beyond current generation dye-sensitized solar cells, Hamann, T.W., Jensen, R.A., Martinson, A.B.F., Van Ryswyk, H and Hupp, J.T., Energy Environ. Sci., 2008, 1, 66-78.

APPENDIX (SELECTED DYES EMPLOYED IN DSSC)

Dye sensitized solar cells (in solution phase, or semi solid or in solid state alone) have been at the door step of commercialization. Si based solid state solar cells have been reducing the cost from nearly $4 per watt to nearly $1.25 per watt and it is expected to go down to $0.70 per watt. In this context one has to compare DSSC with these solid state solar cells at the same levels of efficiencies. This being a fast growing field with development on day to day basis, the coverage in this chapter may not be comprehensive or uptodate. Secondly, it should be remarked though DSSC modules have already been fabricated and possibly marketed too, a thorough understanding of the overall life times and degradation mechanisms of the new and developing DSSCs has yet to evolve. In addition, the module designs require further detailed investigation.It is appropriate if we can at least list some of the recent reviews in this field for the sake of interested readers. The market penetration details are available in the site: http://en.wikipedia.org/wiki/Dye-sensitized_solar_cell (data till 2013)

Some of the recent important references on DSSC In addition to the compilation by K.Kalyanasundaram, Dye Sensitized Solar Cells, EPFL Press (2010)

1. Brian E Hardin, Henry J. Snaith and Michael D.McGehee, The renaissance of dye sensitized solar cells, Nature Photonics, Vol.6,162 (2012)
2. Ajay Jena, Shyama Prasad Mohanty, Pragyensh Kumar, John Naduvath, Vivekanand Gondane, P. Lekha, Jaykrushna Das, Harsh Kumar Narula, S.Mallick and P.Bhargava, Dye Sensitized Solar cells, A Review, Transactions of the Indian Ceramic Society, 71,1-16 (2012)
3. Hongsik Choi, Changwoo Nahm,Jongmin Kim,Suji Kang, Taehyun Hwang and Byungwoo Park, Toward highly efficient quantum dot and dye sensitized solar cells, Current applied Physics, 13, S2-S13, 2013).
4. Juliana ds Santos de Souza, Leilane Oliverira, Martins de Andrade and Andre Sarto Polo, Nano materials for solar energy conversion: Dye Sensitized Solar cells Based on Ruthenium (II) Tris-Heteroleptiv compounds or natural dyes, Nano-energy, (F.L.De Souzs and E.R.Leite (Eds) Springer-verlag, Berlin Heidelberg (2013)
5. Amaresh Mishra, Markus K.R.Fischer and Peter Bauerle, Metal free organic dyes for Dye Sensitized solar cells: From structure:property relations to design rules, Angew. Chem. int. Ed., 48,2474-2499 (2009)
6. Jason B. Baxter, Coomercialization of dye sensitized solar cells: Present status and future research needs to improve efficiency, stability and manufacturing, Journal of Vacuum Science and Technology, 30,020801 (2012)

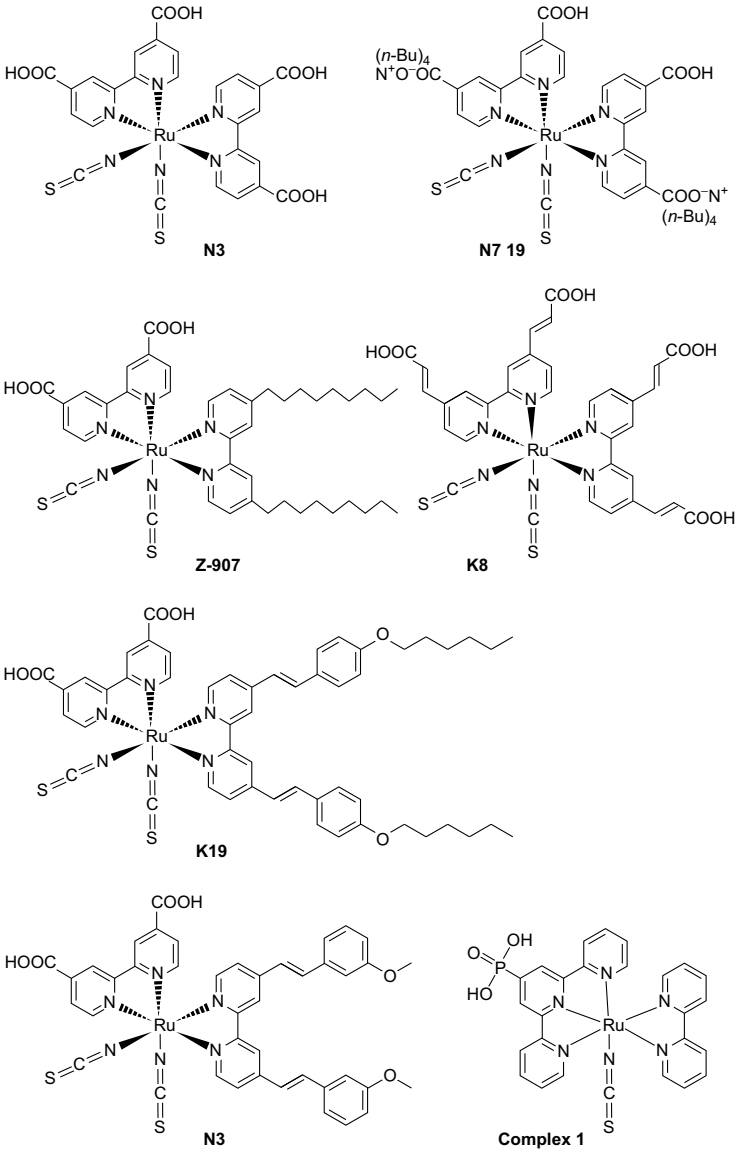

Figure 4.6 ***Molecular structures of the Ruthenium based charge transfer sensitizerin DSSC, especially N3, and N719, most commonly employed.***

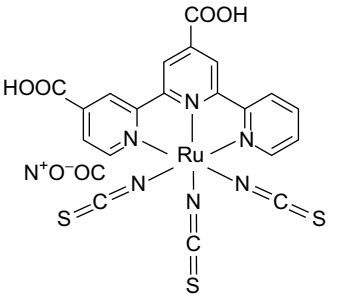

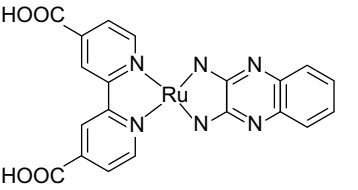

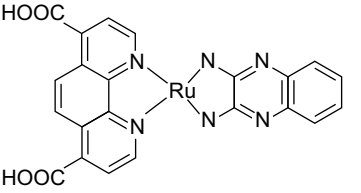

Complex 4
1.72%

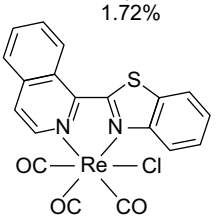

Complex 5
1.46%

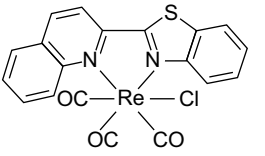

Complex 6
1.43%

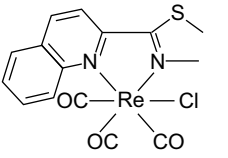

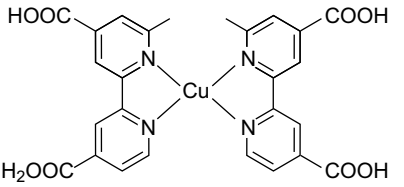

Complex 7 1.9%

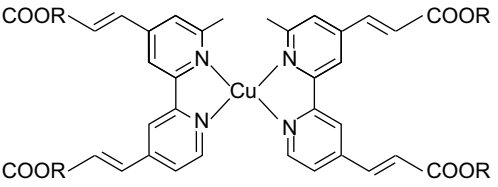

Complex 8 2.3%

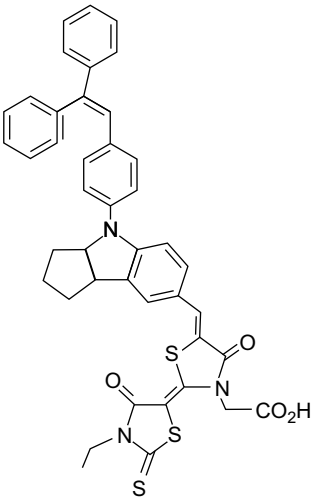
S
O
O
N
S
N
CO2H
N
S
S

(a)

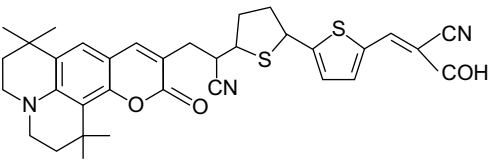
S
S
CN
COH
CN
N
O
O

(b)

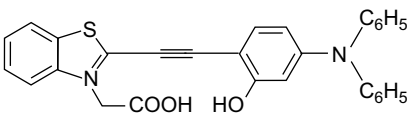
S
N
C6H5
N
C6H5
COOH
HO

(c)

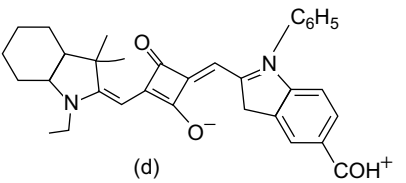
C6H5
O
N
N
O−
COH+

(d)

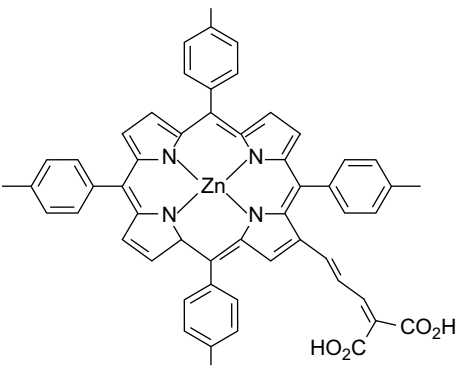
N
N
Zn
N
N
CO2H
HO2C

(e)

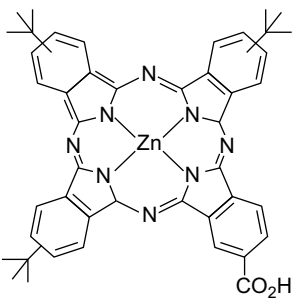
N
N
N
Zn
N
N
N
N
CO2H

(f)

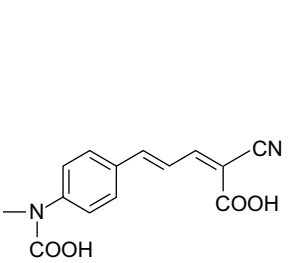

NKX-2553

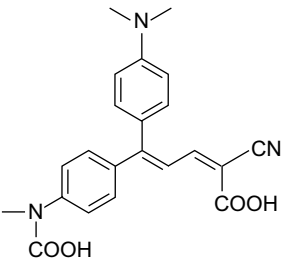

NKX-2553

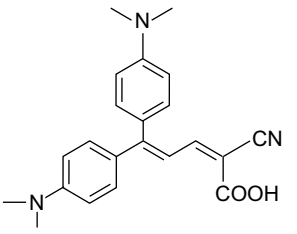

NKX-2569

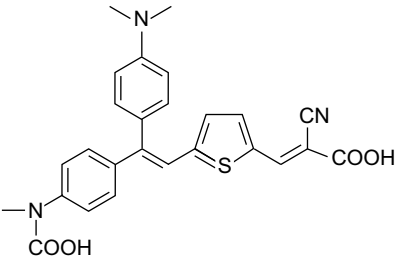

NKX-260*

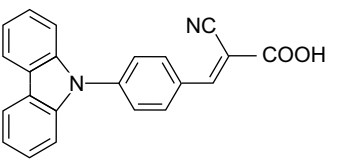

TC301

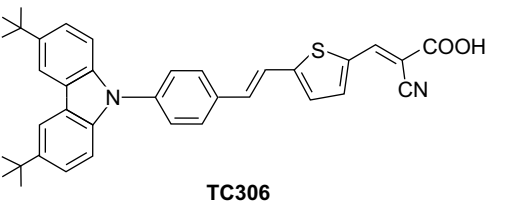

TC306

b

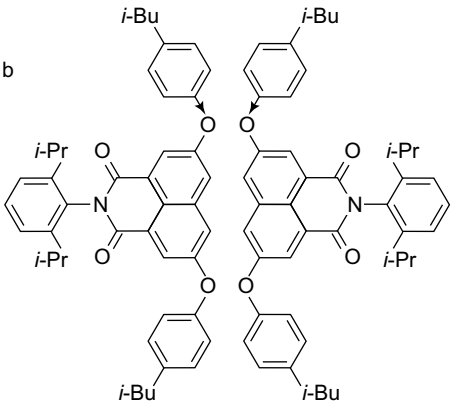

PICD1 (Energy relay dye)

c

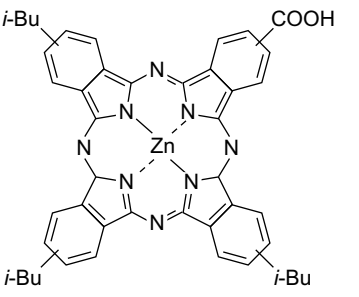

TT1 (Sensitizing dye)

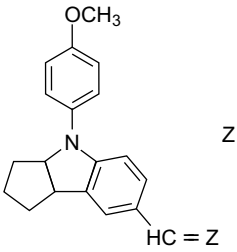

Z =

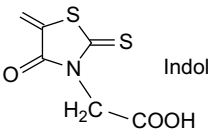

Indoline Dyes

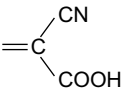

Indoline Dyes

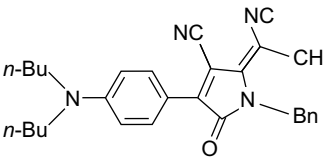

2:93%

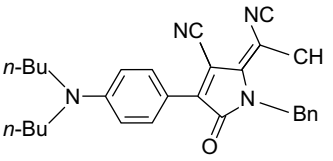

2:93%

5 Photocatalytic Decontamination of Water

5.1 INTRODUCTION

One of the major spin off of Photo-electrochemical decomposition of water in addition to the generation of hydrogen is the decontamination of water by photo-catalytic means. Photo-catalysis has been defined in various forms in other chapters of this monograph. However, it is necessary that the definition as given in Glossary of terms used in photo-chemistry is also stated in this text. It is defined catalytic reaction involving the production of a catalyst by absorption of light [1]. The relative positions of the top of the valence band (VB) and the bottom of the conduction band (CB) decide the oxidizing and reducing powers of the system. In the case of metals, since these two bands overlap, it can exhibit predominantly one of these two functions. Semiconductors and insulators can exhibit both oxidizing and reduction functions if electrons in CB and holes in VB are available. However, this situation requires higher energy photons in the case of insulators and hence the appropriate material for photo-catalytic behaviour is the semiconductors [2]. Semiconducting nanocrystalline materials especially nanocrystalline titanium dioxide (NTO) are multi-functional photo-catalysts that can be an energy conversion catalyst (for production of hydrogen from the splitting of water), an environmental catalyst (in water and air purification or can also function as electron transport medium in DSSC [3].

Over the last three decades there has been increasing global concern over the impact of environmental pollution on public health, and the suffering through various diseases. Various resources in our environment namely water, land and air have been continuously affected by pollution. Most of the diseases facing mankind today occur due to prolonged exposure to environmental pollution. However, most of the environment related diseases are not easily detected and may be acquired during childhood and become noticeable later in adulthood. In addition, pollution leads to depletion of the ozone layer, global warming and climate change. Furthermore, various flora and fauna in the contaminated region are either threatened or made extinct by the pollution. Most polluted

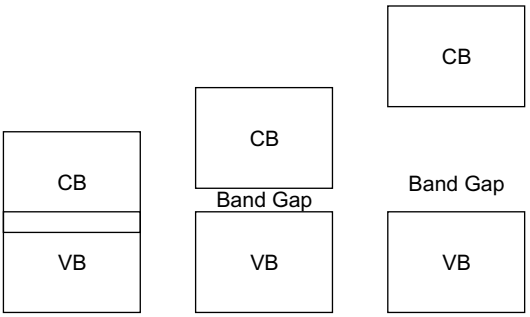

Figure 5.1 ***The positions of valence band and conduction bands in Metals, Semiconductors and Insulators.***

places in the world include China, India, Peru and Russia [4]. Indoor plus outdoor air pollution is the sixth-leading cause of death, causing over 2.4 million premature deaths worldwide [5].

5.2 WATER POLLUTION

Water covers over two thirds of Earth's surface and less than a third is taken up by land. As population of Earth continues to grow, there is ever-increasing pressure on the planet's land and water resources. Oceans, rivers, and other inland waters are being continuously polluted by human activities leading to a gradual decrease in the quality of water. Water pollution is mostly about the quantity of certain substances in water. If the concentration of a certain substance in water exceeds the specified limits, it is considered to be polluted. Water pollution has its impact on both surface water and ground water. Untreated sewage, industrial waste water, pesticides, fertilizers, heavy metals, radioactive waste, chemical wastes like polychlorinated phenols, dyes, oil and plastics are the major sources of water pollution. Water polluted by oil will devastate and affect the marine living organisms in the aqueous eco-system. Thus toxic species in water bodies indirectly enter our food chain through aquatic food. Data on recommended tolerance level of pollutants in water are given in Chapter 1.

The common pollutants in water can be classified into two types namely inorganic pollutants and organic pollutants. The common contaminants in the inorganic class are metal ions, nitrates, nitrites, ozone, ammonia, azides and halide ions.

Organic pollutants are generally oxidized to carbon dioxide,water and inorganic mineral acids. Typical class or organic pollutants are alkanes mostly propane and methane, chlorinated aromatics of the type chlorophenols, chlorobenzenes, chlorinated surfactants, chlorinated aliphatic compounds

like trichlormethane, CCl_4, CH_3Cl, chlor acetic acid, nitrogen containing compounds like nitrophenols, methylene blue, nitrobenzene, azobenzene, and other organics like acetone, benzene, ethylbenzene, methanol, ethanol, acetaldehyde and many other common organic substances. It may be worthwhile to realize the effect of some of these pollutants in the human health. A simple compilation is given in chapter 1.

5.3 METHODS OF WATER TREATMENT

Treatment of water involves three steps:

- Primary treatment: Physical processes that remove non-homogenizable solids and homogenize the remaining effluents.
- Secondary treatment: Biological processes that remove most of the Biological Oxygen Demand (BOD).
- Tertiary treatment: Physical, biological, and chemical processes to remove nutrients like phosphorus and inorganic pollutants like heavy metals. To decolourise organic pollutants present in effluent water, and to carry out further oxidation.

In order for the treated water to be discharged into a water body, it should be free from various soluble organic and inorganic species. These species cannot be removed by the primary and secondary treatments of water. Primary and secondary treatments are part of conventional waste water treatment plants. However, secondary treatment plant effluents are still significantly polluted with some BOD. Neither primary nor secondary treatment is effective in entirely removing phosphorus and other large organic compounds or toxic substances. Hence tertiary treatment is necessary to completely decontaminate the water. Various tertiary treatment methods are aerobic oxidation, super-chlorination, reverse osmosis, ultra filtration, UV treatment and Advanced Oxidation Processes (AOPs).

5.4 ADVANCED OXIDATION PROCESSES

This aspect has been briefly considered in Chapter 1. Methods which utilize hydroxyl radicals for carrying out the oxidation of the pollutants are grouped as Advanced Oxidation Processes. Irrespective of the method of generation of hydroxyl radicals, these processes are called Advanced Oxidation Processes. OH radicals are extraordinarily reactive species and have one of the highest oxidation potentials.(see values of oxidation potential of speices elsewhere in chapter 1) Hydroxyl radicals are known to attack the part of organic molecules with rate constant values of the order of 10^6 to 10^9 $M^{-1}s^1$ [7-9]. In addition, hydroxyl radicals have very little selectivity on the position of attack in a molecule, which is a useful aspect for an oxidant used in waste

water treatment. The fact that the production of OH radicals can be made by a variety of methods adds to the versatility of Advanced Oxidation Processes, thus allowing a better compliance with the specific treatment requirements. An important consideration to be made in the application of AOP to waste water treatment is the requirement of expensive reactants like H_2O_2 and/or O_3. Hence, the Advanced Oxidation Processes cannot replace the application of more economic treatments such as the biological degradation whenever possible. The typical values of second order rate constant for oxidation by ozone and hydroxyl radical for some typical compounds are given in Chapter 1. In Table 5.1 an expanded compilation of oxidant sources in AOP process is given though a similar compilation is available in Chapter 1.

Table 5.1 ***Oxidant Sources in Advanced Oxidation Process.***

Source of Oxidants	*Name of the Process*
H_2O_2/Fe^{3+}	Fenton
H_2O_2/Fe^{3+}	Fenton like
$H_2O_2/Fe^{2+}(Fe^{3+})/UV$	Photo assisted Fenton
H_2O_2/Fe^{3+}-oxalate	Not Applicable
Mn^{2+}/oxalic acid/Ozone	Not Applicable
$TiO_2/h\nu/O_2$	Photo-catalysis
O_3/H_2O_2	Not Applicable
O_3/UV	Photoassisted oxidation
H_2O_2/UV	photoassited oxidation

5.4.1 Fenton Process

This process involving Fe^{2+} ions and H_2O_2 was discovered by Fenton in the 19th century [10]. However, its application for the oxidation of pollutants in water started only later in the 1960s. Currently, the application of Fentons reagent to destroy toxic compounds such as phenols and herbicides in waste water is well known. In the Fenton process, the addition of H_2O_2 to Fe^{2+} salts generate the hydroxyl radicals [11].

$$Fe^{2+} + H_2O_2 \rightarrow Fe^{3+} + OH^- + OH^{\cdot} \tag{5.1}$$

Neither special reactants nor special apparatus are required for this simple way of producing OH radicals. Since iron is abundant as well as non-toxic element and also as the hydrogen peroxide is easy to handle and environmentally safe, this is an attractive oxidative system for waste water treatment. On the basis of this single reaction, the behaviour of the Fenton

system cannot be completely explained (Equation 5.1). In fact, as pointed out in recent studies [12] the adoption of a proper value of pH (2.7-2.8) can result in the reduction of Fe^{3+} to Fe^{2+} (Equations 5.2 and 5.3) proceeding at an appreciable rate. Under these conditions, iron can be considered as the real catalyst.

$$Fe^{3+} + H_2O_2 \rightleftharpoons H^+ + FeOOH^{2+} \tag{5.2}$$

$$FeOOH^{2+} \rightarrow HO_2 + Fe^{2+} \tag{5.3}$$

5.4.2 Photo-assisted Fenton Processes

When irradiated by UV-Visible light, the rate of degradation of organic pollutant with Fenton and Fenton-like reagents is strongly accelerated [13,14]. Irradiation with UV-Visible light of wavelength values higher than 300 nm was found to accelerate the Fenton oxidation reactions. On UV-Visible irradiation Fe^{3+} generated from the Fe^{2+} ions were reduced back to the ferrous ions (Equation 5.4) and the Fenton reaction continues due to the presence of H_2O_2 (Equation 5.1).

$$Fe(OH)^{2+} + h\nu \rightarrow Fe^{2+} + HO \tag{5.4}$$

Despite the great deal of work devoted by researchers to these processes, there are very little industrial applications. This is for the reason that the applications of Fenton processes require strict pH control.

5.4.3 Ozonisation Process

In order to understand the functioning of the O_3/H_2O_2, a look in to the ozone chemistry in aqueous alkaline solutions is required. Hoigne [15] has comprehensively studied this mechanism in order to give a chemical reasoning to the short life time of ozone in alkaline solutions. He showed that the decomposition of ozone in aqueous solution takes place through the formation of OH radicals. OH^- ion function as an initiator in the reaction mechanism (equations 5.5–5.11):

$$HO^- + O_3 \rightarrow O_2 + HO_2^{\cdot} \tag{5.5}$$

$$HO_2^- + O_3 \rightarrow HO_2^{\cdot} + O_3^- \tag{5.6}$$

$$HO_2 \rightleftharpoons H^+ + O_2^{\cdot} \tag{5.7}$$

$$O_2^- + O_3 \rightarrow O_2 + O_3^- \tag{5.8}$$

$$O_3 + H^+ \rightarrow HO_3 \tag{5.9}$$

$$HO_3 \rightarrow HO + O_2 \tag{5.10}$$

$$HO + O_3 \rightarrow HO_2 + O_2 \tag{5.11}$$

In an alkaline solution hydrogen peroxide exists as HO_2^-. As can be seen from equation 5.6, HO_2^- plays a significant role in the ozone decomposition. Hence, addition of HO_2^- into a solution containing ozone will facilitate the decomposition of O_3 and the simultaneous formation of hydroxyl radicals. In addition, the involvement of HO_2^- demonstrates the role played by pH in the formation of hydroxyl radicals from ozone. Hence an increase of pH and the addition of H_2O_2 to the aqueous O_3 solution will result in higher rates of OH radicals production and the attainment of higher steady-state concentrations of OH radicals in the radical chain decomposition process [16].

5.4.4 Photocatalysis

In the photocatalytic processes, semiconductors function as the catalyst and oxygen is used as the oxidizing agent [17]. Among the many catalysts tested so far, only the anatase phase of TiO_2 seems to have the most of the desired attributes such as high stability, good performance and low cost [18]. The photocatalytic processes are initiated by the absorption of the radiation by the semiconductor leading to the formation of electron-hole pairs (equation 5.12)

$$TiO_2 + h\nu \rightarrow e^- + h^+ \tag{5.12}$$

The photogenerated electrons have potential to reduce some metals and dissolved oxygen leading to the formation of the superoxide radical ion, O_2^-. Even though, superoxide radical ions can oxidize organic compounds, their contribution to the overall oxidization process is small. Superoxide radical ions further react in different ways leading to the formation hydroxyl radicals [19] (Equations 5.13-5.17).

$$TiO_2(e^-) + O_2 \rightarrow O_2^- \tag{5.13}$$

$$2O_2^- + 2H^+ \rightarrow H_2O_2 + O_2 \tag{5.14}$$

$$H_2O_2 + e^- \rightarrow HO + OH^- \tag{5.15}$$

$$H_2O_2 + O_2^- \rightarrow HO + HO^- + O_2 \tag{5.16}$$

$$H_2O_2 + h\nu \rightarrow 2HO^- \tag{5.17}$$

On the other hand, the holes are capable of oxidizing adsorbed H_2O or HO to reactive HO radicals (Equations 5.18 and 5.19)

$$TiO_2(h^+) + H_2O_{ads} \rightarrow TiO_2 + HO_{ads} + H^+ \tag{5.18}$$

$$TiO_2(h^+) + HO^-_{ads} \rightarrow TiO_2 + HO_{ads} \tag{5.19}$$

These reactions are important in the oxidative degradation processes due to the high concentration of adsorbed H_2O and HO on the particle surface. Direct oxidation of some of the substrates adsorbed on the semiconductor surface also takes place (Equation 5.20)

$$TiO_2(h^+) + RX_{ads} \rightarrow TiO_2RX^+_{ads} \tag{5.20}$$

Among the three AOPs mentioned, photocatalysis is the most promising method. This is attributed to its potential to utilize energy from the sun without the addition of other forms of energy or reagents. Photoelectrochemistry involves compounds having an energy gap between the highest occupied molecular orbital (HOMO) or valence band and the lowest unoccupied molecular orbital (LUMO) or conduction band. The condition for a compound to be able to get activated by light is that the energy gap between LUMO and HOMO should be equal to that of the energy of the light used. The reactions carried out by the photocatalysts are classified into two categories namely homogeneous and heterogeneous photocatalysis.

5.4.5 Heterogeneous Photocatalysis

Heterogeneous catalysis is based on the semiconductors which are used for carrying out various desired reactions in both liquid and vapour phase. Photocatalysis involves the excitation of electrons from the valence band to the conduction band on exposing the catalyst to the radiation. This leads to the formation of highly reactive electrons and holes in the conduction band and valence band respectively. The electrons are capable of carrying out reduction reactions and holes can carry out oxidation reactions. Various processes involved in semiconductor photocatalysis are shown in Figure 5.2. The electrons and holes move to the surface of the photocatalyst and are trapped there. The trapped electron and hole react with acceptor (step c) or donor molecules (step d), respectively, or recombine at surface trapping sites (step a). The electron and hole can also be trapped at bulk trapping sites and recombine with the release of heat (b). These electrons and holes can be exploited by a variety of means as given below:

1. For producing electricity (solar cells) – photovoltaics
2. For decomposing or removing pollutants – photooxidation
3. For the synthesis and production of useful chemicals – photocatalysis
4. For the photo electrolysis of water to produce H_2 – photoelectrochemistry

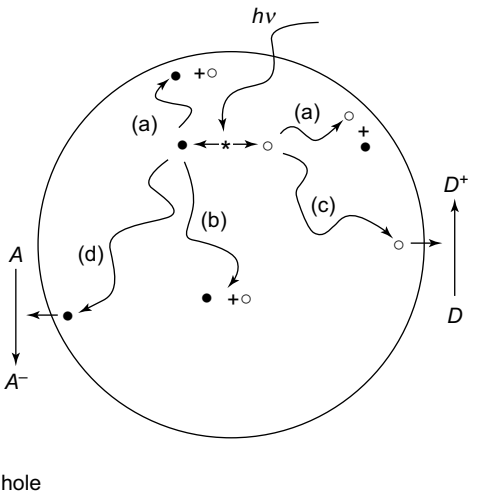

Figure 5.2 ***Fate of photo-excited electrons and holes in a semiconductor particle.***

5.4.6 Charge Carrier Trapping

The recombination of excited electron-hole pair should be minimized for efficient charge transfer reaction between semiconductor and adsorbed species. Trapping the excited electron by surface states increases the lifetime of the excited electron. As a result, the direct recombination of electron-hole pairs is reduced. In the case of nanocrystalline TiO_2 films, the recombination can be delayed, with a lifetime on the scale of microsecond (μs) [20, 21]. The recombination process is competing with the slow charge transfer of electrons to molecular oxygen. In order to trace the trapped electrons and holes in the nanoparticles of TiO_2 after irradiation, electron paramagnetic resonance (EPR) technique is commonly used [22, 23]. Trapped electrons can be detected in the form of Ti^{3+} at low temperatures. Upon adsorption of O_2 at the surface of TiO_2, the Ti^{3+} EPR signals were found to be removed. In addition, trapped holes are also observed and are considered to be localized as deep trap states. Even though, much of the photogenerated holes are trapped in deep or shallow trapping sites, a large portion of the photo-excited electrons exist in a nearly free, untrapped state in the interior of the TiO_2 particle [24]. EPR

and IR studies [25] have found that a major fraction (greater than 90%) of photo-excited electrons remained in the conduction band and were silent in EPR spectra under high-vacuum conditions, even at the low temperature of 90 K.

5.4.7 Semiconductor-electrolyte Interface

Briefly considering this interface, in the interface between a semiconductor and an electrolyte solution, a variety of situations exist. In order for the two phases to be in equilibrium, the electrochemical potential of the two phases must be the same. The redox potential of the electrolyte solution determines the electrochemical potential of the solution and the redox potential of the semiconductor is determined by the Fermi level. If the redox potential of the solution and the Fermi level were not at equal energy, a movement of charge between the semiconductor and the solution is essential in order to equilibrate the two phases. Unlike a metallic electrode, the excess charge that is now located on the semiconductor, does not lay at the surface. The excess charge extends into the electrode for a significant distance (10-1000 nm). This region is referred to as the space charge region, and has an associated electrical field. Consequently, there exists two double layers: the interfacial (electrode/electrolyte) double layer, and the space charge double layer. In the case of an n-type semiconductor electrode at open circuit, the Fermi level is in general more negative than the redox potential of the electrolyte. Hence, transfer of electrons will take place from the electrode into the solution. As a result, the space charge region has a positive charge which results in an upward bending (Note this terminology has significance only if one were to consider the two dimensional representation of the band diagram in reality the band bends towards lower energy in the absolute scale or to more negative value in the electrochemical scale) of the band edges. This region is referred to as a depletion layer, as majority of the charge carriers of the semiconductor are removed from this region. In the case of a p-type semiconductor, the Fermi level is normally lower (caution in two dimensional representation only) in energy than the redox potential of the solution. This will result in flow of electrons from the solution to the electrode to attain equilibrium. This leads to the formation of a negative charge in the space charge region, resulting in a downward bending in the band edges. This is again called a depletion layer, as the holes in the space charge region are removed by this process. For metallic electrodes, changing the potential applied to the electrode shifts the Fermi level. In the case of semiconductor, the band edges in the interior (i.e., away from the depletion region) also vary with the applied potential in the same way as that of the Fermi level. However, the changes in the applied potential will not affect the energies of the band edges at the interface. Therefore, on moving

from the interior of the semiconductor to the interface, a change in the energies of the band edges is observed. Hence, the variation in the applied potential will vary the magnitude and direction of band bending. Three different situations are possible [26] (a) The Fermi energy and the redox potential of the solution lies at the same energy at certain applied potential. There is no band bending as there is no net transfer of charge. Hence, this potential is called as the flatband potential, E_{fb}. (b) At potentials positive of the flatband potential, depletion regions occur for an n-type semiconductor. For a p-type semiconductor, depletion regions occur at potentials negative of the flatband potential. (c) In the case of n-type semiconductor, at potentials negative of the flatband potential, there is an excess of electrons in the space charge region, and hence denoted as an accumulation region. In the case of a p-type, an accumulation region arises at potentials more positive than the flatband potential. For a semiconductor, the ability to transfer charge depends on whether there is an accumulation layer or a depletion layer. The semiconductor electrode behaves similar to a metallic electrode, if there is an accumulation layer. This is because, there is an excess of the majority of charge carriers available for charge transfer. On the other hand, if there is a depletion layer, then there are only a small amount of charge carriers available for transfer. Hence, if at all electron transfer reactions take place, will occur slowly.

5.4.8 Effect of Electron-hole Recombination

Electron-hole recombination plays a major negative role in photocatalysis, as no chemical reactions take place if the photogenerated electron and hole pairs recombine instead of reacting with the substrates adsorbed on the surface. Unlike the measurement of the rate of reaction of the electrons and holes, measuring the rate of recombination directly is not easy. The crystallinity of the semiconductor plays a major role in the extent of recombination [27]. It was found that the recombination takes place at the surface defects [28]. Recombination takes place mostly at the surface where the crystal is terminated thereby the larger the surface area, the faster the recombination. It was found that amorphous TiO_2 was found to have a higher recombination rate than the crystalline TiO_2. Despite the fact that both forms of TiO_2 are thermodynamically capable of reducing O_2, rutile possesses lower photocatalytic activity (higher electron-hole recombination) than anatase because of its lower capacity to adsorb O_2 [29].

5.4.9 Importance of Position of Energy Levels

The ability of a photocatalyst to carry out a particular reaction depends on the position of the energy levels of the catalyst as well as the substrate. For a compound to be able to carry out the reduction reaction, the potential of conduction band or LUMO should be more negative than that of the potential

required for the reduction reaction. For a compound to be able to carry out the oxidation reaction the potential of the valence band or the HOMO should be more positive than the potential required for the oxidation reaction. Let us consider the reaction of the photocatalytic splitting of water as an example. The following are the two reactions involved.

$$4H^+ + 4e^- \rightarrow 2H_2 \tag{5.21}$$

$$2H_2O \rightarrow O_2 + 4H^+ + 4e^- \tag{5.22}$$

The oxidation reaction leading to oxygen evolution mentioned in equation (5.22) will take place at a potential +1.23 V (NHE) where as the reduction reaction leading to the hydrogen evolution will take place at 0.00 V (NHE). The reduction reaction mentioned in equation (5.21) will happen only if the potential of conduction band of photocatalyst is more negative than 0.00 V. Likewise the oxidation reaction mentioned in equation (5.22) will happen only if the potential of the valence band of the photocatalyst is more positive than +1.23 V. Accordingly, depending on the positions of CB and VB, the systems can be classified as OR type (both reactions possible), O type (only oxidation is feasible), R type (only reduction is feasible) and X type (neither reactions can occur).

5.4.10 Choice of the Photocatalyst

Among the available semiconductors, WO_3 and Fe_2O_3 cannot carry out the photosplitting of water since their conduction band potentials are less negative than the hydrogen evolution potential. Most of the semiconductors can carry out the oxygen evolution reaction. However among all of them, only a few were studied for water splitting reaction because of other problems like photo corrosion, cost, higher bandgap and stability. Another important parameter to be taken into account while choosing the photocatalyst is the percentage of ionic character of the cation-anion bond. A system which has higher percentage ionic character (40%) will have higher band gap and will not be able to absorb light in the visible region. A catalyst which has a percentage ionic character between 20–30% with suitable positions of the valence and conduction band potentials with respect to the reaction under consideration will be successful for carrying out the reaction [30]. It is important to mention that the commercial success of a photocatalyst depends on its ability to function by utilizing the visible light. This is because of the composition of sunlight which has 46% visible radiation, 47% IR radiation and only less than 7% UV radiation. But TiO_2, which is the most efficient and stable photocatalyst available, can

function only by using the UV light. Hence, research all over the world is focussed on finding a photocatalyst or modifying the available catalysts so that they can function by absorbing light in the visible region.

5.4.11 Visible Light Photocatalysis

Unlike photocatalysis in green plants, the titanium dioxide photocatalyst in itself does not allow the use of visible light and can make use of only 7% of solar radiations that reach the earth. To address these problems, photocatalytic systems which are able to operate effectively and efficiently not only under UV but also under the most environmentally ideal energy source, sunlight, must be developed. It is vital to design and develop unique TiO_2 photocatalysts which can absorb and operate with high efficiency under solar and/or visible light irradiation. These efforts include doping TiO_2 with metal impurities [31-39], doping TiO_2 with anions (non-metal doping) [40-42], coupling TiO_2 with narrow band-gap semiconductors [43-52] and preparing oxygen-deficient TiO_2 [53-56]. During the recent years, doping with non-metals has been widely studied. Studies were carried out with various non-metallic elements such as nitrogen [57-64], sulphur [65-70], carbon [71-75], fluorine [76-80], phosphorus [81-84] and boron [85-87]. All these elements on doping showed a red shift in the absorption spectrum of TiO_2.

5.4.12 Importance of Adsorption in Heterogeneous Photocatalysis

As the recombination of the photogenerated electron and hole occurs on a picosecond time scale, electron transfer at the interface can kinetically compete with recombination only when the donor or acceptor is adsorbed on the semiconductor before irradiation. Hence, adsorption of the substrate prior to irradiation is important for efficiency of the heterogeneous photocatalytic process [88]. Hydroxyl groups or water molecules adsorbed on the surface can serve as traps for the photogenerated hole, leading to the formation of hydroxyl radicals, in the case of metal oxide suspensions. Strong adsorption of acetone and 2-propanol on ZnO has been observed during temperature-programmed desorption[89] and X-ray photoelectron spectroscopy [90]. Metal oxide surfaces have a surface density of about 4-5 hydroxyl groups/nm^2. These surface hydroxyl groups have different sets of acidities [91, 92], as has been shown by the continuous distribution of adsorption energies in the Freundlich isotherm [93]. Many organic substrates were found to play the role of adsorbed traps for the photo-generated holes. For example, in a colloidal suspension of TiO_2 in acetonitrile, radical ions are detected directly during flash excitation [89].

5.4.13 Alternatives to TiO_2 Photocatalyst

In recent years an increasingly great number of new photocatalysts have been designed and tested as possible alternatives to TiO_2. These materials are not derived from TiO_2 by any of the usual modifications such as doping, coupling with an additional phase or morphological changes. Instead, they are completely different compounds with distinct composition and structure. Various tantalates [94-96] and niobates [97-98] were found to be effective photocatalysts for water splitting. Oxides of bismuth like $Bi_2W_2O_9$, Bi_2WO_6, [99], Bi_2MoO_6, $Bi_2Mo_2O_9$, $Bi_2Mo_3O_{12}$ [100] and oxides of Indium such as In_2O_3 [101, $Ba_2In_2O_5$ [102], MIn_2O_4 (M=Ca, Sr)[103] were found to be capable of photosplitting water. Tantalum nitride (Ta_3N_5) [104], and Tanatalum oxynitrides (TaON) [105] were also found to be effective catalysts for water splitting.

5.4.14 Concluding Remarks

The photocatalytic decontamination has certain advantages over other conventional methods. These include (1) ambient operating temperature and pressure, (2) complete mineralization of parent and their intermediate compounds without secondary pollution and (3) low operating costs. The highly Reactive Oxygen Species (ROS) generated as a result of the photo-induced charge separation on TiO_2 surfaces for microbial inactivation and organic mineralization without creating any secondary pollution is well-Known. So far, the application of such TiO_2 catalysts for water treatment experiences a number of technical issues. (1) The post-separation of the semiconductor catalyst after water treatment is one of the major difficulty towards adopting as an industrially viable process. The fine particle size of the semiconductor, and the large surface area-to-volume ratio and surface energy favours the catalyst agglomeration during the operation which is detrimental. (2) Another challenges is the catalysts development with broader photoactivity and the integration with feasible photocatalytic reactor system. (3) The understanding of the theory behind the common reactor operational parameters and their interactions are inadequate and hence process optimization has become difficult. (4) Deficiencies in the kinetic modelling of both the photomineralization and photo-disinfection have been seen over the years. Few other important aspects of this process have not been considered in this presentation like the reactor design, Kinetic modelling (the data is most often treated in terms of first order rate equation while concentration versus time data (more importantly plots) can show different types of variations, life cycle assessment of the chosen photocatalytic water treatment processes and the deficiencies involved in the kinetic modellings that are presently adopted.

These aspects have been covered in two reviews by Meng Nan Chang et al., [106] and S. Malato et al., [107].

References

1. J. W. Veerhoeven, Pure Appl. Chem., 68, 2223 (1996).
2. B. Viswanathan, Bull. Catal. Soc. India, 2, 71 (2002).
3. M. A. Lazar, S. Varghese and S. S. Nair, catalysts, 2, 572 (2012).
4. M. Block, and D. Hanrahan (2009) Worlds worst polluted places report 2009, Blacksmith Institute, New York.
5. C. Murray and A. Lopez (2002), The World Health Report 2002, Annex to Table 9, pp. 224, World Health Organization, Geneva.
6. K. C. Agarwal, Industrial Power Engineering and Applications, Butterworth-Heinemann, pp. 565 (2001).
7. R. Andreozzi, V. Caprio, A. Insola and R. Marotta Catalysis Today, 53, 51 (1999).
8. A. Farhataziz and B. Ross, Natl. Stand. Ref. Data Ser., USA National Bureau of Standards, Notre Dame, 59, 22 (1977).
9. J. Hoigne, and H. Bader, Water Res., 17, 185(1983).
10. H. J. H. Fenton, J. Chem. Soc. Trans., 65, 899 (1894).
11. Haber, F. and J. Weiss, Proc. R. Soc. Lond. A, 147, 332(1934).
12. J. J. Pignatello, Environ. Sci. Technol., 26, 944 (1992.
13. J. Kiwi, C. Pulgarin, P. Peringer and M. Gratzel, Appl. Catal. B: Environ., 3, (1993).
14. C. Pulgarin, and J. Kiwi, Chimia, 50, 50 (1996).
15. J. Hoigne, (1998) Chemistry of aqueous ozone and transformation of pollutants by ozone and advanced oxidation processes, in: J. Hrubec (Ed.), The Handbook of Environmental Chemistry, vol. 5, part C, Quality and Treatment of Drinking Water, Part II, Springer, Berlin Heidelberg.
16. W. H. Glaze, and J.W. Kang, Ind. Eng. Chem. Res., 28, 1573 (1989).
17. D. Ollis, and H. Al-Ekabi (1993) Photocatalytic purification of water and air. Elsevier, New York.
18. K. Rajeshwar, J. Appl. Electrochem., 25, 1067 (1995).
19. A. Fujishima, X. Zhang and D. A. Tryk, Surf. Sci. Rep., 63, 515(2008).
20. A. M. Peiro, C. Colombo, G. Doyle, J. Nelson, A. Mills and J.R. Durrant, J. Phys. Chem B, 110, 23255 (2006).
21. T. Yoshihara, R. Katoh, A. Furube, Y. Tamaki, M. Murai, K. Hara, S. Murata, H. Arakawa and M. Tachiya, J. Phys. Chem. B, 108, 3817 (2004).

22. R. F. Howe and M. Gratzel, J. Phys. Chem., 89, 4495 (1985).
23. D. C. Hurum, A. G. Agrios, K. A. Gray, T. Rajh and M. C. Thurnauer, J. Phys. Chem. B, 107, 4545 (2003).
24. A. Yamakata, T. A. Ishibashi, K. Takeshita and H. Onishi, Top. Catal., 35, 211 (2005).
25. T. Berger, M. Sterrer, O. Diwald, E. Knozinger, D. Panayotov, T. L. Thompson and J.T. Yates, J. Phys. Chem. B, 109, 6061 (2005).
26. A. W. Bott, Current Separations,17:3, 87 (1998).
27. M. Kaneco, and I. Okura (2002) Photocatalysis: Science and Technology. Springer-Verlag, Berlin.
28. P. T. Landsberg, (1991) Recombination in Semiconductors. Cambridge University Press, Cambridge.
29. N. Serpone, and E. Pelizzetti (1989) Photocatalysis-fundamentals and applications. Wiley Interscience, New York.
30. B. Viswanathan, Bull. Catal. Soc. India, 2, 71 (2002).
31. L. G. Devi, N. Kottam, S. G. Kumar and K. E. Rajashekhar, Cent. Eur. J. Chem., 8, 142 (2010).
32. L. G. Devi, S. G. Kumar, B. N. Murthy and N. Kottam, Catal. Commun., 10, 794 (2009).
33. D. Dvoranova, V. Brezova, M. Mazur and M. A. Malati, Appl. Catal. B Environ., 37, 91 (2002).
34. M. Iwasaki, M. Hara, H. Kawada, H. Tada and S. Ito, J. Colloid Interf. Sci., 224, 202 (2000).
35. H. Sayilkan, Appl. Catal. A-Gen., 319, 202 (2007).
36. C. D. Valentin, G. Pacchioni, H. Onishi and A. Kudo, Chem. Phys. Lett., 469, 166(2009).
37. Y. Wu, J. Zhang, L. Xiao and F. Chen, Appl.Catal. B-Environ., 88, 525 (2009).
38. J. Yu, Q. Xiang and M. Zhou, Appl. Catal. B-Environ., 90, 595(2009).
39. M. Zhou, J. Yu and B. Cheng, J. Hazard. Mater., 137, 1838(2006).
40. R. Nakamura, T. Tanaka and Y. Nakato, J. Phys. Chem. B, 108, 10617 (2004).
41. J. H. Park, S. Kim and A. J. Bard, Nano Lett., 6, 24 (2006).
42. G. R. Torres, T. Lindgren, J. Lu, C.G. Granqvist and S.E. Lindquist,J. Phys. Chem. B, 108, 5995(2004).
43. R. A. Doong, C. H. Chen, R. A. Maithreepala and S. M. Chang, Water Res., 35, 2873 (2001).

44. C. A. K. Gouvea, F. Wypych, S. G. Moraes, N. Duran, N. Nagata and P. P. Zamora, Chemosphere, 40, 433 (2000).
45. W. Ho, J. C. Yu, J. Lin, J. Yu and P. Li, Langmuir, 20, 5865 (2004).
46. W. Ho, and J. C. Yu, J. Mol. Catal. A-Chem., 247, 268 (2006).
47. H. Huang, D. Li, Q. Lin, W. Zhang, Y. Shao, Y. Chen, M. Sun and X. Fu, Environ. Sci. Technol., 43, 4164 (2009).
48. S. C. Lo, C. F. Lin, C. H. Wu and P. H. Hsieh, J. Hazard. Mater., 114, 183 (2004).
49. M. Miyauchi, M., A. Nakajima, K. Hashimoto and T. Watanabe, Adv. Mater., 12, 1923 (2000).
50. R. S. Parra, I. H. Perez, M. E. Rincon, S. L. Ayala and M. C. R. Ahumada, Sol. Energ. Mat. Sol. C., 76, 189 (2003).
51. D. Robert, Catal. Today, 122, 20 (2007).
52. H. Tada, T. Mitsui, T. Kiyonaga, T. Akita and K. Tanaka, Nature Mater., 5, 782 (2006).
53. F. M. Hossain, G. E. Murch, L. Sheppard and J. Nowotny, Solid State Ionics, 178, 319 (2007).
54. T. Ihara, M. Miyoshi, M. Ando, S. Sugihara and Y. Iriyama, J. Mater. Sci., 36, 4201 (2001).
55. I. Justicia, P. Ordejon, G. Canto, J. L. Mozos, J. Fraxedas, G. A. Battiston, R. Gerbasi and A. Figueras, Adv. Mater., 14, 1399 (2002).
56. H. Kikuchi, M. Kitano, M. Takeuchi, M. Matsuoka, M. Anpo and P. V. Kamat, J. Phys. Chem. B, 110, 55379(2006).
57. R. Asahi, T. Morikawa, T. Ohwaki, K. Aoki and Y. Taga, Science, 293, 269 (2001).
58. H. Irie, Y. Watanabe and K. Hashimoto, J. Phys. Chem. B, 107, 5483(2003).
59. G. Liu, H. G. Yang, X. Wang, L. Cheng, J. Pan, G. Q. M. Lu and H. M. Cheng, J. Am. Chem. Soc., 131, 12868 (2009).
60. G. Liu, X. Wang, Z. Chen, H. M. Cheng and G. Q. M. Lu, J. Colloid. Interf. Sci., 329, 331 (2009).
61. M. Maeda, M. and T. Watanabe J. Electrochem. Soc., 153, C186 (2006).
62. S. Sakthivel, M. Janczarek, and H. Kisch, J. Phys. Chem. B, 108, 19384 (2004).
63. M. Sathish, B. Viswanathan, R. P. Viswanath and C. S. Gopinath, Chem. Mater., 17, 6349 (2005).
64. M. Sathish, B. Viswanathan and R. P. Viswanath, Appl. Catal. B-Environ., 74, 307 (2007).

65. C. W. Dunnill, Z. A. Aiken, A. Kafizas, J. Pratten, M, Wilson, D. J. Morgan and I. P. Parkin, J. Mater. Chem., 19, 8747 (2009).
66. W. Ho, J. C. Yu and S. Lee, J. Solid State Chem., 179, 1171 (2006).
67. Y. Izumi, T. Itoi, S. Peng, K. Oka and Y. Shibata, J. Phys. Chem. C, 113, 6706 (2009).
68. T. Ohno, T. Mitsui and M. Matsumura, Chem. Lett., 32, 364 (2003).
69. T. Ohno, M. Akiyoshi, T. Umebayashi, K. Asai, T. Mitsui and M. Matsumura, Appl. Catal. A-Gen., 265, 115 (2004).
70. J. C. Yu, W. Ho, J. Yu, H. Yip, P. K. Wong and J. Zhao, Environ. Sci. Technol., 39, 1175 (2005).
71. M. Sathish, M., R. P. Viswanath and C. S. Gopinath, J. Nanosci. Nanotechno., 9, 423 (2009).
72. Y. Huang, Y., W. Ho, Z. Ai, X. Song, L. Zhang and S. Lee Appl. Catal. B. Environ., 89, 398 (2009).
73. H. Irie, S. Washizuka and K. Hashimoto, Thin Solid Films, 510, 21 (2006).
74. S. Sakthivel, and H. Kisch, Angew. Chem. Int. Edit., 42, 4908 (2003).
75. Q. Xiao, J. Zhang, C. Xiao, Z. Si and X. Tan, Sol. Energy, 82, 706 (2008).
76. X. Yang, C. Cao, L. Erickson, K. Hohn, R. Maghirang and K. Klabunde, J. Catal., 260, 128 (2008).
77. F. B. Li, X.Z. Li, C.H. Ao, S.C. Lee and M. F. Hou, Chemosphere 59, 787 (2005).
78. M. Pelaez, A. A. de la Cruz, E. Stathatos, P. Falaras and D. D. Dionysiou, Catal. Today, 144, 19 (2009).
79. J. Xu, Y. Ao, D. Fu and C. Yuan, Appl. Surf. Sci., 254, 3033 (2008).
80. S. Yang, C. Sun, X. Li, Z. Gong and X. Quan, J. Hazard. Mater., 175, 258 (2010).
81. J. C. Yu, J.G. Yu, W. K. Ho, Z. T. Jiang and L.Z. Zhang, Chem. Mater., 14, 3808 (2002).
82. F. Li, Y. Jiang, M. Xia, M. Sun, B. Xue, D. Liu and X. Zhang, J. Phys. Chem. C, 113, 18134(2009).
83. L. Lin, W. Lin, Y. Zhu, B. Zhao and Y. Xie, Chem. Lett., 34, 284 (2005).
84. R. Zheng, Y. Guo, C. Jin, J. Xie, Y. Zhu and Y. Xie, J. Mol. Catal. A-Chem., 319, 46 (2010).
85. R. Zheng, L. Lin, J. Xie, Y. Zhu and Y. Xie, J. Phys. Chem. C, 112, 15502 (2008).
86. D. Chen, D. Yang, Q. Wang and Z. Jiang, Ind. Eng. Chem. Res., 45, 4110 (2006).

87. T. Ochiai, K. Nakata, T. Murakami, A. Fujishima, Y. Yao, D. A. Tryk and Y. Kubota, Water Res., 44, 904 (2010).
88. W. Zhao, W. Ma, C. Chen, J. Zhao and Z. Shuai, J. Am. Chem. Soc., 126, 4782 (2004).
89. M. A. Fox and M. T. Dulay, Chem. Rev., 93, 341 (1993).
90. M. A. Fox, C. C. Chen and B. A. Lindig, J. Am. Chem. Soc., 104, 5828 (1982).
91. G. Munuera, J. P. Espinoa, A. Fernandez, P. Malet and A. R. G. Elipe, J. Chem. Soc., Faraday Trans., 86, 3441 (1990).
92. M. Pichat, A. A. De ka Cruz, E. Stathatos, P. Falaras and D. D. Dionysiou, J. Chem. Soc. Faraday Trans., I, 83, 697 (1987).
93. T. Yamanaka and K. Tanabe, J. Phys. Chem., 79, 2409 (1975).
94. S. Tybesu and M. Anderson, J. Phys. chem, 95, 3399 (1991).
95. H. Kato, K. Asakura and A. Kudo, J. Am. Chem. Soc., 125, 3082 (2003).
96. H. Kato and A. Kudo, J. Phys. Chem. B., 105, 4285 (2001).
97. F. E. Osterloh, Chem. Mater., 20, 35 (2008).
98. K. Domen, J. Yoshimura, T. Sekine, A. Tanaka and T. Onishi, Catal. Lett., 4, 339 (1990).
99. Y. Ebina, N. Sakai, and T.Sasaki, J. Phys. Chem., B, 109, 17212 (2005).
100. J. Yoshimura, Y. Ebina, J. Kondo, K. Domen and A. Tanaka, J. Phys. Chem, 97, 1970 (1993).
101. Y. Shimodaira, H. Kato, H. Kobayashi and A. Kudo, J. Phys. Chem., B, 110, 17790 (2006).
102. A. Kudo and I. Mikami, Chem. Lett., 27, 1027 (1998).
103. D. F. Wang, Z. G. Zou and J. H. Ye, Chem. Mater., 17, 3255 (2005).
104. J. Sato, N. Saito, H. Nishiyama and Y. Inoue, J. Phys. Chem., B, 107, 7965 (2003).
105. G. Hitoki, A. Ishikawa, T. Takata, J. N. Kondo, M. Hara and K. Domen, Chem. Lett., 31, 736 (2002).
106. G. Hitoki, T. Takata, J. N. Kondo M. Hara, H. Kobayashi and K. Domen, Chem. Commun., 1698 (2002).
107. M. N. Chong, Bo Jin, C. W. K. Chow and C. Saint, Water Research, 44 (2010) 2997-3027.
108. S. Malato, P. Fernandez-Ibanez, M. I. Maldonado, J. Blanco and W. Geernjak, Catalysis Today, 147 (2010) 1-59.

6 Photo-catalytic Routes for Chemicals

Langford [1] in a recent publication defined photocatalysis "as a term that combines the basic notion of a catalyst as a material that enhances the rate as a reaction approaches equilibrium without being consumed with the notion that the reaction is accelerated by photons which of course are consumed. Thus it is a bybrid concept". Following the report by carey et al. in 1976 [2] on the photodechlorination of polychlorinated biphenyls (PCBs), there have been a spate of publications in this area. Rajeshwar has reported in his review [3] that the number of papers in this area grew from 249 in 1975-80 to nearly 16755 in 2000-2010. The photocatalysis research area has seen three generations of development according to Langford [1]. The first generation was focussed on the understanding of semiconductor-solution interface, the second generation devoted to development of thin films doped semiconductors, dye sensitization and the third generation centred around nanostate and self organized materials as photo catalysts.

Petroleum and natural gas have been serving as the primary source of the chemicals, reagents, solvents and polymers used in various applications. However, nature has been successful in synthesizing starch from water and carbon dioxide. Most of the reactions involve electron transfer or redox chemistry. For this to take place in a facile manner, the donor and acceptor levels of the species should be energetically and symmetrically matched between substrate and the system. Nature possibly adapts this by the manipulation of the species. For example, the activation of dinitrogen by nitrogenase enzyme is achieved by the ability of the enzyme to perturb the orbitals of dinitrogen such that the LUMO of dinitrogen will become suitable for electron transfer which destabilises dinitrogen and makes it active.

6.1 PHOTOCATALYSIS

Photo-catalysis involves the excitation of electrons from the valence band or HOMO to the conduction band or LUMO on exposing the catalyst to the radiation. This leads to the formation of highly reactive electrons and holes in the conduction band and valence band respectively. Various processes involved

in semiconductor photo-catalysis are shown in Fig. 6.1. The electrons are capable of carrying out reduction reactions and holes can carry out oxidation reactions. This process can be exploited in various ways. The three main ways are: (i) For producing electricity (ii) For decomposing or removing pollutants and (iii) For the synthesis and production of useful chemicals

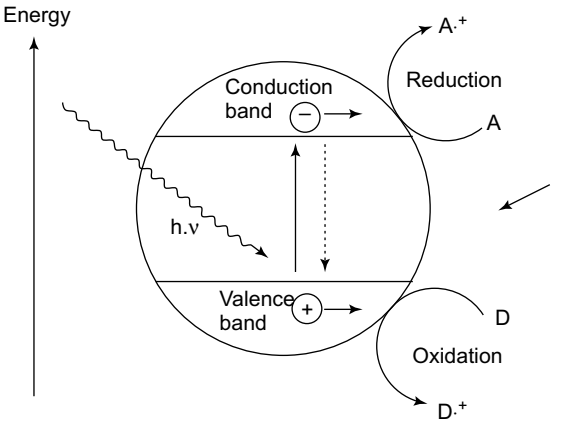

Figure 6.1 *Simple representation of the process involved in photocatalysis [4,5].*

6.2 PHOTOCATALYTIC CHEMICAL PRODUCTION

Photo-catalytic synthesis of compounds can be carried out utilizing the electrons and holes created. So, the reaction should be either a reduction or oxidation or a combination of both. As previously stated for a reaction to take place the potential of the energy levels of the catalyst and the reactant should be suitable for the electron transfer to take place. The photo-catalytic splitting of water has received considerable attention and the literature is extensive on this aspect and is dealt with in other chapters.

6.2.1 Photo-catalytic Oxidation

Conventional oxidizing agents used in organic synthesis like potassium dichromate, potassium permanganate, various acids and peroxides are toxic in nature. These oxidizing agents are difficult to handle and release dangerous fumes and gases during the reaction. If one can carry out oxidation reactions using solar irradiation, it will be an environment friendly process. This has led to many attempts to carry out oxidation reactions photo-catalytically [6].

6.2.2 Oxidation of Alcohols

Oxidation of alcohols to the aldehydes and ketones is an integral part of organic synthesis. There are variety of reagents used for this purpose and their

separation after the oxidation is a difficult task. Photo-catalytic oxidation by using semiconductors will be an easier method since the separation of the catalyst is not necessary. One more advantage of photo-catalytic oxidation is that the products will be free from solvent. Photo-catalytic dehydrogenation of 2-propanol has attracted general interest from the energy-storing viewpoint (ΔH_0 = 69.9 kJ mol^{-1}, ΔG_0 = 25.0 kJ mol^{-l}) There is no theoretical limit on the quantum efficiency for the photo-catalytic dehydrogenation of 2-propanol in the liquid phase, since this reaction becomes exergonic ($\Delta G < 0$) due to the spontaneous evolution of the product hydrogen.

Table 6.1 ***Various photo-catalytic oxidation reactions, catalysts in mostly liquid phase and at RT (RT = Room temperature).***

Reaction Studied	*Catalyst Employed*	*Ref*
Benzylic and allylic alcohols to aldehydes, ketones	molecular iodine	[6]
Benzyl alcohol to benzaldeehyde	9-phenyl-10- methylacridinium ion	[7]
2-propanol to acetone	TiO_2 (110)	[8]
	$(Bu_4N)_4[W_{10}O_{32}]$	[9]
	cis-$Rh_2Cl_2(CO)_2(dpm)_2$	[10]
	(Dioctadecyl dimethylammonium)$_4$ $[W_{10}O_{32}]$	[11]
	Ag/TiO_2	[12]
	Pt dispersed on Brookite	[13]
	Trans$[IrCl_2(SnCl_3)_4]^{3-}$	[14]
	Chloro(tetraphenyl porphyrinato)Rh(III)	[15]
	$RhCl(CO)(PPh_3)_2$	[16]
	Pt dispersed on TiO_2	[17]
	Chloro(tetraphenyl porphyrinato)Rh(III)	[18]
2-propanol to acetone	5wt%Pt dispersed on TiO_2	[19]
Ethanol to acetaldehyde	TiO_2 and ultrasonication	[20]
Methanol, ethanol and n-propanol to aldehydes Secondary alcohols to ketones Allyl alcohol to acrolein Propargyl alcohol to aldehyde	Heteropoly tungstates	[21]
Aromatic secondary Alcohols	silica encapsulated Heteropoly tungstate	[22]
Benzyl alcohol 1-Phenyl ethanol, Benzhydrol 4-Chlorobenzhydrol 44'-dichlorohydro Benzoin	TiO_2(anatase)	[23]

Table 6.1 ***(Continued)***

Reaction Studied	*Catalyst Employed*	*Ref*
4,4'-dimethoxyhydro Benzoin to oxidation products		
Benzyl alcohol to Benzaldehyde	$[Hex_4N]_4[S_2Mo_{18}O_{62}]$ $[Bu_4N][S_2W_{18}O_{62}]$	[24]
Ethanol to acetaldehyde	Pd dispersed on CdS	[25]
Methanol to formaldehyde	Rutile (110)	[26]
Methanol to HCHO	silica coated CdS	[27]
Methanol to HCHO	cis $Rh_2Cl_2(CO)_2(dpm)_2$	[28]
Methanol to HCHO	$[IrH(SnCl_3)_5]_3$	[29]
Ethanol to acetaldehyde;CH_3OH to HCHO	Pt dispersed on CdS	[30]
Ethanol to CH_3CHO	titanium tetraisopropoxide/tetraethoxide	[31]
Ethanol to acetaldehyde	Pt dispersed on CdS	[32]
n-octanol to n-octanal	TiO_2	[33]
Ethanol to acetaldehyde	$CuCl_2$ in HCl	[34]
Dehydrogenation of Cyclohexanol	Chloro(tetraphenyl porphyrinato Rh(III)	[35]
Dehydrogenation ofCH_3OH	cis-$[Rh_2Cl_2(CO)_2(dpm)_2]$	[36]

The presence of surface hydroxyl groups increases the oxidation reaction and the oxygen vacancies were found to play an important role in the oxidation of 2-propanol to acetone using TiO_2. Reaction in vapour phase is limited to 623 K above which thermal desorption takes place. The list of photocatalytic oxidation reactions studied are given in Table 6.1.

The dehydrogenation of 2-propanol using cis-$[Rh_2Cl_2(CO)_2(dpm)_2]$ gave acetone, pinacol and cyclohexanol. The yield of acetone was maximum when the wavelength was 312 nm. In Table 6.2 the data are given to substantiate this statement.

Table 6.2 ***Yields (in micromoles) of photocatalytic oxidation products of 2-propanol using cis $[Rh_2Cl_2(CO)_2(dpm)_2]$ as catalyst [10].***

Wavelength(nm)	260	285	312	338	364	390	414	440
acetone	258	754	945	344	45.9	11.5	8.4	5.6
Pinacol	Trace	6.6	7.9	Trace	0.00	0.00	0.00	0.00
Cyclohexanol	0.08	0.59	1.17	0.15	0.00	0.00	0.00	0.00

Benzylic and allylic alcohols are oxidized to aldehydes and ketones using iodine as the photo-catalyst. The oxidation of the substrates was found to be dependent on the solvent used [6]. Various products formed by the oxidation of allylic and benzylic alcohols by molecular iodine and their yields are given in Table 6.3

Table 6.3 ***Products and yields during the photocatalytic oxidation of allylic and benzylic alcohols using molecular iodine [6].***

Substrate	*Product*	*Irradiation Time (h)*	*Yield*
$C_6H_5CH_2OH$	C_6H_5CHO	5	88
p-$MeOC_6H_4CH_2OH$	p-$MeOC_6H_4CHO$	3	92
o-$MeOC_6H_4CH_2OH$	o-$MeoC_6H_4CHO$	3	90
m-$MeoC_6H_4CH_2OH$	m-$MeOC_6H_4CHO$	3	88
2,4$(Meo)_2C_6H_3CH_2OH$	2,4$(MeO)_2C_6H_3CHO$	2	96
3,4,5$(MeO)_3C_6H_2CH_2OH$	3,4,5$(MeO)_3C_6H_2CHO$	2	85
p-$ClC_6H_4CH_2OH$	p-ClC_6H_4CHO	6	85
2,4 $Cl_2C_6H_3CH_2OH$	2,4 $Cl_2C_6H_3CHO$	6	85
$C_6H_5CH{=}CHCH_2OH$	$C_6H_5CH{=}CHCHO$	6	85
p-$MeC_6H_4CHOHCH_3$	p-$MeC_6H_4COCH_3$	2	94
p-$NO_2C_6H_4CHOHCH_3$	p-$NO_2C_6H_4COCH_3$	5	80
$PClC_6H_4CHOHC_6H_5$	P-$ClC_6H_4COC_6H_5$	3.5	84
p-$NO_2C_6H_4CHOHC_6H_5$	p-$NO_2C_6H_4COC_6H_5$	4.5	77
(p-$FC_6H_4)_2$ CHOH	(P-$FC_6H_4)_2CO$	7	78
p-$MeC_6H_4CHOHCH_2OH$	P-$MeC_6H_4COCH_2OH$	7	78
p-$ClC_6H_4CHOHCH_2OH$	p-$ClC_6H_4COCH_2OH$	6	75
p-$NO_2C_6H_4CHOHCH_2OH$	p-$NO_2C_6H_4COCH_2OH$	8	50

6.3 METHANE TO METHANOL

Methane is a major component of natural gas. Methane can be directly used as a fuel. But most of the sources are located off-shore or in remote places inland. The transportation of methane containing natural gas is difficult because of the difficulty in compression of methane and it is not economically favourable. Because of this limitation, in many cases the natural gas containing methane is flared at the source. Goal gasification also produces upto 18% methane. This places a condition that the gaseous methane has to be converted to a liquid which can be directly used as a fuel or used for the production of chemicals. Direct conversion of methane and carbon dioxide to oxygenated compounds is preferable route. The limited data available in literature are given in Table 6.4.

6.4 PHOTO-CATALYTIC DEHYDROGENATION REACTION

Selective oxidation of hydrocarbons by molecular oxygen (refer to Table 6.5) is an important goal for economic, environmental and scientific reasons.

Table 6.4 ***Catalysts and reaction conditions for the conversion of methane to methanol.***

Catalyst	*Reaction Conditions*	*Ref*
La/WO_3	Hg Lamp	[37,38]
WO_3	Visiblelight laser	[39]
WO_3, TiO_2, NiO	UV Laser	[40]
SiO_2	Hg lamp	[41]
TiO_2/SiO_2		
CdS-TiO_2/SiO_2		
Cu/CdS-$TiO_2/SiO-2$		
Products are acetic acid, ethane, acetone and CO		

Table 6.5 ***Alkane Dehydrogenation Reactions.***

Reaction	*Catalysts*	*Reaction Conditions*	*Ref*
Dehydrogenation of alkane	$RhCl(CO)(PR_3)$	400W Hg lamp	[42]
Cyclohexane to benzene	MOO_x/TiO_2	40W fluorescent lamp	[43]

6.4.1 Conversion of Benzene to Phenol

The total production of phenolic of the order 5×10^6 tones per year. The current process called the cumene process is a multistage process and hence has a low overall yield, energy intensive and gives rise to various undesirable side products like 2-phenylpropan-2-ol and methyl styrene. The direct formation of phenol from hydrocarbon sources like benzene will be attractive for various reasons and the attempts in this direction are given in Table 6.6.

Table 6.6 ***Details of catalysts and reaction conditions for the oxidation of benzene to phenol.***

Reaction	*Catalysts*	*Conditions*	*Irradiation*	*Ref*
Benzene to Phenol, hydro-quinone and catechol	TiO_2 P-25 with Fe^{3+}, H_2O_2 Pt/TiO_2P25 Fluorinated TiO_2 Polyoxometalate	liquid phase	450W Xe lamp >300nm	[44]
Benzene to Phenol Toluene, Benzaldehyde benzylalcohol, cresols	$UO_2{}^{2+}$	Liquid RT	Dye laser	[45]

6.4.2 Oxidation of Cyclohexane

Oxygenation of cyclohexane is an important reaction for the production of alcohols and ketones which are precursors for the synthesis of adipic acid which is an intermediate in the production of nylon. Some of the available data are given in Table 6.7.

Table 6.7 ***Catalysts for the oxidation of cyclohexane in liquid phase at room temperature (RT).***

Cyclohexane to	*Catalysts*	*Irradiation*	*Ref*
Cyclohexanone cyclohexanol	like $(Et_4N)_4W_{10}O_{32}$	400 W Hg lamp	[46]
Cyclohexne to cyclohex-2-en-1-one and epoxide	Iron(III) meso-tetrakiss (2,6dichlorophenyl) Porphyrin	>350nm	[47]
Cyclohexane to Cyclohexanone	TiO_2	125W Hg Lamp 350 nm	[48]

6.4.3 Oxidation of Light Alkanes to Oxygenated Products

Selective conversion to partial oxidative products is difficult due to the low chemical reactivity of light alkanes. The main interest is devoted to the dehydrogenation of n-butane to butenes and butadiene which are precursors for manufacturing synthetic rubber. The relevant data are given in Table 6.8.

6.4.4 Oxidation of Cyclic Hydrocarbons Present in Petroleum

A selective and environment friendly photo-catalytic route for the conversion of cyclic hydrocarbons present in petroleum is desirable for various reasons like for the production fine chemicals and other industrial chemicals. Selective oxidative dehydrogenation of cycloalkane has been the subject of many studies because of the importance of refining and reforming process in petroleum industry. There are only a few practical processes for converting alkanes to more valuable products and some of these are given in Table 6.9.

In Table 6.10, the data for the oxidation of aromatic compounds are summarized.

There are various other oxidation reactions of importance in synthetic organic chemistry which can be carried out by photocatalytic means. the important ones are oxidation of hydrocarbons, phosphines, sulfides and olefins, benhydrol to benzophenone diphenyl sulfides to aromatic aldehydes and sulfoxides, Fluorene to Fluorenone, dihydroanthracene to anthracene, diphenyl

Table 6.8 ***Data on the oxidation of light alkanes, in mostly liquid phase or vapour phase.***

Reaction	*Catalysts*	*Irradiation*	*Ref*
Ethane to acetaldehyde	MoO_3 on SiO_2	75 W Hg	[49]
Propane to aldehyde and ketone	Na, K, and Rb loaded on V_2O_5 on SiO_2	300 W Xenon	[50]
Isobutene to acetone	Tin oxide on SiO_2	310 nm	[51]
Propane to acetone and propanaldehyde	MoO_3 on SiO_2	1000 W Xe lamp	[52]
	Rh on V_2O_5 on SiO_2	300 W Xe lamp	[53]

Table 6.9 ***Data on oxidation of cyclic and aromatic hydrocarbons in liquid phase and room temperature.***

Reaction	*Catalyst*	*Irradiation Source*	*Ref*
Toluene to benzaldehyde and and benzyl alcohol oxidation of cumene, benzyl alcohol and benzaldehyde	UO_2^{2+}	275 W tungsten halogen lamp	[54]
Substituted aromatics to hydroxylated aromatics	TiO_2	125 W Hg lamp	[55]
4-substituted toluenes to aryl aldehydes and ketones	TiO_2, TiO_2/HY	125W Hg	[56]
Naphthalene to 2-formyl Cinnamaldehyde	TiO_2	500W Hg lamp	[57]
Cyclopentene to cyclopenten-2-en-1-one	TiO_2	250 W Hg	[58]
Hexene-1 to acetaldehyde propaionaldehyde, Butyraldehyde	Titaniusm stearate	Hg Lamp	[59]

methane to benzophenone or acetophenon, cumene to cumyl alcohol, tolune to benzaldehyde.

6.5 PHOTOCATALYTIC REDUCTIONS

6.5.1 Photocatalytic Reduction of Carbon Dioxide and Dinitrogen

These are two important reactions and have been investigated by a number of workers. These two reactions have some relevance to photo synthesis and nitrogen cycle. In view of the importance these two reactions need to be dealt with separately. However for a compilation of the relevant data please refer to Magesh et al., [5].

Table 6.10 ***Yields of aromatic hydroxylated species for 45 minutes irradiation time using TiO_2 [55].***

Substrate	*Conversion %*	*Total Yield OH derivative*	*O:m:p ratio*
Phenol	70	75	54.5:0.5:45.0
phenylamine	40	50	49.7:0.0:50.3
N-phenylacetamide	50	60	20.0:03.0:77.0
Nitrobenzene	50	20	29.0:34.0:37.0
Cyanobenzene	60	30	45.0:30.0:25.0
1-Phenylthanone	55	30	38.5:21.0:40.5

6.5.2 Photocatalytic Reduction of Carbonate

When carbon dioxide present in the atmosphere dissolves in water it is mostly present in the form of carbonates. Therefore it is appropriate to study the photo-catalytic reduction of carbonate to form various chemicals. The results involving the photo-catalytic reducion of carbonate species to organic chemicals are given in Table 6.11.

Table 6.11 ***Products, catalysts, and reaction conditions for photocatalytic reduction of carbonate.***

Reaction	*Catalysts*	*Reaction Condition*	*Ref*
Methanol	MoS_2, ZnTe,CdSe P25 TiO_2	125 W Hg	[60]
Methanol and methane	TiO_2	15W lamp 365 nm	[61]
CH_3OH, HCHO $HCOO^-$	Cr and Mg doped TiO_2	125 W Hg	[62]
HCOOH, HCHO CH_3OH	$SrFeO_3$	450W Hg	[63]
Bicarbonate,acetate propionate	MnS	450W Hg	[64]

6.5.3 Photocatalytic Reduciton of other Nitrogen Containing Compounds

The reduction of nitrate is of interest as a means of mimicking reduction of nitrogen oxyanion substrates in nature and developing novel nitrogen fixation systems [66,67]

6.5.4 Photocatalytic Hydrogenation

Hydrogenation of olefins is an important reaction and has applications in Fischer-Tropsch process, preparation of edible oils and in organic synthesis. some relevant data are given in Table 6.12.

Table 6.12 ***Products,catalysts, and conditions for reduction of various hydrocarbons.***

Reaction	*Catalysts*	*Irradiation*	*Ref*
1-pentene	$Fe(CO)_5$	Laser Irradiation	[67]
Ethylene	$H_4Ru_4(CO)_{12}$	450 W Hg	[68,69]
norbornadiene	$Cr(CO)_6$	1-80 atm	[70]
1-octene	cis-$HMn(CO)_4PPh_3$	100 W Hg	[71]
alkenes	$H_4Ru_4(C))_{12}$	355 nm	[72-74]
diphenylacetylene	Pt,Rh Pd on TiO_32	125 W Hg	[75]
1,5cyclooctadience	$Rh_4(CO)_{12}$	500W Hg	[76]

Table 6.13 ***Catalysts and Conditions in the Photocatalytic formation of Hydrogen Peroxide.***

Reaction	*Catalysts*	*Irradiation*	*Ref*
Oxygen to H_2O_2	Ru(II) complex	500 W Xe	[77]
	Ru(II) Complex	500W W-X lamp	[78]
	metal porphyrins	500W W-Xlamp	[79]
	TiO_2-fluoride	40W lamp	[80]
water to H_2O_2	TiO_2	> 400 nm	[81]

6.5.5 Reduction of Organic Nitro Compounds to Amines

The reduction of various nitro compounds to the corresponding amines plays an important role in synthetic chemistry for various drugs, dyes and polymers. Anilines are widely present in the drug and dye molecules. The reduction of nitro compounds is also environmentally significant because of the toxic effects of nitro aromatic compounds.

6.5.6 Photocatalytic Formation of Hydrogen Peroxide

Hydrogen peroxide plays an important role as oxidising agent in a variety of pollution control systems. It is also used in organic synthesis as Fenton's reagent. It is used as a disinfectant, as propellant and also for the production of various peroxides and production of oxyacids. Few typical examples are given in Table 6.13.

6.5.7 Other Organic Photocatalytic Reactions

There are a variety of isomerization reactions which can be carried out by photocatalytic means. Polymerization is a important industrial process and

the dependence of world today on polymers is high. Various polymerization reactions have been carried out by photocatalytic means using both homogeneous and heterogeneous catalysts.

In addition to various reactions considered in this chapter, there are also other reactions like condensation, bond cleavage which can be carried out by photo-catalytic means. Though considerable effort has already been placed on photo-catalytic transformations, the production of chemicals by this route has yet to be fully realized though the feasibility has already been established. The transformation of these processes from laboratory to industrial production though may not have reached the required maturity, it is only a matter of time, when this can occur. When it takes place the production of chemicals can become a neat process with acceptance from people with environmental concerns.

References

1. C. H. Langford, Catalysts, 2: 327 (2012)
2. Carey, J. H., Lawerence, J. and Tosine H. M. Photocatalytic treatment of polychlorinated biphenyls on TiO_2. Bull. Environ. Contam. Toxicol. 1976, 16, 696701.
3. Rajeshwar K., Solar energy conversion and environmental remediation using inorganic semiconductor liquid interfaces: The road traveled and the way forward. J. Phys. Chem. Lett. 2, 1301 (2011).
4. http://$www.isc.fraunhofer.de/german/portal/index\_tec\_18.html$
5. G. Magesh, B. Viswanathan, R. P. Viswanath and T. K. Varadarajan, Photo/Electro-chemistry and Photobiology in Environment, Energy and Fuel, pp. 321-357 (2007).
6. S. Farhadi, A. Zabardasti and Z. Babazadeh, Tetrahedron Lett., 47, 8953 (2006).
7. K. Ohkubo, K. Suga and S. Fukuzumi, Chem. Commun., 19: 2018 (2006).
8. D. Brinkley and T. Engel, Surf. Sci., 415, L1001 (1998)
9. K. Nomiya, Y. Sugie, T. Miyazaki, M. Miwa, Polyhedron, 5(7),1267 (1986).
10. S. Shinoda, A. Kobayashi, T. Aoki and Y. Saito, J. Mol. Catal., 38, 279 (1986).
11. I. Moriguchi, K. Orishikida, Y. Tokuyama, H. Watabe, S. Kagawa and Y. Teraoka, Chem. Mater. 13, 2430 (2001).
12. A. Sclafani, Marie-Noelle Mozzanega and P. Pichat, J. Photochem. Photobiol., A, 59, 181(1991)

13. B. Ohtani, Jun-ichi Handa, Sei-ichi Nishimoto, T. Kagiya, Chem. Phys. Lett., 120 (3), 292 (1985)
14. T. Matsubara, Y. Saito, T. Yamakawa and S. Shinoda, J. Mol. Cat., 67, 175 (1991).
15. R. Irie, X. Li and Y. Saito, J. Mol. Catal., 18,263 (1983).
16. T. Yamakawa, T. Katsurao, S. Shinoda and Y. Saito, J. Mol. Catal., 42,183(1987).
17. I. Ait-Ichou, M. Formenti, B. Pommier and S. J. Teichner, J. Catal., 91, 293(1985).
18. R. Irie, X. Li and Y. Saito, J. Mol. Catal., 23, 17 (1984).
19. B. Ohtani, M. Kakimoto, S. Nishimoto and T. Kagiya, J. Photochem. Photobiol., A, 70, 265 (1993).
20. Y. Kado, M. Atobe and T. Nonaka, Ultrason. Sonochem., 8, 69 (2001).
21. A. Hiskia and E. Papaconstantinou, Polyhedron, 7(6), 477(1988)
22. S. Farhadi, M. Afshari, M. Maleki and Z. Babazadeh, Tetrahedron Lett., 46, 8483 (2005)
23. O. S. Mohamed, A. El-Aal M. Gaber and A. A. Abdel-Wahab, J. Photochem. Photobiol., A, 148, 205 (2002).
24. T. Ruther, A. M. Bond and W. R. Jackson, Green Chem., 5, 364 (2003).
25. Y. Wu, Y. Li and Q. Zhuang, J. Photochem. Photobiol., A, 62, 261 (1991).
26. M. Miyake, H. Yoneyama and H. Tamura, J. Catal., 58, 22 (1979).
27. B. Pal, T. Torimoto, K. Iwasaki, T. Shibayama, H. Takahashi and B. Ohtani, J. Phys. Chem. B 108, 18670 (2004).
28. H. Yamamoto, S. Shinoda and Y. Saito, J. Mol. Catal., 30, 259 (1985).
29. K. Nomura, Y. Saito and S. Shinoda, J. Mol. Catal., 50, 303 (1989).
30. J. Zhenzheng, L. Qinglin, F. Liangbo, C. Zhengshi, Z. Xinhua and X. Chanjuan, J. Mol. Catal., 50, 315, (1989).
31. S. Yamagata, B. H. Loo and A. Fujishima, J. Electroanal. Chem., 260, 447 (1989).
32. Z. Jin, Q. Li, X. Zheng, C. Xi, C. Wang, H. Zhang, L. Feng, H. Wang, Z. Chen and Z. Jiang, J. Photochem. Photobiol., A, 71, 85 (1993).
33. T. Hirakawa, J. K. Whitesell and M. A. Fox, J. Phys. Chem. B, 108, 10213 (2004).
34. K. Tennakone, U. S. Ketipearachchi and S. Punchihewa, J. Mol. Catal., 61, 61 (1990).
35. X Li, S. Shinoda, Y. Saito, J. Mol. Catal., 49, 113(1989).
36. T. Takahashi, S. Shinoda, Y. Saito, J. Mol. Catal., 31, 301 (1986).
37. R. P. Noceti, C.E. Taylor, J. R. D'Este, Catal. Today, 33, 199 (1997).

38. C. E. Taylor and R. P. Noceti, Catal. Today, 55, 259 (2000).
39. M. A. Gondal, A. Hameed and A. Suwaiyan, Appl. Catal., A, 243, 165 (2003).
40. M. A. Gondal, A. Hameed, Z. H. Yamani and A. Arfaj, Chem. Phys. Lett., 392, 372 (2004)
41. D. Shi, Y. Feng, S. Zhong, Catal. Today, 98, 505 (2004).
42. K. Nomura, Y. Saito, J. Mol. Catal., 54,57 (1989).
43. P. Ciambelli, D. Sannino, V. Palma, V. Vaiano, Catal. Today, 99, 143 (2005).
44. H. Park and W. Choi, Catal. Today, 101, 291 (2005).
45. Y. Mao and A. Bakac, Inorg. Chem., 35, 3925 (1996).
46. A. Molinari, R. Amadelli, A. Mazzacani, G. Sartori and A. Maldotti, Langmuir, 18, 5400 (2002)
47. A. Maldotti, A. Molinari, G. Varani, M. Lenarda, L. Storaro, F. Bigi, R. Maggi, A. Mazzacani and G. Sartori, J. Catal., 209, 210 (2002)
48. W. Mu, Jean-Marie Herrmann and P. Pichat, Catal. Lett., 3, 73 (1989).
49. K. Wada, K. Yoshida, Y. Watanabe and T. Suzuki, App. Catal., 74, Ll (1991).
50. T. Tanaka, T. Ito, S. Takenaka, T. Funabiki and S. Yoshida, Catal. Today, 61, 109 (2000).
51. L. V. Lyashenko, V. M. Belousov, F. A. Yampolskaya, React. Kinet. Catal. Lett., 20 (1-2), 59, (1982)
52. K. Marcinkowska, S. Kaliaguine and P. C. Roberge, J. Catal., 90, 49 (1984).
53. F. Amano, T. Ito, S. Takenaka and T. Tanaka, J. Phys. Chem. B, 109, 10973 (2005).
54. Y. Mao and A. Bakac, J. Phys. Chem., 100, 4219 (1996).
55. G. Palmisano, M. Addamo, V. Augugliaro, T. Caronna, E. Garca-Lopez, V. Loddo and L. Palmisano, Chem. Commun., 9, 1012 (2006).
56. C. Bouquet-Somrani, A. Finiels, P. Geneste, P. Graffin, A. Guida, M. Klaver, Jean-Louis Olive and A. Saaedan, Catal. Lett., 33, 395 (1995).
57. T. Ohno, K. Tokieda, S. Higashida and M. Matsumura, App. Catal., A, 244, 383 (2003).
58. P. Kluson, H. Luskova, L. Cerveny, J. Klisakova and T. Cajthaml, J. Mol. Catal. A: Chem., 242, 62 (2005).
59. V. I. Stepanenko, L. V. Lyashenko and V. M. Belousov, React. Kinet. Catal. Lett., 21 (1-2), 45 (1982).

60. M. A. Malati, L. Attubato, K. Beaney, Sol. Energy Mater. Sol. Cells, 40, 1, (996)
61. Y. Ku, Wan-Hui Lee, Wen-Yu Wang, J. Mol. Catal. A: Chem., 212, 191 (2004).
62. M. W. Raphael, M. A. Malati, J. Photochem. Photobiol., A, 46, 367 (1989).
63. Q. H. Yang, X. X. Fu, Chin. Chem. Lett., 14 (6), 649 (2003).
64. X. V. Zhang, S. T. Martin, C. M. Friend, M. A. A. Schoonen and H. D. Holland, J. Am. Chem. Soc., 126, 11247 (2004).
65. K. T. Ranjit, B. Viswanathan, J. Photochem. Photobiol., A, 107, 215 (1997).
66. J. Chatt, J. R. Dilworth and R. L. Richards, Chem. Rev., 78, 589 (1978).
67. R. L. Whetten, Ke-Jian Fu and E. R. Grant, J. Chem. Phys., 77 (7), 3769 (1982).
68. Y. Doi, S. Tamura and K. Koshizuka, J. Mol. Catal., 19, 213,(1983).
69. Y. Doi, S. Tamura and K. Koshizuka, Inorg. Chim. Acta., 65, L63 (1982).
70. M. J. Mirbach, D. Steinmetz and A. Saus, J. Organomet. Chem., 168, Cl3 (1979).
71. P. L. Bogdan, P. J. Sullivan, T. A. Donovan and J. D. Atwood, J. Organomet. Chem., 269, C51 (1984).
72. E. Samuel, J. Organomet. Chem., 198, C65 (1980).
73. J. L. Graff and M. S. Wrighton, Inorg. Chim. Acta., 63, 63 (1982).
74. H. Moriyama, A. Yabe and F. Matsui, J. Mol. Catal., 50, 195 (1989).
75. C. Hoang-Van, P. Pichat and Marie-Noelle Mozzanega, J. Mol. Catal., 92, 187 (1994).
76. Taka-aki Hanaoka, T. Matsuzaki and Y. Sugi, J. Mol. Catal., A: Chem., 149, 161 (1999).
77. M. Fukushima, K. Tatsumi, S. Tanaka and H. Nakamura, Environ. Sci. Technol., 32, 3948 (1998).
78. R. Atkinson, Chem. Rev., 86, 69 (1986).
79. H. Muraki, T. Saji, M. Fujihira and S. Aoyagui, J. Photochem. Photobiol., A, 115, 227 (1998). 80219. J. Premkumar, R. Ramaraj, J. Chem. Soc., Dalton Trans., 21, 3667 (1998).
80. J. Premkumar, R. Ramaraj, J. Mol. Catal. A: Chem., 142, 153 (1999).
81. V. Maurino, C. Minero, G. Mariell and E. Pelizzetti, Chem. Commun., 20, 2627 (2005).

7 Basic Principles of Photosynthesis

7.1 INTRODUCTION

In this chapter, the principles of photosynthesis will be examined in an elementary form since they are relevant for the understanding of photo-electrochemical cells. In its complete form Photosynthesis is a complex phenomenon involving various steps and only the basic principles of this process has a direct relevance to PEC and hence those aspects alone will be outlined in this chapter. In the simplest language, photosynthesis can be considered to be the reduction of carbon dioxide to carbohydrate (molecular state containing carbon and hydrogen with other atoms) species simultaneously making use of water and sunlight. A simple pictorial representation of the basis of photosynthesis is given in Fig. 7.1.

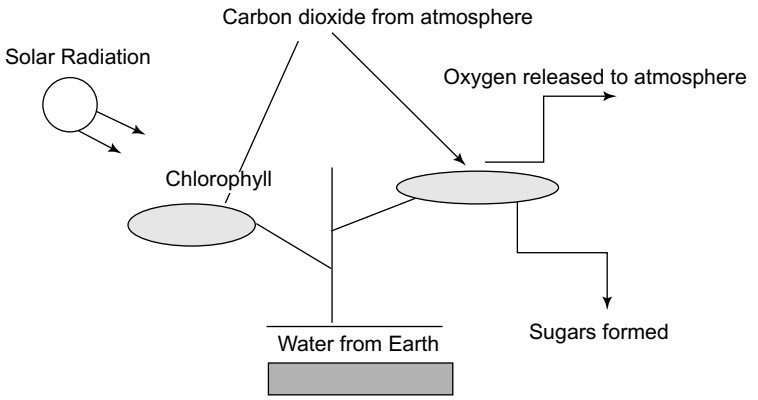

Figure 7.1 ***A simple pictorial representation of the photosynthesis process.***

It is known that the ecosystem of earth is directly connected with the solar radiation that the earth receives on daily basis. Essentially, in simple language photosynthesis involves the capture of photon energy and incorporating them in chemicals. This is what happens in green plants, algae, and some kinds of bacteria. Organisms can be put into two groups, namely autotrophs, which by

themselves can carry out photosynthesis and thus manufacture their own food and also food for others and heterotrophs, which are incapable of carrying out photosynthesis themselves but must consume autotrophs or other organisms that ate autotrophs. In other words, photosynthetic organisms are at the base of the food chain, and with only a very few exceptions all organisms on earth depend upon photosynthesis as the source of their food and energy. Photosynthesis consists of two parts namely the light reactions wherein light energy is converted into high energy chemicals while in dark reaction carbon dioxide is converted into carbohydrates. This process requires hydrogen generated from the decomposition of water together with the evolution of molecular oxygen. In this sense, this process assumes importance for the photo-electro-chemical decomposition of water for the production of hydrogen which can be used as fuel. The evolved oxygen molecule can give rise to ozone in the upper atmosphere which can form a protective layer from ultraviolet radiation on earth. It is necessary to learn the light reactions from the point of green plants though other organisms may also follow a similar path. The first law of photo-chemistry states that for a photo-chemical reaction to take place, photons must be absorbed by the system. In plants the photon absorbing pigments are the chlorophylls and carotenoids. Chlorophylls consist of a light absorbing porphrin ring system with a central magnesium ion with suitable species that can attach to the membrane. Light reactions are generally considered as the energy conversion processes in all plants and since they absorb red and blue parts and hence appear green but other combination of absorbing colours and appearance colours are possible. Carotenoids are one such pigment which are always present but appear only when chlorophylls break down. The photosynthetic pigments are available in the membranes (choloroplasts) and the porous system called stomata allow the passage of uncharged molecules like carbon dioxide and molecular oxygen. The pigment containing membranes are called thylakoids and their arrangement in stacks as pigment protein complexes and probably the arrangement of these species enables efficient harvesting of light energy. The non-membraneous portion of the chloroplast called stroma contains an aqueous solution of enzymes which is responsible for the reduction of carbon dioxide. There are some governing principles for the light reactions. They are:

(1) The pigment protein must be capable of absorbing the photon available and must go to the excited state.
(2) The excess energy available in the protein from the photon must be capable being transferred to the adjacent molecule and this energy transfer path necessarily facilitates the ultimate energy transfer and reduction of normally difficult to reduce carbon dioxide.

(3) These molecules which receive the excitation energy are contained in a thylakoid membrane and thus probably create the necessary reaction centres in highly structured arrangement.

Two kinds of energy-containing molecules are formed in the light reactions of photosynthesis namely adenosine triphosphate (ATP) and reduced nicotinamide adenine dinucleotide phosphate (NADPH), which are the sources of reducing power. The Photosystems and other reaction centers are connected by a series of compounds that act as electron carriers. An excited electron in a Photo system II reaction center enters this chain of carriers and moves from one to the next until it reaches a Photosystem I reaction center. This transport of an electron between the two types of reaction centers results in the pumping of hydrogen ions (H^+) across the thylakoid membrane, thus forming a gradient with a high H^+ concentration inside the thylakoid compartments and a relatively low concentration on the stroma side. The potential energy associated with this gradient is then used to form ATP by a mechanism similar to that by which ATP is generated in mitochondria.

The next step in the process is that an excited electron in Photo system I is transferred to a molecule of NADP, along with an H^+, thereby reducing it to NADPH. Notice that the electrons leaving Photo system I are being replaced by ones that came through the electron carriers from Photo system II. Finally, in order for this process to continue, the electrons that were removed from Photo system II have to be replaced. This is achieved by the splitting of an H_2O molecule, which yields electrons, H^+, and oxygen. The oxygen from two water molecules forms O_2, which then passes through the stomata into the atmosphere. In summary, what has been achieved is the conversion of photon energy into chemical energy in the form of ATP and NADPH, with the concomitant formation of O_2.

7.1.1 Reduction of Atmospheric CO_2 to Carbohydrate

The second major phase of photosynthesis involves the conversion of CO_2 from the atmosphere into carbohydrates and other biological molecules. This set of reactions is sometimes referred to as the "dark reactions" of photosynthesis because light is not directly involved. However, this terminology is somewhat misleading because light is required for the formation of the ATP and NADPH needed for energy and reducing power. If a photosynthesizing plant was suddenly put in the dark, the so-called dark reactions would only continue until the supply of ATP and NADPH was depleted. The conversion of CO_2 into carbohydrate takes place in the chloroplast stroma and follows a complex metabolic pathway called the Calvin Cycle or the Reductive Pentose Phosphate Pathway, each step of which is catalyzed by a specific enzyme. Its overall form is shown in Fig. 7.2.

Carbon dioxide first combines with a five carbon compound called ribulose-1,5 -bisphosphate (RUBP), which then immediately splits into two three carbon compounds. Using energy and reducing power from ATP and NADPH, these are converted into 3-phosphoglyceraldehyde (3PGAL), which can be used by the plant to manufacture carbohydrates and various other biological molecules and to regenerate RUBP.

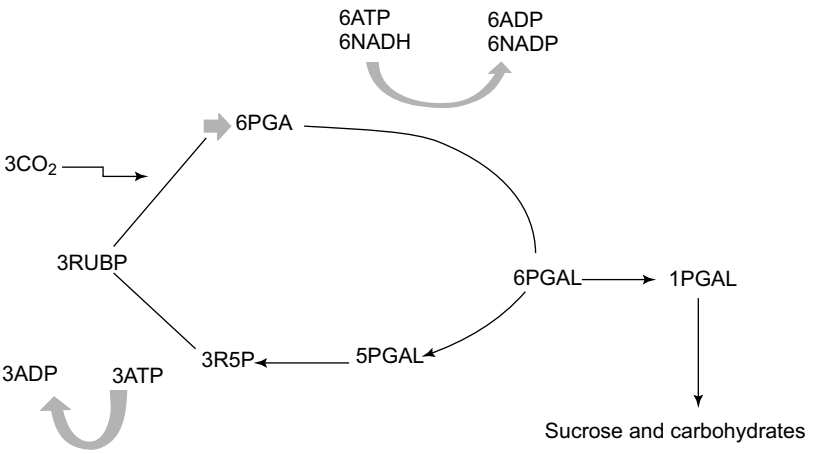

Figure 7.2 ***The Calvin Cycle. In this series of reactions, only a few of which are shown, carbon dioxide from the atmosphere is converted into carbohydrates. Understanding this cycle earned a Nobel Prize for Melvin Calvin in 1961.***

In order for the Calvin Cycle to continue, there must be a continuous supply of RUBP. Thus not all of the 3PGAL produced can go into the synthesis of carbohydrates-a significant portion (about 5 molecules out of 6) must be used to make fresh RUBP. This also requires ATP coming from the light reactions, and is what gives the pathway its cyclic nature. In summary, ATP and NADPH formed in the light reactions of photosynthesis are used to convert atmospheric CO_2 into carbohydrates, which represent a stable, long term form of energy storage. Overall, energy that originated as photons from the sun is now contained in carbohydrates and other molecules that serve as food for the plant or for an animal that eats the plants.

7.1.2 Environmental Aspects of Photosynthesis

Because of the fundamental biological significance of photosynthesis and its importance in agricultural productivity, a considerable amount of research has been directed towards understanding the effects that environmental factors such as light, temperature, rainfall, salinity, and disease have on the process. In recent years, the effects of elevated atmospheric CO_2 and of increased ultraviolet radiation exposure due to depletion of the Earth's

ozone layer have received considerable attention. The potential for forests and other photosynthetic ecosystems to mitigate increasing atmospheric CO_2 is also an active area of research. Different species, and in some cases even different cultivaters of the same species, vary widely in their ability to tolerate the multitude of environmental stresses that a photosynthesizing plant may encounter. The natural geographic distribution of plant species can be understood in terms of their ability to photosynthesize efficiently under the range of conditions that they encounter in the Earth's various ecosystems. Likewise, environmental factors govern the range over which specific agricultural crops can be successfully introduced and cultivated. Both traditional plant breeding methods and the techniques of modern molecular biology are being used to produce plants that can maintain their vigor and sustain high rates of photosynthesis when subjected to environmental stress. These approaches have been very successful in the past and promise to further increase crop productivity and decrease the need for fertilizers, herbicides, and insecticides.

The overall reaction that takes place in plants in the photosynthesis can be represented by

$$6CO_2 + 6H_2O \rightarrow C_6H_{12}O_6 + 6O_2 \tag{7.1}$$

(Carbon dioxide) + Water + light energy Sugar (carbohydrate) + Oxygen

The term Photosynthesis encompasses many dimensions. The simplest one is shown by the equation (7.1). However, it is necessary that we outline some essential aspects of photosynthesis in a simple language. These include:

1. If photosynthesis were to occur as has been shown by equation (7.1) with evolution of molecular oxygen with rearrangement of carbon dioxide and water to yield sugar then the process is termed as oxygenic photosynthesis.
2. Hence it must be possible that some bacteria can carry out the photosynthesis in an anoxygenic pathway without the release of oxygen.
3. Photosynthesis can also be understood in terms of carbon fixation wherein carbon dioxide undergoes reduction (probably stepwise) and hence involves reducing species and energy. This can be considered to be the opposite of cellular respiration wherein glucose and other sugars undergo oxidation to produce carbon dioxide, water and chemical energy.
4. Instead of water, it is possible to employ other reducing agents like arsenite which can act as electron donors and thus reduce carbon dioxide to carbon monoxide (which is subsequently reduced to sugars) and this type of harnessing can take place in some microbes.
5. It is possible one can write a variety of such possibilities for photosynthesis.

> However, essentially photosynthesis takes place in two steps wherein light dependent steps involves the storage of energy in molecules like ATP and NADPH. The light independent second reaction, namely, capture and chemical reduction of carbon dioxide takes place.

It may be necessary if one follows the whole act of photosynthesis in a sequence. The light is harvested by the proteins which are embedded in cell membranes. The membrane may be tightly folded into cylindrical sheets termed as thylakoids. This membrane architecture and its occupancy will be such that it provides large surface area to harness as much light as possible. There can be multiple layers of membranes and usually termed as phospholipid inner or outer membrane together with an aqueous fluid called stroma. This aqueous fluid contains the thylakoids where the act of photosynthesis is taking place. The thylakoid membrane contains membrane proteins together with some pigments that absorb light for the photosynthesis. Even though the primary pigment is chlorophyll, other pigments like carotenes, xanthophylls, phycocyanin (green algae), phycoerythrin (red algae) and flucoxanthin (brown algae) all these ppigments are embedded in special antenna-proteins. When these pigments are arranged in such a way that they work in conjunction, then these proteins are called light harvesting complex to denote that light harvesting effort is a joint effort and not by a single molecular species. This is one of the difficulties faced in artificial photosynthesis since light harvesting species though can be identified the sequence required has to be appropriately stitched and capturing antenna has to be provided for. This whole architecture has to be built mostly in leaves with a fine surface coating of the leaf with a hydrophobic waxy material so that water loss is restricted. Let us consider the light dependent reactions in a little more detailed form. The light dependent reaction has two components conventionally called cyclic and non-cyclic forms. The sequence of reactions is termed as Z scheme. In a simple language, the cyclic form in the Z Scheme generates ATP while in non-cyclic form NADPH is created. At the Photosystem II, light is harvested through light harvesting antenna complexes and other pigments and the electron is transferred to the electron acceptor molecule namely pheophytin. At the same time oxygen evolving complex dissociates water and produce molecular oxygen and protons. The electron from the phenophytin travels along a transport chain and passes through photosystem I to reduce the co-enzyme NADP to NADPH which has a role in the light independent reactions. The cyclic reaction also takes a similar route but is involved in chemiosmotic synthesis of ATP utilizing the energy provided by the electron transport chain of the Z scheme. The generation of the reducing agent NADPH at the terminal step of Z scheme means that the chlorophyll in photosystem II will be in the oxidized form (termed as P680) and its return to its original

state is made possible by the oxygen evolving complex (consisting of four manganese ions and one calcium ion) which binds two molecules of water and thus is capable of storing four oxidizing equivalents. The hydrogen ions thus generated provides the chemiosmotic potential for proton migration and ATP synthesis. In the description given above we have not utilized carbon dioxide which is the source for the carbon fixation. This fixation and its conversion is carried out in photosynthesis in the so called dark reaction. Carbon dioxide from the atmosphere is captured by the enzyme called RuBisCO and the formed NADPH is utilized to generate three carbon sugars which is then converted to the final carbohydrate molecules. These are the starting material for the subsequent generation of cellulose, amino-acids and also the so called fuel for cellular respiration. There are other variations for carbon fixation. The important ones are: (i) The carbon dioxide can be directly fixed to three carbon molecule phophoenolpyruvate (PEP) promoted by an enzyme PEP carboxylase. The oxaloaceitc acid or malate synthesized is then decarboxylated to three carbon sugar 3-phosphoglyceric acids. The plants that do not use PEP-carboxylase for carbon fixation are called C3 plants.

(ii) The CAM (crassulacean acid metabolism) plants fix carbon dioxide at night in the form of malic acid though carboxylation of phosphoenolpyruvate to oxaloacetate which is subsequently reduced to malate. The malate is then decraboxylated in day time releasing carbon dioxide thus facilitating the carbon fixation as 3-phophoglycerate by the conventional enzyme RuBisCO. The energy harnessing in photosynthesis takes place in four steps and the respective time scales are given in Table 7.1.

Table 7.1 ***Time scales of each of the steps of the energy harvesting in photosynthesis.***

	Details of Processes	*Time Scale*
1.	Energy transfer in antenna chlorophyll	Femto second (10-15s) to pico second
2.	Transfer of electrons in photo chemical reactions	Pico to nano second scale Micro to Milli second
3.	Electron transport chain and ATP synthesis	Millisecond to second scale
4.	Fixation of carbon and export of the stable product	

In this short presentation we have shown how the Photosynthesis is taking place and the redox processes are taking place in a step wise manner with appropriate species in relation to the redox potential values. Similar situation exists in Photo-electro-chemical decomposition of water but the

only difference being the redox potential of water is fixed for hydrogen and oxygen evolution and hence the system (in this case the semiconductor) which absorbs radiation has to have its band positions at the appropriate values of water decomposition reaction. In the case of photosynthesis, these species are multiple in nature and also in sequence and hence appears to be a facile process.

References

1. Blankenship, R. E. 2002. Molecular Mechanisms of Photosynthesis. Blackwell Science Publishers, Oxford, UK, Malden, MA, USA.
2. Jansson, J. 1994. The Light-Harvesting Chlorophyll a/b-Binding Proteins. Biochimica Biophysica Acta, 1184: 1919.
3. Long, S. P., E. A. Ainsworth, A. Rogers, and D. R. Ort. 2004. Rising Atmospheric Carbon Dioxide: Plants FACE the Future. Annual Review of Plant Biology, 55: 591-628.
4. Nelson, N. and C. F. Yocum. 2006. Structure and Function of Photosystems I and II. Annual Review of Plant Biology, 57: 521-565.
5. Raghavendra, A. S., ed. 1998. Photosynthesis: A Comprehensive Treatise. Cambridge University Press, Cambridge, UK, New York, USA.
6. Raven, P. H., G. B. Johnson, J. Losos, and S. Singer. 2005. Biology, 7th. ed. McGraw-Hill, New York.
7. Szalai, V. A. and G. W. Brudvig. 1998. How Plants Produce Dioxygen. American Scientist, 86: 542-551.
8. Taiz, L. and E. Zeiger. 2006. Plant Physiology, 4th. ed. Sinauer Associates, Sunderland, MA.
9. Wild, A. and R. Ball. 1997. Photosynthetic Unit and Photosystems: History of Research and Current View. Backhuys Publishers, Leiden.

8 Plasmonic Photocatalysis

8.1 INTRODUCTION

The anxiety to make use of the visible and low energy photons of the solar radiation has led to the development of plasmonic photo-catalytic systems based on metal nano-particles deposited on the surface of polar semiconductors or insulators. Nano particles (NP) of noble metals especially (Ag, Au and Pt) can strongly absorb visible light due to their Surface Plasmon Resonance (SPR) which can be tuned by the control of the size or shape or surroundings of NPs. Conventionally, the visible light plasmonic photo-catalysts is a composite system composed of noble metal NP and a polar semiconductor (like AgCl, AgBr) but however, other materials like carbon, graphene oxide (GO), graphene and a few other insulators which are used as supports and/or charge carriers to form the plasmonic photo-catalytic systems.

8.2 PHENOMENON OF SPR

The conducting electrons of NPs undergo collective oscillation (excitation) by the oscillating electric field of the incident light. When the frequency of the incident light coincides with the resonance conditions of the noble metals NPs, the SPR appears because of the light (regions of visible, infrared or near IR) absorption [1]. The SPR of mostly spherical metal particles is dominated by the dipolar mode and is described in terms of the polarizability.The SPR frequency depends on the nature of the metal, the size and shape of the metal NP and the dielectric property of the surrounding medium, these variables can be used to tune the NP optical properties [2-4]. The noble-metal NPs deposited on the surface of support (example polar semiconductor) possibly charge-polarized work as light trapping, scattering and concentration centres.The SPR of the noble-metal NPs can induce electron transfer from the photo-excited noble metal NP to the support to which the NP is attached. The presence of noble metal NPs in contact with the support surface can also facilitate the redox reaction between the support and the substrate.

8.3 TYPES OF PLASMONIC PHOTO-CATALYSTS

There are various combinations of support and metal can be exploited as plasmonic photo-catalysts. These can be grouped as follows:

1. A semiconductor or insulator (A) with NPs of the metal(M) on the surfaces of the support, designated as M-A.
2. Noble metals M with nano-particles of the support (either a semiconductor or insulator) possibly deposited on the surface denoted as A-M.
3. A combination of the support A/A′ with NPs of metal deposited on the surface is referred to as M-A/A′.
4. Sensitizer molecule S anchored on the surface of noble metal and the noble metal supported on the semiconductor referred as S-M-A.
5. A noble metal M coated with an insulator A is denoted as A(M) and any other combination with support is designated as A′-A(M).

These designations are only indicative and one can generate many other combinations and they can be conveniently abbreviated using this type of notation.

8.4 PROCESS OF PLAMONIC PHOTO-CATALYSIS

In this mode of action, the Metal NPs absorb the visible light, the resulting photo-generated electrons and holes are separated by the metal support interface and the redox reaction take place on the surface of the plasmonic photo-catalyst. Alternatively, there can be radiative energy transfer between the noble metal NPs and the semiconductor in which the strong SPR induced electric field localized in the vicinity of the noble metal NPs can affect the electron hole formation and their transfer [5]. If the noble metal especially Au is supported on insulating support like ZrO_2, SiO_2, or zeolite, then the support cannot sustain the charge transfer and hence the metal NPs can be quickly heated up by the absorption of the visible light thereby activating the organic substrate [6]. A listing of the reported plasmonic photo-catalysts have been complied [2] together with the preparation methods and photo-catalytic reactions like water splitting, oxidation of organic substrates or molecules like methylene blue or rhodamine blue.

8.5 PHOTO-CATALYSTS BASED ON SILVER NANO-PARTICLES

It has been recognized that small silver clusters upto 8 atoms exhibit molecule-like optical transition [7, 8]. As the size of the silver particles are

big enough (more than 2 nm) then they develop optical absorption SPR bands due to their free electrons [9,10]. Since the complex dielectric constant of silver has small imaginary component, this leads to large local field enhancement and small loss of the surface plasmon propagation. Therefore, the SPR of silver nanoparticles induces large absorption amplitude. A variety of plasmonic photo-catalysts composed of silver nano partices on TiO_2, silver halides, composite semiconductors, carbon and graphene have been reported in literature.

8.5.1 Plasmonic Photo-catalyst Composed of Ag, NP and TiO_2

Awazu et al. fabricated $TiO_2/SiO_2/Ag$ photo-catalyst. The photo-catalytic activity of this catalyst under UV illumination for methylene blue is enhanced 7 times compared with that of TiO_2 [11]. Controlling the thickness of the SiO_2 shell can be used to further increase in enhancing the photo-catalytic activity. Kumar et al. studied the system TiO_2-SiO_2(Ag) by tuning the thickness of SiO_2 layer 2, 5, 10 and 20 nm and showed that the photo-catalytic activity gradually increases with a decrease in SiO_2 layer thickness [12]. Nitrogen containing TiO_2 with silver nano particles showed enhanced water-splitting performance compared to TiO_2 alone [13]. They gave evidence to show that the electron-hole pairs near the semiconductor surface are readily separataed from each other and migrate to the surface thus accounting for the enhanced performance.

8.5.2 Plasmonic Photocatalysts–Silver Nanoparticles and Silver Halides

Silver halide (Cl, Br and I) particles generate an electron hole pair on absorption of photon and the photogenerated electron combines with an Ag^+ ion to form Ag^0 atom. Using this principle, Kukuta et al., [14] observed that Ag^0 species are formed on AgBr and is not destroyed under successive illumination. This led to the development of first plasmonic photocatalyst Ag@AgCl (i.e. Ag-AgCl) [15]. A variety of Ag@AgCl systems have been generated and these systems showed strong absorption in the visible region, which is almost as strong as in the UV region. The photocatalytic activity evaluated for the dye degradation is 8 times greater than that observed with N-TiO_2. It is conceived that the visible light induced electron-hole pair in the Nano silver particle is separated such that an electron moves to the surface of the silver nano particle from the interface, and the hole moves to the surface of the AgCl particle which is then used to oxidise chloride ions to chlorine atoms. The chlorine thus formed will oxidise the dye and thus get reduced to chloride (Cl^-) ions.It is possible that the photogenerated electrons are trapped by oxygen dissolved in solution to form superoxide ions O_2^- ions or other

reactive species [16]. The architectures in terms of shape, morphology, (rods, hollow spheres, irregular balls, nanocubles, nano wires) and other features of the AgCl have been shown to have considerable influence in the catalytic decomposition of methylene blue under sunlight and showed high stability and recyclability [17-23]. The system Ag@Ag(Br, I) or Ag@AgBr was studied by [17] wang et al. and they have shown that the photogenerated electrons at the conduction band of the semiconductor are transferred to the silver nano particles, since the Fermi level of the nano particle lie lower in energy than the Conduction band minimum of the semiconductor. Among these two systems, the reducing power of the Ag@Ag(Br, I) is stronger than that of Ag@AgBr and the photogenerated electrons could reduce Cr (VI) to Cr (III) under visible light with high efficiency. Huang et al. [24] studied silver nano particles supported on silver salts like chloride, bromide, iodide, chromate, phosphate, $PW_{12}O_{40}{}^{3-}$ and $SiW_{12}O_{40}{}^{4-}$ and have shown that the charge on the counter anion strongly affects the photocatalytic activity.

8.5.3 Silver Nano Particles on Composite Semiconductors

Composite photo-catalysts of the type $Ag/AgBr/WO_3.H_2O$ have been examined since the CBM (conduction band minimum) and VBM (valence band maximum) for these two substances are at -3.7 and 5.95 eV and at -4.404 and -6.574 eV respectively. In this configuration, the visible light can be absorbed by AgBr or WO_3 and the silver nano particles and hence the oxidizing ability of this system will be higher than that of Ag@AgBr. This superior behaviour of this system has been demonstrated in the photo catalytic destruction of E. Coli. Other systems that have been studied include Ag/AgBr/BiOBr; $Ag\text{-}AgBr/Al_2O_3$; TiO_2-Ag/AgBr and $Ag/AgCl/TiO_2$. These systems have shown visible light photo activity for the sterilization of pathogenic organisms and also for the degradation of dyes [25-28]. Another plasmonic photo catalyst system that has been demonstrated is $Ag\text{-}AgI/Al_2O_3$ for the degradation and mineralization of chlorophenols (2,2,4 and tri) which has been identified to perform through two electron transfer process one from the photo excited Ag NPsto the AgI conduction band resulting in the formation of O_2^- and the other electron transfer from chlorophenol to the Ag NPs [29]. Another similar system studied is $Ag\text{-}AgI/Fe_3O_4@SiO_2$ [30].

8.5.4 Plasmonic Photo Catalysts with Ag NPs and Carbon

Core shell nano composite Ag@C (Ag-C) has been prepared by hydro-thermal process [31]. This system showed strong absorption in the visible region. The prepared Ag@C catalyst exhibits a high photocataltyic activity for the decomposition of tetraethylated rhodamine blue and acetaldehyde under visible light irradiation. A similar system namely TiO_2@C/Ag showed

photo-catalytic activity for the degradation of rhodamine blue and methyl orange [32].

8.5.5 Plasmonic Photo Catalysts with Ag NPs and Graphene

A photo catalyst of the composition Ag/AgCl/GO in which Graphene oxide is used as carrier (The favourable properties of graphene like transparency, high surface area, conjugated aromatic system, and unique electronic properties make them as excellent carriers for active components). The systems containing graphene oxide showed 4 time plasmonic photo catalytic activity for rhodamine degradation as compared to the Ag@AgCl system. This enhancement is due to the effective charge transfer from the plasmon-excited Ag nanocrystal to graphene which may suppress the electron hole recombination [33].

8.6 PLASMONIC PHOTO CATALYSTS OF AU NPs

Gold nanoparticles have unique place in plasmon resonance phenomenon. They show absorption of visible light and exhibit a variety of colours. Their size, shape and surrounding environment all can change the colour that is exhibited by these nano particles. Particles in the range of 10 nm show strong absorption maximum around 520 nm while increase in size there is a red shift. Another method of tuning the SPR is through the change of the shape of NPs. Depending on the aspect ratio, the rod shaped NPs show two resonances. When the length to radius ratio increases the SPR shows red shift. The surroundings also can change the SPR peak position. Au NPs have been deposited on insulators like Zeolite Y, ZrO_2 and SiO_2 and these systems have been efficient for the selective oxidation of hydrocarbons and volatile organic compounds like CO, methanol and formadehyde. The observed process can be accounted for in the heating up of the nano particles or the interaction between oscillating local electromagnetic fields and polar molecules may assist in the activation of the molecules for oxidation. The observed catalytic activity can be considered to arise only from the SPR effect of Au NPs.

8.6.1 Plasmonic Photo Catalysts with Au NPs and TiO_2

Au-TiO_2 system has received considerable attention with respect to plasmonic photo-catalyst. Liu et al., [34] used Au-TiO_2 to split water and demonstrated that Photo catalytic splitting under visible light illumination is enhanced by a factor of 66 with the addition of Au Nanoparticles. It has been proposed that the excitation in the Au Nps and the photo generated electrons is injected into the conduction band of TiO_2. Hou et al., [35] reported the use of plasmonic photo catalyst Au/TiO_2 for the reduction of carbon dioxide to hydrocarbon

fuels. This plasmonic photo catalyst has been used for photo-degradation of acetic acid and 2-propanol [36].

8.7 PLASMONIC PHOTO-CATALYSTS BASED ON PT NPs

There are only limited reports on this system. Li et al., [37] prepared a plasmonic photo catalyst Pt/Bi_2O_3, the conduction band receives the photogenerated electrons from Pt NPs and thus promotes the plasmonic catalysis. This system has also been explored for the photo degradation of benzene and oxidation of alcohols to aldehydes [38, 39].

8.8 CONCLUSION

Noble metal NPs supported on a variety of insulator surfaces does not operate through the injection of the photo excited electrons from NPs to the oxide and thus the latter does not directly participate in photo-catalysis. However,semiconductor supports can directly participate in the plasmonic photo catalysis since the electron transfer between the photo excited NPs and the semiconductor support can take place. The initial inertia in the studies of plasmonic photo catalysis using visible light has been overcome by a number of studies reported in literature and it is hoped that this field will evolve into an active field in the near future.

References

1. H. A. Atwater and A. Polman. Nat. Mater., 9: 205-213, 2010.
2. Peng Wang, Baibiao Huang, Ying Dai and Myung-Hwan Whangbo. Plasmonic photocatalysis: harvesting visible light with noble metal nanoparticles. Phys. Chem. Chem. Phys., 14: 9813-9825, 2012.
3. W. L. Barnes, A. Dereux and T. W. Ebbesen. Nature, 424: 824-830, 2003.
4. U. Kreibig. Optical properties of metal clusters, volume 25. Springer, Berlin, 1995 vol 25.
5. S. Linic, P. Christopher and D. B. Ingram. Nat. Mater., 10: 911-921, 2011.
6. X. Chen, H.-y. Zhu, J.-C. Zhao, Z.-F. Zheng and X.-P. Gao. Angew. Chem., Int. Ed., 47: 5353-5356, 2008.
7. T. H. Lee and R. M. Dickson. Proceedings National Academy of Sciences, USA, 100: 3043-3046, 2003.
8. C. M. Ritchie, J. R. Kiser K. R. Johnsen, Y. Antoku, R. M. Dickson and J. T. Petty. Journal of Physical Chemistry C, 111: 175-181, 2007.
9. J. P. Wilcoxon, J. E. Martin and P. Provencio. J. Chem. Phys., 115: 998-1008, 2007.

10. C. M. Aikens, S. Z. Li and G. C. Schatz. Journal of Physical Chemistry C, 112: 11272-11279, 2008.
11. K. Awazu, M. Fujimaki, C. Rockstuhl, J. Tominaga, H. Murakami, Y. Ohki, N. Yoshida and TWatanabe. J. Am. Chem. Soc., 130: 1676-1680, 2008.
12. M. K. Kumar, S. Krishnamoorthy, L. K. Tan, S. Y. Chiam, S. Tripathy and H. Gao. ACS-Catalysis, 1:300-308, 2011.
13. D. B. Ingram, P. Christopher, J. L. Bauer and S. Linic. ACS-Catal, 1: 1441-1447, 2011.
14. N. Kakuta, N. Goto and H. Ohkita and T. Mizushima. J. Phys. Chem. B, 103: 5917-5919, 1999.
15. P. Wang, B.B. Huang, X. Y. Qin, X. Y. Zhang, Y. Dai, J. Y. Wei and M-H. Whanbo. Angew. Chem., Int. Ed., 47: 7931-7933, 2008.
16. M. R. Hoffmann, S. T. Martin, W. Choi and W. Bahnemann. Chem. Rev., 95: 69-96, 1995.
17. P. Wang, B. B. Huang, Q. Q. Zhang and X. Y. Zhang, X. Y. Qin, Y. Dai, J. Zhan, J. X. Yu, H. X. Liu and Z. Z. Lou. Chemistry - European Journal, 16: 10042-10047, 2010.
18. J. Jiang and L. Z. Zhang. Chemistry - European Journal, 17: 3710-3717, 2011.
19. C. H. An, R. P. Wang ad S. T. Wang and X. Y. Zhang. J. Mater. Chem., 21: 11532-11536, 2011.
20. Z. Z. Lou, B. B. Huang, Z. Y. Wang PWang, X. Y. Qin, X. Y. Zhang, H. F. Cheng, Z. K. Zheng and Y. Dai. Dalton Trans., 40: 4104-4110, 2011.
21. C. H. An, S. Peng and Y. G. Sun. Adv. Mater. (Weinheim, Ger.), 22: 2570-2574, 2010.
22. Y. P. Bi and J. H. Ye. Chem. Commun., pages 6551-6553, 2009.
23. L. Han, P. Wang, C. Z. Zhu, Y. M. Zhai and S. J. Dong. Nanoscale, 3: 2931-2935, 2011.
24. H. Huang, X. R. Li, Z. H. Kang, Y. Liu, X. D. He, S. Y. Lian, J. L. Liu and S. -T. Lee. Dalton Trans., 39: 10593-10597, 2010.
25. H. F. Cheng, B. B. Huang, P. Wang, Z. Y. Wang, Z. Z. Lou, J. P. Wang, X. Y. Qin, X.Y . Zhang and Y. Dai. Chem. Commun., pp. 7054-7056, 2011.
26. X. F. Wang, S. F. Li, Y. Q. Ma, H. G. Yu and J. G. Yu. Journal of Physical Chemistry C, 115: 14648-14655, 2011.
27. Y. Hou, X. Y. Li, Q.D. Zhao, X. Quan and G. H. Chen. J. Mater. Chem., 21: 18067-18076, 2011.
28. J. G. Yu, G. P. Dai and B.B. Huang. J. Phys. Chem., 113: 16394-16401, 2009.

29. X. X. Hu, C. Hu, T.W. Peng, X.F. Zhou and J. H. Qu. Environ. Sci Tech, 44: 7058-7062, 2010.
30. J. F. Guo, B. W. Ma, A.Y. Yin, K.N. Fan and W. L. Dai. Appl. Catal., B, 101: 580-586, 2011.
31. S. M. Sun, W. Z. Wang, L. Zhang, M. Shang and L. Wang. Catal. Commun., 11: 290-293, 2009.
32. P. Zhang, C. L. Shao, Z.Y. Zhang, M.Y. Zhang, J. B. Mu, Z. C. Guo, Y. Y. Sun and Y. C. Liu. Journal Materials Chemistry, 21:17746-17753, 2011.
33. M. S. Zhu, P. L. Chen and M. H. Liu. ACS Nano, 5:4529-4536, 2011.
34. Z. W. Liu, W. B. Hou, P. Pavaskar, M. Aykol and S. B. Cronin. Nano Lett., 11: 1111-1116, 2011.
35. W. B. Hou, W. H. Hung, A. Goeppert P. Pavaskar, M. Aykol and S. B. Cronin. ACS-Catal, 1: 929-936, 2011.
36. E. Kowalska, O. O. P. Mahaney, R. Abe and B. Ohtani. Phys. Chem. Chem. Phys., 12: 2344-2355, 2010.
37. R. H. Li, W. X. Chen, H. Kobayshi and C. X. Ma. Green Chemistry, 12: 212-215, 2010.
38. W. Y. Zhai, S. J. Xue, A. W. Zhu, Y. P. Luo and Y. Tian. ChemCatChem, 3: 127-130, 2011.
39. Z. K. Zheng, B. B. Huang, X. Y. Qin, X Y. Zhang, Y. Dai and M.H. Whangbo. Journal Materials Chemistry, 21: 9079-9087, 2011.

9 Photocatalytic Reduction of Carbon Dioxide by Water: A Step Towards Formation of Fuels and Chemicals

9.1 INTRODUCTION

9.1.1 Heterogeneous Photo-catalysis

The rigorous study of photo-catalytic reactions is continuous from 1970. The concept and the term 'heterogeneous photo-catalysis' were introduced and developed in Lyon to describe the partial oxidation of alkanes and olefinic hydrocarbons. The reactions took place at ambient temperature in the presence of a photo-catalyst conventionally titanium dioxide (TiO_2, anatase) under UV irradiation. Heterogeneous photo-catalysis is defined as "catalytic process during which one or more reaction steps occur by the involvement of electron-hole pairs, photo-generated on the surface of semiconducting materials illuminated by light of suitable energy". This pathway differs from the usual thermal reaction sequence and leads to reaction product selectivity patterns different from those observed with the thermal catalyzed reactions.

9.2 PRINCIPLES OF PHOTO-CATALYSIS

The band gap is one of the characteristic parameters for the electronic structure of any semiconductor and is defined as the energy interval (ΔE_g) between the valence band (VB) and the conduction band (CB). VB is defined as the highest energy band in which all or most of the energy levels are occupied by electrons, whereas CB is the lowest energy band whose energy states will be unoccupied or partially occupied with electrons. The band gap model proposed by Demeestere et al., [1] is shown in Fig. 9.1.

Electrons from VB are transferred to the CB when the semiconductor is illuminated with photons having energy content equal to or higher than the value of the band gap, creating electron-hole pairs (1). After migration to the

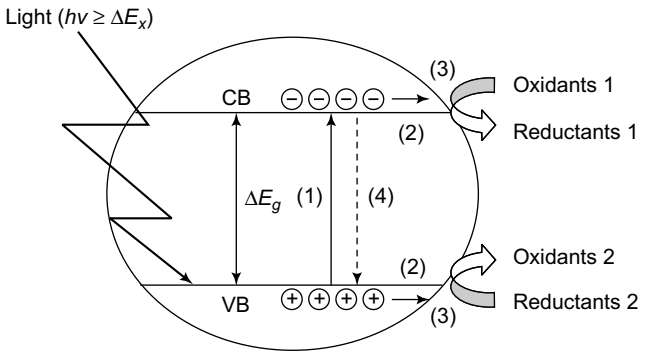

Figure 9.1 ***Pictorial representation of the "band gap model.": (1) Photo induced electron-hole pair creation; (2) charge migration to the surface; (3) redox reactions; (4) recombination. VB and CB represent valence band and conduction band, respectively.***

semiconductor surface (2), electron-hole pairs may induce redox reactions with adsorbates having suitable redox potentials (3). From a thermodynamic point of view, VB holes can oxidize adsorbed compounds if the redox potential of the holes/electrons of the VB is more positive than that of the adsorbates. Similarly, CB electrons can reduce adsorbed species if they have a more negative redox potential than that of the adsorbates. In a sense the energy of the top of the valence band denotes the oxidising power and the energy of the bottom of the conduction band denotes the reducing capacity of the semi-conductor. In the absence of suitable adsorbates, electron-hole pair recombination occurs with release of thermal energy and/or light (4).

The rate of a photo catalytic reaction depends on the type of the photo-catalytic semi-conductor and on the light radiation used [2]. Other factors that influence a photo-catalytic reactions are:

- pH of the medium with which the semiconductor surface is in contact.
- concentration of the substrate influencing the reaction kinetics.
- stream of photons, as oversupply of light accelerates electronhole recombination.
- temperature, higher temperatures usually cause frequent collision between the semiconductor and the substrate.

9.3 APPLICATIONS

A variety of applications ranging from anti-fogging, anti-microbial and self cleaning surfaces, through to water (conisdered in a separate chapter) and air purification, disinfection of water and solar induced hydrogen production (dealt with in separate chapter), have been developed and many of these

have made their way into commercial products. However, extensive research continues to further optimise this technology and to widen the spectrum of potential applications, especially in the following areas:

- Conversion of water to hydrogen gas by photo-catalytic water splitting: The ultimate target of water splitting is to provide clean hyrogen fuel through the utilization of solar energy. Efficiencies of differing magnitudes for solar water splitting have been reported for the photo-voltaic-photoelectrolytic device of Khaselev and Turner and for the photovoltaic-electrolytic device of Licht [3]. [see for a detailed consideration in another chapter]
- Conversion of carbon dioxide into hydrocarbons in the presence of water: In this case, Photo-catalysis provides a way to mimic photosynthesis by employing a semiconductor catalyst to absorb and utilize solar energy to convert chemicals into other forms.
- The application of illuminated semiconductors for the remediation of contaminants has been used successfully for a wide variety of compounds such as alkanes, aliphatic alcohols, aliphatic Conversion of carbon dioxide into hydrocarbons in the presence of water:

  In this case, Photo-catalysis provides a way to mimic photosynthesis by employing a semiconductor catalyst to absorb and utilize solar energy to convert chemicals into other forms.
- The application of illuminated semiconductors for the remediation of contaminants has been used successfully for a wide variety of compounds such as alkanes, aliphatic alcohols, aliphatic carboxylic acids, alkenes, phenols, aromatic carboxylic acids, dyes, Polychlorinated biphenyls (PCB), simple aromatics, halogenated alkanes and alkenes, surfactants, and pesticides as well as for the reductive deposition of heavy metals (e.g., Pt^{4+}, Au^{3+}, Rh^{3+}, Cr(VI)) from aqueous solution to surfaces [4]. Some of the aspects of this application will be dealt with in a separate chapter.
- Use of titanium dioxide in self-cleaning surfaces: Free radicals generated from TiO_2 can oxidize organic matter.
  Photo-catalytic surfaces have the potential to act against a variety of air pollutants and odours. This process can be used to remove microbes, oxidize volatile organic carbons (VOC), formaldehyde, ammonia and inorganic gaseous substances such as nitrogen- or sulphur-oxides (NO_X, SO_X).

9.4 COMPONENTS OF A PHOTO-CATALYST

In addition to the photo catalyst, whose primary function is to absorb light energy, several other components can be added to modify the photo-catalyst

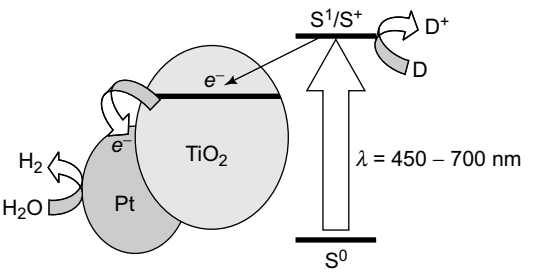

Figure 9.2 ***Pictorial representation of the operation of the photo-catalytic system for the release of hydrogen from water based on metalsemiconductor and a dyesensitizer. Legend: S^0, S^1, and S^+. are the sensitizer in the ground, excited, and one electron oxidized states of the dye, respectively [5].***

system based on their specific application and for improving the overall efficiency of the process [5].

9.4.1 Photo-catalytic Systems Based on Semiconductors and Sensitizers

The large group of the light-sensitive materials that have been investigated as photo-catalysts includes fairly wide-band semiconductors, mostly elemental semicondcutors, metal oxides and sulphides (a listing is given in another place) that absorb UV light. One method of extending their light sensitivity to the visible region of the spectrum is the use of colored substances or sensitizers. In systems with sensitizers, the dyes absorb visible light and in the excited state inject electrons into the semiconductor.

9.4.2 Photo-catalytic Systems based on Semiconductor Hetero-structures

In binary systems based on narrow-band and wide-band semiconductors the absorption of visible light by the narrow-band component leads to the injection of an electron into the wide-band semiconductor. The hole remains spatially separated from the electron and interacts with the electron donor.

9.4.3 Photo-catalyst Systems based on Semiconductors Doped with Metal Cations

The doping of wide-band semiconductors with transition metals creates local energy states in the forbidden gap. The excitation of electrons from those local energy states by visible light leads to the transfer of electrons into the conduction band.

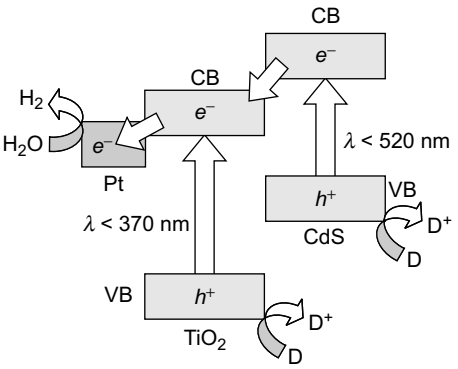

Figure 9.3 ***Simplified pictorial diagram for the spatial separation of the photo-generated charges in the CdS/TiO_2 hetero structures and the formation of hydrogen from water during the action of visible light [5].***

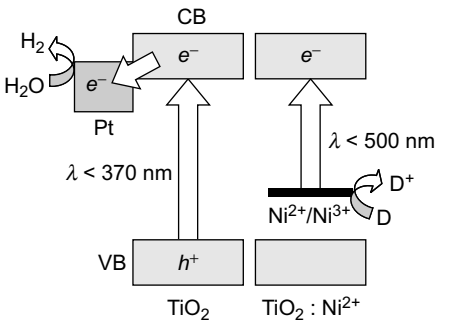

Figure 9.4 ***Schematic diagram of the operation of the Photo-catalytic system for the release of hydrogen from an aqueous solution of electron donor D with the participation of titanium dioxide doped with Ni^{2+} (TiO_2:Ni^{2+}) [5].***

9.4.3 Photo Catalyst Systems based on Semiconductors Doped with Anions

One of the approaches for decreasing the forbidden band gap in oxide semiconductors is partial substitution of the oxygen by other elements especially nitrogen, carbon, and sulfur since their p wave functions will have energy and symmetry close to that of the wave functions of the valence band. This type of substitution makes it possible to realize "band design," i.e., intentional shift of the position of the valence band of the photocatalyst since the p orbitals of the so called substitutional atoms are expected to be situated in the top of the valence band above the p orbitals of the oxygen, thereby narrowing the forbidden band without substantially altering the bottom of the

conduction band. The energy band scheme for such a substituted system (for example nitrogen substituted system is shown in Fig. 9.5.

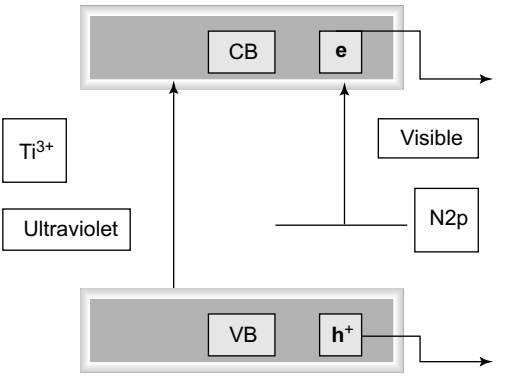

Figure 9.5 ***Schematic energy level diagram for nitrogen substituted TiO2 [Bare semiconductor absorbs UV radiation while the localized energy levels of nitrogen above valence band facilitates the visible light absorption] [5].***

9.5 CO_2 MANAGEMENT–PHOTO-CATALYSIS FOR CO_2 MITIGATION

CO_2 is a colorless and odorless gas. The molecule is linear with a double bond between the carbon and oxygen atoms (O=C=O). CO_2 occurs in nature and serves as source of carbon for photosynthesis by plants and crops. It is present in atmosphere with a volumetric concentration of 0.039% (389 parts per million by volume, ppmv). Other characteristics of CO_2 are given in Table 9.1 together with that of CO and $COCl_2$.

Table 9.1 ***Comparion of properties of Various C_1 building blocks.***

Factors	*CO*	*$COCl_2$*	*CO_2*
MAK Value	30 ppm	0.1 ppm	5000 ppm
Toxicology	Affinity for Hemoglobin 210 times that of oxygen	War gas	Danger of asphysiation at 10 vol% in air
Environmental Hazard	Yes	High	Negative
Flammability	12-74%	No	No
Boiling point	81K	291 K	195 K (sublime)
Storage	Only at less than 5 Mpa	Difficult	No problem
Transport	Gas bottles or tanks in kg ‘quantities	possible	Gas bottles or tanks

The emission of carbon dioxide into the atmosphere, released mainly by the burning of fossil fuels is one of the most serious problems with regard to the greenhouse effect [6]. All human activity generates about 37 billion tons (37 Gt) of CO_2 emissions each year, with about 30 Gt of this coming from energy-related emissions.

Total emissions were less than 25 Gt, twenty years ago, and under business as usual scenarios, emissions are projected to rise to over 50 Gt in twenty years from now. Burning 1 t of carbon in fossil fuels releases more than 3.5 t of carbon dioxide [7]. The Earths surface temperature has risen by approximately 0.6 K in the past century, with particularly significant warming trends over the past two decades. Hence CO_2 reduction/management (capture, storage and sequestration) have become key issues in controlling global warming.

9.6 REDUCTION OF CO_2 EMISSIONS

The reduction of CO_2 emissions can be achieved by three approaches [8]:

(1) Efficient use of carbon-based energy sources.
(2) Use of alternative or carbon-free energy sources.
(3) Use of a post treatment carbon-capture technology.

Carbon capture refers to the removal of CO_2 from industrial flue gas by a gas separation process prior to release to the atmosphere.

9.6.1 Sequestration

Carbon sequestration (storage) is the isolation of carbon dioxide (CO_2) from the earth's atmosphere. Sequestration can play a significant role in preventing continued CO_2 build-up in the atmosphere.

Geological sequestration involves storing CO_2 underground in rock formations that can retain large quantities of CO_2 for long periods of time. The CO_2 would be held in small pore spaces inherent in rocks. It is possible that CO_2 injection into coal seams and mature oil fields could assist in the extraction of coal bed methane or oil that would otherwise be left in the ground, which could help offset the costs of sequestration.

9.6.2 Other Carbon Capture Technologies

Currently, technologies such as gas absorption into chemical solvents, permeation through membranes, cryogenic distillation, and gas adsorption onto a solid sorbent are available for the capture of CO_2 from flue gas. However these are not economically feasible [8].

9.6.3 CO_2 Conversion

CO_2 is the most oxidized form of carbon, and therefore the only chemical transformation at normal energies that would be possible is to reduce it. A wide range of CO_2 conversion techniques are under investigation [9] which include chemical reduction by metals which takes place at relatively high temperatures.

$$2Mg + CO_2 \rightarrow 2MgO + C$$

$$Sn + CO_2 \rightarrow SnO_2 + 2CO$$

$$2Na + 2CO_2 \rightarrow Na_2C_2O_4$$

Thermochemical conversion in presence Ce^{4+} and temperatures higher than 1173 K

$$CO_2 \longrightarrow CO + (1/2)O_2$$

Radio-chemical Method using gamma radiation

$$CO_2 \longrightarrow HCOOH, HCHO$$

Photo-chemical Conversion in presence radiation

$$CO_2 \longrightarrow CO, HCOOH, HCHO$$

Bio-chemical conversion in presence of bacteria

$$CO_2 + 4H_2 \longrightarrow CH_4 + 2H_2O$$

The bacteria Methanobacterium thermoautotrophicum can be immobilized in a fixed bed or on hollow fibres, and feeding stoichiometric ratios for the reaction attains 80% of the theoretical yield.

Electro-chemical conversion (eV)

$$CO_2 + xe^- + xH^+ \longrightarrow CO, HCOOH, (COOH)_2$$

Bio-photochemical Conversion

The bio part of the energy consists in catalysis and information content of an enzyme

CO2 + Oxoglutaric acid $\longrightarrow$ isocitirc acid Electro-photo-chemical conversion (radiation and eV) $CO_2 + 2e^- + 2H^+ \longrightarrow CO + 2H_2O$ Conventional catalytic reduction of CO_2 to chemicals (formic acid, methanol, methane etc.) with external hydrogen is feasible [10] but hydrogen has to be produced via renewable resources to render it viable and sustainable.

9.6.4 Photo-catalytic CO_2 Reduction

The CO_2 reduction process is thermodynamically uphill as illustrated by its standard free energy of formation (G = −394.359 kJ/mol) [11]. Economical

CO_2 fixation is possible only if renewable energy, such as solar energy, is used as the energy source. Equally difficult is the reduction / splitting of water to yield hydrogen and hence requires similar combination of activation steps. The most ideal and desirable process would then be the simultaneous reduction of CO_2 and water to yield hydrocarbons, which essentially works out to artificial photosynthesis.

The utilization of solar energy via chemical storage can be achieved by photo-catalytic or photo-electrochemical activation of light-sensitive catalytic surfaces. When comparing the two systems, photo-catalytic system is simpler and easy to construct. Photo-catalytic process occurs via the direct absorption of photons with energy greater than or equal to the band gap of the photo-catalyst to generate electron-hole pairs. The initial excitation and electron energy transfer to the adsorbed reactants on the photo- catalyst make chemical reactions in the photo-catalytic process possible.

9.6.5 Thermodynamics

There are two conceptual routes to produce renewable carbon containing fuels using solar energy [11].

- Direct photo-reduction of CO_2 using water as a reductant.
- Photolysis of water to generate hydrogen and further reaction of this hydrogen with carbon dioxide forming C_1-C_2 fuels.

Water splitting and carbon dioxide reduction take place simultaneously on the photo–catalyst/co-catalyst surface, and thermodynamic requirements of these processes put constraints on the band gap of the materials used as photo-catalysts. Hydrogen formation from water involves a free energy change (ΔG_0) of 237 kJ/mol and an enthalpy change (ΔH_0) of 285 kJ/mol; the corresponding values for CO formation from CO_2 are 257 and 283 kJ/mol at 298 K (1atm). Hence, the minimum energy required for water and CO_2 splitting processes are, respectively, 1.229 and 1.33 eV (per photon). In theory, the band gap of a photo-catalyst used for co-splitting of CO_2 and water should be at least 1.33 eV [11]. One, two, four, six and eight electron reduction potentials (vs. NHE) for CO_2 reduction and H_2O oxidation at pH 7 and 298 K assuming unit activities for all gaseous and aqueous species are given below [11].

From the above scheme it is clear that CO_2 photo- reduction is not a single-step reaction. Upon transfer of one electron, the structure changes from linear to bent structure which results in irreversible reduction [9]. Additionally, single electron transfer to CO_2 is highly endergonic, because of the negative adiabatic electron affinity of CO_2. The initial step in the photo-catalytic reduction of CO_2 is the generation of electron-hole pairs upon absorption of

Reaction	$E^0_{redox} Vvs NHE$
$2H^+ + 2e^- \longrightarrow H_2$	-0.41
$H_2O \longrightarrow 1/2\ O_2 + 2H^+ + 2e^-$	0.82
$CO_2 + e^- \longrightarrow CO^{2-}$	-1.9
$CO_2 + H^+ + e^- \longrightarrow HCO_2$	-0.49
$CO_2 + 2H^+ + 2e^- \longrightarrow CO + H_2O$	-0.53
$CO_2 + 4H^+ + 4e^- \longrightarrow HCHO + H_2O$	-0.48
$CO_2 + 6H^+ + 6e^- \longrightarrow CH_3OH + H_2O$	-0.38
$CO_2 + 8H^+ + 8e^- \longrightarrow CH_4 + 2H_2O$	-0.24

photons of energy greater than or equal to the band gap of the photo-catalyst. The time scale of this electron-hole recombination is two to three orders of magnitude faster than other electron transfer processes. Therefore, any process which inhibits electron-hole recombination would greatly increase the efficiency and improve the rates of CO_2 photo-reduction. The kinetics of CO_2 photo reduction are also dependent upon many other factors such as intensity of incident light, fraction of the incident light absorbed by the photo-catalyst, the specific surface area of the photo-catalyst absorbing the light, etc.

9.6.6 Effect of Wavelength, Band Gap and Light Intensity

Semiconductors absorb light radiation with the threshold wavelength that provides sufficient photon energy to overcome the band gap between the valence and conduction bands. This threshold wavelength, required to promote the excited state, corresponds to the minimal photon energy and depends on the band-gap energy, e.g. for TiO_2 anatase with band gap energy of 3.2 eV corresponds to 387.5 nm [2].

The wavelength of light influences the yield of CO_2 photo-catalytic reduction products; irradiation using the light with shorter wavelength (254 nm) is significantly more effective for the CO_2 reduction using TiO_2 than that with the wavelength of 350 nm [12].

Electron excited states are produced via electronic transitions, the probability of which depends on the light intensity. At low light intensities, the CO_2 reduction rate increases linearly with the light intensity, at mid-range light intensities, the photo-catalytic reaction rate is dependent on the square root of light intensity; and at high light intensities the rate is independent of the light intensity [2].

Large-band-gap semiconductors are the most suitable photo-catalysts for CO_2 reduction, because they provide sufficient negative and positive redox potentials in conductance and valence bands, respectively. The disadvantage of

using wide band-gap semiconductors is the requirement for high energy input [13].

Even though some of the semiconductors have smaller band gap values, only some of them are catalytically active since the energy levels of either the conduction band or valence band are not appropriate for CO_2 reduction or water decomposition. Some of these semiconductors also undergo photocorrosion as well.

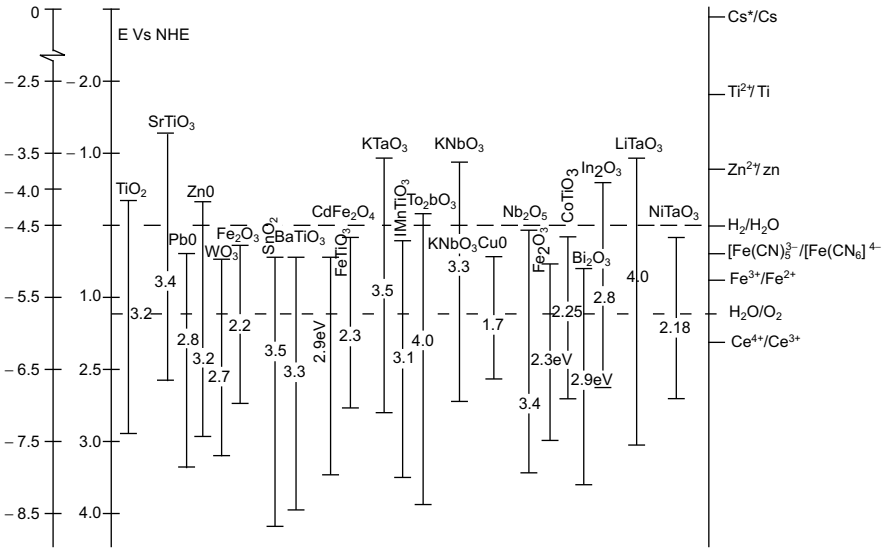

Figure 9.6 ***Conduction band and valence band potentials of semiconductor photocatalysts relative to energy levels of the redox couples [13].***

9.6.7 Photocatalytic Reduction of CO_2 with Water: State of the Art

The possible photo-catlytic reaction pathways are shown in Figure 9.2.

The state of art in this possibility can be summarized as follows:

1. Primary criterion for catalysts for hydrogen evolution from water by activation by photon.
2. Majority of investigations pertain to titania based catalyst with varying characteristics.
3. Titania is the preferred catalyst in various crystalline, morphological and nanostructural (tubes, sheets, films and foams) forms modified by doping with metals and anions coupled with various semiconductor oxides and sensitizers have been investigated extensively.
4. Doping with metals and non-metls to extend the light absorption range and achieve charge separation.
5. Pt,Cu, Ru and Ag are the metals used to improve hydrocarbon yields.

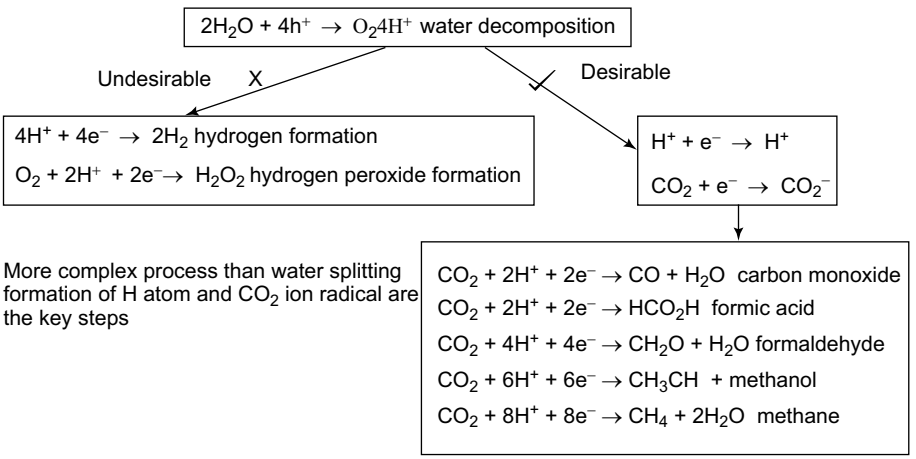

Figure 9.7 ***The Possible CO_2 + H_2O photo catalytic pathways.***

6. Maximum yield of methanol is 2655 micro moles on 3% Cu/TiO_2 catalyst at 333K under UV light, 2450 ν W/cm^2 after 6 hrs, slurry phase, 0.3 g catalyst in 300 ml water;QE- 19 %- Slamet et.al., Catalysis Communications 6 (2005) 313-319.
7. Maximum methane to HC yield was 200 ppm, Pt-Cu on N doped TiO_2 nano tube arrays, sunlight, 100 mW/cm^2 low pressure static reactor using CO_2 and water vapor.
8. Alkali metal and alkaline earth tantalates, titanates and bi-metallics-could be viable options.

Inoue et al., [14] have reported the photocatalytic reduciton of CO_2 in aqueous solutions to produce a mixture of formaldehyde, formic acid, methanol and methane using various wide-band gap semiconductors such as tungsten trioxide (WO_3), titanium dioxide (TiO_2), zinc oxide (ZnO), cadmium sulfide (CdS), gallium phosphide (GaP), and silicon carbide (SiC). These semiconductors were activated by both xenon and mercury lamp irradiation. The formaldehyde and methyl alcohol yield was highest in the presence of SiC, a behavior attributed to the relative position of the SiC conduction band with respect to the $HCHO/H_2CO_3$ redox potential. The SiC conduction band edge lies at a higher position (more negative) than the HCHO/ H_2CO_3 redox potential, which is believed to be responsible for the high rates of product formation. The absence of methyl alcohol when WO_3 was used as catalyst, with a conduction band at a position lower than the $HCHO/H_2CO_3$ redox potential, further indicates the influence of band-edge positions on CO_2 reduction.

Investigations related to the photosynthesis reaction of CO_2 with water vapor to form CH_4 over metal-loaded $SrTiO_3$ have also been conducted. Due

to its higher conduction band edge position compared to the redox potential of CH_3OH/H_2CO_3, strontium titanate could effectively reduce carbon dioxide dissolved in an aqueous electrolyte [15,16]. The effect of doping transition and noble metals such as Ru, V, Cr on TiO_2 has also been studied. It has been found that the production rate of organic compounds such as formic acid, formaldehyde and methanol increased when TiO_2 was doped with RuO_2 . The highest initial energy conversion obtained was found to be 0.04%.

Anpo et al., [6] studied the photo-catalytic reduction of CO_2 with water on various titanium oxide catalysts. The anatase phase of the catalyst with large band gap with sufficient surface-OH groups showed good efficiency for the formation of methane. The yields depended on the ratio of CO_2 to water, the reaction temperature. They observed that the best mole ratio of H_2O /CO_2 for the conversion of carbon dioxide is 5. Addition of Pt to the TiO_2 led to an increased methane yield compared to methanol formation. In another report Anpo et al., [17] reported the use of highly dispersed titanium oxide on glass for the photo catalytic reduction of carbon dioxide. From the direct detection of intermediate species, they proposed that methane formation resulted from the reaction between carbon radicals and atomic hydrogen.

The use of Cu as a co-catalyst was reported by Adachi et al [18] in which Cu-loaded TiO_2 powder was suspended in a CO_2 pressurized solution at ambient temperature, with methane and ethylene produced under Xe lamp illumination. Tseng et al (2004) also studied the effect of copper loading on titania. The methanol yield of 2.0 wt.% Cu/TiO_2 was 118 νmol/g following 6 h of UV illumination. The yield was higher than those of sol-gel TiO_2 and Degussa P25. The redistribution of the electric charge and the Schottky barrier of Cu and TiO_2 facilitates electron trapping via supported Cu. The photocatalytic efficiency of Cu/TiO_2 was markedly increased because of the lowering of the re-combination probability for hole-electron pairs. The highest quantum and energy efficiencies achieved were 10 and 2.5%, respectively. Slamet et al [19] suggested that CuO may be the most active dopant compared to the other copper species. Because Cu_2O has the highest positive value of redox potential Cu^+, Cu_2O dopant should effectively act as an electron trap to prohibit electron-hole recombination. However, owing to the relatively strong interaction between TiO_2 and the dopant particle implanted in the vacant sites of TiO_2 , the dopant with more positive potential redox exceedingly catches electron from conduction band edge. Consequently the dopant-trapped electrons are more difficult to be transformed to the adsorbed species on catalyst surface and hence it may play a role as a center of electron-hole recombination.

Guan et al., [20] studied the reduction of CO_2 with water over a hybrid catalyst, in which a Pt-loaded $K_2Ti_6O_{13}$ photo-catalyst was combined with a

Fe-based catalyst supported on a dealuminated Y-type zeolite (Fe-Cu-K/DAY). In this reaction system, $Pt/K_2Ti_6O_{13}$ catalyst decomposes water to produce H_2 and the Fe-Cu-K/DAY catalyst reduces CO_2 with the resulting H_2 incorporated into organic compounds. When the reaction temperature is increased from room temperature to 600K by concentrating the solar irradiation, the product yield of hydrogen increased from 13.7 νmol/g-h to 20.5 νmol/g-h. Also additionally formic acid, methanol and ethanol were obtained. Guan et al., [21] also reported the use of Pt-loaded $K_2Ti_6O_{13}$ photo catalyst combined with a CO_2 hydrogenation catalyst Cu/ZnO. When the composite catalyst was used under concentrated sunlight, CH_3OH was successfully formed in addition to the above products. Guan et al., [22] also investigated the reduction of CO_2 over zero-valent FeO and FeO-based composites in an aqueous solution at room temperature. It was found that H_2 can be effectively evolved from water over zero-valent FeO in the presence of gaseous CO_2 together with a small amount of hydrocarbons. When FeO was combined with Cu, K, and Al components, hydrocarbons such as CH_4 and C_3H_8 and alcohols such as CH_3OH and C_2H_5OH were also effectively produced. The XPS, XRD, and photoemission yield measurements revealed that the FeO surface as well as the bulk was oxidized to Fe_3O_4 and other possible oxides during the reaction. This corrosion process is promoted by the dissolution of CO_2 in water and the resultant protons oxidize FeO to evolve H_2. Moreover, the evolved H_2 serves as the reactant for the CO_2 hydrogenation on the active site of FeO, especially for the FeOKAl and FeOCuKAl composites.

Kaneco et al., [23] studied the CO_2 photoreduction using TiO_2 powders in liquid CO_2 medium. Carbon dioxide has limited solubility in water. Also reduction of CO_2 is competitive with hydrogen formation via water. To overcome this disadvantage, liquid CO_2 system has been explored. The protonation reaction was performed using water after the end of illumination. The main reduction product was exclusively formic acid. Tan et al., [24] studied the photo-catalytic reduction of carbon dioxide using TiO_2 pellets. Pellet increased the contact areas and adsorption capacity. The yield was significant when compared to the system generated using thin film coating technique.

Koci et al., [25] studied the effect of TiO_2 particle size on photo catalytic reduction of carbon dioxide. As the particle size decreased, higher yields of methanol and methane over the TiO_2 nano particles under the illumination of light were obtained. The optimum particle size corresponding to the highest yields of both products was 14 nm. For crystal sizes smaller than 14 nm the catalyst activity dropped probably due to the changes in optical and electronic properties of the nanometer crystal. The observed optimum particle size was a result of competing effects of specific surface area, charge-carrier dynamics

and light absorption efficiency. Liu et al., [26] have studies the photo catalytic reduction of CO_2 on sol gel derived titania supported CoPC system. The nano particles of cobalt phthalocyanine loaded on titania showed eficient CO_2 reduction activity. This has been attributed to the effective electron transfer to titania surface and also the reduction of the recombination of electron and hole. Lo et al., [27] studied the photo-reduction of carbon dioxide with H_2 and H_2O over TiO_2 and ZrO_2 in a circulated photo-catalytic reactor. Experimental results indicated that the highest yield for the photo-reduction of CO_2 was obtained using TiO_2 with H_2 + H_2O and ZrO_2 with H_2. Photo-reduction of CO_2 over TiO_2 with H_2 + H_2O formed CH_4, CO, and C_2H_6 with the yield of 8.21, 0.28, and 0.20 mmol/g, respectively, while the photo-reduction of CO_2 over ZrO_2 with H_2 formed CO at a yield of 1.24 mmol/g. The detected reaction products supported the proposition of two reaction pathways for the photo reduction of CO_2 over TiO_2 and ZrO_2 with H_2 and H_2O, respectively. A one-site Langmuir Hinshelwood (L-H) kinetic model was applied to simulate the photo-reduction rate of CO_2.

Koci et al., [28] studied the influence of reactor geometry on photoreduction of carbon dioxide using two annular batch reactors. The dependence of products yields on the reactor diameter and on the volume of the liquid phase confirmed the fact that the requirement of perfect mixing is difficult to fulfill in the annular configuration of the reactor. The highest yields of the photo catalytic reduction were achieved in a configuration where the lamp just touches the surface of the liquid in the reactor and the configuration of the reactor was not annular.

Wu et al., [29] applied an optical fibre reactor to the photo reduction of CO_2 with H_2O using TiO_2, Cu/TiO_2, Ag/TiO_2, Cu-Fe/TiO_2-SiO_2 and dye-sensitized Cu-Fe/P25 coated optical fibers. Compared with a traditional packed-bed reactor, an optical fiber provides a medium to transmit light uniformly throughout a reactor. In addition, a higher processing capacity is possible because the photo-catalyst can be dispersed on the optical fibers with large surface area in a given reactor volume. Ulagappan et al., [30] used Ti-silicalite molecular sieves as a catalyst for 266 nm UV laser radiation induced reduction of CO_2 and H_2O gas mixtures, obtaining HCOOH, CO, and $HCOOCH_3$. Product origins were studied by IR spectroscopy, indicating that CO originated from the secondary photolysis of HCOOH, while $HCOOCH_3$ was the result of spontaneous Tishchenko reaction of CH_2=O.

Anpo et al., [31] carried out the CO_2 photo reduction using Ti-MCM-41 and Ti-MCM-48 mesoporous zeolite catalysts. Photo-catalysts prepared within the zeolite cavity and frame-work have unique local structure and high selectivity in photo-reduction. The titanium oxide species included within the zeolite

framework have been found to exist as isolated tetrahedral titanium oxide species. These Ti-containing zeolite catalysts exhibited high photo-catalytic efficiency and selectivity for the formation of methanol.

Some researchers have attempted to replace water with other reductants. This provides a high reaction yield and high selectivity to desired products by changing the mechanism. Liu et al., [32] conducted an experiment with CdS in various solvents including water, methanol, ethanol, and 1-propanol with dielectric constants of 80, 33, 24.3 and 20.1 respectively. The results indicated that, if low-dielectric constant solvents or low-polarity solvents are used, CO_2^- anion radicals can be strongly adsorbed on the surface through the carbon atom of another CO_2^- anion radical because these radicals are not well dissolved in low-polarity solvents. Here, CO is produced as the major reduction product of CO_2. If a high-dielectric-constant solvent is used (e.g., water), the CO_2^- anion radicals can be greatly stabilized by the solvent, resulting in weak interactions with the photo catalyst surface. Subsequently, the carbon atom of the radical tends to react with a proton to produce formic acid. Dey [33] showed that photo-catalytic reduction of CO_2 using TiO_2 suspension in aqueous solutions containing 2-propanol as a hole scavenger leads to the formation of methane.

Titania per se is active for photo-catalytic reduction of CO_2 with H_2O, but the rates are extremely low since its conduction band edge is not suitable for water and CO_2 reduction, though it can readily oxidize water [34]. Promotion with co-catalysts like Pt [35], Ru [36], Rh [37], Ni [38] and Ag [39] vastly enhance the rate in several ways, like, charge separation, retarding re-combination and trapping of charge carriers, besides activation of CO_2 and water reduction and facilitating further surface transformations leading to hydrocarbon products.

Effect of bimetallics on TiO_2 was also studied. Luo et al., [40] studied the CO_2 reduction on Copper and Cerium Co-Doped Titanium dioxide. Photo-catalysts copper and cerium co-doped titanium dioxide were prepared via the equivalent-volume incipient wetness impregnation method. The methanol yield could reach up to 180.3 νmol/g-cat rapidly. Ce atoms activated water and CO_2 molecules, while Cu atoms act as the channel of photo-electrons in real time and prevent the recombination of electrons and holes. Xia et al., [41] studied the reduction of CO_2 with water using multi-walled carbon nanotube supported [MWCNT] TiO_2. The catalysts were prepared by both sol-gel and hydrothermal method. In using the sol-gel method, the MWCNTs were coated with anatase TiO_2 nanoparticles, and by the hydrothermal method, rutile TiO_2 nanorods were uniformly deposited on the MWCNTs. The composite catalysts prepared by the sol-gel method lead to the main formation of ethanol, while HCOOH is found to be the major product on the sample prepared by the hydrothermal method.

When CO_2 present in the atmosphere dissolves in water it is mostly present in the form of carbonate. Many of them have studied photo-catalytic reduction of carbonate to form various chemicals. Ku et al., [42] studied the photo-catalytic reduction of carbonate in aqueous solution by the UV/TiO_2 process. The photo-catalytic reduction of carbonate proceeded faster in acidic solutions than in alkaline solutions. The main products of the photo-catalytic reduction of carbonate by the UV/TiO_2 reduction process were found to be methanol and methane. A Langmuir-Hinshelwood type kinetic equation was developed for modeling the photo catalytic reduction of carbonate.

Sayama et al., [43] investigated the effect of carbonate salt addition on the photo catalytic decomposition of liquid water over Pt-TiO_2 catalyst. It has been found that an addition of carbonate salts to Pt-loaded suspensions led to highly efficient stoichiometric photo-catalytic decomposition of liquid water into H_2 and O_2. Neither the pH nor cation directly contributes to the water splitting. The presence of a high concentration of carbonate ions is essential for the catalytic photo-decomposition of water. The carbonate ion affects both the Pt particles and the TiO_2 surface. The Pt was covered with some titanium hydroxide compounds and therefore, the rate of the back reaction (H_2O formation from H_2 and O_2) on the Pt was suppressed effectively in the presence of carbonate ions. On the other hand, the TiO_2 surface was readily covered with several types of carbonate species. It is considered that these carbonate species aid desorption of O_2 from the TiO_2 surface.

A significant breakthrough in the photocatalytic reduction of gas phase CO_2 by solar radiation has recently been achieved by Varghese and co-workers [34], using nitrogen doped TiO_2 nanotube arrays co-catalyzed with copper and/or Pt nanoparticles, in which water vapor saturated carbon dioxide was reduced to methane and other hydrocarbons under natural sunlight. The yield of methane was reported to be 160 νL/gh.The high rate of carbon dioxide conversion can be attributed to the high surface area and nanoscale wall thickness of the nanotubes, enabling the surface species to readily receive both charge carriers generated near the surface due to the wave function overlap and those generated deep inside the wall via diffusion. The quantum efficiency was found to be 0.74 %.

Many researchers have studied the Photocatalytic reduction of CO_2 using external hydrogen. Tsuneok et al., [44] performed this over MgO, CaO, ZrO_2, Ga_2O_3, and Al_2O_3. Ga_2O_3 exhibited the highest photo-catalytic activity in this process, and CO gas was selectively generated at room temperature and atmospheric pressure. The amount of CO gas evolved depended not only on the amount of CO_2 but also on the amount of H_2 adsorbed on Ga_2O_3. The chemisorbed CO_2 species involved in the photo catalytic reduction of CO2 over Ga_2O_3 was not the bidentate bicarbonate species but the mono dentate

bicarbonate species. The dissociatively adsorbed hydrogen on Ga_2O_3 reduced the mono dentate bicarbonate to the bi-dentate formate under photo irradiation. The bi dentate formate, which was an intermediate in the photocatalytic reduction, decomposed to CO. They proposed that photo-catalytic reduction of CO_2 over Ga_2O_3 takes place via a Langmuir-Hinshelwood-type mechanism, which is not the case for ZrO_2 or MgO. Teramura et al., [45] carried out the Photo-catalytic reduction of CO_2 using H_2 as reductant over $ATaO_3$ photo-catalysts [A = Li, Na, K]. Only CO gas was generated over all samples under photo- irradiation. The photo-catalytic activity was higher in the order corresponding to $LiTaO_3 > NaTaO_3 > KTaO_3$. The order of the photo catalytic activities was consistent with that of the E_g [optical band gap] values. The amount of evolved CO gas almost strongly depends on the amount of chemisorbed CO_2 in the case of $ATaO_3$ [A = Li, Na, K]. In addition, the photo-catalytic activity increased with increasing the calcination temperature of $LiTaO_3$. This means that a smooth charge separation in a $LiTaO_3$ photo-catalyst and chemisorption of CO_2 on the surface contribute to effective reduction of CO_2 in the presence of H_2.

Catalyst systems other than TiO_2 were also intensively studied. Watanabe et al., [46] studied the Photosynthesis of methanol and methane from CO_2 and water molecules on a ZnO surface. The photochemical synthesis of methanol and methane from CO_2 and water molecules was observed at 278 K by irradiating ZnO powder with visible light under high pressures of 25 to 35 kg/cm^2 of CO_2 gas. The best conversion efficiency was found to be about 6% with respect to reactant water molecules using a 75 W Xe lamp. Kanemoto et al., [47] studied the photo-reduction of Carbon dioxide over ZnS Quantum Crystallites. The dissolution of CO_2 in water gives an aqueous solution of pH 3.7 under a pressure of 1 atm. ZnS is unstable under acidic conditions, decomposing into H_2S and Zn^{2+} by the reaction with acid. Freshly prepared colloidal ZnS suspensions effectively catalyze photo-reduction of CO_2 in water at pH 7 with NaH_2PO_2 in the coexistence of Na_2S under UV irradiation. Wang et al., [48] carried out the Photocatalytic hydrogen evolution from water in the presence of Carbon dioxide over $NiO/Ca_2Fe_2O_5$. The catalyst $NiO/Ca_2Fe_2O_5$ was studied in the photo catalytic splitting of water in the presence of carbon dioxide. It is believed that CO_2 may react with water to form HCO_3^- and CO_3^{2-}, which promote the scavenging of holes by OH, and thus enhance the photo-catalytic activity. At the same time, a portion of CO_2 is photo-catalytically reduced to formic acid.

Ahmed et al., [49] studied the Photocatalytic conversion of carbon dioxide into methanol using zinc-copper-M [III] [M = aluminum, gallium] layered double hydroxides. These LDH compounds were applied as photo catalysts

to convert gaseous CO_2 [2.3 kPa] to methanol or CO under UV-visible light using hydrogen. Zn Al LDH was the most active for CO_2 photo-reduction and the major product was CO formed at a rate of 620 nmol $h^{-1}g^{-1}$ cat, whereas methanol was the major product formed by the inclusion of Cu in the LDH photo-catalysts, e.g., at a formation rate of 170 nmol $h^{-1}g^{-1}$ cat using Zn-Cu-Ga photo-catalyst. Yan et al., [50] studied the CO_2 photo reduction using meso porous $ZnGa_2O_4$. A reactive templating route to prepare meso porous $ZnGa_2O_4$ at room temperature has been reported. By using RuO_2 as co-catalyst, the as-prepared meso porous $ZnGa_2O_4$ shows high photo catalytic activity for converting CO_2 into CH_4 under light irradiation, because of strong gas adsorption and large specific surface area of the mesoporous photo-catalyst.

In short the state of art and challenges in this area are as follows:

1. The reaction rate is slow and the yields obtained are also low.
2. The catalysts are often deactivated and arresting the deactivation has to be attempted.
3. The quantum efficiency of the process is often very low.
4. For economic viability one has to prepare catalysts which will be active in the visible region and also will give more than 10% quantum efficiency.
5. One has to generate catalyst systems which will be able to harness light energy effectively and possibly one can generate systems containing macro cyclic ligands like porphrins and Phthalocyanins.

The current situation on the selection of photo-catalytic materials for water splitting has been depicted pictorially by D. Payne Department of Chemistry, University of oxford from Osterloph, 2008. This representation reproduced in Figure 9.3 clearly shows that one has to develop photo-catalytic materials which will be active in the wavelength region 400 nm and also should be capable of providing quantum efficiencies greater than 10%.

9.6.8 Future Directions

As described earlier, photo-catalytic reduction of carbon dioxide with water to fuels/chemicals (methane, methanol, etc.,) is an emerging area of research towards utilizing the abundant sunlight. The process has the potential to become a viable and sustainable alternative energy source to fossil fuels. However, it has thrown up several tough challenges to the scientists and technologists, namely,

- The process centers around the activation of two thermodynamically most stable molecules, CO_2 and water.

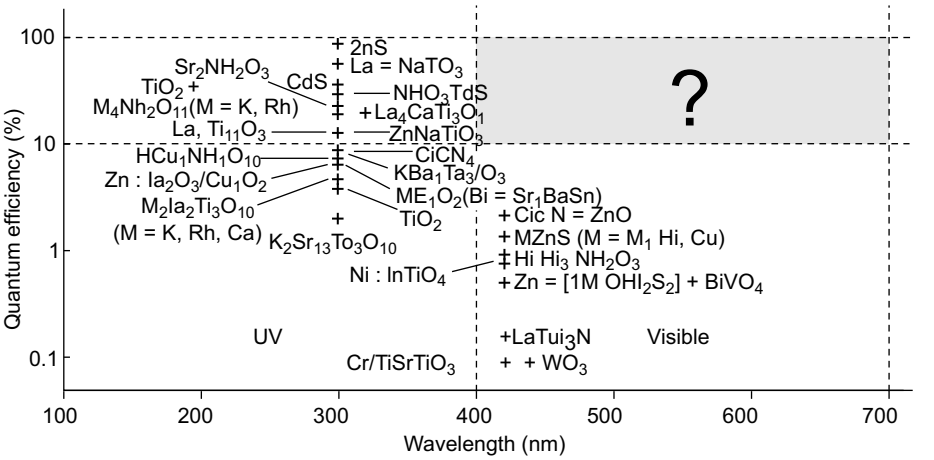

Figure 9.8 ***The pictorial representation of the known and exploited semiconductors and their efficiencies for water splitting reaction. [reproduced from Phil. Trans. R. Soc., 368,3343 (2010)].***

- Conversions achieved so far are extremely small, less than 1%, occurring at very slow rate.
- Catalysts tend to get deactivated over short period.
- CO_2 photo reduction process is highly complex, involving mult-electron transfer and non-selective, leading to a range (C_1-C_3) of hydrocarbon products.
- Design of catalysts, consisting of photo catalysts and co-catalysts aided by metal ion/anion doping and light harvesting components/sensitizers, is equally complex.
- Ideal catalysts are expected to display maximum efficiency towards solar energy absorption and possess requisite band energy level characteristics to drive the redox reactions.
- The process involves two steps, spitting of water and reduction of carbon dioxide, which are thermodynamically not favourable. Since the second step involves multi-electron transfer,the rates are small relative to the first. These two steps are to be synchronized to achieve higher yields of hydrocarbons.

Nevertheless, research efforts on these fronts are being pursued with full vigour by many laboratories round the globe. Design of efficient catalyst systems and achieving higher yield of desired products are the two key issues being pursued by the researchers. Though titania continues to be the most extensively studied photocatalyst [51-54], efforts to develop alternative catalysts, based on various semiconducting metal

oxides/sulfides/nitrides/phosphides, layered titanates, binary and ternary oxides of Nb, Ta, Ga and In in conjunction with alkaline, alkaline earth and rare earth oxides and with a host of co-catalysts and sensitizers, are in full swing [55-59].

References

1. Demeestere K., J. Dewulf and H. V. and Langenhove (2007) "Heterogeneous Photo-catalysis as an Advanced Oxidation Process for the Abatement of Chlorinated, Monocyclic Aromatic and Sulfurous Volatile Organic Compounds in Air: State of the Art". Critical Rev. in Environmental Science and Technology, 37, 489-538.
2. Ko, K., L. Obalov and Z. Lacn (2008) Photocatalytic reduction of CO_2 over TiO_2 based catalysts. Chemical Papers, 62, 1-9.
3. Fujishimaa A., X. Zhang Donald and A. Tryk (2007) Heterogeneous photocatalysis: Fromwater photolysis to applications in environmental cleanup. Int. J. Hydrogen Energy, 32, 2664-2672.
4. Hoffmann M. R., S. T. Martin, W. Choi and D. W. Bahnemann (1995). Environmental Applications of Semiconductor Photocatalysis. Chem. Rev., 95, 69-96.
5. Stroyuk L., A. I. Kryukov, S. Y. Kuchmii and V. D. Pokhodenko (2009). Semiconductor Photocatalytic systems for the Production of Hydrogen by the action of visible light. Theoretical and Experimental Chem., 45, 209-233.
6. Anpo M., H. Yamashita, Y. Ichihashi and S. Ehara, (1995) Photocatalytic reduction of CO_2 with water on various Titanium Oxide catalysts. J. Electroanal. Chem., 396 ,21-26.
7. Maginn E. J, (2010) What to Do with CO_2 J. Phy. Chem. Lett., 1, 3478-3479.
8. Usubharatana P., D. McMartin, A. Veawab and P. Tontiwachwuthikul, (2006) Photocatalytic Process for CO_2 Emission Reduction from Industrial Flue Gas Streams. Ind Eng. Chem. Res, 45, 2558-2568.
9. Scibioh M. A. and B. Viswanathan, (2004) Electrochemical Reduction of Carbon dioxide: A Status Report. Proc Indian National Science Academy, 70A, 407-462.
10. Nam S. S., H. Kim, G. Kishan, M. J. Choi and K. W. Lee, (1999) Catalytic conversion of CO_2 to hydrocarbons over rare earth promoted iron catalysts supported on KY Zeolite. Appl. Catal. A. Gen., 179, 155-159.
11. Indrakanti V. P., J. D. Kubickib and H. H. Schobert (2009), A Photoinduced activation of CO_2 on Ti-based heterogeneous catalysts:

Current state, chemical physics-based insights and outlook. Energy Environmental Science, 2, 745-758.

12. Matthews, R. W. and S. R. McEvoy, (1992) A comparison of 254 nm and 350 nm excitation of TiO_2 in simple photocatalytic reactors. J. Photochem. Photobiol. A: Chem, 66, 355-366.
13. Roy S. C, O. K. Varghese, M. Paulose and C. A. Grimes (2010) Toward Solar Fuels: Photocatalytic Conversion of Carbon Dioxide to Hydrocarbons. Am. Chem. Soc. Nano letters, 4, 1259-1278.
14. Inoue T., A. Fujishima, S. Konishi and Honda K., (1979). Photoelectrocatalytic Reduction of Carbon-Dioxide in Aqueous Suspensions of Semiconductor Powders. Nature, 277, 637-638.
15. Halmann, M., M. Ulman and B. A. Blajeni, (1983) Photochemical Solar Collector for the Photoassisted Reduction of Aqueous Carbon-Dioxide. Sol. Energy, 31, 429-431.
16. Halmann M., V. Katzir, E. Borgarello and J. Kiwi, (1984) Photoassisted Carbon dioxide Reduction on Aqueous Suspensions of Titanium Dioxide. Sol. Energy Mater., 10, 85-91.
17. Anpo M. and K. Chiba, (1992) Photocatalytic Reduction of CO_2 on Anchored Titanium-Oxide Catalysts. J. Mol. Catal., 74, 207-212.
18. Adachi K., K. Ohta and T. Mijuma (1994) Photocatalytic Reduction of Carbon-Dioxide to Hydrocarbon Using Copper-Loaded Titanium-Dioxide. Solar Energy, 53, 187-190.
19. Slamet H. W. Nasution, E. Purnama, S. Kosela and J. Gunlazuardi, (2005) Photocatalytic reduction of CO_2 on copper-doped Titania catalysts prepared by improved-impregnation method. Catal. Commun., 6, 313-319.
20. Guan G., T. Kida T. Harada, M. Isayama and A. Yoshida, (2003). Photoreduction of carbon dioxide with water over $K_2Ti_6O_{13}$ Photocatalyst combined with Cu/ZnO catalyst under concentrated sunlight. App. Catal. A: General, 249, 11-18.
21. Guan G., T. Kida and A. Yoshida, (2003) Reduction of Carbon Dioxide with Water under Concentrated Sunlight Using Photocatalyst combined with Fe-Based Catalyst. App. Catal., B, 41, 387-396.
22. Guan G., T. Kida, T. Ma, K. Kimura, E. Abe and A. Yoshida, (2003). Reduction of aqueous CO_2 at ambient temperature using zero-valent iron-based composites. Green Chem., 5, 630-634.
23. Kaneco S., H. Kurimoto, K. Ohta, T. Mizuno and Akira, (1997) Photocatalytic reduction of CO_2 using TiO_2 powders in liquid CO_2 medium. J. Photochem. Photobiol. A: Chemistry, 109, 59-63.

24. Tan S. S., L. Zou and E. Hu, (2006) Photocatalytic reduction of carbon dioxide into gaseous hydrocarbon using TiO_2 pellets. Catal. Today, 115, 269-273.
25. K. Koci, L. Obalova, L. Matejova, D. Placha, Z. Lacny, J. Jirkovsky and O. Solcova, (2009). Effect of TiO_2 particle size on the photocatalytic reduction of CO_2 Applied Catalysis B: Environmental 89, 494-502.
26. Liu S., Z. Zhao and Z. Wang, (2007) Photocatalytic reduction of carbon dioxide using sol-gel derived titania-supported CoPc catalysts. Photochem. Photobiol. Sciences, 6, 695-700.
27. Lo C.C., C. H. Hung, C. S. Yuan and J. F Wu, (2007) Photoreduction of carbon dioxide with H_2 and H_2O over TiO_2 and ZrO_2 in a circulated photocatalytic reactor. Sol. Energy Mater. Sol. Cells, 91, 1765-1774.
28. Koc K., MartinReli, O. Kozk, Z. Lacny, DanielaPlach, PetrPraus and LucieObalov (2010) Influence of reactor geometry on the yield of CO_2 Photocatalytic reduction. Catal. Today doi:10.1016/j.cattod.2010.12.054
29. Wu J. C. S., T.-H. Wu, T. Chu, H. Huang and D. Tsai, (2008) Application of Optical-Fiber Photoreactor for CO_2 Photocatalytic Reduction. Topic in Catalysis, 47, 131-136.
30. Ulagappan N., and H. Frei, (2000) Mechanistic Study of CO_2 Photoreduction in Ti Silicalite Molecular Sieve by FT-IR Spectroscopy. J. Phy. Chem. A, 104, 7834-7839.
31. Anpo M., H. Yamashita, Y. Ichihashi, Y. Fujii and M. Honda, (1998). Photocatalytic Reduction of CO_2 with H_2O on Titanium Oxides Anchored within Micropores of zeolites: Effects of the Structure of the Active Sites and the Addition of Pt. J. Phys. Chem. B, 101, 2632-2636.
32. Liu B.-J., T. Torimoto and H. Yoneyama, (1998) Photocatalytic reduction of CO_2 using surface-modified CdS photocatalysts in organic solvent. J. Photochem. Photobiol. A: Chem., 113, 93-96.
33. Dey G. R., (2007) Chemical Reduction of CO_2 to different Products during Photo Catalytic Reaction on TiO_2 under Diverse Conditions: an Overview J. Natural Gas Chem., 16, 217-226.
34. Varghese O. K, M. Paulose and T. J. Latempa, (2009) High-Rate Solar Photocatalytic conversion of CO_2 and Water Vapor to Hydrocarbon Fuels. Nanoletters, 9, 731-737.
35. Zhang Q. H., W. D. Han, Y. J. Hong and J. G. Yu, (2009) Photocatalytic reduction of CO_2 with H_2O on Pt-loaded TiO_2 catalyst. Catal. Today, 148, 335-340.
36. Sasirekha, N., Basha, S.J.S. and Shanthi, K., (2006) Photocatalytic performance of Ru doped anatase mounted on silica for reduction of carbon dioxide. Appl. Cataly, B, 62, 169-180.

37. Kohno Y., H. Hayashi, S. Takenaka, T. Tanaka, T. Funabiki and S. Yoshida, (1999) Photocatalytic reaction of H_2O+CO_2 over pure and doped Rh/TiO_2. J. Photochem. Photobiol. A: Chem., 126, 117-123.
38. Fan J., E-Z. Liu, L. Tian, X-Y. Hu, Qi He and T. Sun, (2010) Study on Synergistic Effect of N and Ni^{2+} on Nano Titania in Photocatalytic Reduction of CO_2. Am. Soc. Civil Engineers. doi: 10.1061/(ASCE)EE. 1943-7870.0000311.
39. Koci K., K. Mateju, L. Obalova, S. Krejcikova, Z. Lacny, D. Placha, L. Capek, A. Hospodkova and O. Solcova, (2010) Effect of silver doping on the TiO_2 for Photocatalytic reduction of CO_2. Appl Catal B: Environmental, 96, 239-244.
40. Luo D., Y. Bi, W. Kan, N. Zhang and S. Hong, (2011) Copper and Cerium Co-Doped Titanium dioxide on Catalytic Photo reduction of Carbon dioxide withWater: experimental and theoretical studies. J. Mol. Structure,doi: .1016/j.molstruc.2011.03.044
41. Xia X-H., Z-J. Jia, Y. Yu, Y. Liang, Z. Wang and L-L. Ma, (2007) Preparation of multi-walled carbon nanotube supported TiO_2 and its Photocatalytic activity in the reduction of CO_2 with H_2O. Carbon, 45, 717-721.
42. Ku Y., W-H Lee and W-Y Wang, (2004) Photocatalytic reduction of carbonate in aqueous solution by UV/TiO_2 process. J. Mol Catal. A: Chemical, 212, 191-196.
43. Sayama K., and H. Arakawa, (1997) Effect of carbonate salt addition on the photocatalytic decomposition of liquid water over Pt-TiO_2 catalyst. J. Chem. Soc. Faraday Trans. 93, 1647-1654.
44. Tsuneoka H., K. Teramura, T. Shishido and T. Tanaka, (2010) Adsorbed Species of CO_2 and H_2 on Ga_2O_3 for the Photocatalytic Reduction of CO_2 J. Phy. Chem. C, 114, 8892-8898.
45. Teramura K., S-i Okuokab, H. Tsuneokab, T. Shishidob and T. Tanaka, (2010) Photocatalytic reduction of CO_2 using H_2 as reductant over $ATaO_3$ photocatalysts (A = Li, Na, K). Appl. Catal. B: Environmental, 96, 565-568.
46. Watanabe M., (1992) Photosynthesis of methanol and methane from CO_2 and H_2O molecules on a ZnO surface. Surface Science Lett., 279, 236-242.
47. Kanemoto M., T. Shiragami, C. Pac and S. Yanagida, (1992) Effective Photoreduction of Carbon Dioxide Catalyzed by ZnS Quantum

Crystallites with Low Density of Surface Defects. J. Phy. Chem., C, 96, 3521-3526.

48. Wang Y., Y. Wang and Y. Gao, (2010) Photocatalytic H_2 evolution from water in the presence of Carbon dioxide over $NiO/Ca_2Fe_2O_5$ Reaction Kinetics Mechanics Cataly., 99, 485-491.
49. Ahmed N., Y. Shibata, T. Taniguchi and Y. Izumi, (2011), Photocatalytic conversion of carbon dioxide into methanol using zinc-copper-M(III) (M = aluminum, gallium) layered double hydroxides. J. Catal.,doi:10.1016/j.jcat.2011.01.004.
50. Yan S C., S. X. Ouyang, J. Gao, M. Yang, J. Y. Feng, X. X. Fan, L. J. Wan, Z. S. Li, J. H. Ye, Y. Zhou and Z. G. Zou, (2010) A Room Temperature Reactive - Template Route to Mesoporous $ZnGa_2O_4$ with Improved Photocatalytic Activity in Reduction of CO_2. Angew. Chem. Int. Ed., 49, 6400-6404.
51. Fujishima, T. N. Rao and D. A. Tryk, "Titanium dioxide Photocatalysis," Journal of Photochemistry and Photobiology C: Photochemistry Reviews,Vol. 1, No. 1, pp. 1-21, 2000.
52. Carp C. L. Huisman and A. Reller, "Photoinduced reactivity of titanium dioxide," Progress in Solid State Chemistry, Vol. 32, No. 1-2, pp. 33-177, 2004.
53. Fujishima X. Zhang, "Titanium dioxide photocatalysis: Present situation and future approaches,"ComptesRendusChimie, Vol. 9, No. 5-6, 750-760, 2006.
54. Fujishima, X. Zhang and D. A. Tryk, "Heterogeneous photocatalysis: From water photolysis to applications in environmental cleanup, " International Journal of Hydrogen Energy, Vol. 32, No. 14, pp. 2664-2672, 2007.
55. F. E. Osterloh, "Inorganic Materials as Catalysts for Photochemical Splitting of Water," Chemistry of Materials, Vol. 20, No.1, pp. 35-54, 2008.
56. G. Palmisano, E. Garca-Lo pez, G. Marc, V.Loddo, S. Yurdakal, V. Augugliaro and L. Palmisano, "Advances in selective conversions by heterogeneous photocatalysis," Chemical Communications, Vol. 46, No. 38, pp. 7074-7089, 2010.
57. Z. Jiang, T. Xiao, V. L. Kuznetsov and P. P. Edwards, "Turning carbon dioxide into fuel" Phil. Trans. R. Soc. Vol. A368 3343-3364 (2010).
58. K. Li, D. Martin and J. Tang, "Conversion of Solar Energy to Fuels by Inorganic Heterogeneous Systems" Chinese Journal of Catalysis, Vol. 32, 879-890, 2011.

59. N. M. Dimitrijevic, B. K.Vijayan, O. G. Poluektov, T. Rajh, K. A. Gray, H. He and P. Zapol "Role of water and carbonates in photocatalytic transformation of CO_2 to CH_4 on titania" Journal of American Chemical Society, Vol. 133, 3964, 2011.

Appendix

A Actinometry

There are a variety of chemical actinometry that have been developed over the years. In this section, a few of the actinometers are described.

A.1 POTASSIUM FERRIOXALATE ACTINOMETRY

The governing chemical reaction is represented as ferric ions + oxalate gives rise to ferrous ions and carbon dioxide i.e., $2Fe^{+++} + C_2O_4{}^{2-} = 2Fe^{++} + 2CO_2$ The ferrous ion thus formed is estimated spectrophotoetrically as its phenanthraline complex at 510 nm. Ferric ions form only weak complex with Phenanthraline and is transparent at 510 nm. This actinometer has some advantages and also some disadvantages. The possible advantages are (1) The method is easy and can be adopted and used quickly (2) Does not depend on difference reading between large numbers to determine the amount of conversion (3) Quantum Yields are accurately known (4) Can be adopted to the blue region of the visible spectrum. The major disadvantages of this method are (1) Only short irradiation is enough (2) High absorption neceessitates light filtering or corrections have to be applied.

A.2 SOLUTIONS REQUIRED

(1) 10 Phenanthroline (0.2 percent by weight) in water (2) Buffer solution (82 grams of sodium acetate +10 ml of concentrated sulphuric acid dilited to 1000 ml with water.) (3) Ferric sulphate solution (100 grams of ferric sulphate hydrated + 55 ml concentrated sulphuric acid diluted to 1000 with water. (4) Standardised 0.1 M EDTA 5.0.08 M $FeSO_4$ in 0.1 M sulphuric acid (6) Standard 0.1N potassium chromate solution (7) One percent diphenylamine in concentrated sulphuric acid [Solutions 5-6 are required only to determine the extinction coefficient of ferrous phenonthroline complex. One can also use a reported value of 1.11×10^4

A.3 EXTINCTION COEFFICIENT OF FERROUS PHENANTHRALINE COMPLEX

The following sequence of steps may be followed for this determination.

1. Titrate of 0.08 M ferrous sulphate solution in 0.1 sulphuric acid with a standard 0.1 N potassium chromate using a few drops of diphenylamine solution as indicator.
2. Dilute 0.08 M ferrous sulphate solution 20 times with 0.1 N sulphuric acid to get 4×10^{-4} M solution of ferrous sulphate.
3. To a series of six 25 ml volumetric flasks add 0, 1, 3, 5, 7, 9 mls respectively the solution in 2.
4. Add enough 0.1 N sulphuric acid to each of these solutions in 3 to bring the volume approximately 12.5 ml.
5. To each of these solutions in 4 add 2 ml of the 0.2% phenanthroline solution.
6. Add six ml of buffer solution to each of the volumetric flasks and dilute to the mark.
7. Measure the absorption of each of these solutions at 510 nm in a 1 cm cell versus a solution prepared as above without ferrous sulphate.
8. Plot the absorption values obtained versus complex concentration and determine the extinction coefficient from the slope.

A.4 PREPARTION OF ACTINOMETER SOLUTION

1. Titrate 0.2 N ferric sulphate solution with standard EDTA using 0.2 g of salicylic acid in 100 ml solution as indicator and buffered with 0.3 g glycine/100 ml solution to a pH of 3 to 4.
2. Prepare a standard solution of $K_2C_2O_4$ such that its molarity is six times that of ferric sulphase solution.
3. When actinometer solution is required, pipete 5 ml of the ferric sulphate solution, add 5 mls of the oxalate into a 100 ml volumetric flask and dilute to the mark with water.

A.5 MEASURMENT OF THE INTENSITY

1. Pipete out into the reaction vessel a volume of $K_3Fe(C_2O_4)_3$ necessary to be irradiated.
2. Irradiate the solution for a definite time period.
3. Mix the irradiated solution and then pipete one ml of the actnometer sotion into a 10 ml volumetric flask.
4. Add 2 ml of 0.2 phenanthroline solution.

Table A.1 ***Quantum yields of ferrous production from potassium ferrioxalate [The data have been reproduced from C. G. Hatchard and C. A. Parker, Proc. Roy. Soc., (London) A235, 518 (1956)].***

$\lambda(nm)$	*Concentration(moles/litre)*	*Quantum yield*
254	0.006	1.25
297	0.006	1.24
313	0.006	1.24
334	0.006	1.24
361	0.006	1.21
405	0.006	1.14
436	0.006	1.11

5. Add a volume of buffer equal to half of the aliquot of actinometer solution taken.
6. Make up to the mark.
7. Prepare a blank solution following steps 3-6 with a nonirradiated volume of actinometer taken.
8. Measure the absorption of the solutions 6 and 7 versus water at 510 nm and note the difference.

A.6 CALCULATION OF LIGHT INTENSITY

From the values given in Table A.1 select the appropriate quantum yield for ferrous production using the absorption obtained, calcuate the light intensity from the following formula I (in Einsteins/min) = $AV_2V_3/tV_1\varepsilon\phi_\lambda$ where A is absorption of irradiated actinometer solution corrected for absorption of the blank; V_1 in mls of the irradiated actinometer solution; V_2 is volume of the actinometer solution irradiated; V_3 is the volume of volumetric flask used for dilution of irradiated aliquot solution; ε is the extinction coefficient of ferrous phenonthroline complex at 510 nm (1.11×10^4); ϕ_λ is quantum yield of ferrous production at the wavelength of light used and t is time of irradiation in minutes.

A.7 URANYL OXALATE ACTINOMETRY

A.7.1 Solutions

1. 0.01 M Uranyl sulphate in 0.05 M oxalic acid solution
2. Standardised 0.04 M $KMnO_4$ solution.

Table A.2 ***Quantum yields of oxalate disappearance for uranyl oxalate [W. G. Leighton and G. S. Forbes, J. Am. Chem. Soc., 52, 313 (1930)].***

λ(nm)	*Quantum yield*
254	0.602
265	0582
302	0.570
313	0.561
366	0492
405	0.563
436	0.584

A.7.2 Procedure

1. Titrate an approximate volume of the actinometer solution with the standardised permanganate solution. Titrate at 333 K in 1 n sulphuric acid solution of the oxalate.
2. Irradiate the desired volume of actinometer solution for appropriate time period.
3. Titrate the irradiated solution with permanganate.
4. Calculate the light intensity.

A.8 BENZOPHENONE-BENZHYDROL ACTINOMETRY

A.8.1 Net Reaction

$$\phi_2\text{(CO)} + \phi\text{-CH(OH)-}\phi \Rightarrow [m]\ \phi\text{-CH(OH)-CH(OH)-}\phi$$

A.8.2 Discussion

The rate expression for the system is $(1/\phi_{Ph_2(CO)}$ = 1 + $k_1/k_2(BH_2)$. If this is multiplied by the quantum yield of disappearance of benzophenone at a specific [BH_2] concentration, then the expression is $\phi_a/\phi_{Ph_2CO} = \phi_a + \phi_a k_1/k_2(BH_2)$. A Plot of the relative quantum yield ratio ϕ_a/ϕ_{2CO} versus reciprocal of the benzhydrol concentration gives an intercept of ϕ_a and the light intensity can be calculated from this value.

A.9 PROCEDURE

1. Prepare 0.1 M ϕ_2CO solution in benzene containing varying concentrations of benzhydrol (e.g. 0.3, 0.1, 0.07 and 0.05 M).
2. Degas with freeze thaw cycles and then irradiate.

Table A.3 ***Quantum yields for 2-hexanone Reactions in hydrocarbon solvent [D. R. Coulson and N. C. Yang, J. Am. Chem. Soc., 88, 4511 (1968)].***

ϕ-hexanone	0.327
$\phi_{acetone}$	0.252
$\phi_{propene}$	0.25
$\phi_{cyclobutanol}$	0.075

3. Dilute each tube 25 times and compare the absorption of each to diluted non irradiated samples.
4. Plot $\phi_a/\phi_P h_2$CO versus 1/[BH_2] where [BH_2] is the average of the initial and final benzhydrol concentrations.
5. Determine ϕ_a from the intercept.
6. Calcualte the light intensity I = $\Delta(\phi_2$CO/$\phi_a)$.

A.10 2-HEXANONE ACTINOMETRY

2-hexanone undergoes Norrish type II photochemical reaction to yield acetone (which can be determined by GC) or the disappearance of 2-hexanone or the formation of propene can also be determined.

A.10.1 Procedure

1. Irradiate an appropriate volume of a 1 M solution of 2-hexanone in pentane, hexane or cyclohexane.
2. Analyse in a carbowax or similar column and compare chromatographic peak areas to those obtained from a standard acetone solution.

For more details on this topic, the reader is requested to refer the book by Steven L. Murov “Handbook of Photochemistry”, Marcel Dekker Inc, 1973.

Appendix

B Band Edge Data

The values are calculated using the following two equations $E_c = -A = -\chi + 0.5E_g$ $E_v = -I = -\chi - 0.5E_g$ where χ is electrongativity, E_g is the value of band gap and A is electron affinity and I is the ionization potential.

Table B.1 ***Data of Band edges and band gap of common sulphide semiconductors.***

Material	*Electronegativity*	*Band Gap*	*Conduction Band*	*Valence Band*
Ag_2S	4.96	0.92	-4.50	-5.42
As_2S_3	5.83	2.50	-4.58	-7.08
CdS	5.18	2.40	-3.98	-6.38
$CuFeS_2$	5.15	0.35	-4.97	5.32
FeS	5.02	0.10	-4.97	-5.07
FeS_2	5.39	0.95	-4.92	5.87
In_2S_3	4.70	2.00	-3.70	-5.70
MnS	4.81	3.00	-3.31	-6.31
MnS_2	5.24	0.50	-4.99	-5.49
MoS_2	5.32	1.17	-4.73	-5.90
NiS	5.23	0.40	-5.03	-5.43
NiS_2	5.54	0.30	-5.39	-5.69
PbS	4.92	0.37	-4.74	-5.11
$PbCuSbS_3$	5.22	1.50	-4.61	-6.11
PtS_2	6.00	0.95	-5.53	-6.48
Rh_2S_3	5.36	1.50	-4.61	-6.11
RuS_2	5.58	1.38	-4.89	-6.27
Sb_2S_3	5.63	1.72	-4.72	-6.44
SnS	5.17	1.01	-4.66	-5.67
SnS_2	5.49	2.10	-4.44	-6.54
TiS_2	5.11	0.70	-4.76	-5.46
WS_2	5.54	1.35	-4.86	-6.21
ZnS	5.26	3.60	-3.46	–7.06
ZnS_2	5.56	2.70	-4.21	-6.91
$Zn_3In_2S_6$	5.00	2.81	-3.59	-6.40
ZrS_2	5.20	1.82	-4.29	-6.11

The values are calculated using the following two equations $E_c = -A = -\chi + 0.5E_g$ $E_v = -I = -\chi - 0.5E_g$ where χ is electronegativity, E_g is the value of band gap and A is electron affinity and I is the ionization potential

Table B.2 ***Data of Band edges and band gap of common oxide semiconductors.***

Material	*Electronegativity*	*Band Gap*	*Conduction Band*	*Valence Band*
	eV	(eV)	Bottom (eV)	top (eV)
Ag_2O	5.29	1.20	-4.69	-5.89
$BaTiO_3$	5.12	3.30	-4.58	-7.88
Bi_2O_3	6.23	2.80	-4.83	-7.63
CdO	5.71	2.20	-4.61	-6.81
$CdFe_2O_4$	5.83	2.30	-4.68	-6.98
Ce_2O_3	5.20	2.40	-4.00	-6.40
CoO	5.69	2.01	-4.39	-6.40
$CoTiO_3$	5.76	2.25	-4.64	-6.89
Cr_2O_3	5.68	3.50	-3.93	-7.43
CuO	5.81	1.70	-4.96	-6.66
Cu_2O	5.32	2.20	-4.22	-6.42
$CuTiO_3$	5.76	2.99	-4.32	-7.31
FeO	5.53	2.40	-4.33	-6.73
Fe_2O_3	5.88	2.20	-4.78	-6.98
Fe_3O_4	5.78	0.10	-5.73	-5.83
$FeTiO_3$	5.69	2.80	-4.29	-7.09
Ga_2O_3	5.35	4.80	-2.96	-7.76
HgO	6.08	1.90	-5.13	-7.03
In_2O_3	5.28	2.80	-3.88	-6.68
$KNbO_3$	5.29	3.30	-3.64	-6.94
$KTaO_3$	5.32	3.50	-3.57	-7.07
La_2O_3	5.28	5.50	-2.53	-8.03
$LiNbO_3$	5.52	3.50	-3.77	-7.27
$LiTaO_3$	5.55	4.00	-3.55	-7.55
$MgTiO_3$	5.60	3.70	-3.75	-7.45
MnO	5.29	3.60	-3.49	-7.09
MnO_2	5.95	0.25	-5.83	-6.08
$MnTiO_3$	5.59	3.10	-4.04	-7.14
Nb_2O_5	6.29	3.40	-4.59	-7.99

Table B.2 ***(Continued)***

Material	*Electronegativity*	*Band Gap*	*Conduction Band*	*Valence Band*
NiO	5.75	3.50	-4.00	-7.50
$NiTiO_3$	5.79	2.18	-4.70	-6.88
PbO	5.42	2.80	-4.02	-6.82
Nb_2O_5	6.29	3.40	-4.59	-7.99
NiO	5.75	3.50	-4.00	-7.50
$NiTiO_3$	5.79	2.18	-4.70	-6.88
PbO	5.42	2.80	-4.02	-6.82
PdO	5.79	1.00	-5.29	-6.29
Sb_2O_3	6.32	3.00	-4.82	-7.82
SnO	5.69	4.20	-3.59	-7.79
SnO_2	6.25	3.50	-4.50	-8.00
$SrTiO_3$	4.94	3.40	-3.24	-6.64
Ta_2O_3	6.33	4.00	-4.33	-8.33
TiO_2	5.81	3.20	-4.21	-8.33
V_2O_5	6.10	2.80	-4.70	-7.50
WO_3	6.59	2.70	-5.24	-7.94
ZnO	5.79	3.20	-4.19	-7.39
$ZnTiO_3$	5.80	3.07	-4.27	-7.34
ZrO_2	5.91	5.00	-3.41	-8.41

Appendix

C Semiconducting Materials Employed in PEC

Table C.1 ***Listing of the possible semiconducting materials for PEC and other applications.***

Group	*Material*	*Chemical Formula*	*Value of Band Gap in eV*	*Type of Band Gap*	*Remarks*
IV	Diamond	C	5.47	Indirect	Good thermal Conductivity
IV	Silicon	Si	1.1	Indriect	Electrical mechanical properties
IV	Germanium	Ge	0.67	Indirect	Radar devices
IV	Silicon Carbide	SiC	2.3	Indirect	LED
IV	Silicon Germanium	SiGe	0.67 to 1.11	Indriect	Hetero Junctions
III-V	Aluminium antimonide	AlSb	1.6/2.2	Indirect/direct	
III-V	Aluminium arsenide	AlAs	2.16	Indirect	
III-V	Aluminium Nitride	AlN	6.28	Direct	Not much use
III-V	Aluminium Phosphide	AlP	2.45	Indirect	
III-V	Boron Nitride (C/ H/NT)	BN	6.36/5.96/ 5.5	Indirect quasi direct	LED
III-V	Boron Phosphide	BP	2	Indirect	
III-V	Boron arsenide	BAs	1.5	Indirect	
III-V	Gallium antimonide	GaSb	0.73	Direct	IR detector and LED
III-V	Gallium arsenide	GaAs	1.43	Direct	Electronic applications
III-V	Gallium nitride	GaN	3.44	Direct	Electronic applications
III-V	Gallium Phosphide	GaP	2.26	Indirect	LED
III-V	Indium antimonide	InSb	0.17	direct	IR detectors
III-V	Indium arsenide	InAs	0.36	direct	Infra red detectors

Table C.1 ***(Continued)***

Group	*Material*	*Chemical Formula*	*Value of Band Gap in eV*	*Type of Band Gap*	*Remarks*
III-V	Indium Nitride	InN	0.7	direct	Solar cells
III-V	Indium Phosphide	InP	1.35	direct	Optoelectronics
III-V	Aluminium gallium arsenide	AlGaAs	1.42 to 2.16	Direct/ indirect	Solar cells
III-V	Indium gallium arsenide	InGaAs	0.36 to 1.43	Direct	IR and thermo -photovoltaics
III-V	Gallium arsenide phosphide	GaAsP	1.43 to 2.26	Direct indirect	LED
III-V	Gallium arsenide antimonide	GaAsSb	0.7 to 1.42	Direct	
III-V	Aluminium gallium nitride	AlGaN	3.44 to 6.28	Direct	
III-V	Aluminium gallium phosphide	AlGaP	2.26 to 2.45	Indirect	LED
III-V	Indium gallium nitride	InGaN	2 to 3.4	direct	LED
II-VI	Cadmium selenide	CdSe	1.74	Direct	Optoelectronics and solar cells
II-VI	Cadmium sulphide	CdS	2.42	Direct	Solar cells
II-VI	Cadmium telluride	CdTe	1.49		Solar cells
II-VI	Zinc oxide	ZnO	3.37	Direct	Photo-catalysis
II-VI	Zinc Selenide	ZnSe	2.7	Direct	Lasers and LED
II-VI	Zinc Sulphide	ZnS	3.54/3.91	direct	Scintillator
II-VI	Zinc Telluride	ZnTe	2.25	Direct	Lasers and LED
II-VI	Cadmium zinc telluride(CZT)	CdZnTe	1.4 to 2.2	direct	X/gamma ray detector
II-VI	Mercury Cadmium telluride	HgCdTe	0 to 1.5		IR detectors
II-VI	Mercury Zinc Telluride	HgZnTe	0 to 2.25	IR detectors	
I-VII	Cuprous chloride	CuCl	3.4	Direct	
I-VI	Copper sulphide	Cu_2S	1.2	Direct	Solar cells
IV-VI	Lead selenide	PbSe	0.27	Direct	IR detectors
IV-VI	Lead(II) sulphide	PbS	0.37		IR detectors
IV-VI	Lead telluride	PbTe	0.32		Thermoelectric material
IV-VI	Tin sulphide	SnS	1.0	Indirect	
IV-VI	Tin sulphide	SnS_2	2.2		
IV-VI	Titanium oxide anatase	TiO_2	3.2		Photocatalytic

Table C.1 ***(Continued)***

Group	*Material*	*Chemical Formula*	*Value of Band Gap in eV*	*Type of Band Gap*	*Remarks*
IV-VI	Titanium oxide rutile	TiO_2	3.02		Photo-catalytic
IV-VI	Titanium oxide Brookite	TiO_2	2.96		
I-VI	Copper (I) oxide	Cu_2O	2.1		Rectifier diodes
I-VI	Copper (II) oxide	CuO	1.2	p-type	
III-VI	Uranium dioxide	UO_2	1.3		Thermoelectric applications
IV-VI	Tin oxide	SnO_2	3.7		
II-IV-VI	Barium Titanate	$BaTiO_3$	3.0		Ferro-electric applications
II-IV-VI	Strontium titanate	$SrTiO_3$	3.3		Ferroelectric
I-V-VI	Lithium niobate	$LiNbO_3$	4.0		Ferroelectric
III-I-VI	Lanthanum copper oxide	La_2CuO_4	2.0		Super conductor
IV	Selenium	Se	1.74		Rectifiers
VIII-VI	Iron disulphide	FeS_2	0.95		Solar cells
VIII-VI	Ferric oxide	Fe_2O_3	2.1		
V-VI	Niobium pentoxide	Nb_2O_5	3.4		
V-VI	Tantalum Pentoxide	Ta_2O_5	3.9 to 4.5		
VIII-VI	Nickel oxide	NiO	1.34/2.92		
IV-V-VI	Tin niobate	$SnNb_2O_6$	1.49		
IV-V-VI	Tin tantalite	$SnTa_2O_6$	2.03		
IV-V-VI	Tin niobate	$Sn_2Nb_2O_7$	1.11		
IV-V-VI	Tin tantalate	$Sn_2Ta_2O_7$	1.41		
VI-VI	Tungsten oxide	WO_3	2.8		
IV-VI	Zirconium oxide	ZrO_2	4.60		
III-VI	Indium oxide	In_2O_3	3.6 to 3.9	direct	
VI-VI	Tungsten sulphide	WS_2	1.80		
V-VI	Bismuth sulphide	Bi_2S_3	1.5 to 1.74		
I-V-VI	Potassium tantalate	$KTaO_3$	3.42		
I-V-VI	Sodium niobate	$NaNbO_3$	3.08		
I-V-VI	Potassium niobate	$KNbO_3$	1.97/3.30		
I-V-VI	Sodium tantalate	$NaTaO_3$	2.35		
V-Vi-VI	Bismuth molybdate	$Bi_2\ MoO_6$	2.70/3.02		
V-VI-VI	Bismuth molybdate	$Bi_2Mo_3O_9$	3.10		

Table C.1 ***(Continued)***

Group	*Material*	*Chemical Formula*	*Value of Band Gap in eV*	*Type of Band Gap*	*Remarks*
V-VI-VI	Bismuth molybdate	Bi_2Mo3O_{12}	2.88		
VI-VI	Tungsten selenide	WSe_2	1.37		
VIII-VI-VI	Nickel molybdate	$NiMoO_4$	2.81		
I-V-VI-VI	Sodium bismuth molybdate	$NaBi(MoO_4)_2$	3.0		
I-V-VI-VI	Silver bismuth molybdate	$AgBi(MoO_4)_2$	2.9		
III-VI-VI	Lanthanum molybdate	$La_2(MoO_4)_3$	2.30		
III-VI-VI	Europium molybdate	$Eu_2(MoO_4)_3$	3.20		
I-V-VI-VI	Sodium bismuth tungstate	NaBi(WO4)2	3.5		
VI-V-VI	Lead niobate	$Pb_3Nb_2O_8$	2.72		
VI-V-VI	Lead niobate	$Pb_3Nb_4O_{13}$	2.95		
I-V-VI	Lithium niobate	$LiNbO_3$	3.7/4.7		
III-V-VI	Lanthanum tantalate	$La4Ti3O_{12}$	3.95		
II-IV-VI	Strontium titanate	$Sr_3Ti_2O_7$	3.2		
II-V-VI	Calsium niobate	$Ca_2Nb_2O_7$	4.3		
IV-VI-VI	Lead tungstate	$PbWO_4$	4.7		
IV-VI-VI	Lead molybdate	$PbMoO_4$	4.0		
VIII-VI	Cobalt sesqioxide	Co_3O_4	1.23/1.54	Direct/indirect	
VIII-III-VI	Cobalt aluminate	$CoAl_2O_4$	2.0		
IV-VI	Tin oxide	SnO_2	3.50		
V-VI	Antimony oxide	Sb_2O_3	3.0		
V-VI	Bismuth oxide	Bi_2O_3	2.80		
V-VI	Tantalum oxide	Ta_2O_5	3.95		
VIII-VI	Cobalt oxide	CoO	2.60		
II-IV-VI	Magnesium titanate	$MgTiO_3$	3.70		
II-IV-VI	Barium titanate	$BaTiO_3$	3.20		
I-V-VI	Lithium Niobate	$LiNbO_3$	3.80		

Appendix

D Data on Dye Sensitized Solar Cells

Table D.1 ***Details on the possible dyes for use in dye sensitized solar cells reported in literature [The data have been assembled from literature].***

System DSSC with the dye	*Name of the dye*	V_{OC} mV	I_{SC} mA/cm^2	%
P1	N-[2,7-Bis-(N,N-diphenylamino) -9,9-spirobifluoren-2-yl] -1,7-bis-(4-t-butylphenoxy)- perylene-3,4-dicarboxylic acid anhydride-9,10-imide	839	0.324	0.27
P4	N-(Pentafluorphenyl) -perylen-3,4:9,10- tetracarboxylicacid -3,4-anhydrid-9,10- imide	626	0.114	0.04
P7	Perylene dicarboxylic acid -3,4-anhydride (P7)	652	0.153	0.06
P8	N-(Diisopropylphenyl) -3,4:9,10-perylene tetracarboxylic acid -3,4-anhydrid-9,10-imide	687	0.306	0.13
P9	1,7-(4-t-butylphenoxy) -3,4:9,10-perylene tetracarboxylic dianhydride	647	0.181	0.07
	Ru(L)(NCS)3 (L = 4,4,4 -tricarboxy-2,2:6,2 -terpyridine (Up to 920 nm)			
	2-cyanoacrylic acid-4- (bis-dimethylfluoreneaniline) dithiophene			
	[M(H3tcterpy)LY]+]: M = Os(II) or Ru(II); (H3tcterpy) is tridentate 4,4,4-tricarboxy-2,2:6,2 -terpyridine, and L is a bidentate ligand like (bpy, 2,2-bipyridine) or (pyq, 2-2-pyridylquinoline) Near IR 50			
	Ruthenium complex with 2-(2,4-Difluorophenyl) pyridine			

Table D.2 ***Data of the Dye sensitized solar cells [The data reported in this table have been assembled from literature]***

Dye	*IPCE* (%)	*Short Circuit Current* J_{SC} (mA/cm^2)	*Open Circuit Voltage* V_{OC}(mV)	*Fill Factor (ff)*	*Efficiency* (%)
Z910	8017.20	777	0.76	10.20	
Z907	72	13.60	721	0.69	6.80
Z955	80	16.37	707	0.6	8.00
K8	77	18.00	640	0.75	8.64
K19	70	14.61	711	0.67	7.00
K73	80	17.22	748	0.69	9.00
K51	70	15.40	738	0.69	9.50
Anthocyanin	67	0.425		0.83	
Black rice (anthocyanin) 560 nm		1.142	551		
Dye1	67	11.18	661	0.57	4.21
Dye2	51	12.35	644	0.56	4.41
Dye3		9.07	559	0.57	2.88
Monoporphyrin acid 1	73	8.86	654	0.71	4.11
Monoporphyrin acid 2	75	9.70	660	0.75	1.80
Monoporphyrin acid 3	5	1.35	490	0.69	0.45
Monoporphyrin acid 4	30	2.05	580	0.75	0.89
Monoporphyrin acid 5	4	1.1	561	0.67	0.41
E490		9.17	482	0.6	2.7
E491		8.6	499	0.66	2.84
E513		4.91	472	0.72	1.68
SG 74-5		7.82	479	0.68	2.53
SG 72-5		7.06	487	0.71	2.43
Rose Bengal (1XC)		7.84	560	0.51	2.4
Eosin-Y (1XC)		4.56	560	0.59	1.5
Rhodamine-B (1XC)		1.88	510	0.62	0.6
Fast Green (1XC)		1.50	480	0.58	0.4
Acridine Orange (1XC)		0.36	370	0.50	0.06
Blended dye above five (1XC:2XC:3XC;2Xc:1XC)		27.9	590	0.51	7.9

Table D.3 ***Data of the Dye sensitized solar cells [The data reported in this table have been assembled from literature] Continued.***

Dye	*IPCE* (%)	*Short Circuit Current* J_{SC} (mA/cm^2)	*Open Circuit Voltage* V_{OC}(mV)	*Fill Factor (ff)*	*Efficiency* (%)
NKX-2553		10.4	710	0.74	5.5
NKX-2554		9.9	740	0.74	5.4
NKX2569		12.9	710	0.74	6.8
NKX-2600		12.5	680	0.69	5.9
Indoline D1	70	14.8	589	0.54	5.11
Indoline D2	80	10.0	622	0.65	4.03
TC301		4.93	1041	0.71	3.66
TC306		7.36	915	0.75	5.07
N-719	85	17.0	820	0.72	10.1
N-749(black Dye)		21.8	720	0.65	10.4
N3(red Dye)	83	15.8	726	0.71	8.2
N945		16.50	790	0.72	9.60
D29		7.98	660	0.47	2.22
D35		12.02	780	0.54	5.07
PT		7.57	580	0.59	2.3
TT		0.39	260	0.45	¡0.05
P1		1.26	529	0.68	0.52
P4		0.39	450	0.61	0.12
P7		0.50	477	0.61	0.17
P8		0.51	455	0.62	0.16
P9		0.52	503	0.62	0.18
L0		2.89	735	0.73	2.89
L1		5.42	735	0.69	5.42
L2		6.42	710	0.68	6.42
L3		6.55	635	0.66	6.55
L4		4.56	560	064	4.56
ZnO	42	9.0	612		2.3
ZnO:I	61	14.0		4.5	